THEORETICAL STUDIES ON TRICARBA-SUBSTITUTION, ENCAPSULATION AND CONDENSATION IN POLYHEDRAL BORANES

A Thesis

Submitted for the Degree of

DOCTOR OF PHILOSOPHY

By

Elambalassery G. Jayasree

School of Chemistry

University of Hyderabad

Hyderabad 500 046

INDIA

January 2004

Dedicated to

My Grandmother,

Whose blessings and advices give me

enough strength to get along....

Whose memories keep me going.....

CONTENTS

STATEMENT i

CERTIFICATE ii

ACKNOWLEDGEMENTS iii

CHAPTER 1: **Introduction: Scope of the Thesis and Computational Methodologies.**

1.1. Scope of the thesis 1

1.1.1. Polyhedral Boranes: A brief history 1

i. Polyhedral boranes and cationic charge 3

a. Heteroatom substitution 3

b. Condensation 4

c. Encapsulation 6

ii. Boron hydrides and hydrocarbons: Diversities and similarities 7

1.2. Computational Chemistry 11

1.2.1. Introduction 11

1.2.2. Ab-initio method 12

i. Hartree-Fock method 15

ii. Basis sets 17

a. Basis functions 18

b. Classification of basis sets 19

iii. Electron correlation 20

a. Configuration interaction 20

b. Moller-Plesset perturbation theory 21

1.2.3. Semi empirical methods 23

1.2.4. Density Functional Theory 25

CHAPTER 2: Cationic *Closo*-tricarbaboranes- Stability and Synthetic Designs

2.0. Abstract 34

2.1. Theoretical investigation on the structure and stability of cationic *closo*-tricarbaboranes, $C_3B_{n-3}H_n^+$ (n=5,6,7,10,12) 35

2.1.1. Introduction 35

2.1.2. The rules that govern the stability of heteroborane isomers 36

2.1.3. Geometries and relative stabilities of the isomers 37

i. 5-vertex clusters 37

ii. 6-vertex clusters 38

iii. 7-vertex clusters 40

iv. 10-vertex clusters 41

v. 12-vertex clusters 43

2.1.4. The stability order of various isomers across the clusters 45

2.1.5. Natural charges and the delocalization 46

2.1.6. Possible applications 48

2.1.7. Conclusions 49

2.2. A possible synthetic strategy towards cationic *closo*-tricarbaboranes 49

2.2.1. Introduction 49

2.2.2. Benzyl cation-tropylium ion analogs in polyhedral boranes 50

2.2.3. Geometry of the dicarboranyl methyl cations: Benzyl cation analogs 50

2.2.4. Boranyl methyl anion-monocarbaborane rearrangement 53

2.2.5. Reaction paths and energy barriers 55

2.2.6. Transition states 57

2.2.7. Conclusions 57

CHAPTER 3: **Endohedral Polyhedral Boranes: Relationship with Sandwich Complexes and their Stability**

3.0. Abstract 63

3.1. The relationship between polyhedral borane sandwiches and endohedral complexes based on their electronic structure 64

3.1.1. Introduction 64

3.1.2. Qualitative analysis of the electronic structure of endohedral and sandwich--complexes 64

3.1.3. Extended 2-atom encapsulation 68

3.1.4. Experimental verification 70

3.1.5. Quantitative verification 70

3.1.6. Conclusions 71

3.2. An analysis on the stability of endohedral carba- and silaboranes, $X@Y_mB_nH_{n+m}^q$ (X=He,Ne,Li,Be; Y=B,C,Si; m=0-3; n=12-9; q=-2 to+2), $(C_2B_4H_6)_2X^q$ (X=Li,Al,Si; q=-3,-1,0), and $X_2@B_{17}H_{17}^q$(X=He,Li; q=-2,0) 71

3.2.1. Introduction 71

3.2.2. Numbering notation 73

3.2.3. Energetics and geometries 74

i. Stability order by various equations 74

ii. Geometrical features 75

3.2.4. Multiatom encapsulation 83

3.2.5. Comparison of the stability of endohedral complexes with exohedral face capped systems 84

3.2.6. Conclusions 84

CHAPTER 4: **Condensation in Polyhedral Boranes**

4.0. Abstract 90

4.1. Structural connections between compounds of boron and carbon 91

4.1.1. Introduction 91

4.1.2. Familiar connections 91

4.1.3. Connection between organic structures and magnesium borides 93

4.1.4. Fullerene (C_{60}) and β-rhombohedral boron 98

4.1.5. Conclusions 101

4.2. The stability of 3-dimensional *closo*- polycondensed polyhedral boranes:- A comparative study with benzenoids 101

4.2.1. Introduction 101

4.2.2. Energetics of various fusion modes 103

i. Benzenoids 104

ii. Edge-sharing condensation 105

iii. Face-sharing condensation 108

iv. Four-atom sharing condensation 110

4.2.3. Aromaticity and NICS values 111

4.2.4. Geometrical features of the condensed systems 112

4.2.5. Conclusions 116

4.3. Benzocarboranes : A comparative analysis on their stability and aromaticity 116

4.3.1. Introduction 116

4.3.2. Condensed product of planar 6-membered ring and 12-vertex icosahedral borane 118

4.3.3. Condensed product of planar 6-membered ring and 10-vertex polyhedral borane 121

4.3.4. Condensed product of planar 6-membered ring and 7-vertex polyhedral borane 122

4.3.5. Condensed product of planar 6-membered ring and 6-vertex polyhedral borane 122

4.3.6. Aromaticity and NICS values 123

4.3.7. Conclusions 124

CHAPTER 5: CO Vertices in Polyhedral Boranes: a New Class of *Hypercloso*-systems

5.0. Abstract 130

5.1.1. Introduction 130

5.1.2. Polyhedral boranes with one CO vertex 132

5.1.3. Polyhedral boranes with two CO vertices 134

i. Clusters involving 5-membered rings 134

ii. Clusters involving 4-membered rings 139

5.1.4. Comaprison of the stability with benzoquinones 142

5.1.5. Aromaticity and NICS values 145

5.1.6. Conclusions 145

STATEMENT

I do hereby declare that the work embodied in this thesis is the result of investigations carried out by me in the **School of Chemistry, University of Hyderabad, Hyderabad, India,** under the supervision of **Prof. Eluvathingal D. Jemmis**.

In keeping with the general practice of reporting scientific observations, due acknowledgements have been made whenever the work described is based on the findings of other investigators.

Jayasree

Elambalassery G. Jayasree

CERIFICATE

Certified that the work embodied in the thesis entitled "**Theoretical Studies on Tricarba-substitution, Encapsulation and Condensation in Polyhedral Boranes**" has been carried out by **Ms. Elambalassery G. Jayasree** under my supervision and the same has not been submitted elsewhere for any degree.

Eluvathingal D. Jemmis

Thesis Supervisor

Dean

School of Chemistry

Dean
School of Chemistry
University of Hyderabad
Hyderabad-500 046, India

ACKNOWLEDGEMENTS

"A teacher affects eternity; he can never tell where his influence stops"

-Henry Adams

I have reached this far in my academic life with the blessings of my teachers. I think of all my teachers I have had over the years with a deep sense of gratitude and recognition. I would not have completed my Ph.D. if my supervisor Prof. Jemmis had not been kind, understanding and supportive throughout the course. His overly enthusiasm and integral view on research and his words that "there is no good or bad works as such, but the effort that we put into each project make them valuable" has made a deep impression on me. I owe him lots of gratitude for having me shown this way of research. Besides, Prof Jemmis and his wife have been always concerned and encouraging during the hardest times of my life.

I thank all the faculty members of the School of Chemistry, University of Hyderabad. Special thanks to Prof. K. D. Sen, Prof. M. Durga Prasad, Prof. T. P. Radhakrishnan and Prof. K. C. Kumara Swamy. The research field is always benefited by the interdependence than independence. It was a pleasant experience to collaborate with the experimental group of Prof. KCK and it unraveled before me another way of approaching the problem at hand.

My sincere thanks to all the non-teaching staffs in the School for providing me their valuable service at the appropriate time.

I thank CSIR, New Delhi for the financial assistance and Computer Centre, University of Hyderabad for the computation time.

One gets the work done fast when the atmosphere around is serene and suitable. I am grateful to all my labmates both past and present for giving me such peaceful environment. My seniors BaLu, Kiran, Pankaz and Aswini helped me in various ways to start my work in full swing. I gratefully acknowledge BaLu for his valuable computer classes which made me comfortable with computers and for the long discussions which attracted me towards the world of polyhedral bonding and structures. My juniors Anoop, Param, Bishu and Prasad created a cooperative and jovial atmosphere which helped me

enjoy my work to the maximum. The critical assessment of each chapter by Param helped me to rectify many errors in this thesis.

As Cicero puts it "Friendship is the only thing in this world, the usefulness of which all mankind are in agreement." I am very fortunate to have got a true friend in my life, Panchu who stood with me in the ups and downs of my life and whom I could rely on at any time.

I thank all my friends at School and hostel for making my stay comfortable here in the campus.

My family has been a perpetual source of encouragement, advocacy, assurance, and emotional refueling that empowers me to venture with confidence into the greater world and to become all that I am now.

"I Thank God Almighty, for every moment of life, and for all my many blessings."

Jayasree

CHAPTER 1

Introduction: Scope of the Thesis and Computational Methodologies.

1.1. Scope of the Thesis

1.1.1. Polyhedral boranes: A brief history

The chemistry of boron hydrides (boranes) started its successful journey with Alfred Stock's discovery of volatile and highly reactive boranes of compositions, B_nH_{n+4} and B_nH_{n+6}.[1] Several experimental studies to explore their chemical properties followed. The understanding of structure and bonding of electron deficient boron hydrides remained a challenge to the chemists until the corroboration of the diborane structure using three centre-two electron (3c-2e) bonds by Longuet-Higgins in 1949.[2] The X-ray diffraction studies, theoretical analyses and structural predictions by Lipscomb and his collaborators were instrumental in furthering this field.[3] Qualitative electron counting rules played a vital role in their development. Lipscomb's 'styx',[3] Wade's (n+1) rule[4] and Mingos rule[5] are the significant ones among them. All these studies established the concept of delocalized multicentre bonding which has become a standard vocabulary in the area.

Wade's rule is applicable to families of monopolyhedral borane structures with and without missing vertices. According to Wade's rule, stable *closo*-structures have 'n+1' electron pairs for its skeletal bonding where 'n' is the number of vertices, *nido* structures(one vertex missing) need 'n+2' electron pairs, *arachno* structures(two vertices missing) 'n+3' electron pairs and so forth (Figure 1.1). This leads to many negative charges to the polyhedral boranes as the cage receives one electron pair from each BH vertex for the skeletal bonding. A whole range of dianionic *closo*- polyhedral boranes ($B_nH_n^{-2}$; n=6-12) have been synthesized and many theoretical as well as experimental studies of their structure and reactivity are known.[3c,d,6] These structures have wide-

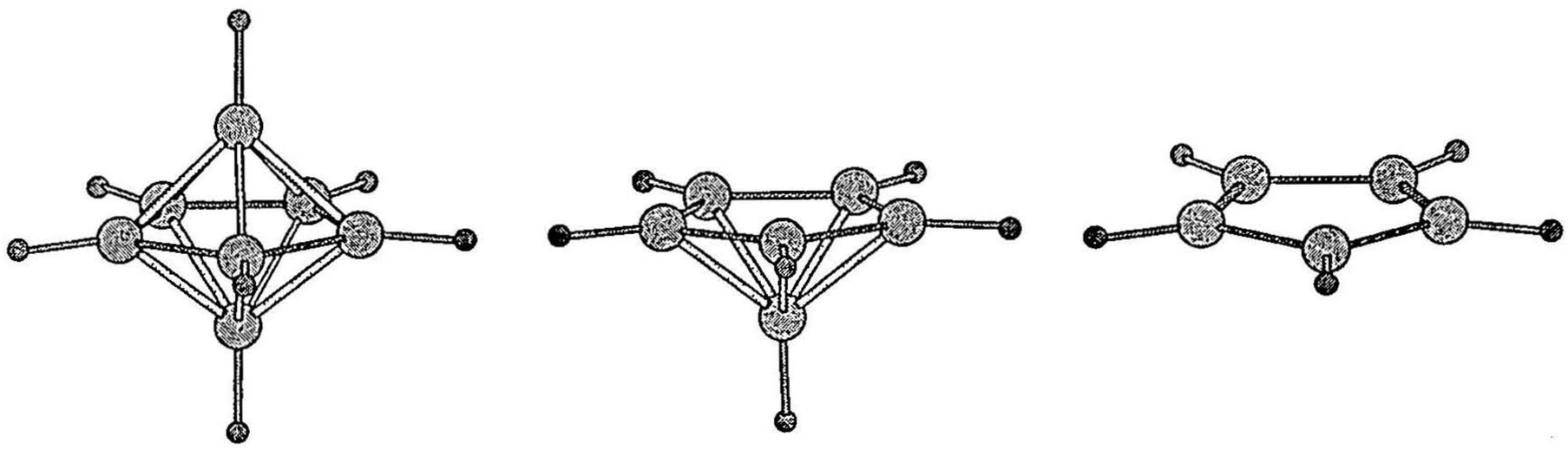

closo-$B_7H_7^{-2}$ *nido*-$B_6H_6^{-4}$ *arachno*-$B_5H_5^{-6}$

Figure 1.1. *Closo*, *nido* and *arachno* forms of a polyhedron. The charges are obtained by the Wade's rule

applications in different areas owing to their peculiar thermal, chemical and photochemical stabilities. The propensity of ^{10}B nucleus to capture a slow neutron, leading to nuclear decay producing high energy $^{4}He^{2+}$ and $^{7}Li^{3+}$ ions forms the basis for Boron Neutron Capture Therapy (BNCT).[7] The polyhedral borane clusters are structurally tuned to vary the properties to make suitable for different applications such as in liquid crystalline materials, Langmuir-Blodgett films, electrophilic catalysts, and weakly coordinating anions.[8]

Recently our group introduced a new electron counting rule, Jemmis' *mno* rule, which covers a whole range of polyhedral structures including metallocenes and condensed polyhedral boranes.[9] According to this, a polyhedron requires m+n+o electron pairs for its skeletal stability where 'm' is the number of cages, 'n' is the number of vertices and 'o' is the number of single vertex sharing present in that polyhedron. This rule forms the basis for discussions of condensed structures in the thesis. The focus of this thesis is on the following aspects of the chemistry of polyhedral boranes.

i. Polyhedral boranes and cationic charge

The dianionic character of the known polyhedral boranes is supported by the electron counting rules. Neutral polyhedral boranes are traditionally obtained by replacing two borons by two carbons in the *closo*-category or by adding bridging hydrogens in the open polyhedral cages such as in *nido* or *arachno* cateogry. It is anticipated that the presence of a large number of electropositive boron atoms may not favor a positive charge. There are a few reports on the cationic boron species, with only one structure belonging to the cluster family (*nido*-$C_5BR_6^+$, a pentacarba-susbstituted analogue of *nido*-$B_6H_6^{-4}$ shown in Figure 1.1):[10] others are derived from diborane and is of the $BH_2L_2^+$ type where L belonging to an acceptor ligand.[3d] Thus, positive charge in the electron deficient borane cage is a novel aspect. Approaches to cationic cages in borane chemistry constitute the major part of this thesis. It is obvious that the factors which can lead to a reduction in the electron deficiency which in turn reduces the anionic charges of the cage can be exploited to arrive at the cationic species in polyhedral boranes. These factors are briefly explained below:

(a) ***Heteroatom substitution***: There are many studies in the literature where the anionic charges in the polyhedral borane clusters are reduced by heteroatom substitution using atoms such as C, N, P, and S.[11] Among them, dicarbaboranes have attracted special attention due to their zero charge, and high thermodynamic and kinetic stability.[12] Icosahedral $C_2B_{10}H_{12}$ has developed a chemistry of its own and is used in biological, medicinal, organic, inorganic, catalytical and materials chemistry. For example, $C_2B_{10}H_{12}$ derivatives are used in Boron Neutron Capture therapy (BNCT), in selective drug transport and in many synthetic reactions like Friedel-Craft's reactions as catalyst.[7,13] The systematic

replacement of increasing number of BH^- of $B_nH_n^{-2}$ by CH should lead to positively charged *closo*-species.

$$B_nH_n^{-2} \underset{BH^-}{\overset{CH}{\rightleftharpoons}} CB_{n-1}H_n^- \underset{BH^-}{\overset{CH}{\rightleftharpoons}} C_2B_{n-2}H_n \underset{BH^-}{\overset{CH}{\rightleftharpoons}} C_3B_{n-3}H_n^+$$

(b) ***Condensation***: Condensations among the deltahedral borane cages also lead to the possibility of positively charged boranes. Two polyhedra can fuse together by sharing a single vertex, an edge, a face or four vertices. The various electron requirements for such condensed systems follow the newly introduced electron counting *mno* rule.[9] This is demonstrated in Table 1.1 using the icosahedral skeleton.

Condensation of two icosahedral $B_{12}H_{12}^{-2}$ sharing four vertices leads to the experimentally known $B_{20}H_{16}$.[14] According to the *mno* rule 22 electron pairs (m, the number of polyhedra =2; n, the number of vertices =20, o, the number of single atom bridges =0) are needed by this structure (Table 1.1). 16 BH vertices provide one electron pair each and the four shared boron atoms give 3 valence electrons each, making the structure neutral. Further condensation by four vertex sharing leads to a structure $B_{28}H_{20}$ with the *mno* count of 31 (m=3, n=28, o=0). 20 BH vertices and 8 shared boron atoms contribute 32 electron pairs making the structure electron excess by 2 units. This structure is not known. Thus, the *mno* rule leads to the homologous series with the molecular formula, $B_{8m+4}H_{4m+8}^{2m-4}$. Each condensation involving the sharing of four vertices reduces the charge by two units.

For the condensed product $B_{21}H_{18}$ formed by the face sharing of two icosahedra. the *mno* rule demands 23 electron pairs (m=2, n=21, o=0). The structure has 18 electron pairs from 18 BH vertices, and 4.5 electron pairs from the three shared boron atoms. Thus.

$B_{21}H_{18}$ should have unit negative charge. Further condensation leads to the neutral $B_{30}H_{24}$ (m=3, n=30, o=0). Face condensation thus, leads to a homologous series with the molecular formula, $B_{9m+3}H_{6m+6}^{m-3}$. The decrease of charge by one unit with each condensation is to be contrasted to the decrease of two charges by the 4-vertex shared -

Table 1.1. Application of the *mno* rule: Variation of charge as a function of increasing condensation of polyhedra with 1, 2, 3 and 4- atom sharing. The only sharing that does not change (neither increase nor decrease) charge is edge-sharing. Experimentally known examples of each condensation are also listed.

	Type of Condensation			
	4-vertex sharing ($B_{8m+4}H_{4m+8}^{2m-4}$)	Face sharing ($B_{9m+3}H_{6m+6}^{m-3}$)	Edge sharing ($B_{10m+2}H_{8m+4}^{-2}$)	Single vertex sharing ($B_{11m+1}H_{10m+2}^{-3m+1}$)
m=1	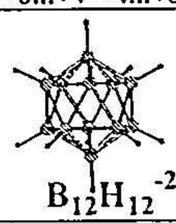 $B_{12}H_{12}^{-2}$	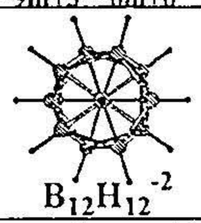 $B_{12}H_{12}^{-2}$	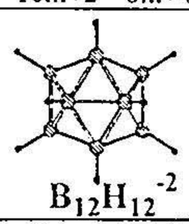 $B_{12}H_{12}^{-2}$	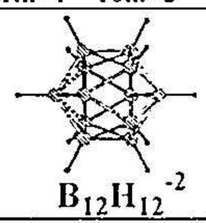 $B_{12}H_{12}^{-2}$
m=2	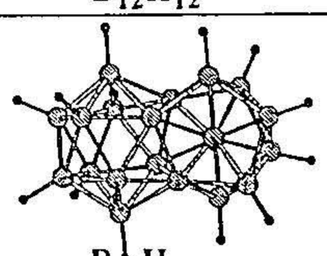 $B_{20}H_{16}$	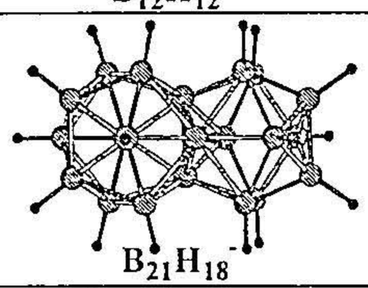 $B_{21}H_{18}^{-}$	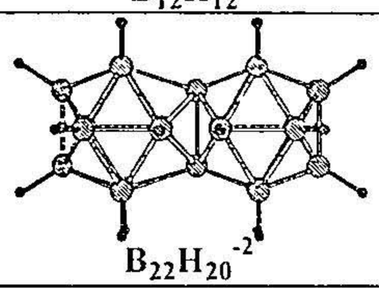 $B_{22}H_{20}^{-2}$	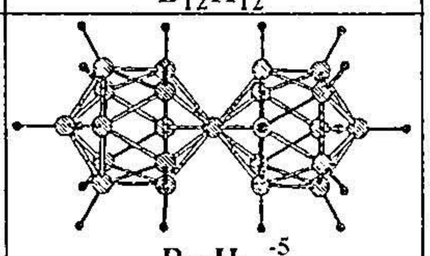 $B_{23}H_{22}^{-5}$
m=3	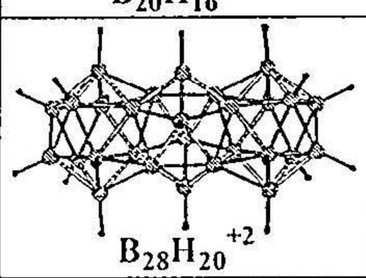 $B_{28}H_{20}^{+2}$	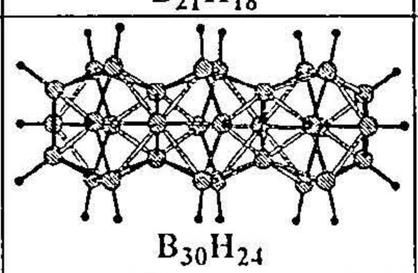 $B_{30}H_{24}$	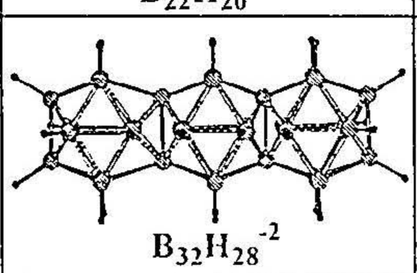 $B_{32}H_{28}^{-2}$	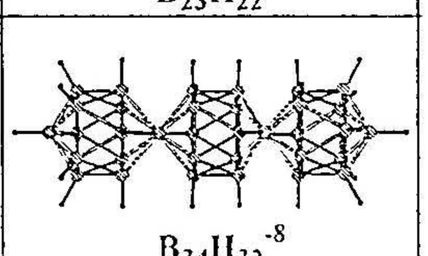 $B_{34}H_{32}^{-8}$
m=4	$B_{36}H_{24}^{+4}$	$B_{39}H_{30}^{+}$	$B_{42}H_{36}^{-2}$	$B_{45}H_{42}^{-11}$
Increment in Charge	+2	+1	0	-3
Known examples.	*closo*-$B_{20}H_{16}^{21}$	*nido*-$B_{20}H_{16}$-$(NCCH_3)_2$ [22a] *nido*-$S_2B_{16}H_{16}$ [22b]	*nido*-$B_{22}H_{22}^{-2}$; [23a] *bisnido*-$B_{18}H_{20}^{-2}$ [23b]	*closo*-$[(B_{11}H_{11})_2Cu]^{-3}$ [24]

condensation. Though these face sharing *closo*- structures are not experimentally characterized, there are several *nido* and *arachno* examples.[15] Face sharing is also observed in boron rich solids.[16]

The edge sharing $B_{22}H_{20}$ (m=2, n=22, o=0) and $B_{32}H_{28}$ (m=3, n=32, o=0) are found to have -2 charges. The molecular formula of the homologous series, $B_{10m+2}H_{8m+4}^{-2}$ shows that the edge-sharing of *closo*- structures does not change the charge. Icosahedral *closo*- structures of this kind are not known owing to the nonbonding interaction between the adjacent atoms of fused cages. However, many edge sharing *nido* systems have been synthesized.[17] The single vertex sharing system $B_{23}H_{22}$ (m=2, n=23, o=1) requires -5 charges for the skeletal bonding and a further condensation increases this requirement to -8 as in $B_{34}H_{32}$ (m=3, n=34, o=0). The molecular formula of this homologous series is $B_{11m+1}H_{10m+2}^{-3m+1}$. Such single vertex sharing systems are known with heavier elements at the shared position.[18]

Thus, the charge requirement for condensation depends on the number of shared vertices (Table 1.1). It is obvious that the four vertex sharing and the face sharing reduce the electron requirement of the system. Thus, these condensation modes are another possible way of achieving the cationic charge in polyhedral boranes.

(c) ***Encapsulation***: A variety of structural patterns such as sandwich structures, and fused structures of borane units are known: all of them are either anionic species or neutral ones.[14,18,19] Though single atom sharing between two cages leads to an enhanced electron requirement,[9] an endohedral structure obtained by reducing the distance between the two rings on either side of the fused atom has a lower electron requirement. This can be demonstrated using a hypothetical structure with molecular formula $B_{12}H_{12}Li$ (Figure 1.2). Thus, in addition to heteroatom substitution and condensation, stuffing an atom within the cage can also be a suitable approach towards cationic boranes.[20]

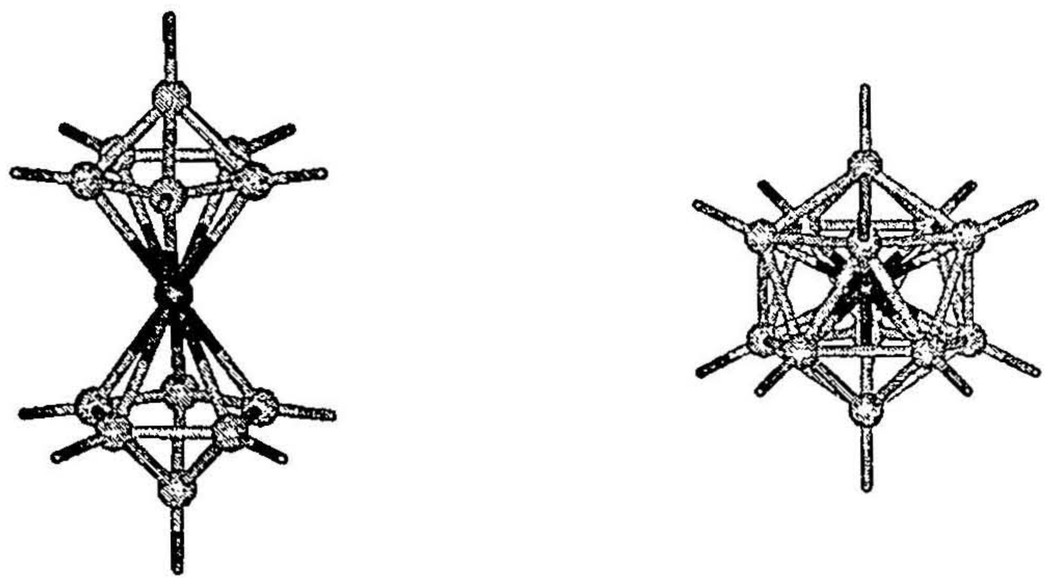

$B_6H_6LiB_6H_6$
By *mno* rule: 2+13+1=16 electron pairs
12 electron pairs(12BH)+ 1 electron (Li)
Charge=-7

$Li@B_{12}H_{12}$
1-13+0-1=13 electron pairs
12 electron pairs(12BH)+ 1 electron (Li)
Charge=-1

Figure 1.2. The figure shows the reduction in charge while going from sandwich structure $B_6H_6LiB_6H_6$ to the endohedral structure $Li@B_{12}H_{12}$.

ii. Boron hydrides and hydrocarbons: Diversities and similarities

The hydrocarbons, in general, have electron sufficient 2c-2e bonds. The sp^3, sp^2, and sp hybridization and the 2-dimensional aromaticity of benzene are common knowledge in chemistry. Boranes do not have sufficient electrons to form 2c-2e bonds. The electron deficient polyhedral boranes have multicentre bonds in order to overcome the electron scarcity. This leads to 3-dimensional delocalization and aromaticity. When the carbon atoms form a part of the polyhedral borane cage, several novel characteristics appears. Carbon atom prefers a position of higher electron density and low coordination number. This has been explained in many ways.[21,22] The carbon sites are more exposed towards many reactions. When the polyhedral cage is a multicarba system, the favorable isomer is found to be the one where there is a maximum overlap between the ring and cap orbitals suggested by Jemmis.[23] The isoelectronic relationship of CH with BH^- obviously steered in establishing the close association between the organic compounds and polyhedral boranes in spite of their marked differences. There exists a whole range of structures which are interconnected. The attempts by Olah, Williams and others provided many leads

to understand the structural patterns of otherwise complicated polyhedral boranes.[24-26] Not only there are structural relations, but also the aromatic stability is governed by the unique (4n+2) π electron rule for both the systems, which is explained by Jemmis and Schleyer with their 6π-interstitial electron rule.[27] According to this rule, 6π electrons are required for the stability of the polyhedral boranes, even though the term "π" is strictly applicable here. Hückel's (4n+2) rule is a special case of the newly introduced *mno* rule for edge-sharing *bisarachno* systems. This is demonstrated by the hypothetical hexagonal bipyramidal molecule, $B_8H_8^{-2}$ (D_{6h}) and edge-sharing condensed system $B_{14}H_{12}^{-2}$ (m=2, n=14, o=0) (Figure 1.3). Removal of two vertices from $B_{14}H_{12}^{-2}$ leads to a *bisnido*-structure $B_{12}H_{10}$ with a -6 charge (Figure 1.3). The *bisarachno*-structure with a -10 charge obtained by the removal of two more vertices is isoelectronic to naphthalene, $C_{10}H_8$. The difference between the Hückel (4n+2) and Jemmis' *mno* electron counts come from the skeletal σ-bonds, which are left out in the Hückel rule. If the number of C-C σ electrons are added to the (4n+2) π electrons, we get the electrons demanded by the *mno* rule. All these connections could bring the structure and bonding of polyhedral boranes close to those of the hydrocarbons.

We have tried to simplify the polyhedral borane chemistry further by drawing more parallels between organic compounds and their polyhedral borane counterparts and by carrying out quantitative comparative studies between them. In our attempts towards the realization of cationic *closo*-tricarbaboranes, we have drawn the analogies of benzyl cation-tropylium ion rearrangement in polyhedral borane chemistry. The possibility of condensation among polyhedral borane cages similar to aromatic hydrocarbons led us to -

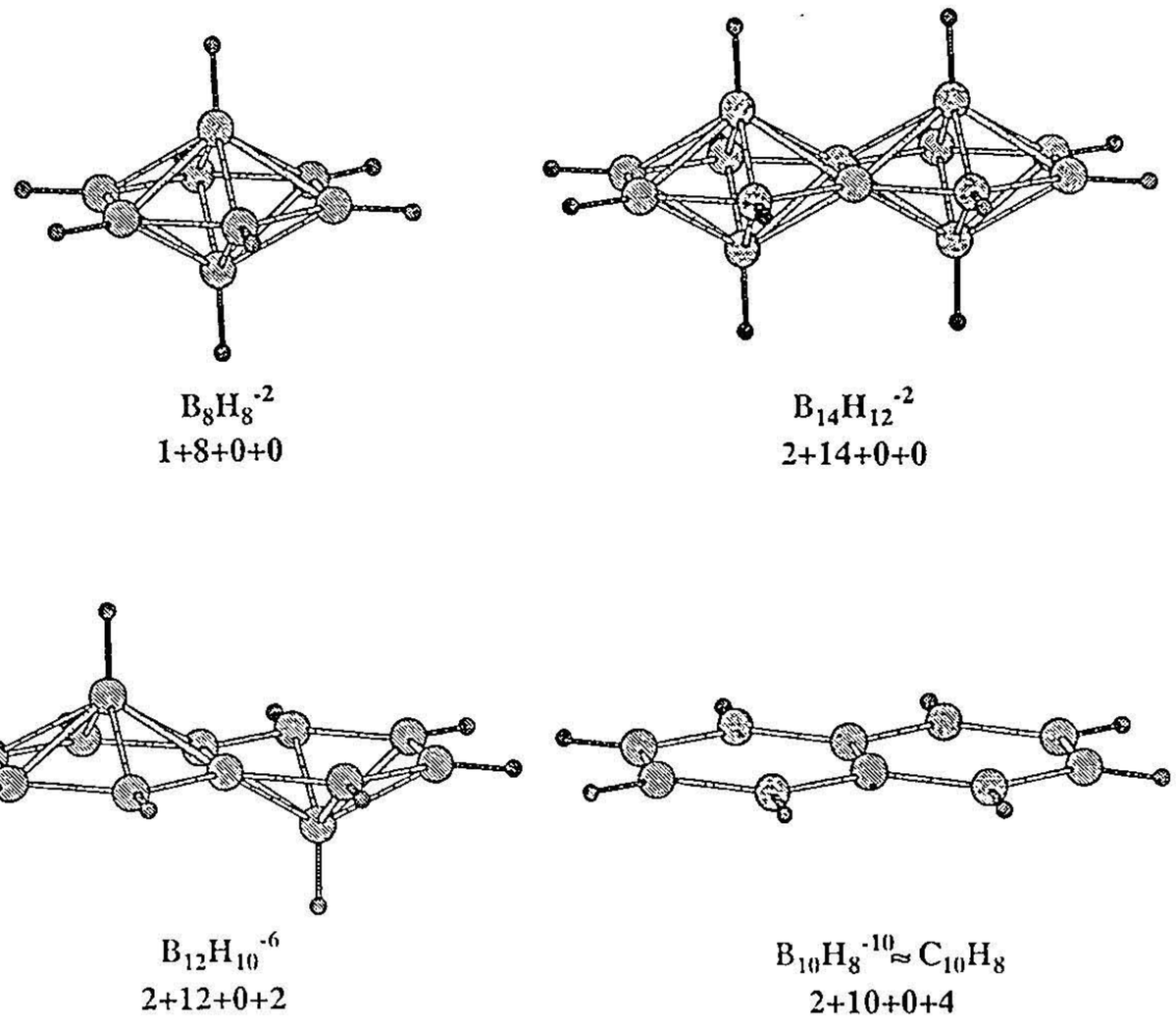

Figure 1.3. The relationship between Hückel aromatic naphthalene and hypothetical hexagonal boranes shows that Hückel's rule is a special case of *mno* rule. The electron counting according to the *mno* rule is also indicated below each structures. For *closo*-$B_8H_8^{-2}$, m= 1, n=8, o=0, p(number of missing vertices) = 0. for *closo*-$B_{14}H_{12}^{-2}$, m= 2, n=14, o=0, p= 0 for *bisnido*-$B_{12}H_{10}^{-6}$, m=2, n=12, o=0, p=2 and for *bisarachno*- $B_{10}H_8^{-10}$, m=2, n=10,o=0, and p=4.

carry out a comparative analysis on their energetics. Similarly a quantitative study on benzoquinone analogs of polyhedral boranes is also included in the thesis.

Besides being able to derive many correlations between boron chemistry and carbon chemistry, the attempts towards cationic polyhedral boranes also led to many novel structures with hypercoordinate carbon atoms. Van't Hoff and LeBel's suggestion of tetrahedral tetracoordination around carbon has been well appreciated and is invariably supported by the basic rules such as octet rule and hybridization concepts.[28] In general, the structures of carbon are well understood and can be explained by these basic rules. Hoffman's theoretical suggestion of planar tetracoordinate carbon (ptC) came as a breakthrough in the organic structural chemistry.[29] This study helped in figuring out the

electronic structure of methane with ptC, according to which it has an electron deficient σ-plane with six electrons and four bonds and a filled pπ-orbital perpendicular to the molecular plane. This report is followed by enormous number of studies designing novel compounds with such unusual structural pattern and towards their experimental realization.[30] Multicentre bonding helps in describing the structures of hypercoordinated carbon compounds where violation of basic octet rule occurs. Nonclassical structures of hydrocarbons such as pentagonal pyramidal $C_6H_6^{+2}$ and transition metal carbido complexes can be immediately pointed out as the earlier examples of hypercoordinate carbon atom.[31] The deltahedral carbaboranes span out a range of structures with hypercoordinate carbons and have many applications.[15,16]

There are many new carbaborane structures proposed in this thesis. The condensed products of benzene and polyhedral boranes- the benzocarboranes[32] and the sandwich structures between two polyhedral carbaborane units are already known in the literature.[21,22] The cationic *closo*-tricarbaboranes, endohedral carbaboranes and the benzoquinone analogs of polyhedral boranes are the fresh candidates in this category.

Studies on various ways of alleviating the anionic charge in *closo*- polyhedral boranes form the main subject of this thesis. These are supported by comparison of the polyhedral systems with known organic compounds. There are many intriguing structures with hypercoordinate carbon in these studies. Most of the calculations for the thesis work were done at the B3LYP/6-31G* level of theory[33] using Gaussian 94 programme.[34] Wherever possible, attempts are made to understand why the numbers turn out the way they do. The theory underlying the various computational techniques is discussed in the next part of this chapter.

1.2. Computational Chemistry[35,36]

1.2.1. Introduction

The beginning of the 20th century witnessed the birth of quantum mechanics to explain the behaviour of atoms and molecules. Quantum mechanics have transfigured the understanding in many areas including chemical science, molecular biology, material science and computer science. It is particularly helpful in solving many fundamental puzzles of the time such as the nature of bonding, chemical reactivities and mechanisms, spectral, electrical and magnetic properties, all of which are essential to provide new insights to the chemists to achieve their primary task of rationally synthesizing and characterizing new compounds. Though the Schrödinger equation can be easily written down for any problem, obtaining the exact solution of the equation presents with many mathematical difficulties and computational expenses. Many approximations are introduced to make the problem solvable. This, combined with the rapid growth in the development of faster computer chips and more memory and disk space, aided the progress of computational chemistry. Despite these, often accurate results for the complicated systems are not easily obtained; the results depend on choosing an appropriate model to which acceptable approximations can be applied. Over the years theoretical chemistry has evolved into a major area and its importance is widely appreciated by experimentalists as complementary.

The quantum mechanics most commonly used in computational chemistry can be divided into two groups- wave function based methods and density based methods. *Ab initio* and semiempirical methods are wave function based approaches whereas density functional method comes under the latter category.[35,36] *Ab initio* methods refer to quantum

chemical methods in which all the integrals are exactly evaluated in the course of a calculation. The semiempirical methods employ many simplifications by deleting different integrals systematically. Thus, these methods are faster than the *ab initio* method. The error introduced by neglecting the integrals is minimized through the use of experimentally derived parameters and thus strive for accuracy. Both these methods are wave function based approaches. In the density functional method, the ground state electronic energy is determined completely by the electron density. The electron density is the square of the wave function, integrated over N-1 electron coordinates for an N-electron system and depends on three coordinates independently of the number of electrons. Thus, while the complexity of wave function approaches increases with the number of electrons, the electron density approach has the same number of variables irrespective of the system size. Each of these methods is explained in the coming sections.

1.2.2. Ab-Initio Method

To describe the stationary state of a many electron system completely, it is adequate to know the solutions of the time independent Schrödinger's equation.[37]

$$H \Psi_k = E_k \Psi_k \qquad (1.1)$$

H is the total energy operator, termed Hamiltonian operator which includes the operators for both kinetic and potential energy. Ψ_k are the wave functions of states with energies E_ks, which depend on the coordinates of both nuclei and electrons and also on the spin coordinates. There are many approximations to simplify the problem of solving this equation. The **Born-Oppenheimer approximation**[38] assumes that the electronic arrangement of a system depends on the positions of the nuclei rather than its momentum in contrast to electrons where the velocity and position matters, as the nucleus is heavier

than the electron. Thus, Schrodinger equation becomes just the electronic Schrodinger equation.

$$H_{el}\Psi_{el}(r,R) = E_{el}(R)\Psi_{el}(r,R) \qquad (1.2)$$

where,

$$H_{el} = -\frac{1}{2}\sum_{i=1}^{n}\nabla_i^2 - \sum_{\mu=1}^{N}\sum_{i=1}^{n}(Z_\mu/r_{\mu i}) + \sum_{i=1}^{n-1}\sum_{j=i+1}^{n}\frac{1}{r_{ij}} \quad \text{in atomic units} \qquad (1.3)$$

The first term in the Hamiltonian corresponds to the kinetic energy of an electron, the second and third terms represent the energy due to electron-nuclei and electron-electron interactions. Here the Hamiltonian corresponds to the motion of electrons in a field of fixed nuclei in the absence of magnetic field. Each nuclear configuration has its own characteristic energy. This approximation gets support from the spectral studies. The approximation fails when nontrivial coupling of electronic and nuclear motion occurs in cases such as Jahn-Teller effect and Renner effect. Further approximations are required to get reliable information on the electronic structure for large molecules.

It is obvious that the accuracy of each molecular orbital method depends on how the basis function is selected initially. In *ab initio* methods the complete wave function for a single electron is the product of molecular orbital, $\psi(x,y,z)$ and spin function, α or β, named as spin orbital.

Spin orbital, $\Phi_i = \psi(x,y,z)\,\alpha(\xi)$ or $\psi(x,y,z)\,\beta(\xi)$ (1.4)

$\psi(x,y,z)$ itself is usually taken as the linear combination of atomic orbitals of the constituent atoms (**LCAO**).[39] This is one of the simplest assumptions and the basis of most of the quantum chemical calculations performed today.

$$\psi(x,y,z) = \sum_{\mu=1}^{N} C\mu i\,\chi\mu \qquad (1.5)$$

The Schrodinger equation is thus, reduced to

$$\hat{F}\,\Phi_i = \varepsilon_i \Phi_i \tag{1.13}$$

The Fock operator,

$$\hat{F} = -\frac{1}{2}\nabla_i^2 - \sum_{\mu} (Z_\mu / r_{\mu i}) + \sum_{j=1}^{n} (2\hat{J}_j - \hat{K}_j) \tag{1.14}$$

$\hat{J}_j$ and $\hat{K}_j$ are the coulomb operator and the exchange operator respectively.

These equations are generally known as Hartree-Fock equations.

Thus, energy,

$$\varepsilon_i = \langle \Phi_i | \hat{F} | \Phi_i \rangle$$

$$= H_{ii} + \sum_{j=1}^{n} (2J_{ij} - K_{ij}) \tag{1.15}$$

where H_{ii} is the average kinetic energy and the nuclear-electronic attraction energy for the electron in Φ_i

$$H_{ii} = \left\langle \Phi_i(1) \left| -\frac{1}{2}\nabla_1^2 - \sum_{\mu} Z_\mu / r_{\mu 1} \right| \Phi_i(1) \right\rangle \tag{1.16}$$

and the energy of interactions among the electron i and all the electrons is given by the sum of coulomb integral, J_{ij} and exchange integral, K_{ij}.

$$J_{ij} = \left\langle \Phi_i(1)\Phi_j(2) \mid 1/r_{12} \mid \Phi_i(1)\Phi_j(2) \right\rangle \tag{1.17}$$

$$K_{ij} = \left\langle \Phi_i(1)\Phi_j(2) \mid 1/r_{12} \mid \Phi_j(1)\Phi_i(2) \right\rangle \tag{1.18}$$

J_{ij} represents the energy due to the classical repulsion between the electrons and K_{ij} is the exchange energy coming out of the antisymmetric nature of the wave function. Thus, ε_i can be termed as orbital energy or one electron energy. The total electronic energy by Hartree-Fock method will be obtained by summing up these one electron energies. However, the interelectronic interactions are counted twice here and should be subtracted.

Thus,

$$E_{HF} = \sum_{i=1}^{n} [2\varepsilon_i - \sum_{j=1}^{n} (2J_{ij} - K_{ij})] \quad (1.19)$$

From equation (1.15) we have

$$E_{HF} = \sum_{i=1}^{n} [2H_{ii} + \sum_{j=1}^{n} (2J_{ij} - K_{ij})] \quad (1.20)$$

$$\text{or,} \quad E_{HF} = \sum_{i=1}^{n} (\varepsilon_i + H_{ii}) \quad (1.21)$$

The total energy is obtained by adding the internuclear repulsion energy for the nuclei:

$$E_{tot} = E_{HF} + V_{NN}$$

$$V_{NN} = \sum_{\mu=1}^{N-1} \sum_{\nu=\mu+1}^{N} \frac{Z_\mu Z_\nu}{r_{\mu\nu}} \quad (1.22)$$

The definition of Fock operator in the equation (1.14) involves an unknown wave function. Thus the method of solving the equation involves an iterative process starting with arbitrary assumed orbitals. The initial guess set is used to generate the Fock operator, which in turn is used to obtain the new wave function and the process is repeated till the coefficients generated in the consecutive steps differ by less than some cutoff value. Since the resulting molecular orbitals are derived from their own effective potentials, the technique is called self consistent field (SCF) theory.[40]

ii. Basis Sets[36e,g]

We have seen that the *ab initio* method involves solving Schrödinger equation incorporating many approximations, one of them being the introduction of basis set. The initial guess function, called as molecular orbitals is represented as a set of known functions called a basis set. The ease of computation depends on the basis set chosen, it is of prime importance to select a basis set appropriate for the problem at hand.

χ_μ s are called basis functions and $C_{\mu i}$ s are called molecular orbital expansion coefficients. The complete wave function for the molecule is the product of the molecular orbitals of single electron.

$$\Psi_{el} = \Phi_1(1)\Phi_2(2)..... \Phi_n(n) \qquad (1.6)$$

Thus chosen wave function must satisfy certain conditions to be the acceptable solutions. It should be orthogonal and normalized.

$$\int \Phi i \Phi j d\tau = 1 \text{ if } i=j;$$

$$=0 \text{ if } i \neq j \qquad (1.7)$$

In addition, the electrons being fermions, the orthonormalized many electron wave function Ψ should be antisymmetric on exchange of a pair of electrons. The complete wave function, which is the product of one electron spin orbitals, are represented by a determinant called *Slater determinant* to incorporate the antisymmetric property.

$$\Psi_{el} = \begin{vmatrix} \Phi_1(1) & \Phi_2(1) & \Phi_3(1) & \cdots & \Phi_n(1) \\ \Phi_1(2) & \Phi_2(2) & \Phi_3(2) & \cdots & \Phi_n(2) \\ & & \vdots & & \\ \Phi_1(n) & \Phi_2(n) & \Phi_3(n) & \cdots & \Phi_n(n) \end{vmatrix} \qquad (1.8)$$

The definition of Slater determinant so as to incorporate the antisymmetry is according to the Pauli's exclusion principle which states that a molecular orbital cannot occupy two electrons of the same spin. If the wave function of a molecule with an even number of electrons is represented by a single determinant with electrons of paired spins occupying identical molecular orbital, the wave function is said to be of *closed shell*.

Thus for a closed shell,

$$\Psi_{el} = \begin{vmatrix} \Phi_1(1) & \Phi_2(1) & \Phi_3(1) \text{ ------ } & \Phi_{n/2}(1) \\ \Phi_1(2) & \Phi_2(2) & \Phi_3(2) \text{ ------ } & \Phi_{n/2}(2) \\ & & \vdots & \\ \Phi_1(n) & \Phi_2(n) & \Phi_3(n) \text{ ------ } & \Phi_{n/2}(n) \end{vmatrix} \qquad (1.9)$$

The next task is to solve the Schrödinger equation after having defined the Hamiltonian operator and the trial wave function.

i. Hartree-Fock Method[40]

Hartree-Fock method approximates the trial wave function to consist of a single slater determinant. Once the trial wave function is generated, the problem now remains to solve the molecular orbital expansion coefficients. Hartree-Fock method is based on variational principle according to which the energy obtained using an antisymmetric wave function is always greater. Substitution of Ψ from equation (1.5) into the electronic Schrödinger equation (1.2) leads to

$$\sum_{\mu=1}^{N} c_\mu \sum_{\mu=1}^{N} c_\nu S_{\mu\nu} E' = \sum_{\mu=1}^{N} c_\mu \sum_{\mu=1}^{N} c_\nu H_{\mu\nu} \qquad (1.10)$$

where, the overlap integral $S_{\mu\nu} = \int \Phi_\mu \Phi_\nu$ and the resonance integral $H_{\mu\nu} = \int \Phi_\mu \hat{H} \Phi_\nu$.

The best wave function is obtained by minimizing the energy with respect to the orbital coefficient, $C_{\mu i}$.

$$\frac{\partial E}{\partial C_{\mu i}} = 0 \qquad (1.11)$$

This leads to a set of algebraic equations which can be written in a determinant form and is called secular determinant.[41]

$$| H\text{-}ES | = 0 \qquad (1.12)$$

(a) ***Basis functions***:- There are two types of basis functions generally used for the electronic structure calculations, Slater Type Orbitals (STOs) and Gaussian Type Orbitals (GTOs).

Slater Type Orbitals (STOs):- The functional form of the STO is

$$\chi_{\rho,n,l,m}(r,\theta,\varphi) = NY_{l,m}(\theta,\varphi)r^{n-1}e^{-\zeta r} \quad (1.23)$$

Where $Y_{l,m}$ is the spherical harmonic function, and N is the normalization constant. It resembles the hydrogen like orbitals which is obvious from the exponential dependence on the distance between the nucleus and the electron. Though the calculation of multicentre-two electron integrals cannot be done analytically using STO, a fast convergence is achieved owing to the exponential dependence. STOs do not have radial nodes, which are incorporated by taking linear combination of STOs. These types of basis functions are used for atomic and diatomic systems.

Gussian Type Orbitals (GTOs):- The functional form of the GTO is

$$\chi_{\rho,n,l,m}(r,\theta,\varphi) = NY_{l,m}(\theta,\varphi)\, r^{(2n-2-l)}\, e^{-\zeta r2} \text{ (in polar coordinates)} \quad (1.24)$$

$$\chi_{\rho,lx,ly,lz}(x,y,z) = N_x{}^{lx}y^{ly}z^{lz}\, e^{-\zeta r2} \text{ (in cartesian coordinates)} \quad (1.25)$$

where lx, ly and lz are integers, x, y and z are cartesian coordinates and ζ is the orbital exponent. In contrast to STOs, there is r^2 dependence in the exponential for GTO. This leads to a zero slope for the GTO at the nucleus and thus, it fails to represent the region near the nucleus. Similarly at higher r values, the GTO falls off rapidly, thus that part of the wave function is represented poorly. Though the use of GTOs makes the computation easier as the product of two GTOs is another GTO, it does not have a close similarity with atomic orbital wave functions. GTOs are generally used for electronic structure calculations of polyatomic molecules though more number of GTOs are necessary for the

accurate results compared to the STOs. To reduce the large number of variables due to the large number of basis functions, certain coefficients of the basis functions are kept constant relative to another, thus forming groups of Gaussian functions. The former is called primitive Gaussian functions and the latter, contracted Gaussian functions (CGTO).

(b) ***Classification of basis sets***:- Minimal basis set involves basis functions corresponding to all the electrons of the neutral atom. For first row elements in the periodic table, it uses two s-functions (1s and 2s) and one set of p-functions. Similarly for second row elements it employs three s-functions and two sets of p-functions.

A double zeta (DZ) type basis function takes into account double the number of basis functions as used in the minimal basis set. For hydrogen, it employs two basis functions (1s and 1s') which differ in their ζ-value and for first row elements, four s-functions (1s, 1s', 2s and 2s') and two sets of p-functions (2p and 2p'). The DZ basis set is evolved in order to account for the electron distribution which is different in different directions such as in σ-type and π-type bonds. Since chemical bonding essentially uses valence orbitals, the doubling of functions can be restricted to these orbitals. Such a basis set is referred to as split valence basis set. Similarly triple zeta (TZ) and triple split valence basis sets are also used according to the requirements of the problems.

In order to allow the tails of the atomic orbitals to be varied to account for the different electronic properties of an element in different molecular environments one extra basis function is needed which permits the electron cloud to be polarised off-centre from the nucleus. These basis functions are called polarization functions. Thus, a polarised basis function allows the variation of shape of the orbitals. It adds d-functions to carbon atoms and f-functions to d-block elements. A diffused basis set allows orbitals to occupy

large region of space. Such basis sets are required for systems where the electrons are comparatively far from the nucleus such as molecules with lone pairs, anions, and molecules in their excited states.

The basis set used in the thesis work is mainly 6-31G* which uses six primitive Gaussians for core orbitals and a split-valence pair of three and one primitives for valence orbitals, and adds a single set of polarization function to the split valence basis set.

iii. Electron Correlation

We have found that the Hartree-Fock wave functions are adequate to describe the ground state of most of the molecules. However the best single determinant wave functions may not always have the full symmetry of the exact wave function. Moreover they are inefficient in dealing with correlation between electrons with opposite spins. These drawbacks are reflected in the qualitative deficiency in the explanations such as the symmetry of degenerate orbitals in some molecules and the bond dissociation energies of molecules. The main methods for calculating the electron correlation are explained below.

(a) ***Configuration Interaction***[42]

The method of Configuration Interaction (CI) is the most common technique employed to improve the wave functions and energy beyond Hartree-Fock level.[42] The wave function used in this method is a linear combination of a set of Slater determinants built from a set of orthonormal, linearly independent basis functions.

$$\Psi = \sum_i c_i \Psi_i \qquad (1.26)$$

where Ψ_i s are called Configuration State Functions (CSFs) which are Slater determinants containing products of spin orbitals with Ψ_0 being the Hartree-Fock wave function.

$$\Psi_0 = (n!)^{-1/2} \mid \Phi_1 \Phi_2 ..... \Phi_n \mid \qquad (1.27)$$

The Φ_i s are subsets of the total set which have been determined in the variational procedure. The remaining unused spin orbitals correspond to unoccupied or virtual spin orbitals. Ψ_i s with i>0 are generally classified into single substitution function where one occupied orbital is replaced by a virtual orbital, double substitution function where two of the occupied orbital are being replaced by virtual orbitals and so forth. In the full CI method, the trial wave function,

$$\Psi = c_0\Psi_0 + \sum_{i>0} c_i\Psi_i \qquad (1.28)$$

where the summation is over all the substituted determinants starting from single substitution till n-substitution in which all occupied spin orbitals are replaced by the virtual orbitals. Thus, a full CI provides an exact solution of the Schrodinger equation within a particular basis set. The difference between the E_{HF} and the full CI energy is the correlation energy within the particular basis set. Though this method is well-defined it is not practical except for very small systems because of the very large number of substituted determinants. Thus, normally the length of the CI expansion is limited by truncating at a given level of substitution. Configuration interaction singles (CIS), Configuration interaction doubles (CID) and Configuration interaction singles doubles (CISD) are generally used models. The major drawback of this method is that it suffers from an incorrect dependence on the number of particles, lack of size-consistency, though at each level it gives an upper bound to the exact energy.

(b) ***Moller-Plesset Perturbation Theory (MPPT)***[43]

An alternative procedure for finding the correlation energy is perturbation theory. To start with, consider a system with known Hamiltonian, eigen values and eigen functions.

$$H_o\Psi_i = E_i\Psi_i \tag{1.29}$$

where Ψi form a complete set. The changes ensue on these upon a small variation or perturbation in the Hamiltonian (H) is then calculated.

$$H = H_0 + \lambda H' \tag{1.30}$$

$\lambda H'$ is the perturbation where λ is a dimensionless parameter. When $\lambda = 0$; $H = H_0$. H_0 is taken as the sum of one electron Fock operators by Moller-Plesset theory.

By Rayleigh-Schrödinger Perturbation Theory we have,

$$\Psi_\lambda = \Psi^{(0)} + \lambda\Psi^{(1)} + \lambda^2\Psi^{(2)} + ... \tag{1.31}$$

$$E_\lambda = E^{(0)} + \lambda E^{(1)} + \lambda^2 E^{(2)} + ... \tag{1.32}$$

Substituting (1.30), (1.31), and (1.32) in the Schrodinger equation, we obtain

$$(H_0 + \lambda H')(\Psi^{(0)} + \lambda\Psi^{(1)} + \lambda^2\Psi^{(2)} + ...) =$$

$$(E^{(0)} + \lambda E^{(1)} + \lambda^2 E^{(2)} + ...)(\Psi^{(0)} + \lambda\Psi^{(1)} + \lambda^2\Psi^{(2)} + ...) \tag{1.33}$$

Collecting terms having similar power, we get equations

$$H_0\Psi^{(0)} = E^{(0)}\Psi^{(0)} \tag{1.34}$$

$$(H' - E^{(1)})\Psi^{(0)} + (H_0 - E^{(0)})\Psi^{(1)} = 0 \tag{1.35}$$

Solving this equation we get first order correction to the energy ($E^{(1)}$)and wave function ($\Psi^{(1)}$).

$$E^{(1)} = \langle\Psi^{(0)} | H' | \Psi^{(0)}\rangle \tag{1.36}$$

$$\Psi^{(1)} = \sum_{j\neq i} \frac{\langle\Psi_j | H' | \Psi_i\rangle}{E_i - E_j}\Psi_j \tag{1.37}$$

When the series (1.31) and (1.32) are truncated after second order, third order etc such methods are referred to as MP2, MP3 and so forth. The perturbation theory results

terminated at any order are not variational as they are not derived as expectation values of the Hamiltonian.

1.2.3. Semi empirical Methods[36]

Semi empirical methods make use of available experimental data as parameters in place of integrals to be evaluated. The simplest among these methods, the Hückel Molecular Orbital Theory (HMOT), introduced in 1931, uses an undefined one electron energy operator and a fundamental basis set of valence shell electrons.[44] The ground state energy is obtained by assigning 'n' electrons to the 'n' lowest lying energy levels and summing up the energies of the occupied orbitals. It works well with planar, conjugated, alternant hydrocarbons, but fails in systems where there is formal charge on atoms. This method was improved by Roothaan who introduced a π-approximation using LCAO approximation within Hartree-Fock model. Though the model takes care of only π-electrons, Parriser, Parr and Pople method (PPP) became popular as it explicitly introduced the electron interaction into the Hamiltonian by adding an additional 2-electron operator. Extended Hückel theory developed in 1963 by Hoffmann uses the empirical one electron Hamiltonian defined by the matrix elements in the atomic valence shell basis.[45] Here all overlap integrals are evaluated using slater orbitals. Off-diagonal elements are approximated from ionization potentials of atoms.

CNDO, INDO, and NDDO are some of the semiempirical methods brought forth by Pople and coworkers (1965). These methods retain all the important features of the Hartree-Fock-Roothan equation and use some empirical parameters and assumptions which simplify the Hamiltonian. One of the primary difficulties encountered in the *ab initio* methods is in solving the electron repulsion integrals. The semi empirical methods

neglect electron repulsion integrals of different kinds depending on the particular method. **Zero differential overlap approximation**[46] is the beginning of a family of such approximations.

According to ZDOA,

$$<\Phi_\mu\Phi_\lambda\frac{1}{r_{12}}\Phi_\nu\Phi_\sigma> = <\Phi_\mu\Phi_\lambda\frac{1}{r_{12}}\Phi_\lambda\Phi_\mu> \delta_{\mu\nu}\,\delta_{\lambda\sigma}$$

and corresponding overlap integrals $S_{\mu\nu} = \int\Phi_\mu(1)\,\Phi_\nu(1)d\tau_i$

are neglected. The core integrals $H_{\mu\nu} = \int\Phi_\mu(1)\,H^{\,core}\,\Phi_\nu(1)d\tau_i$

are incorporated in order to account for the possible bonding effect of the overlap. Various semi empirical methods are named based on the extent to which this zero differential overlap approximation is involved in the evaluation of electron repulsion integrals.

In Complete Neglect of Differential Overlap (CNDO), the zero differential overlap approximation is used for all products of different atomic orbitals along with another approximation that the remaining two electron integrals depend on the nature of the atoms to which those orbitals belong. Thus this method introduces electron-electron repulsion in a moderate manner. The different interactions between the two electrons on the same atom are not considered, and thus, it fails to explain different states arising from the same configuration. The PPP method mentioned earlier can be considered as a CNDO approximation involving only valence p-orbitals. Intermediate Neglect of Differential Overlap (INDO) retains the monatomic differential overlap, but only in one centre integrals. Another method, Neglect of Diatomic Differential Overlap (NDDO) retains the dipole-dipole interactions as well. It neglects differential overlap only for the atomic orbitals on different atoms. There are many improved versions of these methods such as MNDO,[47] AM1,[48] PM3[49] etc which are being widely used today.

1.2.4. Density functional theory[50]

The computations based on density functional theory (DFT) achieved more popularity over the years as it gives more information regarding the properties of the system at a lower cost than the traditional *ab initio* wave function techniques. Starting from the free electron theory in 1920s one could go through the emergence of DFT through Slater's Xα model and Hohenberg-Kohn theorem in the 1960s. The first Hohenberg-Kohn (HK) theorem states that the electron density ρ(r) determines the external potential υ(r) and the total number of electrons, N.

$$\int \rho(r)dr = N \tag{1.38}$$

N and υ(r) defines the molecular Hamiltonian, consequently, energy is also a function of υ and ρ.

$$E = E_{\upsilon}(\rho) \tag{1.39}$$

Thus, the electron density ρ(r) determines all the properties of the system considered.

The second HK theorem arrived at the energy of the system as

$$E_{\upsilon}(\rho) = \int \rho(r)\upsilon(r)dr + F_{HK}(\rho) \tag{1.40}$$

$$F_{HK}(\rho) = T(\rho) + Vee(\rho) \tag{1.41}$$

where $F_{HK}(\rho)$ is the Hohenberg-Kohn functional containing the electronic kinetic energy functional T(ρ) and the electron-electron interaction functional Vee(ρ), which are not known. Later Kohn and Sham in their studies introduced orbitals such that the kinetic energy could be computed accurately. According to their model, the Hamiltonian of an N-electron non interacting refernce system is defined as

$$H_{ref} = \sum_{i}^{N} \frac{1}{2}\nabla_i^2 + \sum_{i}^{N} \nu_i(r) = \sum_{i} h_{ref,i} \tag{1.42}$$

Here electron-electron interactions are excluded. All physically acceptable densities of the non-interacting system can be written as

$$\rho_s = \sum_i^N |\Psi_i|^2 \tag{1.43}$$

where Ψ_i is eigen function of the one-electron operator, orbitals.

The Hohenberg-Kohn functional, F_{HK} can thus be written as

$$F_{HK}(\rho) = T_s(\rho) + J(\rho) + E_{xc}(\rho) \tag{1.44}$$

where T_s represents the kinetic energy functional,

$$Ts(\rho) = \sum_i^N <\Psi_i | -\frac{1}{2}\nabla_i^2 | \Psi_i > \tag{1.45}$$

$J(\rho)$ represents the classical coulombic interaction energy,

$$J(\rho) = \frac{1}{2} \iint \frac{\rho(r)\rho(r')}{r-r'} dr dr' \tag{1.46}$$

and $E_{xc}(\rho)$ is the exchange-coorelation term and represents the remaining part of the electron-electron interaction energy. This energy comes from the exchange energy due to the antisymmetric nature of the wave function and the correlation energy due to the motion of the individual electrons. These energy functionals can be of two types, local functional and gradient functionals; the former depend entirely on the electron density and the latter depend both on electron density and its gradient. There are many forms of these functionals, the most popular being Becke-Perdew (BP), Vosko-Wilk-Nussair (VWN) and Lee-Yang-Parr's functionals (LYP).

The computations carried out for the work embedded in the thesis is done at B3LYP level which is a hybrid functional and includes Hartree-Fock and DFT exchange and DFT correlation.

References

1. (a) Stock, A.; Nassenez, C. *Chem. Ber.* **1912**, *45*, 3529. (b) Stock, A. *Hydrides of Boron and Silicon*, Cornell University Press, Ithaca, New York, **1933**.
2. Longuet-Higgins, H. C. *J. Chim. Phys.* **1949**, *46*, 268.
3. (a) Eberhardt, W. H.; Crawford Jr., B. L.; Lipscomb, W. N. *J. Chem. Phys.* **1954**, *22*, 989. (b) Dickerson, R. E.; Lipscomb, W. N. *J. Chem. Phys.* **1957**, *27*, 212. (c) Lipscomb, W. N. *Boron Hydrides*, Benjamin, New York, **1963**. (d) Muetterties, E. L. *Boron Hydride Chemistry*, Academic Press, New York, **1975**.
4. (a) Wade, K. *Chem. Commun.*, **1971**. 792. (b) Wade, K. *Adv. Inorg. Chem. Radiochem.*, **1976**, *18*, 1.
5. (a) Mingos, D. M. P. *Acc. Chem. Res.*, **1984**, *17*. 311. (b) Mingos, D. M. P. *J. Chem. Soc. Chem. Commun.*, **1983**, 706.
6. (a) Lipscomb, W. N. *J. Less- Common Met.* **1981**. *82*, 1. (b) Dixon, D. A.; Klier, D. A.; Hallgreen, T. A.; Hall, J. H.; Lipscomb, W. N. *J. Am. Chem. Soc.* **1977**, *99*, 6226.
7. Hawthorne, M. F. *Angew. Chem. Int Ed Engl* **1993**. *32*, 950.
8. (c) Hawthorne, M. F.: Zheng, Z. *Acc. Chem. Res.* 1997, *30*, 267.
9. (a) Jemmis, E. D.; Balakrishnarajan, M. M.; Pancharatna, P. D. *J. Am. Chem. Soc.* **2001**, *123*, 4313. (b) Jemmis, E. D.; Balakrishnarajan, M. M.; Pancharatna, P. D. *Chem. Rev.* **2002**, *102*, 93.
10. (a) Jutzi, P.; Seufert, A. Angew. Chem. Int. Ed.Engl. 1977, 16, 330. (b) Dobmeier, C.; Köppe, R.; Robl, C.; Schnöckel, H. *J. Organomet. Chem.* **1995**, *487*, 127.

11. (a) *The Borane, Carborane, Carbocation Continuum*, Casanova, J. Ed., John Wiley, New York, **1998**. (b) Vondrak, T.; Hermanek, S.; Plesek, J. *Polyhedron* **1993**, *12*, 1301. (c) Muller, J.; Runsink, J.; Paetzold, P. *Angew. chem. Int Ed Engl* **1991**, *30*, 175. (d) Hynk, D.; Buhl, M.; Schleyer, P. v. R.; Volden, H. V.; Gundersen, S.; Muller, J.; Paetzold, P. *Inorg. Chem.* **1993**, *32*, 2442. (e) Little, J. C.; Moran, J. T.; Todd, L. J. *J. Am. Chem. Soc.* **1967**, *89*, 5495. (f) Getman, T. D.; Deng, H-B.; Hsu, L-Y.; Shore, S. G. *Inorg. Chem.* **1989**, *28*, 3612. (f) Hynk, D.; Vajda, E.; Buhl, M.; Schleyer, P. v. R. *Inorg. Chem.* **1992**, *31*, 2464. (g) Pretzer, W. R.; Rudolph, R. W. *J. Am. Chem. Soc.* **1973**, *95*, 931.

12. (a) Blanch, R. J.; Li, J.; Bush, L. C.; Jones, M., Jr. *J. Am. Chem. Soc.* **1992**, *114*, 9236. (b) Blanch, R. J.; Bush, L. C.; Jones, M. Jr. *Inorg. Chem.* **1994**, *33*, 198. (c) Cunningham, R. J.; Bian, N.; Jones, M. Jr. *Inorg. Chem.* **1994**, *33*, 4811. (d) Ho, D. M.; Cunningham, R. J.; Brewer, J. A.; Bian, N.; Jones, M. Jr. *Inorg. Chem.* **1995**, *34*, 5274. (e) Zharov, I.; Saxena, A.; Michl, J.; Miller, R. D. *Inorg. Chem.* **1997**, *36*, 6033.

13. *Advances in Boron Chemistry*, Siebert, W. Ed., University of Heidelberg, Germany, **1997**.

14. (a) Miller, H. C.; Muetterties, E. L. *J. Am. Chem. Soc.* **1963**, *85*, 3506. (b) Dobrott, D. R.; Friedman, L. B.; Lipscomb, W. N. *J. Chem. Phys.* **1964**, *40*, 866. (c) Miller, N. E.; Forstener, J. A.; Muetterties, E. L. *Inorg. Chem.* **1964**, *3*, 1690.

15. (a) Enemark, J. H.; Friedman, H.; Lipscomb, W. N. *Inorg. Chem.* **1966**, *5*, 2165. (b) Jelinek, T.; Kennedy, J. D.; Stibr, B. *J. Chem. Soc. Chem. Commun.* **1994**, 1415.

16. (a) Hoard, J. L.; Sullenger, D. B.; Kennard, C. H. L.; Hughes, R. E. *J. Solid State Chem.* **1970**, *1*, 268. (b) Slack, G. A.; Hejna, C. I.; Garbauskar, M. F.; Kasper, J. S. *J. Solid State Chem.* **1988**, *76*, 52. (c) Slack, G. A.; Hejna, C. I.; Garbauskar, M. F.; Kasper, J. S. *J. Solid State Chem.* **1988**. *76*, 64.

17. (a) Pitochelli, A. R.; Hawthorne, M. F. *J. Am. Chem. Soc.* **1962**, *84*, 3218. (b) Hosmane, N. S.; Franken, A.; Zhang, G.; Srivastava, R. R.; Smith, R. Y.; Spielvogel, F. *Main group met. Chem.* **1988**, *21*,319.

18. Kester, J. G.; Keller, D.; Huffmann, J. C.; Benefiel, M. A.; Geiger, W. E.; Atwood, C.; Siedle, A. R.; Korba, G. A.; Todd, L. J. *Inorg. Chem*. **1994**, *33*, 5438.

19. (a) Siriwardane, U.; Islam, M. S.; West, T. A.; Hosmane, N. S.; Maguire, J. A.; Cowley, A. H. *J. Am. Chem. Soc*. **1987**, *109*, 4600. (b) Hosmane, N. S.; Meester, P.; de Siriwardane, U.; Islam, M. S.; Chu, S. S. C. *J. Chem. Soc., Chem. Commun.* **1986**, 1421. (c) Schubert, D. M.; Rees, W. S. Jr.; Knobler, C. B.; Hawthorne, M. F. *Organometallics*. **1990**, *9*, 2938.(d) Schubert. D. M.; Bandman, M. A.; Rees, W. S. Jr.; Knobler, C. B.; Lu, P.; Nam, W.; Hawthorne, M. F. *Organometallics*. **1990**, *9*, 2046.

20. Jemmis, E. D.; Balakrishnarajan, M. M. *J. Am. Chem. Soc*., **2000**, *122*, 7392.

21. (a) Gimarc, B. M. *J. Am. Chem. Soc*. **1983**, *105*, 1979. (b) Ott, J. J.; Gimarc, B. M. *J. Am. Chem. Soc.* **1986**, *108*, 4303. (c) Gimarc, B. M.; Ott, J. J. *J. Am. Chem. Soc.* **1986**, *108*, 4298.

22. (a) Williams, R. E. *Adv. Inorg. Radiochem*. **1976**, *18*, 67. (b) Williams, R. E.; Gerhart, F. J. *J. Am. Chem. Soc.* **1965**, *87*, 3513. (c) Williams, R. E. *Carboranes, in Progress in Boron Chemistry*, Vol.2, Brotherton, R. J.; Steinberg, H. Eds., Pergamon, Oxford, **1970**.

23. Jemmis, E. D. *J. Am. Chem. Soc.* **1982**, *104*, 7017.

24. (a) Olah, G. A.; Westerman, P. W.; Mo, Y. K.; Klopman, G. *J. Am. Chem. Soc.* **1972**, *94*, 7859. (b) Rasul, G. A.; Olah, G. A. *Inorg. Chem.* **1997**, *36*, 1278. (c) DePuy, C. H.; Gareyev, R.; Hankin, J.; Davico, G. E.; Damrauer, R. *J. Am. Chem. Soc.* **1997**, *119*, 427. (d) Olah, G. A.; Rasul, G. *J. Am. Chem. Soc.* **1996**, *118*, 8503.

25. Williams, R. E. *Inorg. Chem.* **1971**, *10*, 210.

26. Olah, G. A. *My search for Carbocations and their role in Chemistry*, Nobel Lectures, Chemistry 1991-1995, World Scientific Publishing Co. Singapore.

27. Jemmis, E. D.; Schleyer, P. v. R. *J. Am. Chem. Soc.* **1982**, *104*, 4781.

28. (a) van't Hoff, J. H. *Arch. Neerl. Sci. Exactes Nat.* **1874**, 445. (b) LeBel, J. A. *Bull. Soc. Chim. Fr.* **1874**, *22*, 337.

29. Hoffmann, R.; Alder, R. W.; Wilcox, Jr., C. F. *J. Am. Chem. Soc.* **1970**, *92*, 4992. (b) Hoffmann, R. *Pure Appl. Chem.* **1971**, *28*, 181.

30. (a) Röttger, D.; Erker, G. *Angew. Chem., Int. Ed. Engl.* **1997**, *36*, 812. (b) Siebert, W.; Gunale, A. *Chem. Soc. Rev.* **1999**, *28*, 367.

31. (a) Hogeveen, H.; Kwant, P. W. *J. Am. Chem. Soc.*. **1974**, *96*, 2208. (b) Hogeveen, H.; Kwant, P. W. *Acc. Chem. Res.* **1975**, *8*, 413.

32. (a) Hota, N. K.; Matteson, D. S. *J. Am. Chem.. Soc.* **1968**, *90*, 3571 (b) Hota, N. K.; Matteson, D. S. *J. Am. Chem. Soc.* **1971**, *93*, 2893. (c) Wu, S.; Jones, Jr., M. *Inorg. Chem.* **1988**, *27*, 2005 (d) Bradley, A. Z.; Link, A. J.; Biswas, K.; Kahne, D.; Schwartz, J.; Jones, Jr., M.; Zhu, Z.; Platz, M. S. *Tetrahedron Lett.* **2000**, *41*, 8691 (e) Bradley, A. Z.; Cohen, A. D.; Jones, A. C.; Ho, D. M. Jones, Jr., M. *Tetrahedron Lett.* **2000**, *41*, 8695.

33. (a) Becke, A. D. *J. Chem. Phys.* **1993**, *98*, 5648. (b) Lee, C.; Yang, W.; Parr, R. G. *Phys. Rev. B.* **1988**, *37*, 785. (c) Vosko, S.H.; Wilk, L.; Nusair, M. *Can. J. Phys.* **1980**, *58*, 1200. (d) Stephens, P. J.; Delvin, F. J.; Chabalowski, C. F.; Frisch, M. J. *J. Phys. Chem.* **1994**, *98*, 11623.

34. Frisch, M. J.; Trucks, G. W.; Schelegel, H. B.; Gill, P. M. W.; Johnson B. G.; Robb, M. A.; Cheeseman, J. R.; Keith, T.; Peterson, G. A.; Montgomery, J. A.; Raghavachari, K; Al-Laham, M. A.; Zakrzewski, V. G.; Ortiz, J. V.; Foresman, J. B.; Cioslowsky, J.; Stefenov, B. B.; Nanayakkara, A.; Challacombe, M.; Peng, C. Y.; Ayala, P. Y.; Chen, W.; Wong, M. W.; Andres, J. L.; Replogle, E. S.; Gomberts, R.; Martin, R. L.; Fox, D. J.; Binkley, J. S.; Defrees, D. J.; Baker, J.; Stewart, J. P.; Head-Gordon, M.; Gonzalez, C.; Pople, J. A. *Gaussian 94*, Revision D.1, Gaussian Inc., Pittsburg PA, **1995**.

35. (a) Levine, I. N. *Quantum Chemistry*, 2nd Edition Allyn and Bacon, Boston. (b) McQuarrie, D. A. *Quantum Chemistry*, Oxford University Press, California, **1983**. (c) Pilar, F. L. *Elementary Quantum Chemistry*. Mc-Graw Hill Publishing Co., NewYork, **1968**. (d) Chandra, A. C. *Introductory Quantum Chemistry*, Tata Mc-Graw Hill Publishing Co., New Delhi, **1988**. (e) Szabo, A.; Ostlund, N. S. *Modern Quantum Chemistry*, Mc-Graw Hill Publishing Co., NewYork, **1982**.

36. (a) Hehre, W. J.; Radom, L.; Schleyer, P. v. R.; Pople, J. A. *Ab-initio Molecular Orbital Theory*, John Wiley & Sons, Inc., New York, **1986**. (b) Pople, J. A.; Beveridge, D. L. *Approximate Molecular Orbital Theory*, Mc-Graw Hill Publishing Co., NewYork, **1970**. (c) Lowe, J. P. *Quantum Chemistry*, Academic Press, New York, **1978**. (d) Schaeffer III, H. F. *Electronic Structure of Atoms and Molecules*,

Addison-Wesley, Massachusetts, USA, **1972**. (e) Foresman, J. B.; Frisch, A. *Exploring Chemistry with Electronic Structure Methods,* Gaussian Inc. Pittsburgh, USA. (f) Richards, W. G.; Cooper, D. L. *Ab initio Molecular Orbital Calculations for Chemists*, Clarendon Press, Oxford, **1983**. (g) Jensen, F. *Introduction to Computational Chemistry*, John Wiley & Sons, New York, **1999**.

37. Schrödinger, E. *Ann. Physik.* **1926**, *79*, 361.

38. Born, M.; Oppenheimer, J. R. *Ann. Physik.* **1927**, *84*, 457.

39. Ritz, W. *J. Reine. Angew. Math.* **1908**, *135*, 1.

40. (a) Hartree, D. R. *Proc. Cambridge. Phil. Soc.* **1928**, *24*, 89. (b) Fock, V. *Z. Phys.* **1930**, *61*, 126.

41. (a) Roothaan, C. C. J. *Rev. Mol. Phys.* **1951**, *23*, 69. (b) Hall, G. G. *Proc. Roy. Soc.***1951**, *A205*, 541. (c) Roothaan, C. C. J. *Rev. Mol. Phys.* **1960**, *32*, 179.

42. (a) Hurley, A. C. *Electron Correlation in Small Molecules* Academic Press, London, **1977**. (b) Wilson, S. *Electron Correlation in Molecules* Clarendon Press, Oxford, **1984**. (c) Raghavachari, K.; Anderson, J. B. *J. Phys. Chem.* **1996**. *100*, 12960.

43. Møller, C.; Plesset, M. S. *Phys. Rev.* **1934**, *46*, 618.

44. Hückel, E. *Z. Phys.* **1931**, *70*, 204.

45. (a) Hoffmann, R.; Lipscomb, W. N. *J. Chem. Phys.* **1962**, *36*, 2179. (b) Hoffmann, R. *J. Chem. Phys.* **1963**, *39*, 1397. (c) Hoffmann, R. *J. Chem. Phys.* **1964**, *40*, 2474. (d) Hoffmann, R. *J. Chem. Phys.* **1964**, *40*, 2480. (e) Hoffmann, R. *J. Chem. Phys.* **1964**, *40*, 2745. (f) Hoffmann, R. *Angew. Chem. Int. Ed. Engl.* **1982**, *21*, 711.

46. (a) Sadley, J. *Semi-empirical Methods of Quantum Chemistry* Wiley, **1985**. (b) Zerner, M. C. *Rev. Comput. Chem.* 1991, 2, 313.

47. Dewar, M. J. S.; Thiel, W. *J. Am. Chem. Soc.* **1977**, *99*, 4899.

48. Dewar, M. J. S.; Zoebisch, E. G.; Healy. E. F.; Stewart, J. J. P. *J. Am. Chem. Soc.* **1985**, *107*, 3902.

49. Stewart, J. J. P. *J. Comput. Chem.* **1989**, *10*, 209.

50. (a) Parr, R. G.; Yang, W. *Density Functional Theory of Atoms and Molecules,* Oxford University Press, Oxford, **1989**. (b) Dreisler, R. M.; Gross, E. K. V. *Density Functional Theory: An Approach to the Quantum Many-body Problem*, Springer-Verlag, Berlin, **1990**. (c) Hohenberg, P. C.; Kohn, W.; Sham, L. J. *Advances in Quantum Chemistry*, vol. 21, Academic Press, **1990**. (d) Kohn, W.; Becke, A. D.; Parr, R. G. *J. Phys. Chem.* **1996**, *100*, 12974. (e) Hohenberg. P. C.; Kohn, W. *Phy Rev.* **1964**, *136*, B864. (f) Kohn, W.; Sham, L. *J. Phys. Rev.* **1965**, *A140*. (g) Geerlings, P.; De Proft, F.; Langenaeker. W. *Chem. Rev.* **2003**, *103*, 1793.

CHAPTER 2

Cationic *Closo*-tricarbaboranes- Stability and Synthetic Designs

2.0. Abstract

Stability of polyhedral borane structures with positive charge is challenging as the electron deficiency of polyhedral boranes is well-known. One of the ways in which the cationic charge can be achieved is by the replacement of three BH^- by three CH groups in the dianionic *closo*-B_nH_n clusters. Computational studies at the B3LYP/6-31G* level showed that all the isomers of cationic *closo*-tricarba isomers are relatively stable; experimental studies must be worthwhile. All the isomers retain the *closo*-framework with B-B, B-C and C-C bond lengths falling within the range observed for the known carbaboranes. The possibility of a rearrangement similar to the benzyl cation - tropylium ion equilibrium in polyhedral borane chemistry renders a method for their exploration. The rearrangements are found to have favorable energy barriers with one transition state. The geometry of the dicarboranyl methyl cations, benzyl cation analogs, with bent CH_2 group favors the rearrangement into the next larger polyhedra. A similar study for the formation of monocarbaboranes shows that this method can be adopted for all the carbaboranes. The structure and stability of cationic *closo*-tricarbaboranes are explained in the first section. The synthetic strategy towards their realization assisted by a comparative study with organic counterparts is explained in the second section of this chapter.

2.1. Theoretical Investigation on the structure and stability of cationic *closo*-tricarbaboranes, $C_3B_{n-3}H_n^+$ (n=5,6,7,10,12)

2.1.1. Introduction

The chemistry of carbaboranes has grown into a wide field of its own in the last few decades with many novel applications. Mono- and dicarba derivatives have been well documented and characterized both as *closo*, *nido*, and *arachno* arrangements .[1,2] Only the *nido* and *arachno* variants are known among the tri or multicarbaboranes.[3] The reaction of alkynes with a variety of polyboranes provides a route to access the carbon excess carbaboranes.[1,4] These compounds have attracted interest due to their diverse structural patterns, which are at the borderline between classical and nonclassical structures even in the context of polyhedral boranes.[1] C*loso* carbaboranes with more than two carbon atoms are not found in literature. A *closo* structure, $C_3B_5H_7$ with a bare boron atom was reported[5] but later proved to bc an incorrect interpretation of the stable *closo*-$C_2B_5H_7$.[6] Obviously *closo* structures with three carbon atoms, $C_3B_{n-3}H_n$, require a positive charge to satisfy the skeletal electron count. This charge requirement and the anticipated reactivity must have been the factors which discouraged their exploration.

The systems that were chosen for theoretical analysis range from 5-vertex to 7-vertex in simple polyhedra. The 10 and 12-vertex systems were selected as models in the stacked polyhedral systems which are also monopolyhedra consist of stacks of rings. The electronic structure and relative energies of the isomers of tricarbaboranes involving trigonal bipyramid(**1**, $C_3B_2H_5^+$), octahedron (**2**,$C_3B_3H_6^+$), pentagonal bipyramid (**3**, $C_3B_4H_7^+$). bicapped square antiprism (**4**,$C_3B_7H_{10}^+$) and icosahedron (**5**, $C_3B_9H_{12}^+$) are studied and discussed in detail.

2.1.2. The rules that govern the stability of heteroborane isomers

In view of the large number of isomers calculated for each of the molecular formula, a brief description of the common rules used in explaining the relative stabilities of *closo*-carbaboranes is indispensable. The common rules, which govern the stability of isoelectronic hetero borane isomers are, 1) William's rule[7,8] 2)Gimarc's topological charge rule[9] 3) Jemmis ring-cap orbital overlap criteria.[10] According to William's rule carbon prefers to be at lower connectivity site and they will take nonadjacent position so as to minimize the repulsive forces. This empirical rule has been successfully used in dicarbaboranes. However it fails in silaboranes.[11] For example, 1,2-$Si_2B_4H_6$ is more favored than the 1,6-isomer contrary to the Williams rule. Gimarc's topological charge rule predicts the location of heteroatoms based on the perturbations caused on the homogeneous systems by a foreign atom. The charge created by this perturbation at various locations in the molecule decides the next preferable position for another incoming atom. This works well for carbaboranes but again is known to fail.[11] The ring-cap orbital overlap criteria is applied through a fragment orbital approach. According to this, a polyhedron can be divided into rings and caps. The orbitals of suitable symmetry on the ring and cap will overlap to its maximum if the diffuseness of the cap orbitals and ring size match perfectly. The maximum ring-cap orbital overlap leads to the most stable isomer. There is a poor overlap between the orbitals of ring and cap in $B_5H_5^{-2}$ (D_{3h}). The longer than usual B-B distance of the 3-membered ring helps to some extent. The 5-membered ring in $B_7H_7^{-2}$ (D_{5h}) presents the reverse problem of larger ring size than ideal for BH caps. The octahedral $B_6H_6^{-2}$ provides an intermediate situation where the B_4H_4 ring is reasonably compatible with BH group in overlap.[12b] An increase in the ring size as in hexagonal

bipyramid has an adverse effect on the perfect ring-cap orbital overlap. For example, $B_8H_8^{2-}$ prefers D_{2d} geometry over the D_{6h}.[13] Another contributory factor to the relative energies is the number of different types of bonds. It is well known that B-C is a stronger bond than C-C, which, in turn, is stronger than B-B (bond energy of B-C, C- C and B-B is 89.0, 82.6 and 70±5 kcal/mol respectively).[14] Thus isomers with more number of inherently stronger B-C bonds will be the thermodynamically more stable isomer. In addition the C-C and B-C bonds, being shorter than B-B bonds reduce the size of a ring.

2.1.3. Geometries and relative stabilities of the isomers

i. 5-vertex clusters: Nonclassical vs. classical nature of bonding in the five vertex $B_5H_5^{-2}$ and $C_2B_3H_5$ have been debated in literature.[15,11b,16] Three isomeric forms of cationic *closo*-tricarbaborane, $C_3B_2H_5^+$ are shown in Figure 2.1.

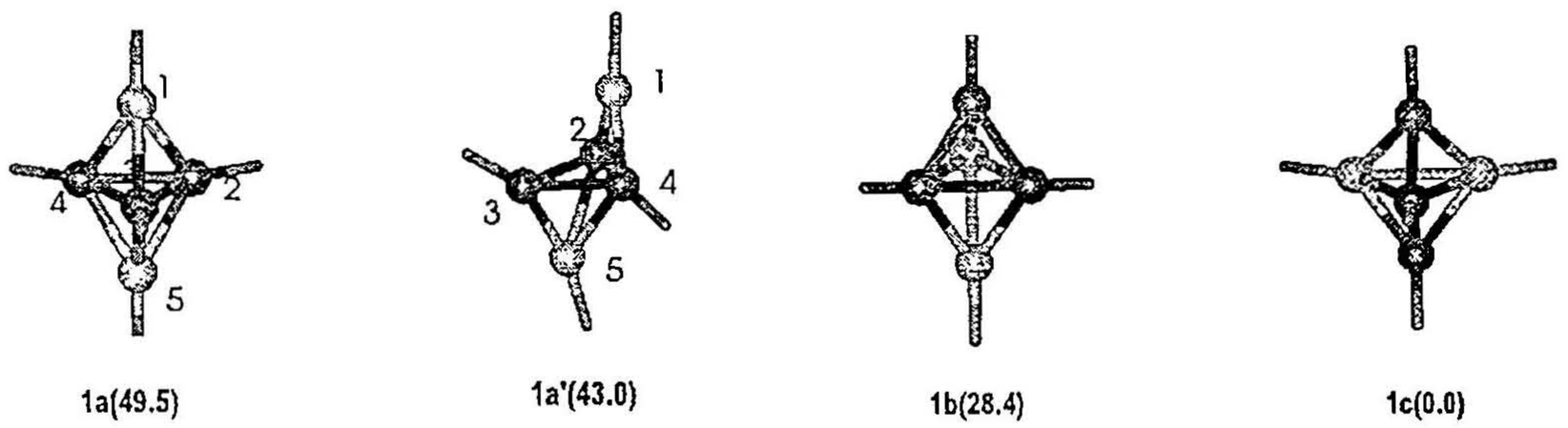

Figure 2.1. Optimized geometries of $C_3B_2H_5^+$ isomers. The relative energies (kcal/mol) are given in parenthesis. The isomer **1a** is a transition state with one imaginary vibrational frequency.

The relative energies have been collected in Table 2.1. The stability order is **1c>1b>1a′**. The D_{3h} structure **1a** is not a minimum on the potential energy surface (PES), while the less symmetric **1c** (C_{2v}) is the most stable form. The relative energy values of these isomers fall in line with the idea of maximum orbital overlap, according to which, a three membered ring prefers a CH group rather than BH as cap so as to allow for maximum overlap of the corresponding orbital. In **1c** the two -CH groups with less diffused orbitals

are at cap positions thus ensuring optimum ring-cap orbital overlap. This structure can also be described as a didehydrogenoallyl cation bridged by a B_2H_2 group. Structure **1b** with one -CH group at the cap comes next. The D_{3h} structure, **1a**, which has two -BH caps interacting with the small C_3H_3 ring, is not even a minimum. A less symmetric structure, **1a′** obtained by breaking one C-B bond is calculated to be a minimum, though 43.0 kcal/mol higher in energy than **1c**. The stabilization of **1c** over **1a′** and **1b** can also be understood from the stability order of $C_2B_3H_5$ isomer; i.e., 1,5-$C_2B_3H_5$ is more stable than the 1,2-and 2,3-isomers. The two C-C bonds in **1c** of 1.449Å (WBI=1.187) are shorter than normal C_{sp^3}-C_{sp^3} distance of 1.54 Å whereas C-C bonds in **1a′** stretch to 1.591 Å (WBI=0.757) and 1.622Å (WBI=0.772). The C-C bonds in **1b** are also long in comparison. (1.629Å (WBI=0.652) and 1.517Å (WBI=0.920)).

ii. Six-vertex clusters: $C_3B_3H_6^+$ cluster can assume only two isomeric forms, (**2b**) with two C-C bonds and (**2a**) with three carbon atoms positioned at the vertices of a trigonal face of an octahedron (Figure 2.2). **2a** is less stable than **2b** by a small energy difference (9.62 kcal/mol). The overlap criterion makes CH capping slightly more favorable than BH capping for four membered rings. Thus two CH caps along with more number of B-C bonds in **2b** clearly explain the lower stability of **2a** over **2b**. Another isomeric form of this compound, trigonal prismatic structure involving C3 and B3 rings eclipsing each other on optimization goes to the most stable octahedral arrangement, **2b**.

Table 2.1. Total Energies (Hartrees), unscaled zero point vibration energies (ZPVE, kcal/mol) and relative energies (RE, kcal/mol) of $C_3B_{n-3}H_n^+$(n=5,6,7,12) isomers at HF/6-31G*. (RE include ZPE, numbers in the parentheses are from B3LYP calculations at 6-31G* level.) All the isomers are minima except 1a which has one imaginary vibrational frequency.

Symmetry	Isomer	Total Energy	ZPVE	RE
D_{3h}	1a	-165.466367 (-166.610431)	46.0 (46.0)	61.6 (49.5)
C_1	1a′	-165.482565 (-166.617842)	47.1 (47.1)	52.5 (43.0)
C_s	1b	-165.514565 (-166.647055)	47.9 (47.9)	33.3 (28.4)
C_{2v}	1c	-165.569610 (-166.694365)	49.2 (49.2)	0.0 (0.0)
C_{3v}	2a	-190.840453 (-192.168999)	59.3 (59.6)	9.0 (9.6)
C_{2v}	2b	-190.854973 (-192.184250)	59.4 (59.4)	0.0 (0.0)
C2v	3a	-216.040945 (217.580399)	67.5 (63.7)	83.0 (69.5)
C_s	3b	-216.083029 (-217.610600)	68.6 (68.6)	57.7 (51.5)
C_s	3c	-216.114937 (-217.638286)	69.3 (69.0)	38.3 (34.6)
C_{2v}	3d	-216.144494 (-217.665643)	69.8 (69.8)	20.3 (18.1)
C_{2v}	3e	-216.177235 (-217.694988)	70.1 (70.1)	0.0 (0.0)
C_{3v}	5a	-342.489713 (-345.013573)	119.2 (112.5)	54.4 (48.1)
C2v	5b	-342.519317 (-345.039338)	120.0 (113.0)	36.6 (32.5)
C_s	5c	-342.548337 (-345.065683)	119.9 (113.3)	18.3 (16.2)
C_{2v}	5d	-342.552425 (-345.070426)	120.0 (113.3)	15.8 (13.3)
C_{3v}	5e	-342.578022 (-345.092057)	120.3 (113.6)	0.0 (0.0)

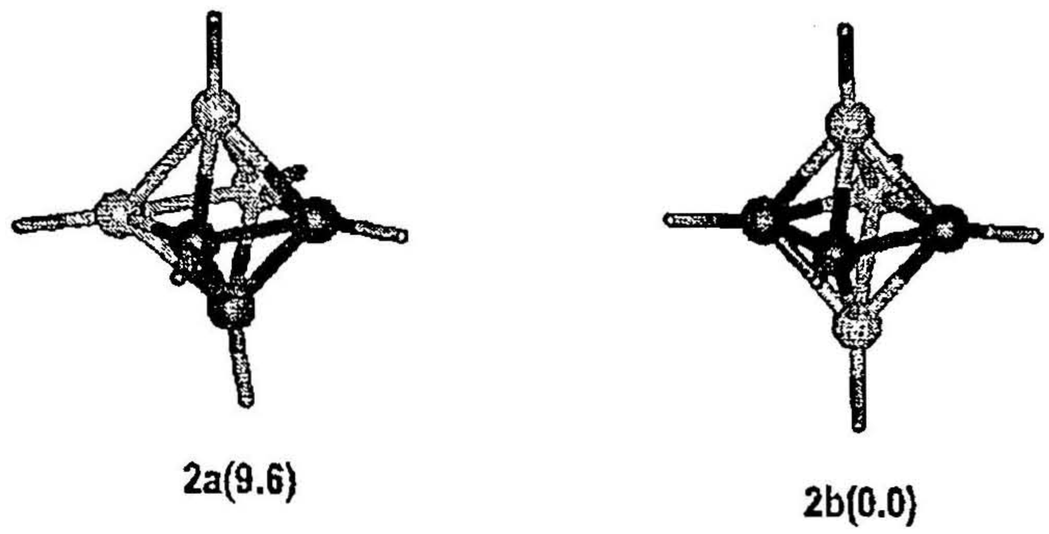

Figure 2.2. Optimized geomtries of $C_3B_3H_6^+$ isomers. The relative energies (kcal/mol) are given in parenthesis.

iii. Seven-vertex clusters: All the isomers are found to be minima on the PES. Calculations indicate that **3e** is the most favored isomer among the five possible isomers of $C_3B_4H_7^+$ (Figure 2.3). A five membered ring prefers a BH group as a cap rather than CH, an outcome of ring-cap compatibility. This explains the stability of **3e** and **3d** over **3a**, **3b and 3c**. The reduction of ring C-C bond length in **3e** to ~1.480 Å from normal C-C bond length of 1.54 Å results in better ring-cap overlap and overall stability. The theoretical prediction of **3e** as the most favorable isomer is also in tune with the large number of B-C bonds. The structures **3b** and **3c** have one BH and one CH caps. The structure **3c** with more number of B-C bonds is lower in energy than **3b**. As expected the CH and BH bonds of the five membered ring are bent away from the BH caps. The next possibility of 2 CH groups capping the five membered ring (**3a**) is highest in energy with the worst ring-cap compatibility.

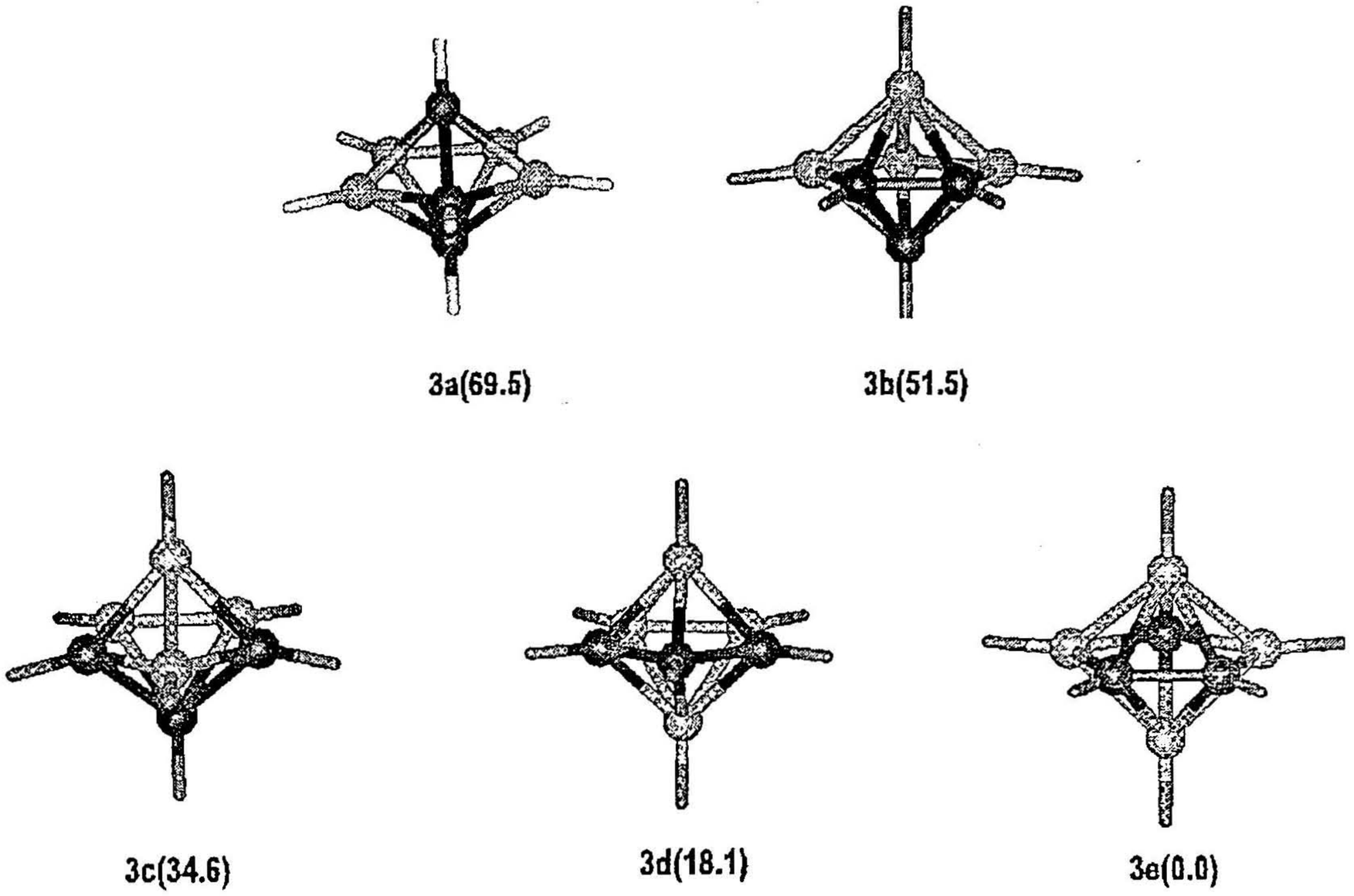

Figure 2.3. Optimized geometries of $C_3B_4H_7^+$ isomers. The relative energies (kcal/mol) are given in parenthesis. All the isomers are minima on the PES.

iv. Ten-vertex clusters: Due to the lower symmetry of $B_{10}H_{10}^{-2}$, there are a large number of isomers for $C_3B_7H_{10}^+$. The insertion of a four membered B_4H_4 ring into the previously studied octahedral structure, $C_3B_3H_6^+$ provides more positions for carbon atoms thereby increasing the number of possible isomers. The energies of all of them are given separately in Table 2.2. All the isomers are calculated to be minima on the PES. The most stable isomer is calculated to be **4a** (Figure 2.4).

The order of relative stability among the 12 possible isomers could be explained easily by the relative positions of 3 CH groups, the number of C-C bonds, and the presence of strained C_3 ring. **4a** with 2 CH caps to 4-membered rings is the most stable isomer, which is a straightforward result of ring cap compatibility. The second type where only

one of the two four membered rings is capped by CH has six possible isomers (**4b-4e,4h,4j**). These are the next lowest set in energy, except for **4h** and **4j**, which have less number of B-C bonds. The remaining isomers form the third category where all the CH groups occupy the ring positions (**4f,4g,4i,4k,4l**). Some of them come in between the second type due to the stability attained from the larger number of B-C bonds in them. These are expected to be high in energy. This is true except for **4f** and **4g**, which have different number of B-C bonds. The least stable structure **4l** has minimum number of B-C bonds, no CH capping to the four membered rings and a strained cyclo $(CH)_3$ fragment. When there is equal number of B-C bonds in two isomers the more stable isomer is the one where the carbon takes a lower coordination position. This explains the stability of **4c** over **4d** and **4f** over **4g**.

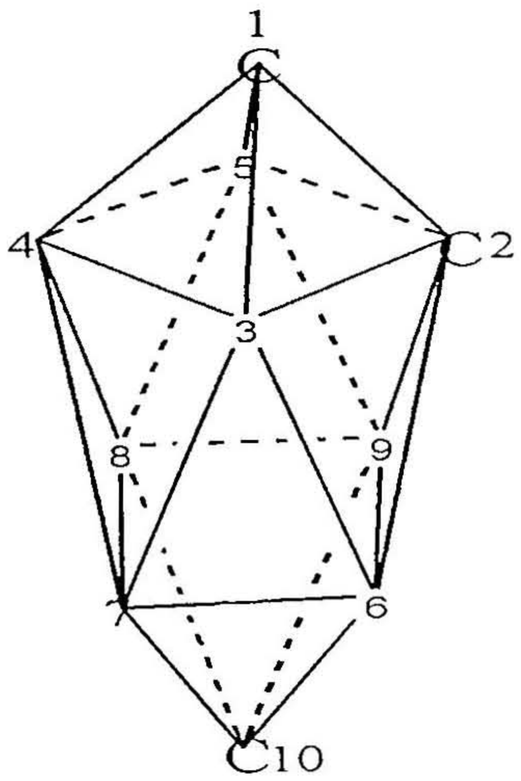

4a

Figure 2.4. The most stable isomer **4a**. The numbering of various vertices is shown.

Table 2.2. Total Energies (Hartrees), unscaled zero point vibration energies (ZPVE, kcal/mol) and relative energies (RE, kcal/mol) of $C_3B_7H_{10}^+$ isomers at HF/6-31G*. The numbers within parenthesis below the isomer number refer to the position of carbon substitution (RE include ZPE, numbers in the parentheses are from B3LYP calculations at 6-31G* level.) All the isomers are minima on the PES.

Symmetry	Isomer	Total energy	ZPVE	RE
C_s	4a (1,2,10)	-291.993209 (-294.113322)	98.7 (93.9)	0.0 (0.0)
C_{2v}	4b (1,6,8)	-291.980752 (-294.104220)	98.7 (93.3)	7.8 (5.1)
C_1	4c (1,6,7)	-291.963165 -294.086174)	98.7 (93.1)	18.8 (16.4)
C_1	4d (1,2,8)	-291.955438 (-294.080785)	93.9 (93.1)	23.6 (19.0)
C_1	4e (1,3,6)	-291.928398 (-294.057750)	98.3 (92.8)	40.3 (33.7)
C_s	4f (2,3,8)	-291.925340 (-294.054170)	98.1 (92.5)	41.9 (35.4)
C_1	4g (2,4,6)	-291.912253 (-294.047456)	97.7 (92.3)	49.8 (39.3)
C_{2v}	4h (1,2,4)	-291.907239 (-294.041898)	98.0 (92.5)	53.2 (43.4)
C_1	4i (2,3,7)	-291.896747 (-294.029926)	97.7 (92.2)	59.5 (50.5)
C_1	4j (1,2,3)	-291.893203 (-294.027124)	97.9 (92.1)	61.9 (52.3)
C_s	4k (2,3,4)	-291.887185 (-294.021788)	97.2 (91.9)	65.0 (55.6)
C_s	4l (2,3,6)	-291.869740 (-294.008640)	97.2 (91.7)	76.0 (63.9)

v. Twelve-vertex clusters: The icosahedral $C_3B_9H_{12}^+$ could exist in five different isomeric forms (Figure 2.5). The stability order emerged from calculations is **5e>5d>5c>5b>5a**. The bond energy consideration alone is sufficient to explain the relative stability order of these clusters. **5e** with larger number of stronger B-C bonds is the most stable isomer. Here all the carbon atoms are positioned such that no two carbon atoms are in direct contact with each other.

The **5a** isomer contains a strained cyclopropenyl ring, where each CH can be considered as a cap to five membered rings with two carbon atoms in it. This makes it incompatible with ring-cap matching. Also closely placed three carbon atoms in the cluster violate the Williams principle. These factors contribute to the energy of this isomer and make it the least preferred one. The **5b** and **5c** isomers, which differ by ca. 8 kcal/mol have been associated with one C-C and two C-C bonds respectively and two CH caps on two five membered rings, each have only one carbon atom and one CH cap to a ring with two carbon atoms. The two C-C bonds in **5b** place it at a higher energy than **5c**. The isomer **5d** with only one C-C connectivity and an isolated third carbon atom in the skeleton, as expected is stable over **5a**, **5b** and **5c**.

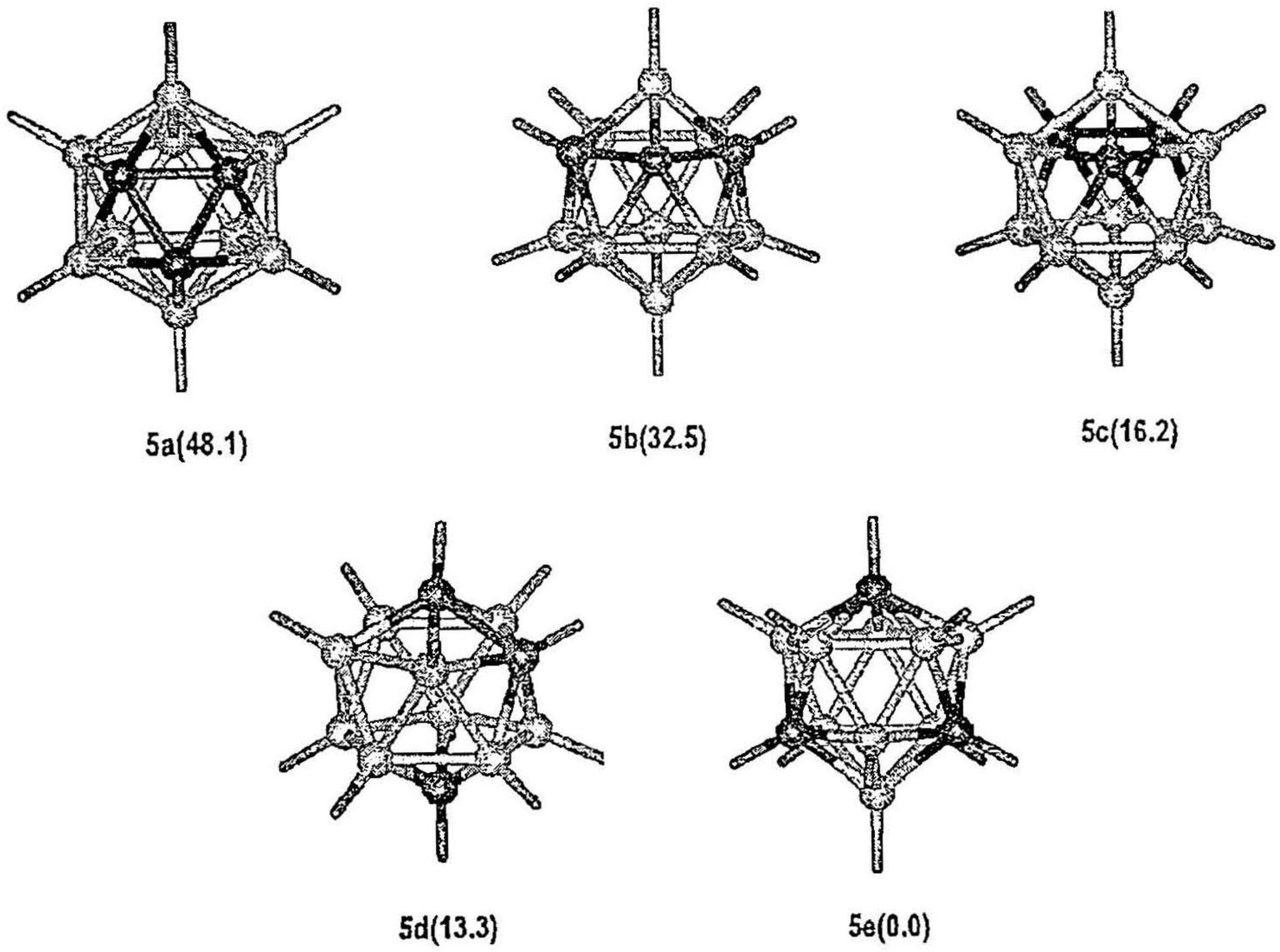

Figure 2.5. Optimized geometries of $C_3B_9H_{12}^+$ isomers. The relative energies (kcal/mol) are given in the parenthesis. All the isomers are minima on the PES.

2.1.4. The stability order of various isomers across the clusters

The perturbation caused by carbon in the borane cage affects both chemical and physical properties. The unusual stability of $B_{12}H_{12}^{-2}$ led to the belief that the stability of polyhedral boranes increases with size of the cluster. While this is true in comparison between $B_{12}H_{12}^{-2}$ and $B_5H_5^{-2}$, it cannot explain the greater stability of $B_6H_6^{-2}$ over $B_7H_7^{-2}$. Many studies were carried out to get a satisfactory explanation of the stability order among the *closo* boranes.[10a,12,15,17a] This was explained finally by the concept of overlap matching.[12d] All the studies led to a stability order for dianionic polyhedral boranes as shown: $B_{12}H_{12}^{-2} \sim B_6H_6^{-2} > B_7H_7^{-2} > B_{10}H_{10}^{-2} > B_5H_5^{-2}$.

The stability of cationic carbaboranes is correlated using the following equations (2.1-2.4) which are nearly isodesmic. Only the most stable isomer in each category is considered here. The equations are calculated using the B3LYP/6-31G* energy values of all species. This gives the order of stability among the members as a relative preference between tricarbaboranes and all boranes with $B_{12}H_{12}^{-2}$ as a standard. Orbital compatibility arguments anticipate the result that structures 1-4 are all benefited by carbon substitution so that all equations are endothermic. Maximum benefit is obtained by the smallest system as the CH caps favor the small three-membered ring over the BH cap and thus, leading to greater overlap. Next comes $C_3B_4H_7^+$. $C_3B_3H_6^+$ and $C_3B_7H_{10}^+$ benefited less from carbon substitution.

	kcal/mol	
$C_3B_2H_5^+ + B_{12}H_{12}^{-2} \longrightarrow C_3B_9H_{12}^+ + B_5H_5^{-2}$	125.4	(2.1)
$C_3B_3H_6^+ + B_{12}H_{12}^{-2} \longrightarrow C_3B_9H_{12}^+ + B_6H_6^{-2}$	82.1	(2.2)
$C_3B_4H_7^+ + B_{12}H_{12}^{-2} \longrightarrow C_3B_9H_{12}^+ + B_7H_7^{-2}$	94.1	(2.3)
$C_3B_7H_{10}^+ + B_{12}H_{12}^{-2} \longrightarrow C_3B_9H_{12}^+ + B_{10}H_{10}^{-2}$	42.5	(2.4)
$C_2H_2 + CH^+ + (n-3)\ BHinc \longrightarrow C_3B_{n-3}H_n^+$		(2.5)

An alternative to evaluate the relative stability of these cations is to employ the equation (2.5), where $E(CH^+)=E((CH_3)_2CH^+)-E(C_2H_6)$. The energy obtained on the LHS of equation (2.5) is just a summation factor and it does not include any additional stabilization of the cluster. The reaction energy of this equation calculated using BHinc from acyclic B_3H_5 ($E(BHinc)=E(B_3H_5)-E(B_2H_4)$[17a])provides the stabilization energy due to delocalization, ring-cap orbital overlap and other factors. The values obtained are -453.6, -350.1, -226.1, -161.0 and -108.9kcal/mol for n=12,10,7,6, and 5 respectively. These absolute values indicate total stability. The inherent stability here may be better approximated by dividing each of these by the number of vertices. Thus we get –37.8, -35.0, -32.3, -26.8 and –21.8 kcal/mol respectively for n=12,10,7,6 and 5, implying maximum inherent stabilization to the icosahedral $C_3B_9H_{12}^+$. What is interesting is that the carbon substitution has changed the order of stability of tricarbaboranes from $B_nH_n^{-2}$. $C_3B_7H_{10}^+$ is more favorable than $C_3B_4H_7^+$, which in turn is more favorable than $C_3B_3H_6^+$. This is contrary to the stability order of $B_nH_n^{-2}$ where 6-vertex polyhedron is more stable than 7- and 10-vertex polyhedra.

2.1.5. Natural charges and the delocalization

The delocalized nature of the isomers is well understood from the charge distribution among the vertices. The monopositive charge is distributed among all the vertices and naturally those BH groups, which are near to the CH vertices, acquire the highest positive charge. For example in the most stable isomer of $C_3B_9H_{12}^+$ **5e**, there are four unique vertices by symmetry. The NBO charges obtained by adding the charge on the hydrogen to the heavy atom on each vertex are shown in Figure 2.6. The three equivalent carbon atoms have NBO charge of -0.336. The three borons (Ba) each of which are in the

vicinity of two carbon atoms and are not bonded to each other have a charge of 0.286. The third set of three boron atoms (Bb), which are bonded to each other and at the same time connected to two carbon atoms have a charge of 0.269. The charge on the remaining 3 boron atoms (Bc), which are connected to only one carbon atom, is 0.113. With the introduction of carbon atoms, the cage is polarized so that the hydrogens on the carbon have more positive character and those on the boron atoms have less acidic character. Thus different derivatisation is possible on both the carbon and boron vertices, forming stable species enabling to vary their constitution and hence the properties. This partial localization of the charge present in all the isomers must provide interesting variation of reactivity at different sites providing versatility in functionalization.

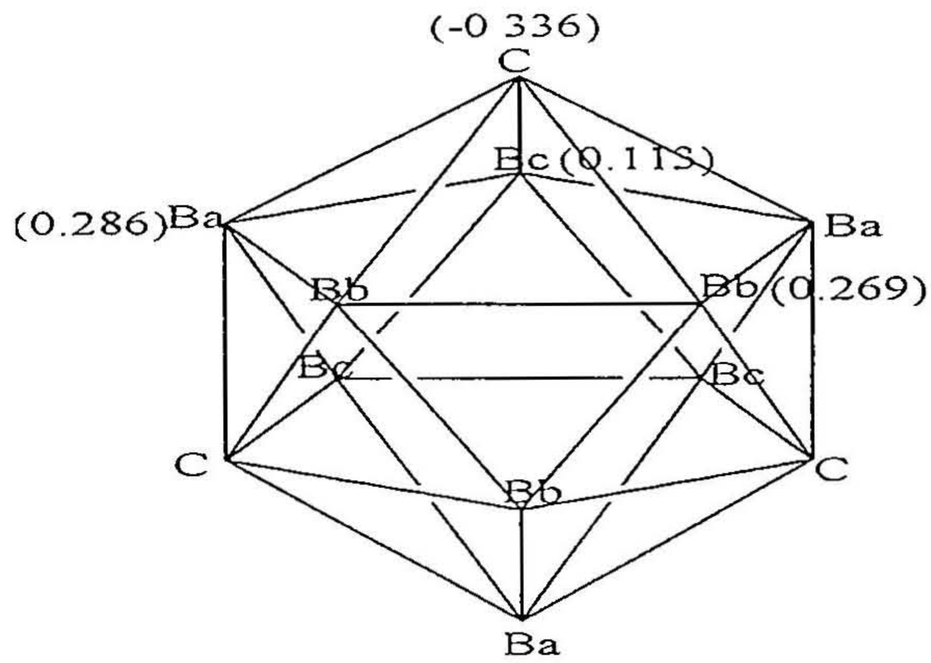

Figure 2.6. The NBO charges on the various vertices of most favorable and symmetric tricarba-isomer is shown

All of the *closo*- tricarbaborane cations studied here are favorable systems with the positive charge delocalized throughout the entire cage with a variety of reactive sites than the neutral and anionic counterparts. The possible ways of stabilizing these cations are the displacement of hydrogens by ligands and thus making it suitable for a variety of uses such as stabilization of unusual anions and as weakly coordinating cations.

2.1.6. Possible applications

Cationic tricarbaborane systems should have promising applications, adding to the many known uses of boranes. Recently a variety of substituted *closo*- carbaboranes like permethylated and perhalogenated carbaborane anions ($CB_{11}R_{12}^-$) have been synthesized.[18] The crystallinity and extremely weak coordination of $CB_{11}R_{12}^-$ have been used profitably to stabilize and to characterize a number of unusual cations.[19] Just as these derivatives of $B_{12}H_{12}^{-2}$ and $CB_{11}H_{12}^-$ have been used as highly noninteracting carbanions in studying reactive cations,[19,20] appropriate derivatives of $C_3B_9H_{12}^+$ should help as versatile cations in stabilizing reactive anions. These cationic tricarbaboranes presumably should have approximate spherical geometry with a highly dispersed charge. Though spherical in shape, the three carbon atoms in them provide opportunities for polarization of charge resulting in weakly acidic sites, which can be used to advantage. For example, fullerene salts with alkali and alkaline earth metal counter ions have been studied extensively. The physics and chemistry of C_{60}^{-3} depend on the counter cations used.[21] The superconductivity of C_{60}^{-3} $(M^+)_3$ is known to depend on the cation M^+. Use of carbaborane based cations allows variation of size of the cationic species and also polarization of the charge depending on the positions of the carbon atoms. Recently MgB_2 with negatively charged graphite like boron sheets and intercalated Mg^{+2} is shown to be superconducting.[22] The nature of the cation may be used to fine tune these electronic properties. There is, thus, a need to develop highly unreactive cations with varying sizes. Cationic carbaboranes are possible candidates.

2.1.7 Conclusions

An electronic and structural analysis is made on the cationic *closo* tricarbaboranes obtained by the isoelectronic replacement of 3 BH^- by 3 CH. Models are taken from both simple and stacked systems. The stability order of all the isomers are explained based on the William's rule, Gimarc's rule and Jemmis ring-cap orbital overlap criterion, which govern a monopolyhedral cage. The stability order is proportional to the number of inherently stronger B-C bonds. The introduction of more carbon atoms on the boron clusters brings in more number of isomers and a reduced delocalization.

2.2. A possible synthetic strategy towards cationic *closo*-tricarbaboranes

2.2.1. Introduction

The previous section of this chapter pointed out the stability of the isomers of *closo*-$C_3B_{n-3}H_n^+$, which are potentially weakly coordinating cations by virtue of the dispersal of charge throughout the cage. Though many synthetic approaches towards the neutral *nido* or *arachno* multi-carba systems are known,[3,4,23] *closo*-cationic tricarbaboranes remain elusive till date. Here a synthetic strategy is proposed towards cationic *closo*-carbaboranes based on the well-known benzyl cation-tropylium ion equilibrium. Though the studies on the relative energies of the various isomers on the potential energy surface of $C_7H_7^+$ and the energy barrier for their interconversion still continue, the stability of tropylium ion over benzyl cation is a well accepted verity.[24] A reaction similar to the expansion of the six-membered ring to seven-membered ring must lead from *closo*-$C_2B_{n-2}H_n$ to *closo*-$C_3B_{n-3}H_n^+$. Theoretical studies of a synthetic strategy involving cage expansion starting from carboranyl carbene 1-CH-1,2-$C_2B_{10}H_{11}$ leading to the formation of neutral *closo*-$C_3B_{10}H_{12}$ are known.[23e]

2.2.2. Benzyl cation-tropylium ion analogs in polyhedral boranes

In comparison to the benzyl cation-tropylium ion rearrangement, which is calculated to be exothermic by 10.2 kcal/mol at B3LYP/6-31G*, the cluster expansion reactions are generally more exothermic (Scheme 2.1). The octahedral 1-CH_2-2,3-$C_2B_4H_5^+$ (**1**) is less stable than 2,4,5-$C_3B_4H_7^+$ (**2**) by 54.0 kcal/mol. The 11-vertex *closo*-dicarboranyl methyl cation, 1- CH_2-7,9-$C_2B_9H_{10}^+$ (**3**) is also less stable than the cationic *closo*-icosahedral tricarba species, 2,8,10-$C_3B_9H_{12}^+$ (**4**) by 41.3 kcal/mol. However, equation III (Scheme 2.1) which generates a 13-vertex *closo*-tricarbaborane (**6**) is endothermic; 2,9,11-$C_3B_{10}H_{13}^+$ (**6**) is higher in energy than 12-vertex 1-CH_2-8,10-$C_2B_{10}H_{11}^+$ (**5**) by 10.5 kcal/mol, possibly from the inherent extra stability of the icosahedral skeleton. There are several isomers possible for each tricarbaborane family; **2** is the most stable isomer among the pentagonal bipyramidal tricarba species and **4** is the second-most stable one among the icosahedral family.

2.2.3. Geometry of the dicarboranyl methyl cations: Benzyl cation analogs

The primary cation, anticipated to be highly reactive, has its CH_2 group tilted towards one of the boron vertex (B_β). This tilting is observed in all the cases except for **1** where the bending is towards an edge forced by the symmetry. In **3** the CH_2 group tilts to one of the vertex by 45.1°. But in the known dicarboranyl methane ($C_2B_9H_{10}CH_3$) there is no tilting for the CH_3 group and methyl carbon is collinear to the capping atoms.[25] It is the interaction of the vacant p-orbital on the CH_2 group with bonding skeletal orbitals 1a' and 2a' of the cage (**A**, Figure 2.7) that leads to the tilting. This delocalization is reflected in the natural charge on the CH_2 group (0.082). The molecular orbitals, 1a' and 2a' are stabilized while 3a' which is the LUMO gets destabilized in this process (**C**, Figure 2.7). If

this is indeed correct, CH_2 substituent with two electrons in the p-orbital should not tilt, as is confirmed from the optimized geometries of $C_2B_nH_{n+1}CH_2^{-1}$. These are minima on their respective potential energy surface as well.

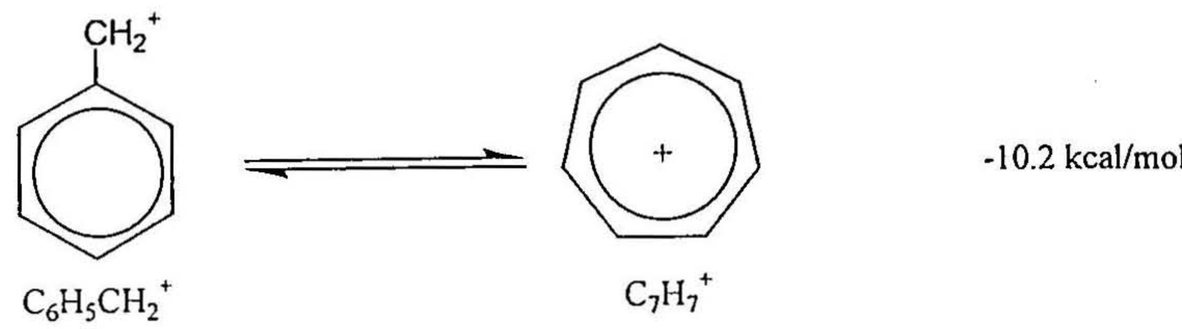

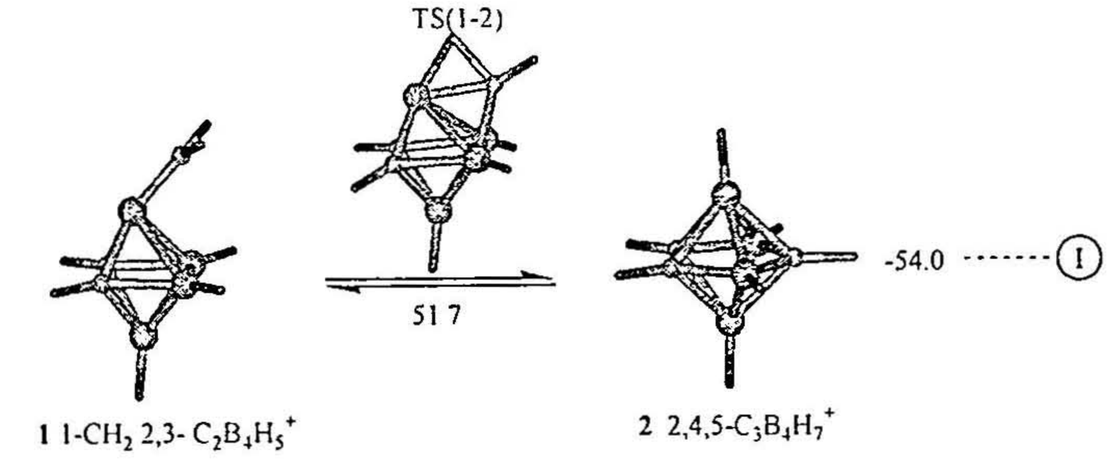

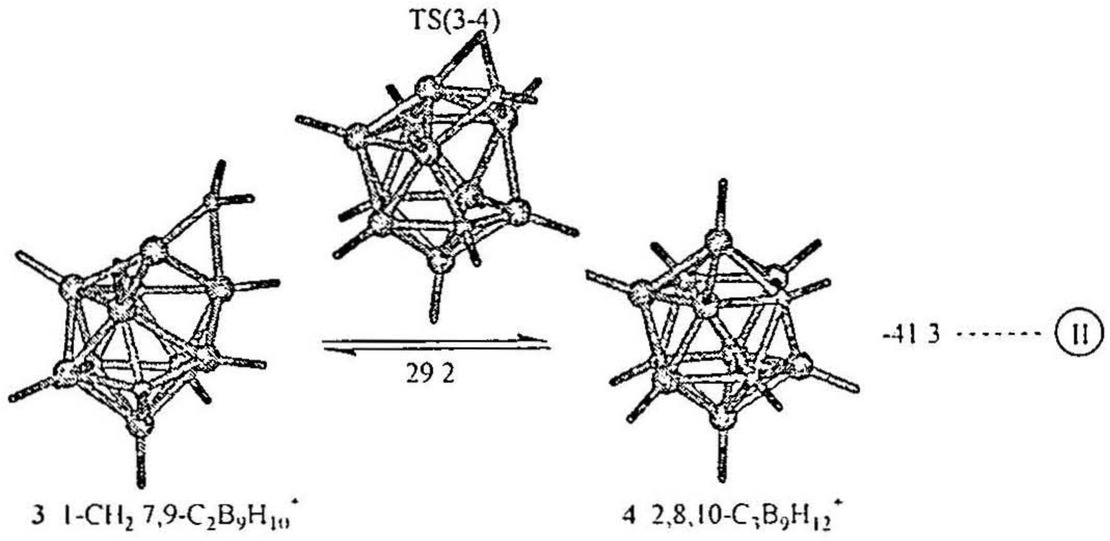

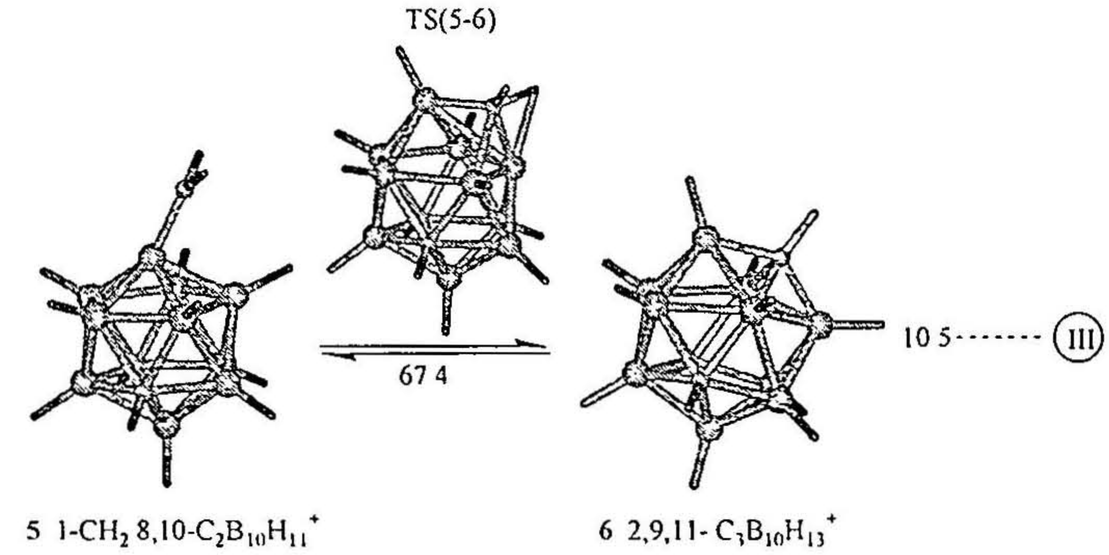

Scheme 2.1. The optimized reactants, transition states and products calculated for the formation of cationic tricarbaboranes. The relative energies and the energy barriers are also given.

The B_α (boron to which the CH_2 carbon is bonded)-C bond length in **3** is 1.482 Å (WBI=1.148).[26] There is a C-B_α-B_β 3-centre bond which shows enhanced delocalization due to the stabilizing interaction. This is further supported by the formation of a weak bond (WBI=0.627) between the carbon and the cage boron (B_β) towards which it is tilted. The tilting angle, bond lengths and the Wiberg bond indices of all the systems studied are given in Table 2.3. The tilting angle is less for **5** (30.4°) where the equilibrium is calculated to be endothermic.

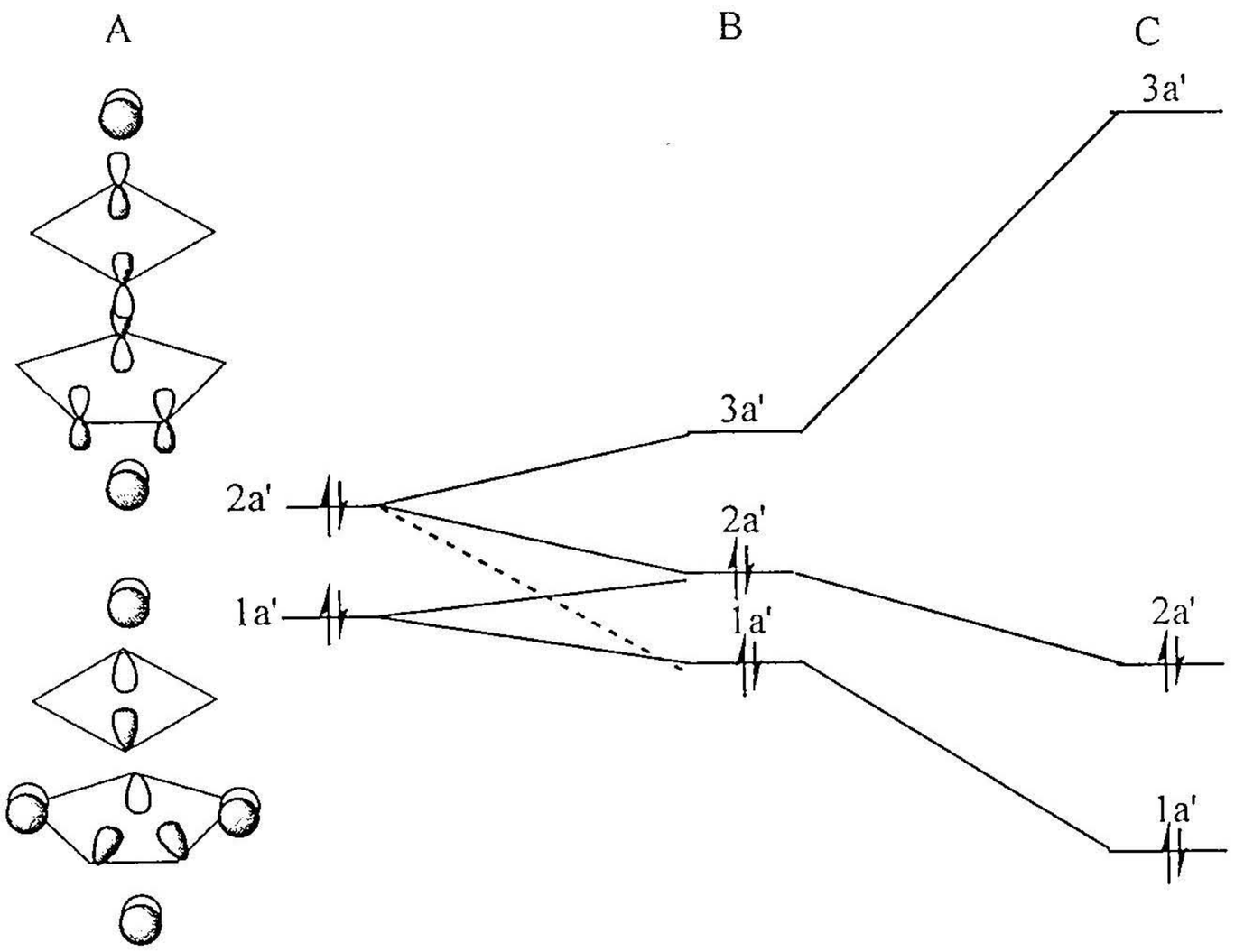

Figure 2.7. The cage orbitals of $C_2B_9CH_2^+$ which has hyperconjugative interaction with the vacant p-orbital of the CH_2 group(A) and the resulting molecular orbitals of $C_2B_9CH_2^+$ with linear CH_2 (B). The tilting of CH_2 group enhances the interaction leading to the stabilization of bonding molecular orbitals, 1a' and 2a' and the destabilization of the LUMO,3a' (C).

2.2.4. Boranyl methyl anion-monocarbaborane rearrangement

A similar trend both in geometry and in energetics is observed in the formation of monocarbaboranes from boranyl methyl systems (**7-12,** Scheme 2.2). The monocarbaboranes precede over the boranyl methyl systems in their stability, thus making this synthetic method a favorable one for their formation as well. The exothermicity of the equilibrium involving the formation of 13-vertex monocarbaboranes in the gas phase, though not very large, implies that the hitherto unknown 13-vertex *closo*-borane is not very far from experimental realization. The recent report of the synthesis of 13-vertex *closo*-dicarbaborane supports our results.[27] There is no bending of the methyl carbon in trianionic boranyl methyl systems also, but is pyramidal in contrast to the planar structure of the dicarboranyl methyl anions (Figure 2.8).

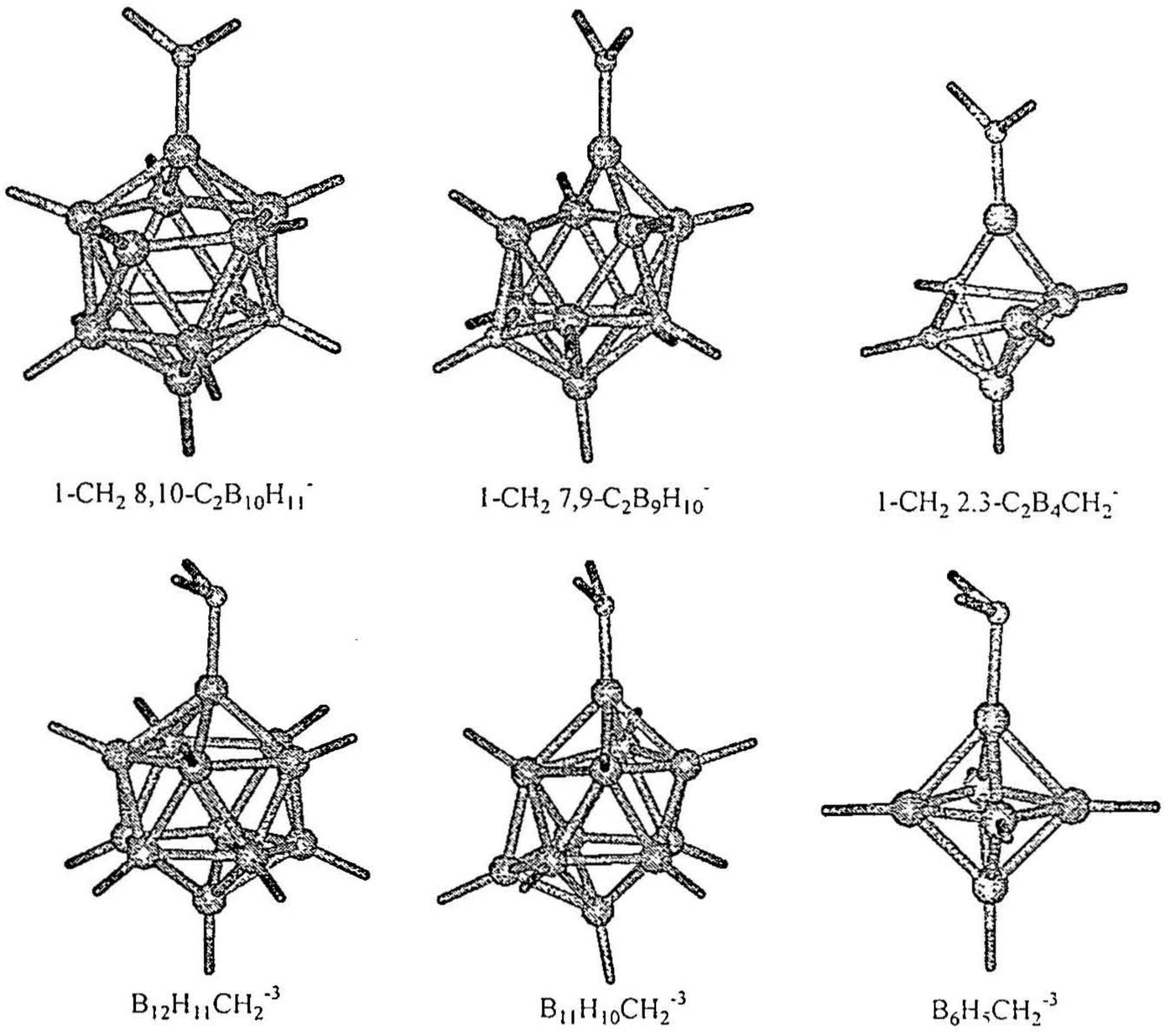

Figure 2.8. Optimized geomtries of dicarboranyl methyl anions and boranyl methyl trianions.

The methyl group is pyramidalized so that the extra electron pair occupies an orbital of more p character with some s mixing and is not involved in the skeletal bonding. In the dicarboranyl methyl systems the cage, due to its electron withdrawing character, incorporates the additional electron pair for the skeletal bonding and opens up. This result is in accord with the fact that the methyl anion is pyramidal whereas the methyl cation takes on a planar arrangement.

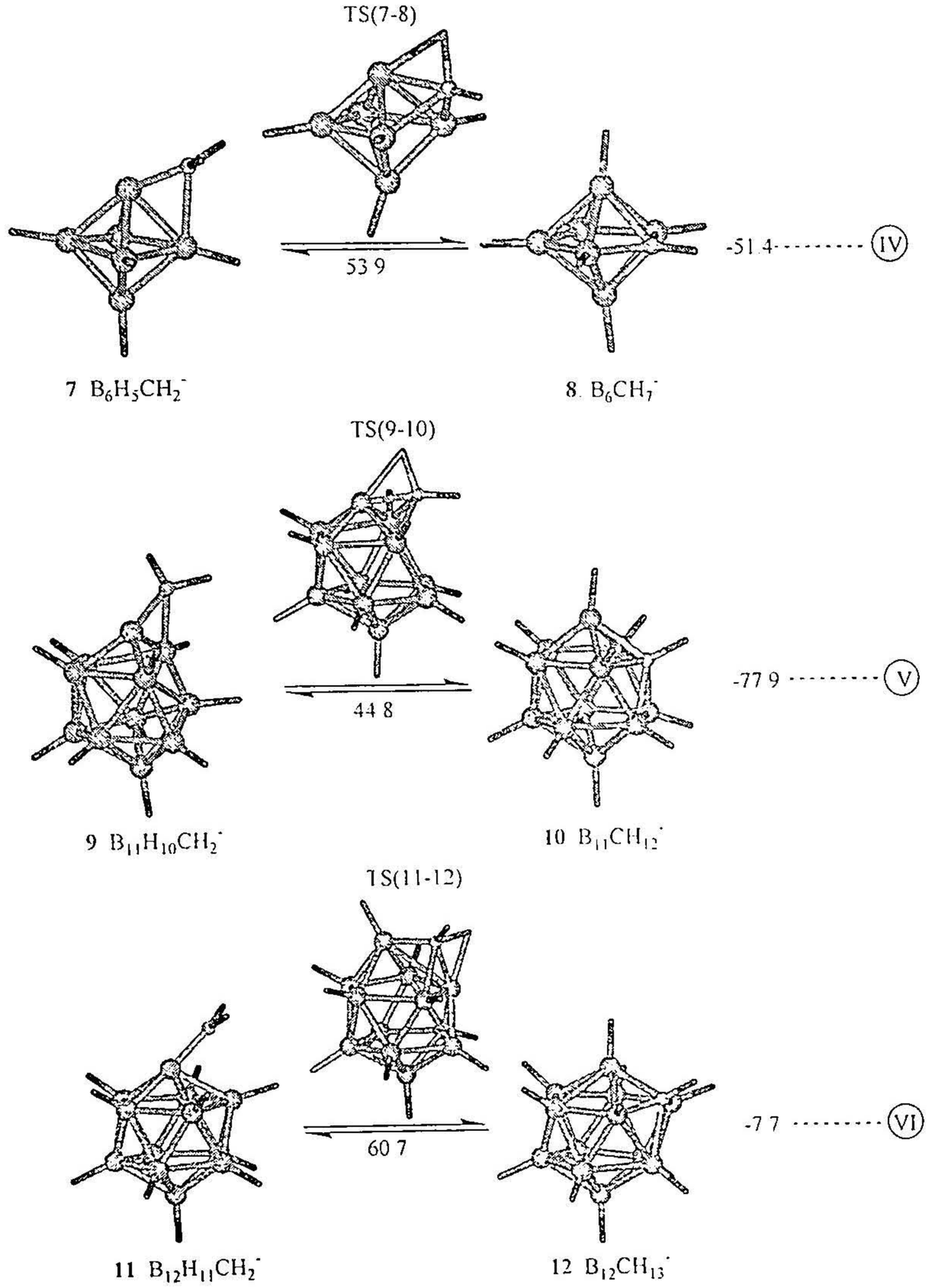

Scheme 2.2. The optimized reactants, transition states and products calculated for the formation of anionic monocarbaboranes. The relative energies and the energy barriers are also given.

The formation of tricarbaboranes is found to be more feasible than the corresponding monocarbaboranes except for 13-vertex *closo*-systems. The rearrangements involving the formation of dicarbaboranes are not studied due to their relative ease of availability and abundance.

Table 2.3. The total energies in au, tilting angle (θ) in degrees, the distance between the methyl carbon and the boron (B_α) to which it is connected (l_1) as well as the boron (B_β) towards which it is bent (l_2), and the corresponding Wiberg bond indices (WBI).

Compound	Energy, au	Tilting angle, θ	C-B_α (Å)		C-B_β (Å)	
			l_1	WBI	l_2	WBI
$C_2B_4H_5CH_2^+$(1)	-217.60895	45.4	1.457	1.308	2.496	0.185
$C_2B_9H_{10}CH_2^+$(3)	-345.00457	45.1	1.463	1.232	1.895	0.472
$C_2B_{10}H_{11}CH_2^+$(5)	-370.50948	30.4	1.499	1.141	2.328	0.198
$B_{12}H_{11}CH_2^-$(7)	-344.39207	44.7	1.481	1.197	2.015	0.390
$B_{11}H_{10}CH_2^-$(9)	-318.87012	49.7	1.482	1.148	1.752	0.627
$B_6H_5CH_2^-$(11)	-191.45219	40.2	1.474	1.266	1.894	0.525

2.2.5. Reaction paths and energy barriers

In the light of favorable exothermicities, the reaction path for the formation of the tropylium ion equivalent structures is traced out by IRC calculations.[28] The energy barrier for the conversions from **1** to **2** is calculated to be 51.7 kcal/mol. The energy barrier involved in the conversion of 11-vertex (**3**) to icosahedral species (**4**) is computed to be 29.2 kcal/mol and the energy barrier for **5** to **6** is computed to be comparatively higher, 67.4 kcal/mol. Thus, the transformation from a less stable 11-vertex to the most stable icosahedral form is more feasible than from either icosahedral or octahedral carbaborane to the corresponding 13-vertex and 7-vertex carbaboranes (Figure 2.9). These are to be compared to the barrier of 62.1 kcal/mol calculated on the path of benzyl cation-tropylium ion conversion.[29] Thus, the energy barriers for the cationic boranes appear to be accessible. All the rearrangements are one-step processes with a transition state that is located on the potential energy surface.

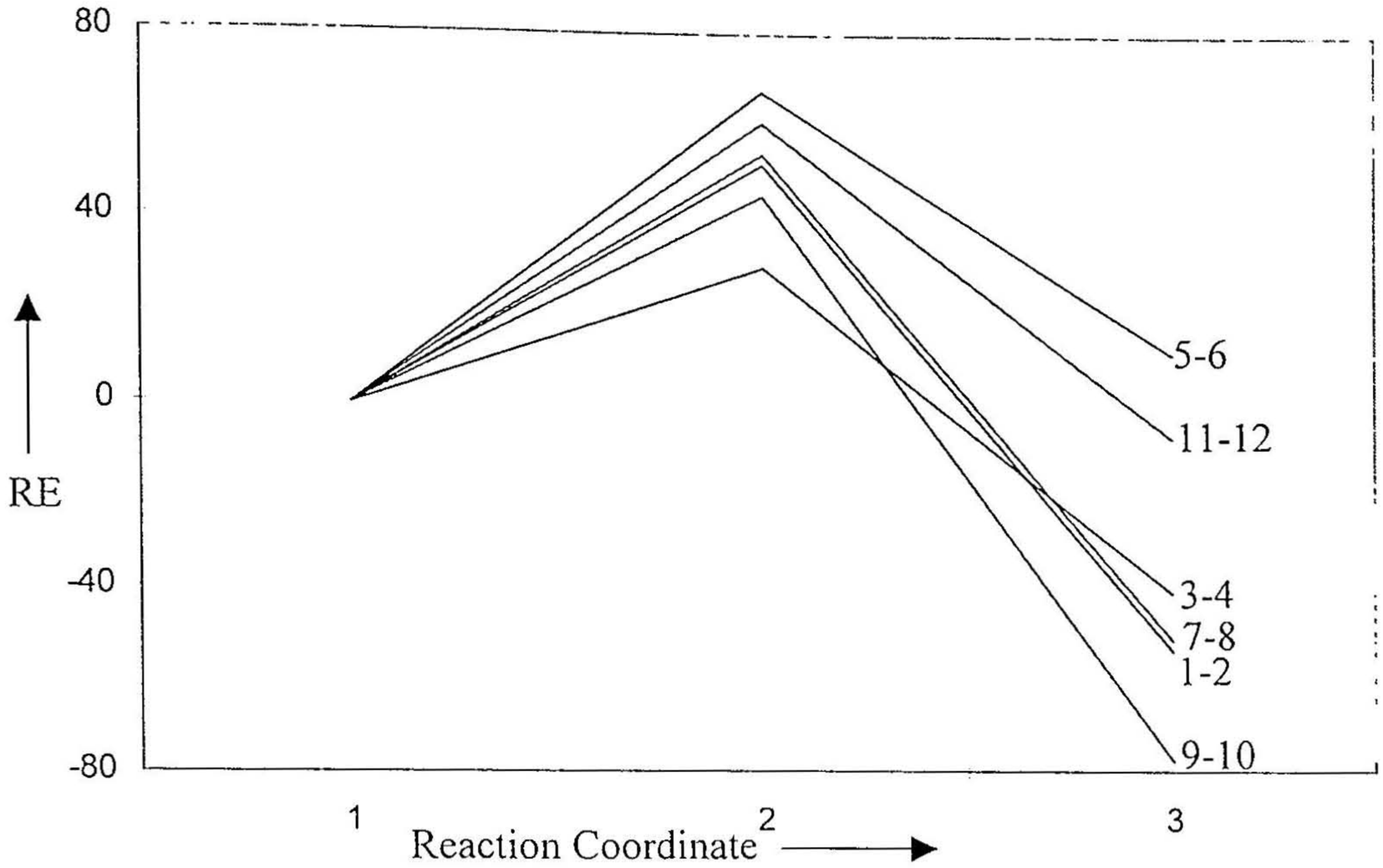

Figure 2.9. The reaction path traced out for all the equilibria shown in Scheme 1 and 2. The reaction coordinate is taken on the X-axis and the relative energy (RE) is plotted along Y-axis. It is obvious that the formation of icosahedral species (3->4 (tricarba-formation) and 9->10 (monocarba- formation)) involves less energy barrier compared to other cases.

The reaction path for the formation of the icosahedral cations starting from CH_2 susbstituted isomers of the experimentally known 11-vertex dicarbaborane are also computed (Figure 2.10).[25b] Two cases are studied here where the reactant is with CH_2 group attached on the boron vertex (**13**) and on the carbon vertex (**15**). Their energy barriers can be compared with II in scheme 2.1. The rearrangement from the (**13**) is slightly less favorable than from (**3**) with an energy barrier of 34.2 kcal/mol and that from the (**15**) is highly unfavorable with a barrier of 70.1 kcal/mol. This shows the lower preference of C-substituted dicarboranyl methyl cation as the reactant.

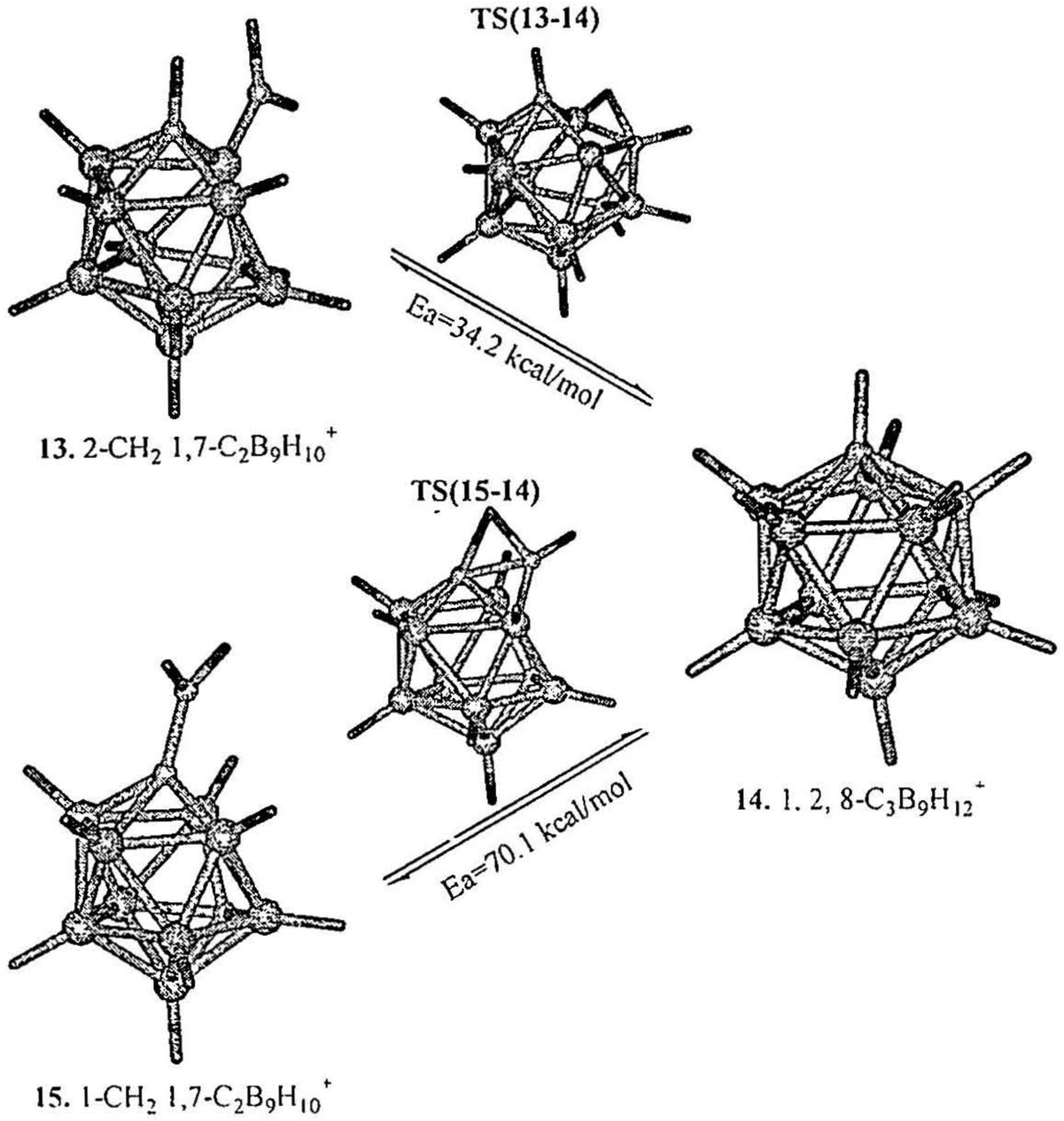

Figure 2.10. The optimized geometries of the reactants, transition states and the product obtained for the experimentally known 11-vertex dicarbaborane reactant. The relative energies and the energy barriers are also given.

2.2.6. Transition states

All the transition states are characterized with one of the -CH_2 hydrogen bridging the carbon-boron bond. One of the ring B-B bond is elongated to 2.780 Å in **TS(3-4)** and 1.980 Å in **TS(1-2)** whereas the B_α-B_β bond is lengthened in **TS(5-6)** (2.292 Å) to accommodate the –CH_2 carbon. The imaginary vibrational frequency and the IRC calculations confirm all the transition states for the respective transformations.

2.2.7. Conclusions

The extension of the well-known organic reaction to polyhedral boranes will not only provide an additional link in our attempts to correlate the carbon chemistry and boron chemistry, but also enrich the carbaborane chemistry as it includes the cage expansion and

the introduction of carbon atoms into the cage. The computational results show that with a proper reactant, the exploration of the cationic polyhedral carbaboranes should be within the realm of the possible. There are many known reactions to emulate. The reactant with an icosahedral framework could be achieved by many ways such as the reaction between $B_{10}H_{12}(ligand)_2$ and acetylenes ($C_2R(R'X)$), halogenaion of the methyl derivatised *closo*-icosahedral borane and insertion of the properly substituted vertex on to a *nido* face.[24]

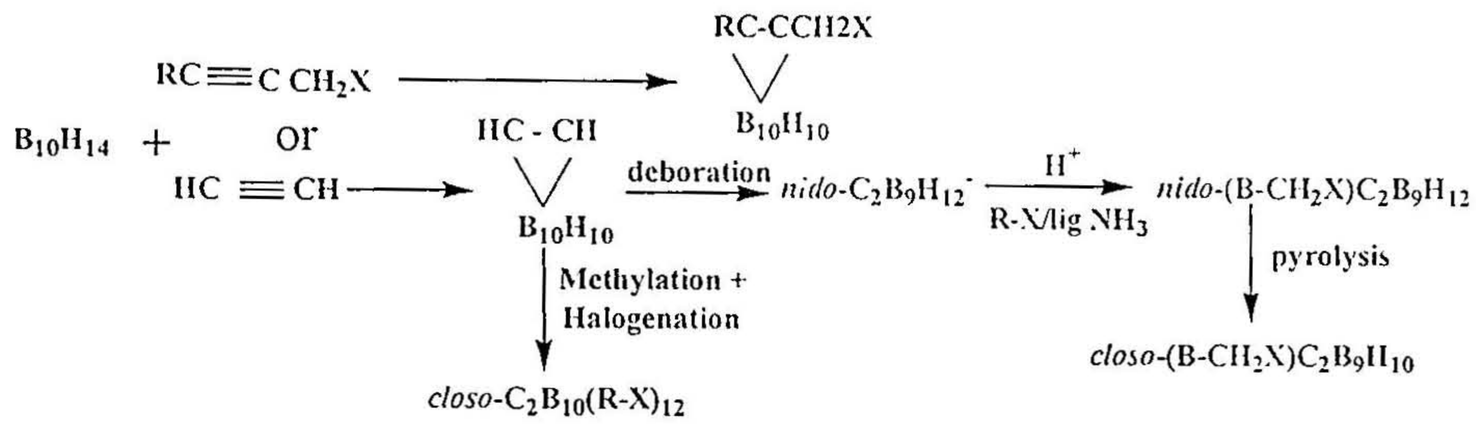

This reactant can be either directly employed for the formation of 13-vertex cluster or made to undergo base promoted degradation to obtain the *nido* product.[30] The pyrolysis of the *nido*- B-derivatized $C_2B_9H_{13}$ leads to the *closo*-11-vertex dicarboranyl methyl system.[31] Thus, the prospect of synthesizing other similar carboranyl systems, either by extending an analogous pathway as that of icosahedral systems or by starting with a B-derivatized *nido*-system, is sure to bring excitement in the area of carbon rich carbaboranes.

References

1. Grimes, R. N. *Carboranes*, Academic Press, New York, **1970**.
2. (a) Brigadze, V. I. *Chem. Rev.* **1992**, *92*, 209. (b) Muetterites, E. L.; Knoth, W. H. *Polyhedral Boranes*, Marcel Dekker, New York, **1968**. (c) Purcell, K. F.; Kotz, J.C. *Inorganic Chemistry*, W. B. Saundes, Philadelphia, **1977**; Chapter 18. (d) Stibr, B. *Chem. Rev.* **1992**, *92*, 225. (e)Onak, T. *Advances in Boron and Boranes*, Liebman, J. F.; Greenberg, A.; Williams, R. E. Eds., VCH; Germany, **1988**, 125. (f) Olah, G. A.; Wade, K.; Williams, R. E. Eds., *Electron Deficient Boron and Carbon Cluster*, John-Wiley and Sons, New York, **1991**. (g) Onak, T. in *Comprehensive Organometallic Chemistry II*, Anel, E. W.; Stone, F. G. A.; Wilkinson, G. Eds., Elsevier Science Ltd., Oxford, UK, **1995**.
3. (a) Onak, T. P.; Wong, G. T. F. *J. Am. Chem. Soc.* **1970**, *92*, 5226. (b) Herberhold, M; Bertholdt, U.; Milius, W.; Glockle, A.; Wrackmeyer, B. *Chem. Commun.* **1996**, 1219. (c) Wrackmeyer, B.; Schanz, H. J.; Milius, W. *Angew. Chem. Int. Ed. Eng.* **1997**, *36*, 1117. (d) Jutzi, P.; Seufert, A. *Angew. Chem. Int. Ed. Eng.* **1977**, *16*, 330. (e) Wrackmeyer, B.; Schanz, H. J.; Hofmann, M.; Schleyer, P. v. R. *Angew. Chem. Int. Ed. Eng.* **1998**, *37*, 1245. (f) Plumb, C. A.; Carroll, P. J.; Sneddon, L. G. *Organometallics*, **1992**, *11*, 1665. (g) Wang, J.; Li, S.; Zheng, C.; Maguire, J. A.; Hosmane, N. S. *Organometallics*, **2002**, *21*, 5149.
4. (a) Hosmane, N. S.; Grimes, R. N. *Inorg. Chem.* **1979**, *18*, 3294. (b) Maynard, R. B.; Borodinsky, L.; Grimes, R.N. *Inorg. Synth.* **1983**, *22*, 211. (c) Fox, M. A.; Greatrex, R.; Nikrahi, A. *Chem. Commun.* **1996**, 175.

5. (a) Thompson, M. L.; Grimes, R. N. *J. Am. Chem. Soc.* **1971**, *93*, 6677. (b) Thompson, M. L.; Grimes, R. N. *Inorg. Chem.* **1972**, *11*, 1925.

6. (a) Bausch, J. W.; Prakash, G. K. S.; Williams, R. E. *Inorg. Chem.* **1992**, *31*, 3763. (b) Fox, M. A.; Greatrex, R. *J. Chem. Soc, Dalton. Trans.* **1994**, 3197.

7. Williams, R. E. *Adv. Inorg. Radiochem.* **1976**, *18*, 67.

8. (a) Williams, R. E.; Gerhart, F. J. *J. Am. Chem. Soc.* **1965**, *87*, 3513. (b) Williams, R. E. *Carboranes*, in Progress in Boron Chemistry, Vol.2, Brotherton, R. J.; Steinberg, H. Eds., Pergamon, Oxford, **1970**.

9. (a) Gimarc, B. M. *J. Am. Chem. Soc.* **1983**, *105*, 1979. (b) Ott, J. J.; Gimarc, B. M. *J. Am. Chem. Soc.* **1986**, *108*, 4303. (c) Gimarc, B. M.; Ott, J. J. *J. Am. Chem. Soc.* **1986**, *108*, 4298.

10. Jemmis, E. D. *J. Am. Chem. Soc.* **1982**, *104*, 7017.

11. (a) Jemmis, E. D.; Subramanian, G; Radom, L. *J. Am. Chem. Soc.* **1992**, *114*, 1481. (b) Jemmis, E. D.; Subramanian, G. *Ind. J. Chem.* **1992**, 645.

12. (a)Porterfield, W. W.; Jones, M. E.; Gill, W. R.; Wade, K. *Inorg. Chem.* **1990**, *29*, 2914. (b) Zhao, M.; Gimarc, B. M. *Polyhedron.* **1995**, *14*, 1315. (c) King, R. B. *Inorg. Chim. Acta.* **1981**, *49*, 237. (d) Jemmis, E. D.; Pavankumar, P. N. V. *Proc Indian Acad. Sci. (Chem. Sci.)* **1984**, *93*, 479. (e) Jemmis, E. D.; Balakrishnarajan, M. M. *Bull. Mater. Sci.* **1999**, *22*, 863.

13. (a) Klier, D. A.; Lipscomb, W. N. *Inorg. Chem.* **1979**, *18*, 1312. (b) Halgern, T. A.; Lipscomb, W. N. *J. Chem. Phys.* **1973**, *58*, 1569.

14. *Inorganic Chemistry : Principles of Structure and Reactivity*, Huheey, J. E.; Keiter, A. E.; Keiter, R. L. Fourth Edition New York, **1993.**

15. Dixon, D. A.; Klier, D. A.; Hallgreen, T. A.; Hall, J. H.; Lipscomb, W. N. *J. Am. Chem. Soc.* **1977**, *99*, 6226.

16. Graham, G. D.; Marynick, D. S.; Lipscomb, W. N. *J. Am. Chem. Soc.* **1980**, *102*, 2939.

17. (a) Schleyer, P. v. R.; Najafian, K. *Inorg. Chem.* **1998**, *37*, 3454. (b) *The Borane, Carborane, Carbocation Continuum*, Casanova, J. Ed., John Wiley, New York, **1998**.

18. (a) King, B. T.; Janousek, Z.; Gruner, B.; Trammel, M.; Noll, B. C.; Michl, J. *J. Am. Chem. Soc.* **1996**, *118*, 3313. (b) Srivastava, R. R.; Hamlin, D. K.; Wilbur, D. S. *J. Org. Chem.* **1996**, *61*, 9041. (c) Tsang, C.; Yang, Q.; Tung-Po Sze, E.; Mak, T. C. W.; Chan, D. T. W.; Xie, Z. *Inorg. Chem.* **2000**, *39*, 5851. (d) King, B. T.; Michl, J. *J. Am. Chem. Soc.* **2000**, *122*, 10255.

19. (a) Xie, W.; Bau, R.; Reed, C. A. *Inorg. Chem.* **1995**, *34*, 5403. (b) Xie, W.; Bau, R.; Benesi, A. *Science*, **1993**, *262*, 402. (c) Reed, C. A. *Acc. Chem. Res.* **1998**, *31*, 133. (d) Strauss, S. H. *Chem. Rev.* **1993**, *93*, 927.

20. (a) Ivanova, S. M.; Ivanov, S. V.; Miller, S. M.; Anderson, O. P.; Solntsev, K. A.; Strauss, S. H. *Inorg. Chem.* **1999**, *38*, 3756. (b) Lupinetti, A. J.; Havighurst, M. D.; Miller, S.M.; Anderson, O. P.; Strauss, S. H. *J. Am. Chem. Soc.* **1999**, *121*, 11920. (c) Reed, C. A.; Fackler, N. L. P.; Kim, K-C.; Stasko, D.; Evans, D. R. *J. Am. Chem. Soc.* **1999**, *121*, 6314.

21. Rosseinsky, M. J. *Chem. Mater.* **1998**, *10*, 2665.

22. Akimitsu, N.; Nakagawa, N.; Muramaka, T.; Zenitani, Y. *Nature.* **2001**, *410*, 63.

23. (a) Plumb, C. A.; Carroll, P. J.; Sneddon, L. G. *Organometallics*. **1992**, *11*, 1665. (b) Su, K.; Carrol, P. J.; Sneddon, L. G. *J. Am. Chem. Soc.* **1993**, *115*, 10004. (c) Štíbr, B.; Holub, J.; Císařová, L.; Teixidor, F.; Viñas, C.; Fusek, J.; Plzák, Z. *Inorg. Chem.* **1996**, *35*, 3635. (d) Maxwell, W. M.; Miller, V. R.; Grimes, R. N. *Inorg. Chem.* **1976**, *15*, 1343. (e) Mckee, M. L. *J. Am. Chem. Soc.* **1992**, *114*, 5856.

24. (a) Nicolaides, A.; Radom, L. *J. Am. Chem. Soc.* **1994**, *116*, 9769. (b) Shin, S. K. *Chem. Phys. Lett.* **1997**, *280*, 260. (c) Lifshitz, C. *Acc. Chem. Res.* **1994**, *27*, 138. (d) Shin, C-H.; Park, K-C.; Kim, S-J.; Kim, B. *Bull. Korean. Chem. Soc.* **2002**, *23*, 337.

25. (a) Peymann, T.; Knobler, C. B.; Hawthorne, M. F. *Inorg. Chem.* **1998**, *37*, 1544. (b) Leonowicz, M. E.; Scholer, F. R. *Inorg. Chem.* **1980**, *19*, 122.

26. Wiberg, K. B. *Tetrahedron*, **1968**, *24*, 1083.

27. Burke, A.; Ellis, D.; Giles, B. T.; Hodson, B. E.; Macgregor, S. A.; Rosair, G. M.; Welch, A. J. *Angew. Chem. Int. Edn.* **2003**, *42*, 225.

28. (a) Gonzalez, C.; Schlegel, H. B. *J. Chem. Phys.* **1989**, *90*, 2154. (b) Gonzalez, C.; Schlegel, H. B. *J. Phys. Chem.* **1990**, *94*, 5523.

29. Ignatyev, I. S.; Sundius, T. *Chem. Phys. Lett.* **2000**, *326*, 101.

30. Struchkov, Yu. T.; Antipin, M.; Stanko, V. I.; Brattsev, V. A.; Kirillova N. I.; Knyazev, S. P. *J. Organomet. Chem.* **1977**, *141*, 133.

31. (a) Tebbe, F. N.; Garrett, P. M.; Hawthorne, M. F. *J. Am. Chem. Soc.* **1964**, *86*, 4222. (b) Garrett, P. M.; Tebbe, F. N.; Hawthorne, M. F. *J. Am. Chem. Soc.* **1964**, *86*, 5016. (c) Wiesboeck, R. A.; Hawthorne, M. F. *J. Am. Chem. Soc.* **1964**, *86*, 1642.

CHAPTER 3

Endohedral Polyhedral Boranes: Relationship with Sandwich Complexes and their Stability

3.0. Abstract

An electronic structural connection is established for sandwich complexes and polyhedral boranes with encapsulated atoms. The charge requirements of these extreme geometrical patterns depend on the size of the central atom and the distance between the adjacent rings. While going from the endohedral to the corresponding sandwich complexes the unoccupied a_{2u} and e_g molecular orbitals are stabilized considerably requiring additional 6 electrons for stability. In the corresponding process starting from the double decker sandwich complexes the two endohedral atoms are found to stabilize the large borane skeleton. The energetics and geometries of the relatively less explored endohedral boranes show that endohedral silaboranes are more stable than the endohedral carbaboranes. In general when an atom is encapsulated in a borane cage its skeletal bonds are elongated. The exo bonds are shortened due to the possible reduction in the torsional strain between the adjacent vertices. A comparison of the endohedral complexes with its exoisomers shows that encapsulation brings in more strain to the system. A qualitative analysis of the relationship between the sandwich systems and the endohedral systems is presented in the first section of the chapter followed by a detailed study on the stability and structure of the relatively unexplored endohedral carbaboranes and silaboranes in the second section.

3.1. The relationship between polyhedral borane sandwiches and endohedral complexes based on their electronic structure

3.1.1. Introduction

Sandwich complexes occupy a prominent place in chemistry. Though a large majority of these are known with Cp^- ($C_5H_5^-$) (Figure 3.1, **1**) and similar planar rings,[1] there are several examples known with polyhedral borane fragments such as the pentagonal pyramidal $C_2B_4H_6^{-2}$ (Figure 3.1, **2,3**),[2-7] the ollide ions $C_2B_9H_{11}^{-2}$ [8-10] and the $B_{11}H_{11}^{-4}$ (Figure 3.1, **5,7**)[11] as ligands. Recognition of the similarity between the frontier orbitals of Cp^- and of the polyhedral fragments $C_2B_9H_{11}^{-2}$ and $C_2B_6H_6^{-2}$ was a turning point in this chemistry.[12] The structural connection between a sandwich complex involving two pentagonal pyramids (Figure 3.1, **3**) and an endohedral icosahedron generated by bringing them closer (Figure 3.1, **9**) cannot be missed. A point of concern is also that there is no sandwich structure of the type **3** available with boron as the central atom. The only sandwich structure with a central boron atom calculated to be a minimum has $Si_3H_3^+$ as ligands.[13] The details of the interaction that precludes **3** with a central boron atom are beginning to be understood.[13] A more general understanding, which examines the interrelationship between the variety of sandwich structures and the corresponding endohedral structures are called for. The requirements for stabilizing sandwich and endohedral complexes involving the main group atoms are studied here based on their electronic structures.

3.1.2. Qualitative analysis of the electronic structure of endohedral and sandwich complexes

The analysis is carried out by constructing a correlation diagram that connects pentagonal pyramidal B_6H_6 fragments, sandwiches of the type **3** (M=Si, B), endohedral

complexes **9** (M=B) and $B_{12}H_{12}^{-2}$ (Figure 3.2). While going from a hypothetical polyhedron made of two pentagonal pyramids with large ring-ring distance (Figure 3.2, B) to a sandwich structure with a large central atom such as silicon (Figure 3.2, C), the -

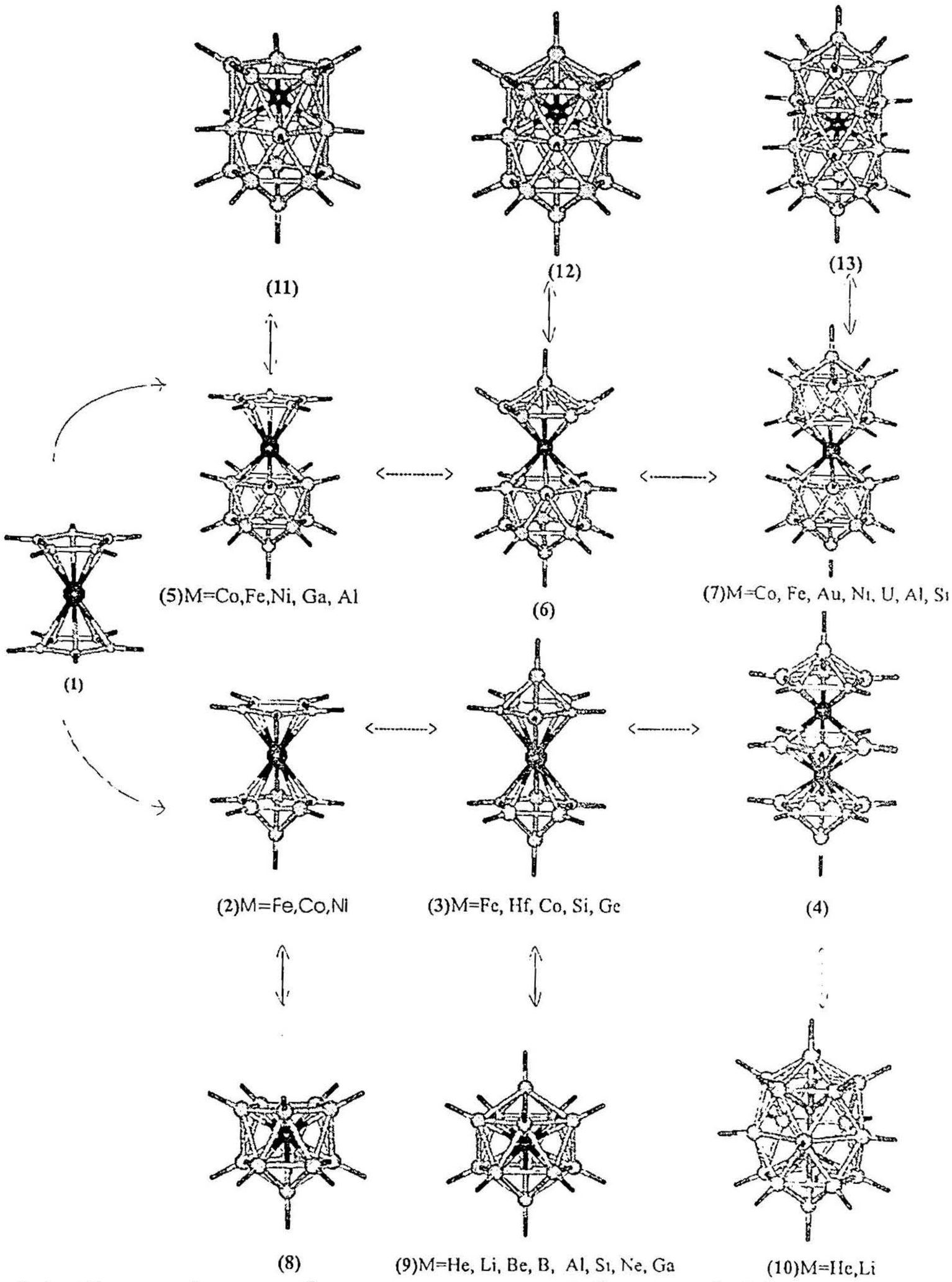

Figure 3.1. The continnum of structures generated from sandwich structures similar to ferrocene and the corresponding endohedral structures. The central atoms of experimentally characterized or theoretically favorable structures are mentioned below each category. Charges of the respective molecules are not given due to the variety in the metal centers.

a_{2u} orbital is significantly stabilized by the favorable interaction with the suitable orbital of the central atom. Many structures of this type are known experimentally.[2-7]

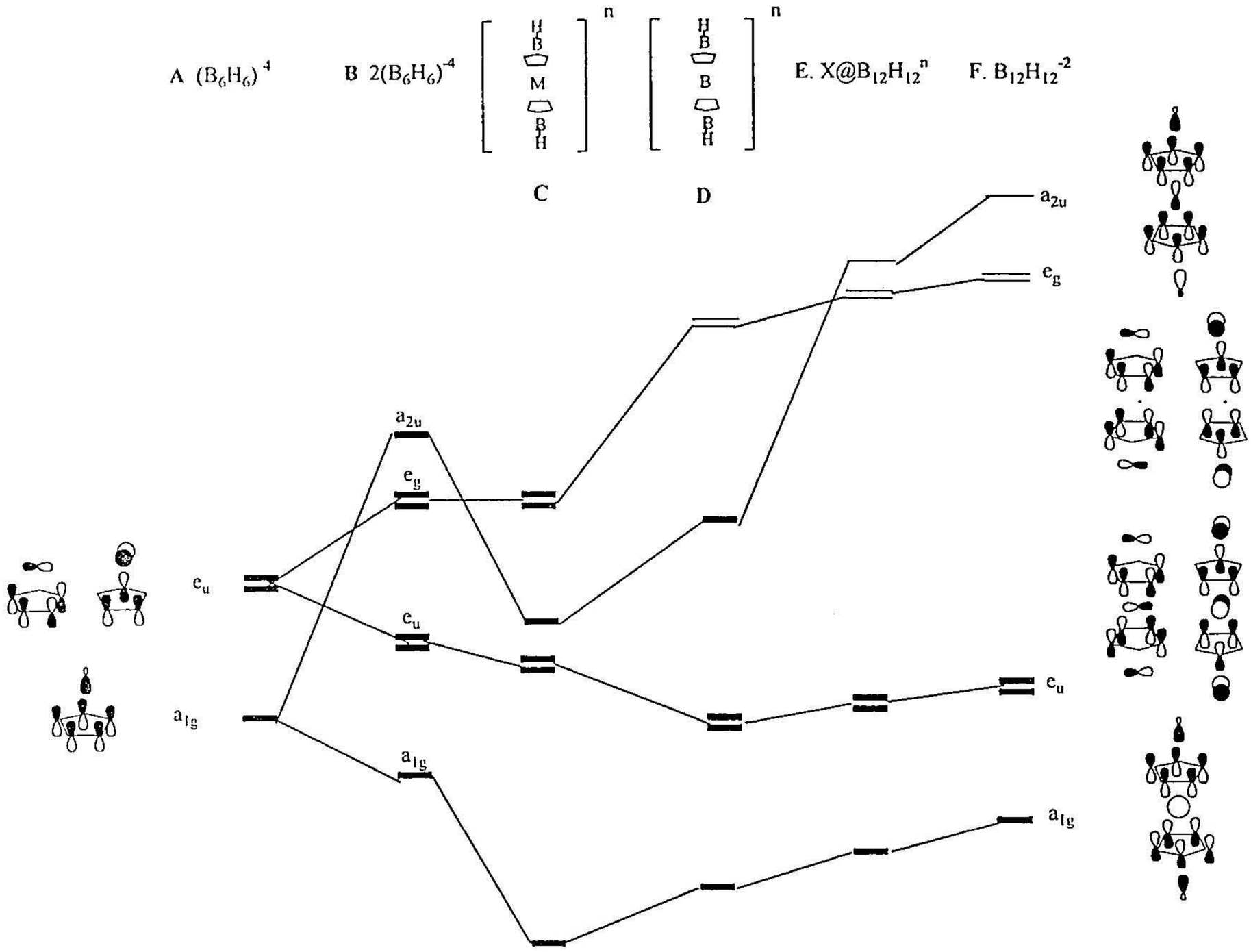

Figure 3.2. Correlation Diagram connecting $2B_6H_6^{-4}$ fragments (A, B), sandwich structures with central atom boron and silicon (C, D), and the endohedral polyhedron (E). F represents the MOs of parent polyhedron, $B_{12}H_{12}^{-2}$. The MOs shown at the right side is that of single atom bridged structures.

Bridging the two pentagonal pyramids by an atom smaller than silicon, for example, boron (Figure 3.2, D), increases the direct unfavorable interactions between the two. Hence a_{2u} and e_g orbitals are pushed up in energy leading to a decreased electronic requirement for the structure. This is in tune with the nonexistence of the sandwich complexes of pure polyhedral boranes. When the rings flanking the central atom are brought closer to result an encapsulated arrangement, the a_{2u} molecular orbital goes up in energy even more

dramatically (Figure 3.2, E). The molecular orbital pattern emerging from this correlation is similar to that of the parent polyhedron without a central atom. Thus, the electronic requirements of the polyhedron do not change by encapsulation. The charge of the endohedral system will differ from the parent cage, reflecting the contribution of the valence electrons of the central atom for skeletal bonding. Hence $B@B_{12}H_{12}$ should have a charge of +1 to compensate the three electrons contributed by the central boron atom to the $B_{12}H_{12}^{-2}$.

The newly established *mno* rule for polyhedral boranes, which is an extension of Wade's rule, explains the HOMO-LUMO separations found for various structures in Figure 3.2.[14] The Walsh diagram connecting the sandwich complex to the corresponding encapsulated polyhedron as a function of ring-ring distance is constructed (Figure 3.3). The stabilization of $1a_{2u}$ and $2e_g$ orbitals in going from the endohedral to the sandwich complex is clear from the diagram. At a ring-ring distance of around 2.6Å or when the bridging atom is small, there is no marked HOMO-LUMO gap since $2e_u$, $1a_{2u}$, $2e_g$ and $3e_g$ are separated by small energies (Figure 3.3) and it is difficult to differentiate the HOMO and LUMO from the Walsh diagram, which shows the variable electronic requirements for such structures. This point corresponds to the boron bridging complexes shown in Figure 3.2, D. A parallel analysis is carried out for the variation of electronic structure for **2**, **5**, **6**, and **7** going to their corresponding endohedral- structures **8**, **11**, **12** and **13**, respectively. The HOMO-LUMO gap and the stabilization of one doubly degenerate and a non-degenerate MO for the sandwich structures are always obtained. Thus, in all the cases the sandwich structures require six electrons more than the endohedral structures. Obviously

the *nido* systems (**2,5**) require 2 more electrons than the *closo*. Examples of complexes (**2**,[15] **3**,[2-7] **5**[16] and **7**[8-10]) are known in the literature.

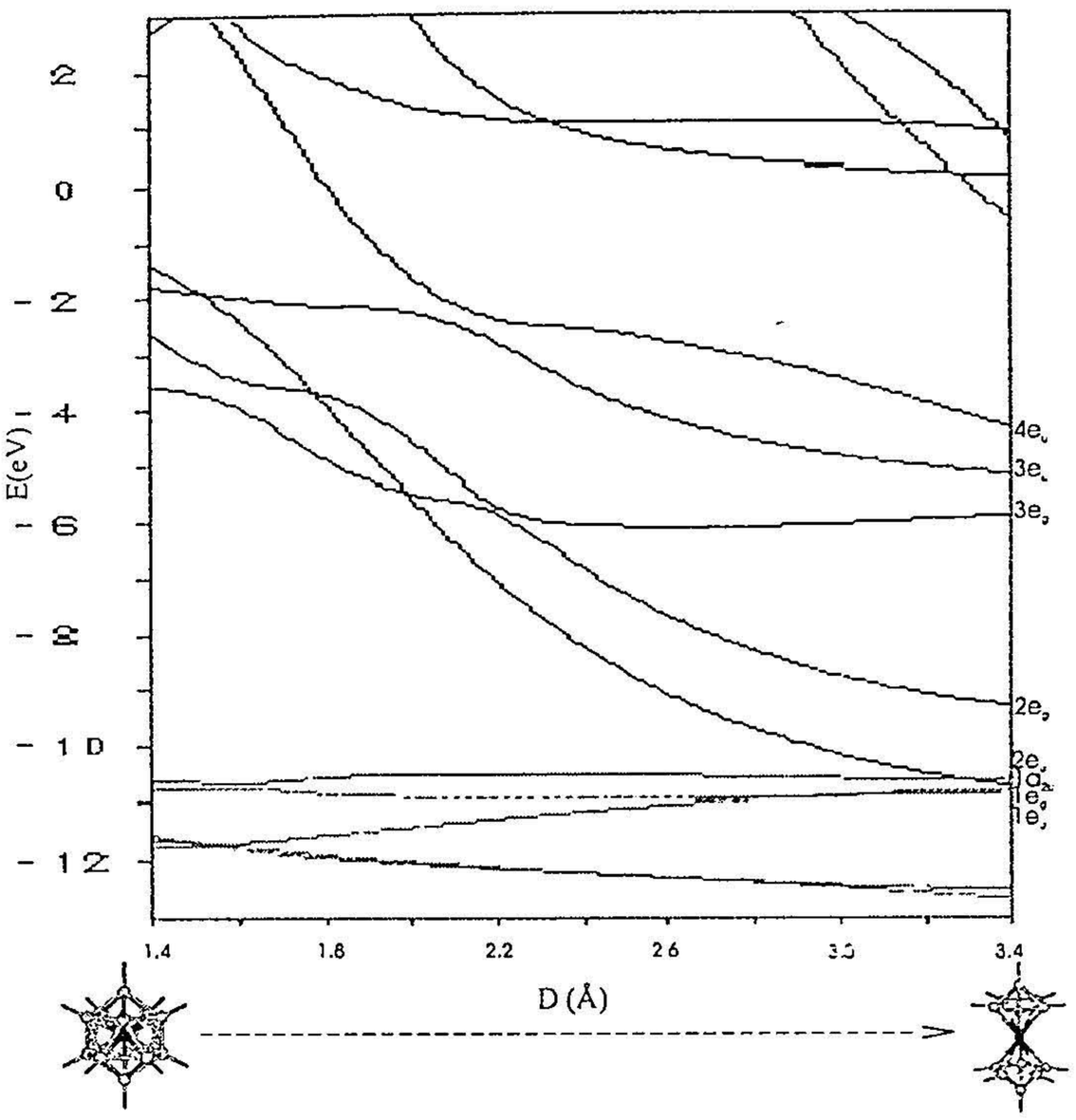

Figure 3.3. The Walsh diagram connecting the encapsulated and single vertex sharing polyhedral $B_{13}H_{12}$ systems. The distance between the two 5-membered rings (D) is plotted along the x-axis. The energy (E) is plotted along the y-axis. e_u is the HOMO of the endohedral system and as the distance between the rings increases gradually e_g and a_{2u} comes down in energy and e_g becomes the HOMO. The optimized structure of the endohedral $B@B_{12}H_{12}^{+}$ is shown.

3.1.3. Extended 2-atom encapsulation

The extension to one more cage will result in structures similar to that in transition metal cluster chemistry. The Walsh diagram for the structure $B_6H_6LiB_5H_5LiB_6H_6$ (**4-Li$_2$**) going to its endohedral analog $Li_2@B_{17}H_{17}$ (**10a-Li$_2$**) is shown in Figure 3.4. The valence electrons of the stuffed atoms satisfy the electronic requirements for the skeletal framework of the polyhedron. As per *mno* rule the structure **4-Li$_2$** requires 24 (3+19+2) electron pairs and the structure **10a-Li$_2$** requires 18 (1+17) electron pairs. BH vertices

provide 17 electron pairs and 2 central lithium atoms together contribute one electron pair in both the structural varieties. Thus, the structure **10a-Li_2** is neutral and the structure **4-Li_2** requires 6 more electron pairs. While going from **10a-Li_2** to **4-Li_2**, the stabilization of two doubly degenerate MOs (2e, 3e) and 2 nondegenerate MOs ($2a_1$, $3a_1$) is obvious from Figure 3.4, which is in agreement with the *mno* rule.

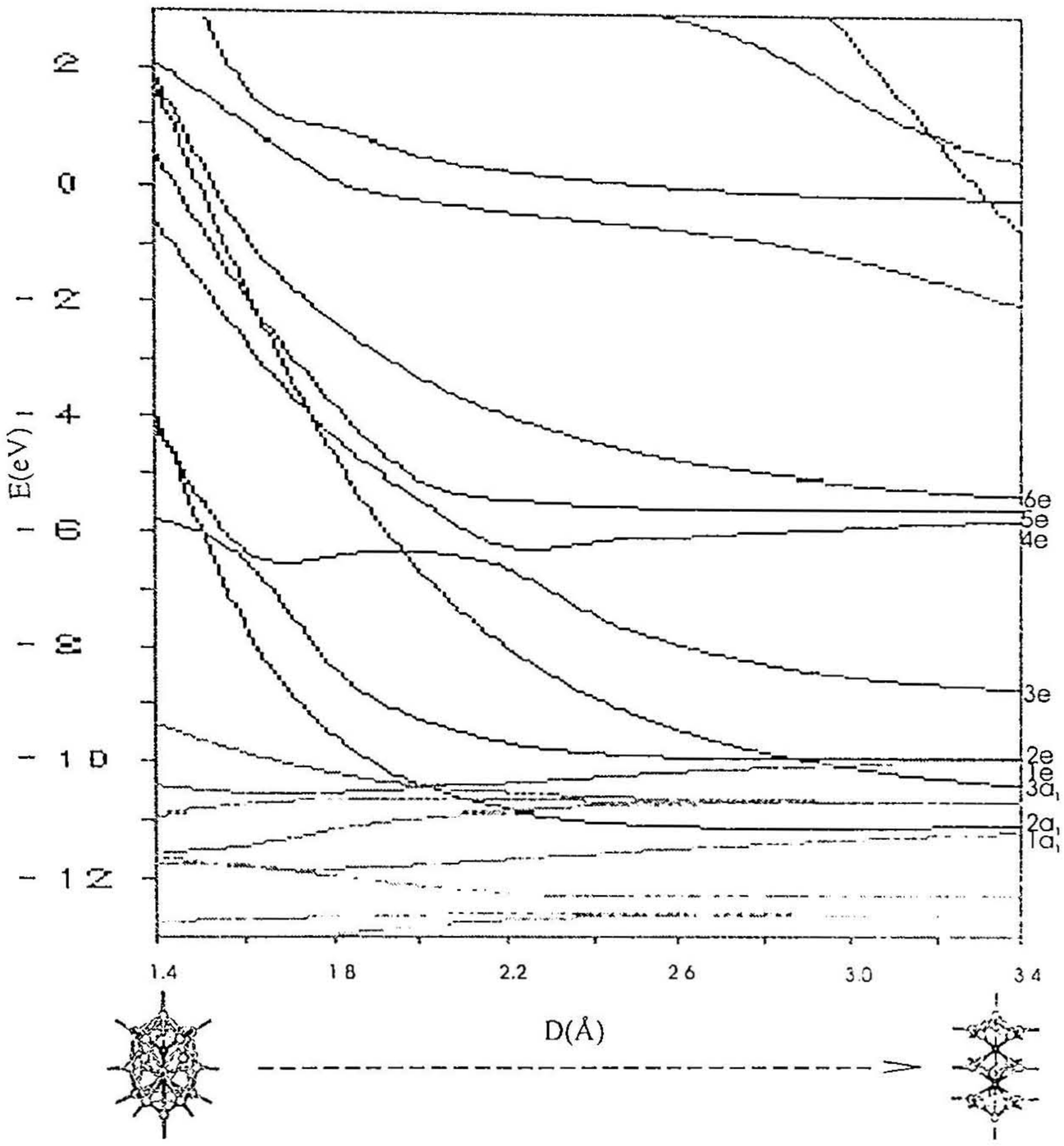

Figure 3.4. The Walsh diagram connecting the three cage single vertex sharing systems [$B_6H_6LiB_5H_5LiB_6H_6$] (**4-Li_2**) and its two atom encapsulated counterparts $Li_2@B_{17}H_{17}$ (**10a-Li_2**). The stabilization of two doubly degenerate MOs (LUMO (2e) and LUMO+1 (3e) of endohedral systems) and two nondegenerate MOs (LUMO+2 ($2a_1$) and another higher lying antibonding orbital ($3a_1$)) in the sandwich structure shows that it requires 6 electron pairs more than the endohedral complex.

3.1.4. Experimental verification

The electronic requirements anticipated by the above analysis are substantiated by the presence of experimentally characterized complexes viz. $[(R_2C_2B_4H_4)Co(C_2B_3H_5)]^-$ **(2)** [15]; $((SiMe_3)_2C_2B_4H_4)_2Si$, $[Li(C_2B_4H_5SiMe_3)_2]^-$, $[((SiMe_3)_2C_2B_4H_4)_2Ga]^-$ **(3)** [2-7]; $[(C_2B_9H_{11})MCp]$[16] (where M=Fe, CO, Ni, Ga, Al) **(5)** and $[(C_2B_9H_{11})_2M]$[8-10] (M=Fe, Co, Ni, Si, Al) **(7)**.

3.1.5. Quantitative verification

The structures $[(C_2B_4H_6)_2Al]^-$ **(3-Al)**, $(C_2B_4H_6)_2Si$ **(3-Si)**, $[(C_2B_4H_6)_2Li]^{-3}$ **(3-Li)** are calculated to be minima on the potential energy surface(PES) with low frequency 27.63, 4.08, and 21.10, respectively (Figure 3.5). The lowest frequencies correspond to the rotation of the rings along the pseudo C_5 axis. But similar sandwich complexes with comparatively smaller atoms as the sharing vertex such as boron and carbon with an identical electron count as that of Al and Si complexes, respectively are found to be higher order saddle points on the PES. This is in accordance with the variable electronic requirements and hence the instability for the structural category of boron bridging complexes in Figure 3.3, D. The unfavorable interactions of these complexes and the high positive charge of the corresponding endohedral isomers (+5 and +6) preclude them experimentally.

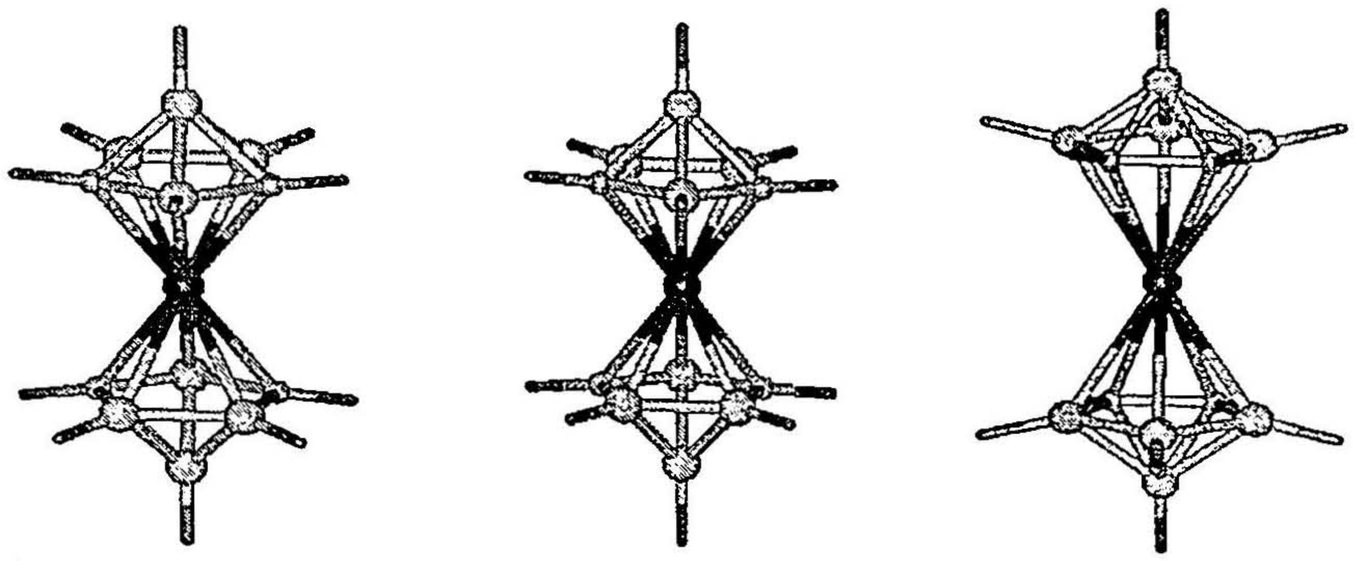

Figure 3.5. The optimized geometries of Si, Al, Li single vertex sharing systems. The total energies (au) and the low frequency values are indicated in the parentheses.

3.1.6. Conclusions

A qualitative analysis explains the electron counts observed for the polyhedral structures with single atom bridging and the corresponding endohedral complexes. Though sandwich complexes are identical to stuffed boranes in molecular composition, the molecular orbital approach shows how it forms a separate class of compounds due to its disparate electronic requirements. The encapsulation does not bring in new molecular orbitals, thus keeping the electron requirement similar to that of the parent polyhedral borane. Multiatom encapsulation in higher cages is found to be favorable on the potential energy surface.

3.2. An analysis on the stability of endohedral carba- and silaboranes, $X@Y_mB_nH_{n+m}^q$ (X=He,Ne,Li,Be; Y=B,C,Si; m=0-3; n=12-9; q=-2 to+2), $(C_2B_4H_6)_2X^q$ (X=Li,Al,Si; q=-3,-1,0), and $X_2@B_{17}H_{17}^q$(X=He,Li; q=-2,0)

3.2.1. Introduction

The icosahedral structure with a central atom belongs to the family of endohedral complexes, which have been studied rigorously during recent years.[17] These are known experimentally with the fullerenes[17a-d] and even with the classical strained hydrocarbon, $C_{20}H_{20}$ with icosahedral symmetry.[17e] To our knowledge, no endohedral complex of

polyhedral borane is reported experimentally even though recent theoretical studies have shown that several of them are minima on their potential energy surface.[18] In view of the many sandwich structures involving the polyhedral fragments, where the central atom belongs to the main group, there is indeed the possibility of generating endohedral structures of the same kind. An encapsulated boron atom inside a polyhedral arrangement is observed in the structure of β-rhombohedral boron.[19] The related $B_{28}H_{18}^{+}$ (C_{3v}) is calculated to be a minimum.[19c]

Icosahedral boranes, carbaboranes, and silaboranes are the stable members of family of polyhedral structures and endohedral complexes are most likely to be generated here. Icosahedral $B_{12}H_{12}^{-2}$ is especially favored because of the orbitals of high symmetry with which the central atom can interact perfectly. Trends in the calculational results of the structures and energies are described. The dependence of the stability of the endohedral boranes on the size of the parent cage as well as the size of the central atom are examined using the mono, di- and tri- substituted twelve vertex carbaboranes and silaboranes varying the central atom (Figure 3.6). A comparison of the relative energies of the stuffed systems with respect to the corresponding exoisomer where the heteroatom caps a face of the polyhedron helps to calibrate the stabilities of various endohedral complexes. Near-isodesmic equations are used to obtain relative preferences in a given series of endohedral complexes.

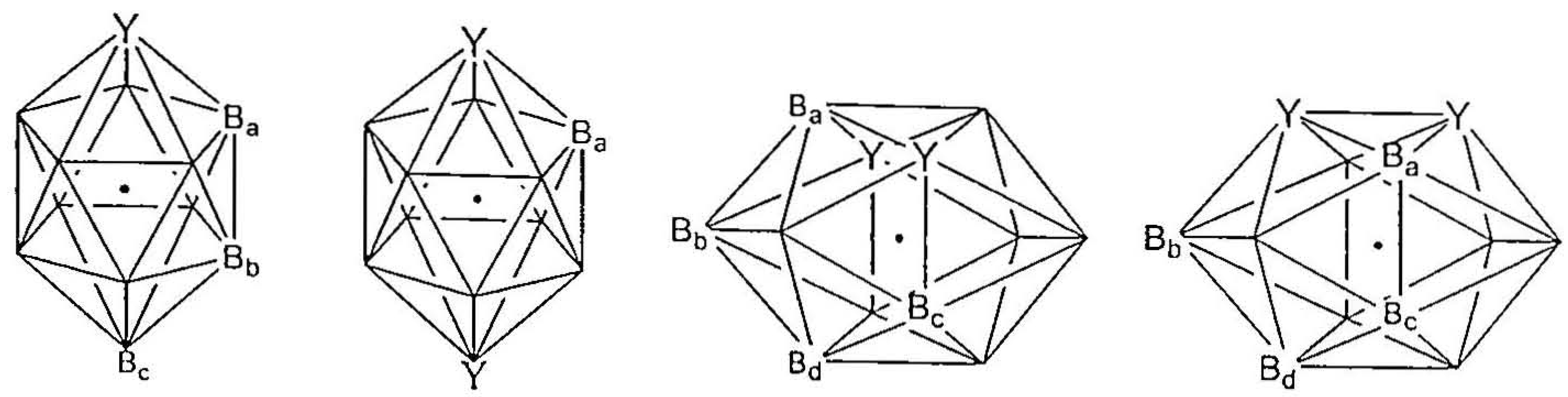

$YB_{11}H_{12}^-$(b,e) p-$Y_2B_{10}H_{12}$(c_1,f_1) m-$Y_2B_{10}H_{12}$(c_2,f_2) o-$Y_2B_{10}H_{12}$(c_3,f_3)

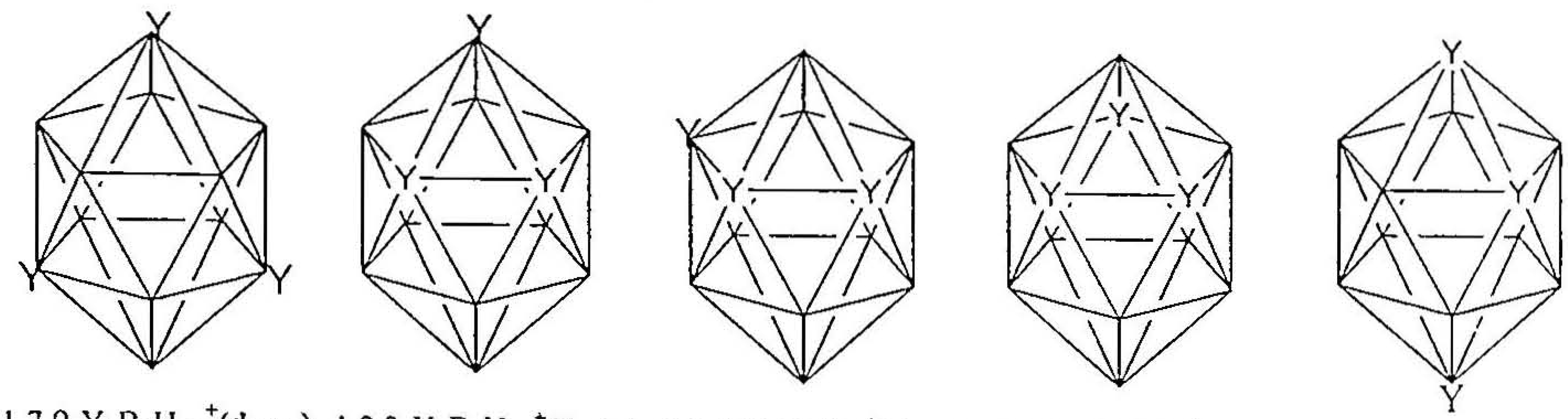

1,7,9-$Y_3B_9H_{12}^+$(d_1,g_1) 1,2,3-$Y_3B_9H_{12}^+$(d_2,g_2) 2,3,4-$Y_3B_9H_{12}^+$(d_3,g_3) 2,4,5-$Y_3B_9H_{12}^+$(d_4,g_4) 1,2,12-$Y_3B_9H_{12}^+$(d_5,g_5)

Figure 3.6. The parent cages along with the vertex symbols used in the text. Y=C, Si. Symbols given in the parentheses are b, for monocarbaborane cage, c for dicarbaboranes and d for tricarbaboranes. Similarly e, f and g represent the mono, di, and trisilaboranes.

3.2.2. Numbering notation

In general the complexes are numbered as N(a-g)-X_n where N corresponds to the number of structure shown in Figure 3.1, X corresponds to the central atom, a-g corresponds to the parent cages (a)$B_{12}H_{12}^{-2}$, (b) $CB_{11}H_{12}^-$, (c) $C_2B_{10}H_{12}$, (d) $C_3B_9H_{12}^+$, (e) $SiB_{11}H_{12}^-$, (f) $Si_2B_{10}H_{12}$, and (g) $Si_3B_9H_{12}^+$ in endohedral complexes. The exohedral isomers are differentiated from the endohedral ones by a prime added at the end of the label. The positional isomers para, meta and ortho of dicarbaborane are identified by the subscripts 1, 2, and 3, respectively and those of tricarbaboranes are given numbers 1 to 5 as is shown in Figure 3.6. Thus, **9a-Li** corresponds to the endohedral complex represented by **9** with the icosahedral $B_{12}H_{12}^{-2}$ skeleton (**a**) with Li^+ inside ($Li@B_{12}H_{12}^-$) and **10a-Li$_2$** stands for $Li_2@B_{17}H_{17}$.

3.2.3. Energetics and geometries

i. Stability order by various equations

The energy involved in the encapsulation (ΔE_{en}) of an atom inside each cage (Figure 3.6) is estimated using the equation,

$$X^a + Y_mB_nH_{n+m}{}^b \text{ ----> } X@Y_mB_nH_{n+m}{}^{a+b} \quad (3.1)$$

Where X = the central atom, Y = B, C or Si. The central atoms are so chosen as to fit within the cavity of a given polyhedral borane. The central atom should not also result in unduly large negative or positive charge to the complex. The total energies for endo and exo- carbaboranes and silaboranes are tabulated in Table 3.1 and Tale 3.2.

The energy of encapsulation, ΔE_{en} obtained from the equation is tabulated in Table 3.3. The varying charge requirements in the different isomers make it difficult to have a uniform comparison across all the isomers using ΔE_{en}. But the endohedral carba- and silaboranes can be compared without any ambiguity. While endohedral interactions are ideal in $B_{12}H_{12}^{-2}$, an external perturbation by substituting boron by a heteroatom such as carbon or silicon causes a reduction in symmetry leading to inequivalent interactions of the orbitals of the central atom with the skeletal orbitals. In addition, substitution of a boron atom by a carbon atom makes the cage size reduce a little thus, making the corresponding endohedral systems more strained. The ΔE_{en} values are 169.8kcal/mol for $He@B_{12}H_{12}^{-2}$ **(9a-He)**, 180.2kcal/mol for the monocarbasubstituted system **(9b-He)** and 191.2 kcal/mol for the dicarbaborane **(9c-He).** Corresponding ΔE_{en} values for the silaboranes are 150.3kcal/mol and 138.1kcal/mol, respectively for **9e-He** and **9f-He** systems. Similar trends continue for Li and Be encapsulation; ΔE_{en} indicates that mono and disilaboranes

with Li and Be as the doped atom ((**9e-Li,9f-Li**); (**9e-Be,9f-Be**)) are more stable than the corresponding stuffed carbaboranes ((**9b-Li, 9c-Li**); (**9b-Be, 9c-Be**)).

Comparison across different endohedral isomers can be done using the near-isodesmic equations,

$$X@B_nH_n^{a-2} + Y_mB_nH_{n+m}^{b} \rightarrow X@Y_mB_nH_{n+m}^{a+b} + B_nH_n^{-2} \quad (3.2)$$

The size of the cage and the size of the central ion play significant role in the energetics of this equation. The He centered cages have a stability order of **9g-He>9f-He>9e-He>9b-He>9c-He>9d-He** which is same as the cage size (Table 3.4). With Li the stability order changes to **9e-Li>9b-Li>9f-Li>9c-Li>9g-Li>9d-Li**. This can be attributed to the smaller size of the Li ion. The size of the lithium ion is such that the lithium encapsulation is more favorable for monosilaboranes, having maximum positive interaction with the orbitals of central atom and skeleton. In disilaboranes due to the large size of the cage, such bonding interactions are reduced. Li stuffed monocarba- and monosilaboranes being neutral are especially important. Similarly for the Be stuffed systems, the order is **9e-Be>9b-Be>9f-Be>9c-Be** identical to that of Li encapsulated systems.

ii. Geometrical features

The steric constraints arising from encapsulation is reflected in the geometrical parameters- skeletal bond lengths (Table 3.5) and the estimated percentage of expansion(Table 3.6). The latter is the percentage change in the distance from the centroid to the atoms on the surface as a result of expansion. The surface B-B distance increases from 1.787Å in $B_{12}H_{12}^{-2}$ to 1.861Å in **9a-He**, 1.874Å in **9a-Li**, 1.871Å in **9a-Be**, 1.859Å in **9a-B** and 1.998Å in **9a-Ne**. In monocarbaborane encapsulated systems the C-B distances

are within the range 1.750-1.900. This is higher than the C-B distance (1.707Å) calculated for the parent cage $CB_{11}H_{12}^-$. Similarly the skeletal B-B bond lengths

Table 3.1a. The total energies[‡] (au), zero point vibration energies (ZPVE, kcal/mol), HOMO-LUMO gap (H-L Gap,eV), charge on the central atom (Q(X)) and the lowest frequency (LF) of endohedral complexes $X@C_nB_{12-n}H_{12}^q$ (X=He,Ne,Li,Be; q = charge of the molecule). The relative energies among the various isomers are given in the parentheses wherever necessary.

No.	*Isomer(No.)*	*Symmetry*	*Energy,au(RE,Kcal /mol)*	*ZPVE(k cal/mol)*	*H-L Gap(eV)*	*Q(X)*	*LF*
9a-He	$He@B_{12}H_{12}^{-2}$	I_h	-308.326599	106.73	8.44	0.10	437.8
9b-He	$He@CB_{11}H_{12}^-$	C_1	-321.614225	110.37	8.17	0.10	390.7
$9c_1$-He	$He@p\text{-}C_2B_{10}H_{12}$	D_{5d}	-334.737114(0.0)	113.21	7.92	0.10	354.6
$9c_2$-He	$He@m\text{-}C_2B_{10}H_{12}$	C_{2v}	-334.729926(4.51)	113.30	7.94	0.10	350.7
$9c_3$-He	$He@o\text{-}C_2B_{10}H_{12}$	C_{2v}	-334.712837(15.23)	112.89	7.84	0.10	359.4
$9d_1$-He	$He@1,7,9\text{-}C_3B_9H_{12}^+$	C_{3v}	-347.681760(0.0)	115.02	8.00	0.10	324.3
$9d_2$-He	$He@1,2,3\text{-}C_3B_9H_{12}^+$	C_{3v}	-347.616409(41.0)	113.74	7.41	0.10	297.6
$9d_3$-He	$He@2,3,4\text{-}C_3B_9H_{12}^+$	C_s	-347.637524(27.8)	114.28	7.47	0.10	325.1
$9d_4$-He	$He@2,4,5\text{-}C_3B_9H_{12}^+$	C_s	-347.660395(13.4)	114.50	7.77	0.10	318.8
$9d_5$-He	$He@1,2,12\text{-}C_3B_9H_{12}^+$	C_s	-347.662260(12.2)	114.54	7.58	0.10	315.2
9a-Li	$Li@B_{12}H_{12}^-$	I_h	-313.133455	106.79	8.50	-2.77	414.3
9b-Li	$Li@CB_{11}H_{12}$	C_{5v}	-326.241299	108.97	8.15	-2.54	357.8
$9c_1$-Li	$Li@p\text{-}C_2B_{10}H_{12}^+$	D_{5d}	-339.179215(0.0)	110.34	7.82	-2.39	306.1
$9c_2$-Li	$Li@m\text{-}C_2B_{10}H_{12}^+$	C_{2v}	-339.178721(0.3)	110.73	7.80	-2.37	319.5
$9c_3$-Li	$Li@o\text{-}C_2B_{10}H_{12}^+$	C_s	-339.157362(13.7)	110.43	7.79	-2.38	307.3
$9d_1$-Li	$Li@1,7,9\text{-}C_3B_9H_{12}^{+2}$	C_{3v}	-351.937654(0.0)	110.83	7.79	-2.23	257.1
$9d_2$-Li	$Li@1,2,3\text{-}C_3B_9H_{12}^{+2}$	C_{3v}	-351.874829(39.4)	109.61	7.46	-2.24	211.8
$9d_3$-Li	$Li@2,3,4\text{-}C_3B_9H_{12}^{+2}$	C_s	-351.895419(26.5)	110.15	7.34	-2.24	258.2
$9d_4$-Li	$Li@2,4,5\text{-}C_3B_9H_{12}^{+2}$	C_s	-351.913736(15.01)	110.57	7.60	-2.23	253.5
$9d_5$-Li	$Li@1,2,12\text{-}C_3B_9H_{12}^{+2}$	C_s	-351.917648(12 6)	110.42	7.66	-2.24	250.8
9a-Be	$Be@B_{12}H_{12}$	I_h	-320.273374	105.66	8.68	1.08	409.7
9b-Be	$Be@CB_{11}H_{12}^+$	C_{5v}	-333.200342	106.55	8.26	1.33	340.4
$9c_1$-Be	$Be@p\text{-}C_2B_{10}H_{12}^{+2}$	D_{5d}	-345.948543(1.46)	106.24	7.83	1.42	267.2
$9c_2$-Be	$Be@m\text{-}C_2B_{10}H_{12}^{+2}$	C_{2v}	-345.950874(0.0)	106.50	7.82	1.45	276.7
$9c_3$-Be	$Be@o\text{-}C_2B_{10}H_{12}^{+2}$	C_s	-345.931086(12.41)	106.23	7 82	1.45	279.8
9a-B	$B@B_{12}H_{12}^+$	I_h	-329.961162	100.75	7.97	0.37	214.9
9a-Ne	$Ne@B_{12}H_{12}^{-2}$	I_h	-433.948481	97.12	7.51	0.09	290.1
9b-Ne	$Ne@CB_{11}H_{12}^-$	C_{5v}	-447.213398	99.57	7.19	0.08	86.8
9a-Ga	$Ga@B_{12}H_{12}^+$	I_h	-2227.892117	104.47	7.68	-4.34	145.3
9a-Si	$Si@B_{12}H_{12}^{+2}$	I_h	-593.993353	95.69	8.05	1.31	219.8
10a-He_2	$He_2@B_{17}H_{17}^{-2}$	C_s	-438.409278	153.25	5.86	0.07	129.9
10a-Li_2	$Li_2@B_{17}H_{17}$	C_s	-447.717853	150.79	6.22	0.66	87.0
3Al	$[(C_2B_4H_6)_2Al]^-$	C_{2h}	-601.094016	110.62	2.11	-0.04	4.1
3Si	$[(C_2B_4H_6)_2Si]$	C_{2h}	-648.009730	111.83	6.25	0.53	27.6
3Li	$[(C_2B_4H_6)_2Li]^{-3}$	C_{2h}	-365.800723	104.61	4.68	-0.53	21.1

[‡]The additional total energies required for the equations are $B_{12}H_{12}^{-2}$ -305.69021; $B_{17}H_{17}^{-2}$ -432.99603 (A. M. Mebel, K. Najafian, P.v R.Schleyer: Inorg. Chem. 1998, 37, 6765); $CB_{11}H_{12}^-$ -318.994288; p-$C_2B_{10}H_{12}$ -332.134854; m-$C_2B_{10}H_{12}$ -332.130514; o-$C_2B_{10}H_{12}$ -332.104338 (E. D. Jemmis, B. Kiran: J. Am. Chem. Soc., 1997, 119, 4076); 1,7,9-$C_3B_9H_{12}^+$ -345.092057; 1,2,3-$C_3B_9H_{12}^+$ -345.013573; 2,3,4-$C_3B_9H_{12}^+$ -345.039338; 2,4,5-$C_3B_9H_{12}^+$ -345.065683; 1,2,12-$C_3B_9H_{12}^+$ -345.070426 (E. D Jemmis, M. Ramalingam, E. G. Jayasree: J Comput. Chem. 2001,22,1542.)

are in the range 1.840-2.050 where for the parent system the B-B bond length is well below 1.800Å. Similar lengthening of skeletal bonds occurs in all the cages.

Table 3.1b. The total energies (au), zero point vibration energies (ZPVE, kcal/mol), the strain energy, the difference between endo and exo isomers (SE), HOMO-LUMO gap (H-L Gap, eV), charge on the central atom (Q(X)) and the lowest frequency (LF) of exo isomers $XC_nB_{12-n}H_{12}^q$(X=He,Ne,Li,Be; q = charge of the molecule). The relative energies are given in the parentheses wherever necessary.

No	*Isomer*	*Symmetry*	*Energy,au(RE,kcal/mol*	*ZPVE(kcal/mol)*	*SE(kcal/mol*	*H-L Gap(eV)*	*Q(X)*	*LF*
9a-He'	$HeB_{12}H_{12}^{-2}$	C_{3v}	-308.597321	104.98	169.88	9.00	0.00	10.4
9b-He'	$HeCB_{11}H_{12}^{-}$	C_s	-321.901584	109.04	180.31	8.79	0.00	20 1
$9c_1$-He'	Hep-$C_2B_{10}H_{12}$	C_s	-335.041869(0.0)	112.01	191.23	8.59	0 00	-32 4
$9c_2$-He'	Hem-$C_2B_{10}H_{12}$	C_s	-335.037518(2.7)	111.81	193.01	8 53	0 00	-18 9
$9c_3$-He'	Heo-$C_2B_{10}H_{12}$	C_s	-335.01165(19.0)	111.48	187.50	8.34	0 00	-17 5
$9d_1$-He'	He1,7,9-$C_3B_9H_{12}^{+}$	C_s	-347.999407(0.0)	113.82	199.32	8.49	0 00	11 9
$9d_2$-He'	He1,2,3-$C_3B_9H_{12}^{+}$	C_s	-347.920910(49.3)	112.63	191.07	7.79	0 00	11 2
$9d_3$-He'	He2,3,4-$C_3B_9H_{12}^{+}$	C_s	-347.946411(33.3)	113.00	193.83	7.93	0 00	-26 7
$9d_4$-He'	He2,4,5- $C_3B_9H_{12}^{+}$	C_s	-347.972982(16.6)	113.47	196.15	8.36	0 00	-7 0
$9d_5$-He'	He1,2,12-$C_3B_9H_{12}^{+}$	C_s	-347.977772(13.6)	113.51	197.98	8.18	0 00	-16 2
9a-Li'	$LiB_{12}H_{12}^{-}$	C_{3v}	-313.318124	107.32	115.88	4 34	0 06	256 7
9b-Li'	$LiCB_{11}H_{12}$	C_s	-326.480831	110.84	150.31	6 02	0 25	210 9
$9c_1$-Li'	Lip-$C_2B_{10}H_{12}^{+}$	C_s	-339.464667(3.4)	112.72	179.12	7.37	0 49	140 3
$9c_2$-Li'	Lim-$C_2B_{10}H_{12}^{+}$	C_s	-339.470142(0.0)	112.74	182.87	7.68	0.46	139 0
$9c_3$-Li'	Lio-$C_2B_{10}H_{12}^{+}$	C_s	-339.440806(18.4)	112.30	177.86	7.36	0 47	129 7
$9d_1$-Li'	Li1,7,9-$C_3B_9H_{12}^{+2}$	C_s	-352.372334(0.0)	113.64	272.76	6.86	1 00	-20 0
$9d_2$-Li'	Li1,2,3-$C_3B_9H_{12}^{+2}$	C_s	-352.225726(92.0)	112.67	220.19	8.01	0 70	59 0
$9d_3$-Li'	Li2,3,4-$C_3B_9H_{12}^{+2}$	C_s	-352.308514(40.1)	112.97	259.22	6.61	1 00	-3 3
$9d_4$-Li'	Li2,4,5-$C_3B_9H_{12}^{+2}$	C_s	-352.333605(24.3)	113.47	263.47	6.70	1.00	6 07
$9d_5$-Li'	Li1,2,12-$C_3B_9H_{12}^{+2}$	C_s	-352.340132(20.2)	113.44	265.11	6.76	1 00	-15 0
9a-Be'	$BeB_{12}H_{12}$	C_{3v}	-320.366166	108.45	58.23	3.87	0.05	406 8
9b-Be'	$BeCB_{11}H_{12}^{+}$	C_s	-333.356353	111.38	97.90	4.56	0 22	398 1
$9c_1$-Be'	Bep-$C_2B_{10}H_{12}^{+2}$	C_s	-346.140060(11.4)	112.07	120.17	7.11	0 45	362 5
$9c_2$-Be'	Bem-$C_2B_{10}H_{12}^{+2}$	C_s	-346.158195(0.0)	112.52	130.10	5.30	0 44	361 8
$9c_3$-Be'	Beo-$C_2B_{10}H_{12}^{+2}$	C_s	-346 126925(19.6)	111.98	122.89	4.93	0 42	352 7
9a-B'	$BB_{12}H_{12}^{+1}$	C_{3v}	-330.057921	106.21	60.72	3.34	0 40	428 0
9a-Ne'	$NeB_{12}H_{12}^{-2}$	C_{3v}	-434.587324	105.30	400.87	9.00	0 02	47 5
9b-Ne'	$NeCB_{11}H_{12}$	C_s	-447.891856	109.25	425.73	8 79	0 22	51 2
9a-Ga'	$GaB_{12}H_{12}^{+}$	C_{3v}	-2228.195507	100.50	190.38	2.40	0 55	-207 1
9a-Si'	$SiB_{12}H_{12}^{+2}$	C_{3v}	-594.237695	99.34	153.33	2 76	0 97	-115 4
10a-He_2'	$He_2B_{17}H_{17}^{-2}$	C_2	-438.809797	150.13	251.33	7.05	0 00	-17 9
10a-Li_2'	$Li_2B_{17}H_{17}$	C_2	-448.086404	154.11	231.27	5.16	0 25	169 8

The percentage of expansion shows that in carbaboranes the largest expansion is observed at the C-H vertex (Table 3.6). The vertex near to the carbon shows a larger expansion among the B-H vertices. As one goes to a vertex which is far from the substituted site the percentage of expansion gets reduced. In silaboranes this trend is

reversed. This shows that the endohedral system adjusts itself to attain a nearly spherical shape so as to enhance the interaction between the orbitals and hence the stability.

Table 3.2a. The total energies[‡] (au), zero point vibration energies(ZPVE, kcal/mol), HOMO-LUMO gap(H-L Gap,eV), charge on the central atom (Q(X)) and the lowest frequency (LF) of $X@Si_nB_{12-n}H_{12}^{q}$ (X=He,Li,Be; q=charge of the molecule). The relative energies are given in the parentheses wherever necessary.

No.	*Isomer*	*Symmetry*	*Energy(au)*	*ZPVE(k cal/mol)*	*H-L Gap(eV)*	*Q(X)*	*LF*
9e-He	$He@SiB_{11}H_{12}^-$	C_{5v}	-573.027881	105.13	7.45	0.10	325.0
$9f_1$-He	$He@p\text{-}Si_2B_{10}H_{12}$	D_{5d}	-837.559458(2.6)	102.68	7.36	0.09	279.2
$9f_2$-He	$He@m\text{-}Si_2B_{10}H_{12}$	C_{2v}	-837.563588(0.0)	102.66	6.31	0.09	177.1
$9f_3$-He	$He@o\text{-}Si_2B_{10}H_{12}$	C_s	-837.563021(0.4)	102.80	6.77	0.09	250.1
$9g_1$-He	$He@1,7,9\text{-}Si_3B_9H_{12}^+$	C_{3v}	-1101.937307(1.9)	99.42	6.10	0.09	178.4
$9g_2$-He	$He@1,2,3\text{-}Si_3B_9H_{12}^+$	C_{3v}	-1101.939681(0.4)	99.88	7.53	0.08	241.0
$9g_3$-He	$He@2,3,4\text{-}Si_3B_9H_{12}^+$	C_s	-1101.940253(0.0)	99.58	7.30	0.08	165.8
$9g_4$-He	$He@2,4,5\text{-}Si_3B_9H_{12}^+$	C_s	-1101.934355(3.7)	99.61	7.17	0.09	142.7
$9g_5$-He	$He@1,2,12\text{-}Si_3B_9H_{12}^+$	C_s	-1101.937203(1.9)	99.39	6.62	0.08	168.6
9e-Li	$Li@SiB_{11}H_{12}$	C_{5v}	-577.647834	104.29	6.76	-2.50	309.1
$9f_1$-Li	$Li@p\text{-}Si_2B_{10}H_{12}^+$	D_{5d}	-842.005437(0.0)	100.96	6.53	-2.27	258.0
$9f_2$-Li	$Li@m\text{-}Si_2B_{10}H_{12}^+$	C_{2v}	-842 005406(0.02)	100.86	5.63	-2.26	204.5
$9f_3$-Li	$Li@o\text{-}Si_2B_{10}H_{12}^+$	C_{2v}	-842.002047(2.1)	100.80	6.81	-2.23	229.8
$9g_1$-Li	$Li@1,7,9\text{-}Si_3B_9H_{12}^{+2}$	C_{3v}	-1106.213376(0.0)	96.68	7.03	-2.06	195.6
$9g_2$-Li	$Li@1,2,3\text{-}Si_3B_9H_{12}^{+2}$	C_{3v}	-1106.205720(4.8)	96.55	6.71	-2.00	196.9
$9g_3$-Li	$Li@2,3,4\text{-}Si_3B_9H_{12}^{+2}$	C_s	-1106.206511(4.3)	96.50	5.82	-2.00	147.7
$9g_4$-Li	$Li@2,4,5\text{-}Si_3B_9H_{12}^{+2}$	C_s	-1106.207960(3.4)	96.81	6.50	-2.04	183.5
$9g_5$-Li	$Li@1,2,12\text{-}Si_3B_9H_{12}^+$	C_s	-1106.209526(2.4)	96.53	6.66	-2 04	170.7
9e-Be	$Be@SiB_{11}H_{12}^+$	C_{5v}	-584.610558	102.05	7.04	1.31	301.5
$9f_1$-Be	$Be@p\text{-}Si_2B_{10}H_{12}^{+2}$	D_{5d}	-848.794720(1.9)	97.58	6.58	1.29	241.8
$9f_2$-Be	$Be@m\text{-}Si_2B_{10}H_{12}^{+2}$	C_{2v}	-848.797677(0.0)	97.70	6.77	1.32	237.7
$9f_3$-Be	$Be@o\text{-}Si_2B_{10}H_{12}^{+2}$	C_{2v}	-848.792394(3.3)	97.55	6.18	1.17	220.1

[‡] The additional total energies required for equations are $SiB_{11}H_{12}^-$ -570.365124; $p\text{-}Si_2B_{10}H_{12}$ -570.365124; $m\text{-}Si_2B_{10}H_{12}$ -834 877723, $o\text{-}Si_2B_{10}H_{12}$ -834.873540 (E D. Jemmis, B. Kiran: J. Am. Chem. Soc., 1997, 119, 4076.); $1,7,9\text{-}Si_3B_9H_{12}^+$ -1099 232179, $1,2,3\text{-}Si_3B_9H_{12}^+$ -1099 226018; $2,3,4\text{-}Si_3B_9H_{12}^+$ -1099.224193 (this study)

Another interesting geometrical feature shown by all the structures is the reduction of the exohedral X-H bonds by the introduction of a central atom. The orbitals of the central atom are found to stabilize some of the bonding molecular orbitals of the cage.[18a] Delocalization of electrons from these exo bonds to the central atom is expected to lengthen the X-H bonds. However, the observed reduction may be attributed to a reduction in the H-X-X-H torsional forces, which would stretch the X-H bonds. Longer X-X distance reduces the torsional strain, leading to a decrease in the X-H bonds. This

reduction of X-H bonds is contrary to endohedral dodecahedrane where lithium insertion shrinks the cage and elongates the exo bonds.[20] This contrasting behavior results from the saturated nature of the $C_{20}H_{20}$ skeleton, the extra electron brought by encapsulation of Li occupies a molecular orbital which is the bonding combination of the C-H σ* orbitals. In polyhedral boranes, the process of encapsulation enlarges the cage thus increasing the -

Table 3.2b. The energies(au), zero point vibration energies(kcal/mol), HOMO-LUMO gap(H-L Gap,eV), charge on the central atom (Q(X)) and the lowest frequency (LF) of $XSi_nB_{12-n}H_{12}^q$(X=He,Li,Be; q=charge of the molecule). The relative energies are given in the parentheses wherever necessary.

No.	*Isomer*	*Symmetry*	*Energy(au)*	*ZPVE(kcal/mol)*	SE	*H-L Gap(eV)*	*Q(X)*	*LF*
9e-He'	$HeSiB_{11}H_{12}^-$	C_s	-573.272118	103.30	153.26	7.77	0.00	-15.0
$9f_1$-He'	Hep-$Si_2B_{10}H_{12}$	C_s	-837.784746(0.0)	100.74	141.37	7.70	0.00	-22.8
$9f_2$-He'	Hem-$Si_2B_{10}H_{12}$	C_s	-837.783644(0.69)	100.78	138.09	7.62	0.00	12.0
$9f_3$-He'	Heo-$Si_2B_{10}H_{12}$	C_s	-837.780544(2.6)	100.73	136.50	6.91	0.00	-32.6
$9g_1$-He'	He1,7,9-$Si_3B_9H_{12}^+$	C_s	-1102.139225(0.0)	97.52	126.70	7.40	0.00	-17.0
$9g_2$-He'	He1,2,3-$Si_3B_9H_{12}^+$	C_s	-1102.133134(3.8)	97.55	121.39	6.83	0.00	-8.98
$9g_3$-He'	He2,3,4- $Si_3B_9H_{12}^+$	C_s	-1102 131276(5.0)	97.52	119.87	6.39	0.00	-16 2
$9g_4$-He'	He2,4,5-$Si_3B_9H_{12}^+$	C_s	-1102.134649(2.9)	97.69	125.68	6.76	0.00	22.37
$9g_5$-He'	He1,2,12-$Si_3B_9H_{12}^+$	C_s	-1102.136750(1.6)	97.59	125.22	6.92	0.00	-27.5
9e-Li'	$LiSiB_{11}H_{12}$	C_s	-577.853047	105.16	128.77	6.01	0 25	223 1
$9f_1$-Li'	Lip-$Si_2B_{10}H_{12}^+$	C_s	-842.219195(5.5)	101.75	134.13	6.97	0.43	148 4
$9f_2$-Li'	Lim-$Si_2B_{10}H_{12}^+$	C_s	-842.227934(0.0)	102.01	139.64	7.21	0.41	170.4
$9f_3$-Li'	Lio-$Si_2B_{10}H_{12}^+$	C_s	-842.218991(5.6)	101.86	136.13	6.76	0.44	119.2
$9g_1$-Li'	Li1,7,9-$Si_3B_9H_{12}^{+2}$	C_{3v}	-1106.450571(3.0)	98 11	148.84	7.42	0.61	101.5
$9g_2$-Li'	Li1,2,3-$Si_3B_9H_{12}^{+2}$	C_s	-1106 455410(0 0)	98.20	156.68	6.80	0 62	97 0
$9g_3$-Li'	Li2,3,4- $Si_3B_9H_{12}^{+2}$	C_s	-1106.450856(2.9)	98.13	153.33	6.54	0.66	44 3
$9g_4$-Li'	Li2,4,5-$Si_3B_9H_{12}^{-2}$	C_s	-1106 449588(3.7)	98.00	151.62	6.84	0.65	-49 1
$9g_5$-Li'	Li1,2,12-$Si_3B_9H_{12}^+$	C_s	-1106.447016(5 3)	97.83	149 03	6 84	0 64	-10 9
9e-Be'	$BeSiB_{11}H_{12}^+$	C_s	-584.737521	105.85	79.67	4.48	0.20	345.1
$9f_1$-Be'	Bep-$Si_2B_{10}H_{12}^{+2}$	C_s	-848.930509(10 9)	102 06	85.21	4.63	0 35	297 8
$9f_2$-Be'	Bem-$Si_2B_{10}H_{12}^{+2}$	C_s	-848 947939(0.0)	102.31	94.29	4.85	0.35	264.7
$9f_3$-Be'	Beo-$Si_2B_{10}H_{12}^{+2}$	C_s	-848 932801(9.5)	101.97	88.11	4.69	0.34	257.1

Table 3.3a. The energy of encapsulation (kcal/mol) of stuffed systems as obtained from the equation, $X^a + Y_mB_nH_{n+m}^b$ ----> $X@Y_mB_nH_{n+m}^{a+b}$

Where X = the central atom, Y = hetero atom on the borane cage, C/Si

a, b, and a+b are the respective charges on the systems.

X	$B_{12}H_{12}^{-2}$	$CB_{11}H_{12}^-$	$C_2B_{10}H_{12}$	$C_3B_9H_{12}^{+1}$	$SiB_{11}H_{12}^-$	$Si_2B_{10}H_{12}$	$Si_3B_9H_{12}^{+1}$
He	169.8	180.2	191.2	199.1	150.3	138.1	119.9
Ne	399.1	423.7	----	----	----	----	----
Li^+	-99.6	23.6	150.7	275.4	1.2	98.4	190.4
Be^{+2}	-584.2	-347.5	-105.5	----	-372.2	-168.7	----

ΔE_{en} value in addition are $B@B_{12}H_{12}^+$ -1413.6; $Ga@B_{12}H_{12}^-$ -898.7; $Si@B_{12}H_{12}^{+2}$ -1723.6

Table 3.3b. The energy of capping (kcal/mol) of systems as obtained from the equation,

$X^a + Y_mB_nH_{n+m}^b$ ----> $XY_mB_nH_{n+m}^{a+b}$

Where X = the capping atom, Y = hetero atom on the borane cage, C/Si

a, b, and a+b are the respective charges on the systems.

X	$B_{12}H_{12}^{-2}$	$CB_{11}H_{12}^-$	$C_2B_{10}H_{12}$	$C_3B_9H_{12}^{+1}$	$SiB_{11}H_{12}^-$	$Si_2B_{10}H_{12}$	$Si_3B_9H_{12}^{+1}$
He	-0.04	-0.2	0.02	-0.19	0.03	0.02	0.002
Ne	-1.7	-2.0	---	---	---	---	---
Li^+	-215.5	-126.8	-34.6	2.7	-127.6	-41.9	34.6
Be^{+2}	-642.4	-445.4	-235.6	---	-451.9	-263.0	---

ΔE_{en} value in addition are $B_{13}H_{12}^+$ -1474.3; $GaB_{12}H_{12}^+$ -1089.0 $SiB_{12}H_{12}^{+2}$ –1876.9

Table 3.4. The ΔE values obtained from the near isodesmic equations of the form

$X@B_nH_n^{a-2} + Y_mB_nH_{n+m}^b \rightarrow X@Y_mB_nH_{n+m}^{a+b} + B_nH_n^{-2}$

Where X = the central atom, Y = hetero atom on the borane cage, C/Si

and a-2, a+b, and b are the charges on the system.

L H S		R H S		ΔE (kcal/mol)
$He@B_{12}H_{12}^{-2}$	$CB_{11}H_{12}^-$	$He@CB_{11}H_{12}^-$	$B_{12}H_{12}^{-2}$	10.32
$He@B_{12}H_{12}^{-2}$	p-$C_2B_{10}H_{12}$	He@p-$C_2B_{10}H_{12}$	$B_{12}H_{12}^{-2}$	21.42
$He@B_{12}H_{12}^{-2}$	1,7,9-$C_3B_9H_{12}^+$	He@1,7,9-$C_3B_9H_{12}^+$	$B_{12}H_{12}^{-2}$	29.30
$He@B_{12}H_{12}^{-2} > He@CB_{11}H_{12}^- >$ He@p-$C_2B_{10}H_{12}$>He@1,7,9-$C_3B_9H_{12}^+$				
$Li@B_{12}H_{12}^-$	$CB_{11}H_{12}^-$	$Li@CB_{11}H_{12}$	$B_{12}H_{12}^{-2}$	123.14
$Li@B_{12}H_{12}^-$	p-$C_2B_{10}H_{12}$	Li@p-$C_2B_{10}H_{12}^+$	$B_{12}H_{12}^{-2}$	250.30
$Li@B_{12}H_{12}^-$	1,7,9-$C_3B_9H_{12}^+$	Li@1,7,9-$C_3B_9H_{12}^{+2}$	$B_{12}H_{12}^{-2}$	375.02
$Li@B_{12}H_{12}^- >$ $Li@CB_{11}H_{12} >$ Li@p-$C_2B_{10}H_{12}^+$>Li@1,7,9-$C_3B_9H_{12}^{+2}$				
$Be@B_{12}H_{12}$	$CB_{11}H_{12}^-$	$Be@CB_{11}H_{12}^+$	$B_{12}H_{12}^{-2}$	236.64
$Be@B_{12}H_{12}$	m-$C_2B_{10}H_{12}$	Be@m-$C_2B_{10}H_{12}^{+2}$	$B_{12}H_{12}^{-2}$	478.66
$Be@B_{12}H_{12} > Be@CB_{11}H_{12}^+ >$ Be@m-$C_2B_{10}H_{12}^{+2}$				
$Ne@B_{12}H_{12}^{-2}$	$CB_{11}H_{12}^-$	$Ne@CB_{11}H_{12}^-$	$B_{12}H_{12}^{-2}$	24.58
$Ne@B_{12}H_{12}^{2-} > Ne@CB_{11}H_{12}^-$				
$He@B_{12}H_{12}^{-2}$	$SiB_{11}H_{12}^-$	$He@SiB_{11}H_{12}^-$	$B_{12}H_{12}^{-2}$	-16.54
$He@B_{12}H_{12}^{-2}$	m-$Si_2B_{10}H_{12}$	He@m-$Si_2B_{10}H_{12}$	$B_{12}H_{12}^{-2}$	-31.78
$He@B_{12}H_{12}^{-2}$	2,3,4-$Si_3B_9H_{12}^+$	He@2,3,4-$Si_3B_9H_{12}^+$	$B_{12}H_{12}^{-2}$	-50.00
He@2,3,4-$Si_3B_9H_{12}^+ >$ He@m-$Si_2B_{10}H_{12} >$ $He@SiB_{11}H_{12}^- > He@B_{12}H_{12}^{2-}$				
$Li@B_{12}H_{12}^-$	$SiB_{11}H_{12}^-$	$Li@SiB_{11}H_{12}$	$B_{12}H_{12}^{-2}$	100.74
$Li@B_{12}H_{12}^-$	p-$Si_2B_{10}H_{12}$	Li@p-$Si_2B_{10}H_{12}^+$	$B_{12}H_{12}^{-2}$	197.99
$Li@B_{12}H_{12}^-$	1,7,9-$Si_3B_9H_{12}^+$	Li@1,7,9-$Si_3B_9H_{12}^{+2}$	$B_{12}H_{12}^{-2}$	289.94
$Li@B_{12}H_{12}^- >$ Li@p-$SiB_{10}H_{12}^+ >$ $Li@Si_2B_{11}H_{12}$> Li@1,7,9-$Si_3B_9H_{12}^{+2}$				
$Be@B_{12}H_{12}$	$SiB_{11}H_{12}^-$	$Be@SiB_{11}H_{12}^+$	$B_{12}H_{12}^{-2}$	211.93
$Be@B_{12}H_{12}$	m-$Si_2B_{10}H_{12}$	Be@m-$Si_2B_{10}H_{12}^{+2}$	$B_{12}H_{12}^{-2}$	415.43
$Be@B_{12}H_{12} >$ Be@m-$Si_2B_{10}H_{12}^{+2} > Be@SiB_{11}H_{12}^+$				

Table 3.5a. Skeletal bond lengths of $X@C_mB_nH_{n+m}^{a+b}$ calculated at B3LYP/6-31G*

Doped atom	Skeletal Bond lengths (Å) of endohedral $CB_{11}H_{12}^-$ systems				
	$C-B_a$	B_a-B_a	B_a-B_b	B_b-B_b	B_b-B_c
He	1.779	1.843	1.850	1.869	1.876
Li	1.796	1.866	1.863	1.888	1.897
Be	1.792	1.871	1.860	1.898	1.916
Ne	1.885	1.952	1.969	2.054	2.089

Doped atoms	Skeletal Bond lengths (Å) of endohedral p-$C_2B_{10}H_{12}$ systems		
	$C-B_a/C-B_b$	B_a-B_b	B_a-B_a/B_b-B_b
He	1.794	1.845	1.852
Li	1.818	1.860	1.884
Be	1.830	1.859	1 904

Doped atoms	Skeletal Bond lengths (Å) of endohedral m-$C_2B_{10}H_{12}$ systems									
	$C-B_a$	$C-B_b$	$C-B_c$	B_a-B_a	B_b-B_b	B_d-B_d	B_a-B_b	B_b-B_c	B_b-B_d	B_c-B_d
He	1.792	1.783	1.774	1.847	1.841	1 879	1.831	1.861	1.863	1.862
Li	1.774	1.815	1.837	1.881	1 859	1.905	1.851	1.893	1 887	1 892
Be	1.767	1.818	1.863	1.896	1.854	1.951	1.857	1.925	1 902	1 910

Doped atoms	Skeletal Bond lengths (Å) of endohedral o-$C_2B_{10}H_{12}$ systems									
	$C-B_a$	$C-B_b$	C-C	B_b-B_b	B_d-B_d	B_a-B_b	B_a-B_c	B_b-B_c	B_b-B_d	B_c-B_d
He	1.778	1.778	1.698	1.852	1.884	1.846	1.842	1.862	1.869	1.888
Li	1.801	1.794	1.709	1.880	1.921	1 870	1.850	1.881	1.890	1.923
Be	1.811	1.787	1.695	1.895	1.974	1.872	1.848	1 889	1 912	1 961

Table 3.5b. Skeletal bond lengths of $X@Si_mB_nH_{n+m}^{a+b}$ calculated at B3LYP/6-31G*

Doped atom	Skeletal Bond lengths (Å) of endohedral $SiB_{11}H_{12}^-$ systems				
	$Si-B_a$	B_a-B_a	B_a-B_b	B_b-B_b	B_b-B_c
He	2.126	1.996	1.831	1 862	1 837
Li	2.139	1.976	1 852	1.880	1 863
Be	2.130	1.942	1.858	1.889	1 877

Doped atoms	Skeletal Bond lengths (Å) of endohedral p-$Si_2B_{10}H_{12}$ systems		
	$Si-B_a/Si-B_b$	B_a-B_b	B_a-B_a/B_b-B_b
He	1.991	1.811	1.994
Li	2.138	1.831	1.985
Be	2.149	1.837	1.965

Doped atoms	Skeletal Bond lengths (Å) of endohedral m-$Si_2B_{10}H_{12}$ systems									
	$Si-B_a$	$Si-B_b$	$C-B_c$	B_a-B_a	B_b-B_b	B_d-B_d	B_a-B_b	B_b-B_c	B_b-B_d	B_c-B_d
He	2.143	2.145	2.107	2.510	1.816	1 836	1.875	1 941	1 836	1 821
Li	2.137	2.160	2.130	2.217	1.827	1.880	1.913	1.957	1.861	1 849
Be	2.135	2.156	2.137	2.031	1.844	1.912	1.914	1.945	1 878	1 865

Doped atoms	Skeletal Bond lengths (Å) of endohedral o-$Si_2B_{10}H_{12}$ systems									
	$Si-B_a$	$Si-B_b$	Si-Si	B_b-B_b	B_d-B_d	B_a-B_b	B_a-B_c	B_b-B_c	B_b-B_d	B_c-B_d
He	2.281	2.103	2.395	2.010	1 821	1 936	1.798	1.831	1 819	1 834
Li	2.268	2.122	2.437	2.001	1.850	1.941	1.833	1 854	1 848	1 865
Be	2.225	2.124	2 443	1.974	1 878	1 922	1.864	1.865	1.867	1 893

Table 3.6a. Distance from the central atom (X) to each of the vertices in $X@C_mB_nH_{n+m}^{a+b}$. Corresponding percentage of expansion is given in parentheses

Doped atom	Distance from X to the surface atoms (Å) in Stuffed $CB_{11}H_{12}^-$			
	C	B_a	B_b	B_c
He	1.681(8.3)	1.778(4.8)	1.750(3.3)	1.729(3.2)
Li	1.692(9.0)	1.801(6.1)	1.764(3.9)	1.740(4.1)
Be	1.725(11.2)	1.830(7.4)	1.748(4.5)	1.704(0.6)
Ne	1.860(19.8)	1.923(13.3)	1.880(12.3)	1.838(8.8)

Doped Atom	Distance from X to the surface atoms (Å) in Stuffed p-$C_2B_{10}H_{12}$	
	C	B_a/B_b
He	1.641(7.5)	1.760(3.8)
Li	1.646(7.8)	1.785(5.3)
Be	1.636(7.1)	1.799(6.2)

Doped atom	Distance from X to the surface atoms (Å) in Stuffed m-$C_2B_{10}H_{12}$				
	C	B_a	B_b	B_c	B_d
He	1.660(7.2)	1.793(5.7)	1.762(3.8)	1.734(3.3)	1.733(2.7)
Li	1 678(8 4)	1.833(8.0)	1.787(5.3)	1.755(4.7)	1.741(3.2)
Be	1 700(9.8)	1.908(12.5)	1.803(6.3)	1.744(4.0)	1.709(1.3)

Doped atom	Distance from X to the surface atoms (Å) in Stuffed o-$C_2B_{10}H_{12}$				
	C	B_a	B_b	B_c	B_d
He	1 687(8.6)	1.798(4.9)	1.765(4.1)	1.740(3.0)	1.719(2.9)
Li	1.717(10.5)	1 840(7.4)	1.790(5.5)	1.748(3.4)	1.721(3.0)
Be	1.780(14.5)	1.906(11.2)	1.804(6.5)	1.727(2.2)	1.684(0.8)

B-B bond lengths, which in turn decreases the H-B-B-H torsional forces. This results in the shortening of the B-H bonds.

The polarization observed on the central atom is given in Table 3.1 and 3.2. In general the noble gases He and Ne do not show any significant charge transfer. Be and Li show rather high polarization. The abnormal charges on the Li atom obtained for Mulliken population analysis in the endohedral complexes prompted us to look at the natural charges. In all the endohedral systems lithium shows a natural charge of 0.6. The central atom in higher carbon substituted borane shows a greater positive charge. This can be attributed to the enhanced electron withdrawing character of the cage as the number of carbon substitution increases.[21] This trend is observed in the silaborane stuffed cages also.

In endohedral carbaboranes the HOMO-LUMO gap reduces in the range 0.2-0.5 eV as the number of carbons increases.

Table 3.6b Distance from the central atom (X) to each of the vertices in $X@Si_mB_nH_{n+m}^{a+b}$. Corresponding percentage of expansion is given in parentheses

Doped atom	Distance from X to the surface atoms (Å) in Stuffed $SiB_{11}H_{12}^-$			
	Si	B_a	B_b	B_c
He	1.877(-4.6)	1.801(2.5)	1.833(8.1)	1.854(8.5)
Li	2.028(3.1)	1.823(3.8)	1.808(6.7)	1.800(5.3)
Be	2.128(8.2)	1.828(4.0)	1.786(5.4)	1.749(2.3)
Doped Atom	Distance from X to the surface atoms (Å) in Stuffed p-$Si_2B_{10}H_{12}$			
	Si		B_a/B_b	
He	1.991(0.5)		1.850(4.8)	
Li	2.063(4.1)		1.849(4.8)	
Be	2.110(6.5)		1.836(4.0)	
Doped atom	Distance from X to the surface atoms (Å) in Stuffed m-$Si_2B_{10}H_{12}$				
	Si	B_a	B_b	B_c	B_d
He	1.933(-0.1)	1.854(2.5)	1.865(5.7)	1.879(7.6)	1.909(10.9)
Li	2.065(3.5)	1.868(3.3)	1.850(4.9)	1.835(5.1)	1.839(6.9)
Be	2.150(7.8)	1.862(3.0)	1.833(3.9)	1.797(2.9)	1.802(4.7)
Doped atom	Distance from X to the surface aoms (Å) in Stuffed o-$Si_2B_{10}H_{12}$				
	Si	B_a	B_b	B_c	B_d
He	1.919(-6.0)	1.832(1.2)	1.865(6.1)	1.907(10.7)	1.925(12.6)
Li	2.076(1.7)	1.865(3.0)	1.849(5.2)	1.846(7.2)	1.836(7.4)
Be	2.202(7.8)	1.881(3.9)	1.825(3.9)	1.800(4.5)	1.763(3.2)

3.2.4. Multiatom encapsulation

The multiatom encapsulation in polyhedral boranes has not been considered before. We predict here two examples of two atom doped *closo* polyhedra (**10**). $He_2@B_{17}H_{17}^{-2}$ **(10a-He_2)** and $Li_2@B_{17}H_{17}$ **(10a-Li_2)** are found to be minima on their potential energy surface with lowest frequencies 87.0 and 129.9. The B-B skeletal distances in both the systems exhibit higher values than the parent $B_{17}H_{17}^{-2}$. The ΔE_{en} value for $He_2@B_{17}H_{17}^{-2}$ is 251.53 kcal/mol and that of $Li_2@B_{17}H_{17}$ is –95.84 kcal/mol. The exothermic value of $Li_2@B_{17}H_{17}$ is comparable to the ΔE_{en} value of $Li@B_{12}H_{12}^-$. As shown in Figure 3.4 He_2 encapsulated complex requires 2 more electrons and its lithium counterpart is neutral. Even though the lithium atoms are surprisingly close (1.431Å) no bonding is observed between them. The Li-Li Wiberg bond index (WBI) from the NBO[22] analysis is only

0.036. It shows that the two Li atoms exist as cations, which are very small in size, within the cage and are stabilized by the surrounding anionic cage.

3.2.5. Comparison of the Stability of Endohedral complexes with Exohedral Face Capped Systems

All the exohedral isomers are more favorable than the endohedral isomers. The relative energies calculated for the stuffed systems with respect to the face capped isomers give a rough estimate of the strain energy involved in encapsulating a heteroatom (SE, shown in Tables 3.1b and 3.2b). These isomers obey the capping principle[23] as well as the *mno* rule[14]. Among the carbaboranes the least strain energy has been evaluated for Be doped systems. $Be@CB_{11}H_{12}^{+}$ **(9b-Be)** has a strain energy of 97.9 kcal/mol. Similarly the $Be@C_2B_{10}H_{12}^{+2}$ **(9c-Be)** isomers have a strain energy of 120-130 kcal/mol. $Li@CB_{11}H_{12}$ **(9b-Li)** has a value of 150.3 kcal/mol where as $Li@C_2B_{10}H_{12}^{+}$ **(9c-Li)** isomers show the strain within a range of 175-179 kcal/mol. The comparatively bigger Ne atom has the highest strain with its encapsulated isomer **(9a-Ne)** less stable by 425.73 kcal/mol compared to the corresponding capped isomer **(9a-Ne')**. All the He face capped isomers have very low value for the lowest frequency with some of them exhibiting an imaginary value even though they are lower in energy than the endohedral isomers. The isomer in which both the lithium atoms are capped on the triangular faces of the $B_{17}H_{17}^{-2}$ **(9a-$Li_{2'}$)** gives a strain energy of 231.27 kcal/mol for the endohedral structure. Silaboranes with its large size shows a low value for the strain energy when compared to the endohedral carbaboranes.

3.2.6. Conclusions

A comparison with the corresponding exoisomer and their specific geometrical features enable to decide over the stability of the given endohedral cluster. The stability

depends on the cage size and the size of the central atom or ion. With the same central atom, the cage size becomes the predominant factor in deciding the stability of the endohedral structures. The geometries and relative energies points out that more symmetrical icosahedral $B_{12}H_{12}^{-2}$ is the most favorable system for encapsulating an atom inside. The endohedral carbaborane systems are relatively less favorable due to the small cage size than the endohedral silaborane systems.

References

1. (a) Togni, A.; Halterman, R. L. Eds, *Metallocenes: Synthesis, Reactivity, Applications,* Wiley-VCH, Weinheim, Germany, **1998**. (b) Long, N. J. *Metallocenes*, Blackwell Science, Oxford, UK, **1998**.
2. (a) Siriwardane, U.; Islam, M. S.; West, T. A.; Hosmane, N. S.; Maguire, J. A.; Cowley, A. H. *J. Am. Chem. Soc*. **1987**, *109*, 4600. (b) Hosmane, N. S.; Meester, P. de.; Siriwardane, U.; Islam, M. S.; Chu, S. S. C. *J. Chem. Soc., Chem. Commun.* **1986**, 1421.
3. Hosmane, N. S.; Lu, K. J.; Zhang, H.; Maguire, J. A. *Organometallics*. **1997**, *16*, 5163.
4. (a) Hosmane, N. S.; Meester, P. de.; Siriwardane, U.; Islam, M. S.; Chu, S. S. C. *J. Am. Chem. Soc.* **1986**, *108*, 6050. (b) Islam, M. S.; Siriwardane, U.; Hosmane, N. S.; Maguire, J. A.; Meester, P. de.; Chu, S. S. C. *Organometallics*. **1987**, *6*, 1936.
5. Hosmane, N. S.; Zhu, D.; McDonald, J. E.; Zhang. H.; Maguire, J. A.: Gray, T. G.; Helfert, S. C. *J. Am. Chem. Soc*. **1995**, *117*, 12362.
6. Hosmane, N. S.; Yang, J.; Zhang, H.; Maguire, J. A. *J. Am. Chem. Soc*. **1996**, *118*, 5150.
7. Hosmane, N. S.; Zhu, D.; McDonald, J. E.; Zhang, H.; Maguire, J. A.; Gray. T. G.; Helfert, S. C. *J. Am. Chem. Soc*. **1995**, *117*, 12362.
8. (a) Schubert, D. M.; Rees, W. S. Jr.; Knobler, C. B.; Hawthorne, M. F. *Organometallics*. **1990**, *9*, 2938. (b) Rees, W. S. Jr.; Schubert, D. M.: Knobler, C. B.; Hawthorne, M. F. *J. Am. Chem. Soc*., **1986**, *108*, 5369.

9. (a) Bandman, M. A.; Knobler, C. B.; Hawthorne. M. F. *Inorg. Chem.* **1988**, *27*, 2399. (b) Bandman, M. A.; Knobler, C. B.; Hawthorne, M. F. *Inorg. Chem.* **1989**, *28*, 1204. (c) Schubert, D. M.; Bandman, M. A.; Rees, W. S. Jr.; Knobler, C. B.; Lu, P.; Nam, W.; Hawthorne, M. F. *Organometallics*. **1990**, *9*, 2046. (d) Rees, W. S. Jr.; Schubert, D. M.; Knobler, C. B.; Hawthorne. M. F. *J. Am. Chem Soc*. **1986**, *108*, 5367.

10. (a) Borodinsky, L.; Sinn, E.; Grimes, R.N. *Inorg. Chem*. **1982**, *21*, 1686. (b) Xie, Z.; Jelinek, T.; Bau, R.; Reed, C.A. *J. Am. Chem. Soc*. **1994**, *116*, 1907. (c)Churchill, M.R.; Gold, K. *J Am. Chem. Soc*. **1970**, *92*, 1180. (d) Kang, H.C.; Lee, S.S.; Knobler, C.B.; Hawthorne, M.F. *Inorg. Chem*. **1991**, *30*, 2024. (e) St. Clair, D.; Zalkin, A.; Templeton, D.H. *J. Am. Chem Soc*. **1970**, *92*, 1173. (f) Vinas, C.; Pedrajas, J.; Bertran, J.; Teixidor, F.; Kivekas. R.; Sillanpaa, R. *Inorg. Chem*. **1997**, *36*, 2482. (g) Hansen, F.V.; Hazell, R.G.; Hyatt, C.; Stucky, G.D. *Acta Chemica Scandinavica*. **1973**, *27*, 1210. (h) Yan, Y.; Mingos, D.M.P.; Williams, D.J.; Kurmoo, M. *J. Chem. Soc., Dalton Trans*. **1995**, 3221. (i) Plešek, J.; Hermanek, S.; Franken, A.; Cisarova, I.; Nachtigal, C. *Collect. Czech. Chem. Commun*. **1997**, *62*, 47. (j) Plešek, J.; Stibr, B.; Cooke, P.A.; Kennedy, J.D.; McGrath, T.D.; Thornton-Pett, M. *Acta Crystallogr., Sect. C*. **1998**, *54*, 36. (k) Franken, A.; Plešek, J.; Fusek, J.; Semrau, M. *Collect. Czech. Chem Commun*. **1997**, *62*, 1070. (l) Yan, Y.; Mingos. D.M.P.; Muller, T.E.; Williams, D.J.; Kurmoo, M. *J. Chem. Soc., Dalton Trans*. **1994**, 1735.

11. Kester, J. G.; Keller, D.; Huffman, J. C.; Benefiel, M. A.; Geiger Jr,W. E.; Atwood, C.; Siedle, A. R.; Korba, G. A.; Todd, L. J. *Inorg. Chem*. **1994**, *33*, 5438.

12. (a) Hawthorne, M. F.; Young, D. C.; Wegner, P. A. *J. Am. Chem. Soc.* **1965**, *87*, 1818. (b) Hawthorne, M. F. *Acc. Chem. Res.* **1968**, *1*, 281.(c) Grimes, R. N. *J. Organomet. Chem.* **1999**, *581*, 1. (d) Fehlner, T. P. *Struct. Bonding* (Berlin) **1997**, *87*, 112. (e) Fehlner, T. P. *Organometallics*. **2000**, *19*, 2643.

13. (a) Srinivas, G. N.; Hamilton, T. P.; Jemmis, E. D.; McKee, M. L.; Lammertsma, K. *J. Am. Chem. Soc*. **2000**, *122*, 1725. (b) Jemmis, E. D.; Pancharatna, P. D. *App. Organomet. Chem.* **2003**, *17*, 480.

14. (a) Wade, K. *Chem. Commun.* **1971**, 792. (b) Wade, K. *Adv. Inorg. Chem. Radiochem.* **1976**, *18*, 1. (c) Jemmis, E. D.; Balakrishnarajan, M. M.; Pancharatna, P. D. *J. Am. Chem. Soc.* **2001**, *123*, 4313. (d) Balakrishnarajan, M. M.; Jemmis, E. D. *J. Am. Chem. Soc*. **2000**, *122*, 4516. (e) Jemmis, E. D.; Balakrishnarajan, M. M.; Pancharatna, P. D. *Chem. Rev*. **2002**, *102*, 93.

15. Pipal, J. R.; Maxwell, W. M.; Grimes, R. N. *Inorg. Chem.* **1978**, *17*, 1447.

16. (a) Brain, P. T.; Bühl, M.; Cowie, J.; Lewis, Z. G.; Welch, A. J. *J. Chem. Soc., Dalton. Trans*. **1996**, 231. (b) Rosair, G. M.; Welch, A. J.; Weller, A. S. *Organometallics*. **1998**, *17*, 3227. (c) McWhannell, M. A.; Rosair, G. M.; Welch, A. J.; Teixidor, F.; Vinas, C. *J. Organomet. Chem*. **1999**, *573*, 165.

17. (a) Hirsch, A.; Chen, Z.; Jiao, H. *Angew. Chem. Int. Ed*. **2000**, *39*, 3915. (b) Bühl, M. *Chem. Eur. J.* **1998**, *4*, 734. (c) Rubin, Y.; Jarrosson, T.; Wang, G.-W.; Bartberger, M. D.; Houk, K. N.; Schick, G.; Saunders, M.; Cross, R. J. *Angew. Chem. Int. Ed*. **2001**, *40*, 1543. (d) Shabtai, E.; Weitz, A.; Haddon, R. C.; Hoffman, R. E.; Rabinovitz, M.; Khong, A.; Cross, R. J.; Saunders, M.; Cheng, P.-C.; Scott,

L. T. *J. Am. Chem. Soc.* **1998**, *120*, 6389. (e) Cross. R. J.; Saunders, M.; Prinzbach, H. *Org. Lett.* **1999**, *1*,1479.

18. (a) Jemmis, E. D.; Balakrishnarajan, M. M. *J. Am. Chem. Soc.* **2000**, *122*, 7392. (b) Charkin. O. P.; Klimenko. N. M.; Moran. D.; Mebel. A. M.; Schleyer. P. v. R. *Russ. J. Inorg. Chem.* **2001**, *46*, 110. (c) Charkin. O. P.; Klimenko. N. M.; Schleyer. P. v. R. *Russ. J. Inorg.Chem.* **2000**, *45*, 1539. (d) Charkin. O. P.; Klimenko. N. M.; Moran. D.; Mebel. A. M.; Charkin, D. O.; Schleyer, P. v. R. *Inorg. Chem.* **2001**, *40*, 6913.

19. (a) Hughes, R. E.; Kennard, C. H. L.; Sullinger, K. G.; Weakliem, H. A.; Sands, D. E.; Hoard, J. L. *J. Am. Chem. Soc.* **1963**, *85*, 361. (b) Hoard, J. L.; Sullinger, D. B.; Kennard, C. H. L.; Hughes, R. E. *J. Solid State Chem.* **1970**, *1*, 268. (c) Jemmis, E. D.; Balakrishnarajan, M. M. *J. Am. Chem. Soc.* **2001**, *123*, 4324.

20. Moran, D.; Stahl, F.; Jemmis, E. D.; Schaefer III. H. F.; Schleyer, P. v. R. *J. Phys. Chem.* **2002**, *106*, 5144.

21. (a) Hawthorne, M. F.; Benry, T. E.; Wegner, P. A. *J. Am. Chem. Soc.* **1965**, *87*, 4746. (b) Leites, L. A.; Vinagradova, L. E.; Kalinin, V. N.; Zakharkin, L. I. Izv. Akad., Nauk SSSR, *Ser Khim*, **1970**, 2596.

22. (a)Reed, A. E.; Weistock, R. B.; Weinhold, F. *J. Chem. Phys.* **1985**, *83*, 735. (b) Reed, A. E.; Curtiss, L. A.; Weinhold, F. *Chem. Rev.* **1988**, *88*, 899. (c)Wiberg, K. B. *Tetrahedron* **1968**, *24*, 1083.

23. Mingos, D. M. P. *Nature. Phys. Sci.*, **1972**, *236*, 99.

CHAPTER 4

Condensation in Polyhedral Boranes

4.0. Abstract

Condensation among polyhedral cages reduces the electron deficiency. The electron requirement of these condensed boranes is explained by the *mno* rule. Here we derive many relationships connecting the hydrocarbons, polyhedral boranes, and metal borides with the aid of the *mno* rule. We also found an electronic structural relationship between fullerenes and β-rhombohedral boron. This relationship is derived by replacing the 12 pentagonal pyramidal B_6^{-4} units by isoelectronic C_5^- units and removing the central B_{12} from the electron deficient B_{84} unit leading to an isoelectronic equivalence of B_{84}^{-50} and C_{60}^{-12}. This relationship is well supported by the experimental realization of $C_{60}M_{12}$ (M=Li, K) and $C_{48}N_{12}$. The condensation between two polyhedral cages can occur by sharing one, two, three or four vertices in contrast to the benzenoids where only 2 vertex sharing is possible. A quantitative comparative analysis on the energetics of condensation of polyhedral boranes and benzene has been carried out. The study showed that stability reduces with increasing condensation except for edge-sharing. Polycondensation by sharing two vertices is energetically favorable. The constancy in charge also renders edge-sharing suitable for polycondenstion. Benzocarboranes, the edge-shared product of benzene and 3-dimensional polyhedral boranes are also theoretically investigated. The aromaticity of the six-membered ring in these condensed structures is calculated to be decreased as seen in geometrical parameters and NICS values. On the otherhand, the aromaticity of the polyhedral cage is not substantially altered.

4.1. Structural connections between compounds of boron and carbon

4.1.1. Introduction

Though neighbors in the periodic table, boron and carbon differ dramatically. Carbon is a keyplayer in much of modern material science; fullerenes and nanotubes are in the foreground. Yet the bonding in carbon is elegantly simple, making it into high school textbooks. The familiar two-dimensional aromatic compounds such as $C_3H_3^+$, $C_5H_5^-$ and C_6H_6 are governed by the Hückel's $(4n+2)\pi$ electron rule, where 'n' is zero or any integer. At a simple level the $(4n+2)\pi$ electron rule is applicable to condensed systems; benzene, naphthalene and anthracene have 6, 10, and 14 π electrons (n=1,2, and 3) respectively. Polycondensation in two-dimension leads to graphite. In contrast, boron provides unimaginable complexity in structure and bonding. The boranes, hydrocarbon equivalents, are well known for their electron deficiency and multicentre bonding, and are characterized by aromatic polyhedral structures, $B_nH_n^{-2}$ (n=5-12).[1] Despite their complexity, structural connections between boranes and elemental boron continue to emerge.[2] While the familiar benzene to graphite connection appears to be far removed from the relationship between icosahedral borane and elemental boron, there are several analogies that are discernible.

4.1.2. Familiar connections

The isoelectronic relationships between the two sets CH_3^+, CH_4, CH_5^+, CH_6^{2+}, CH_7^{3+} and BH_3, BH_4^-, BH_5, BH_6^+, BH_7^{2+} are obvious.[3,4] Equally obvious, but of rather recent origins, is the connection between C and B^- in extended binary structures. The adjacent stacks of boron and lithium synthesized by Nesper are indeed structurally reminiscent of polycarbyne: the crystal structure shows a linear borynide chain $(B^-)_n$, isoelectronic to polycarbyne.[5] While the extent of charge transfer can be debated, the

connection to sp-hybridized carbon is obvious in this 1-dimensional structure. MgB_2 provides a close analogy to the graphite structure.[6,7] The graphite-like boron sheets (B^-) alternating with a similar sheet of magnesium (Mg^{+2}) with hexagons twice as large and one Mg in the center of the Mg_6 hexagon establish the link (Figure 4.1, **1**).

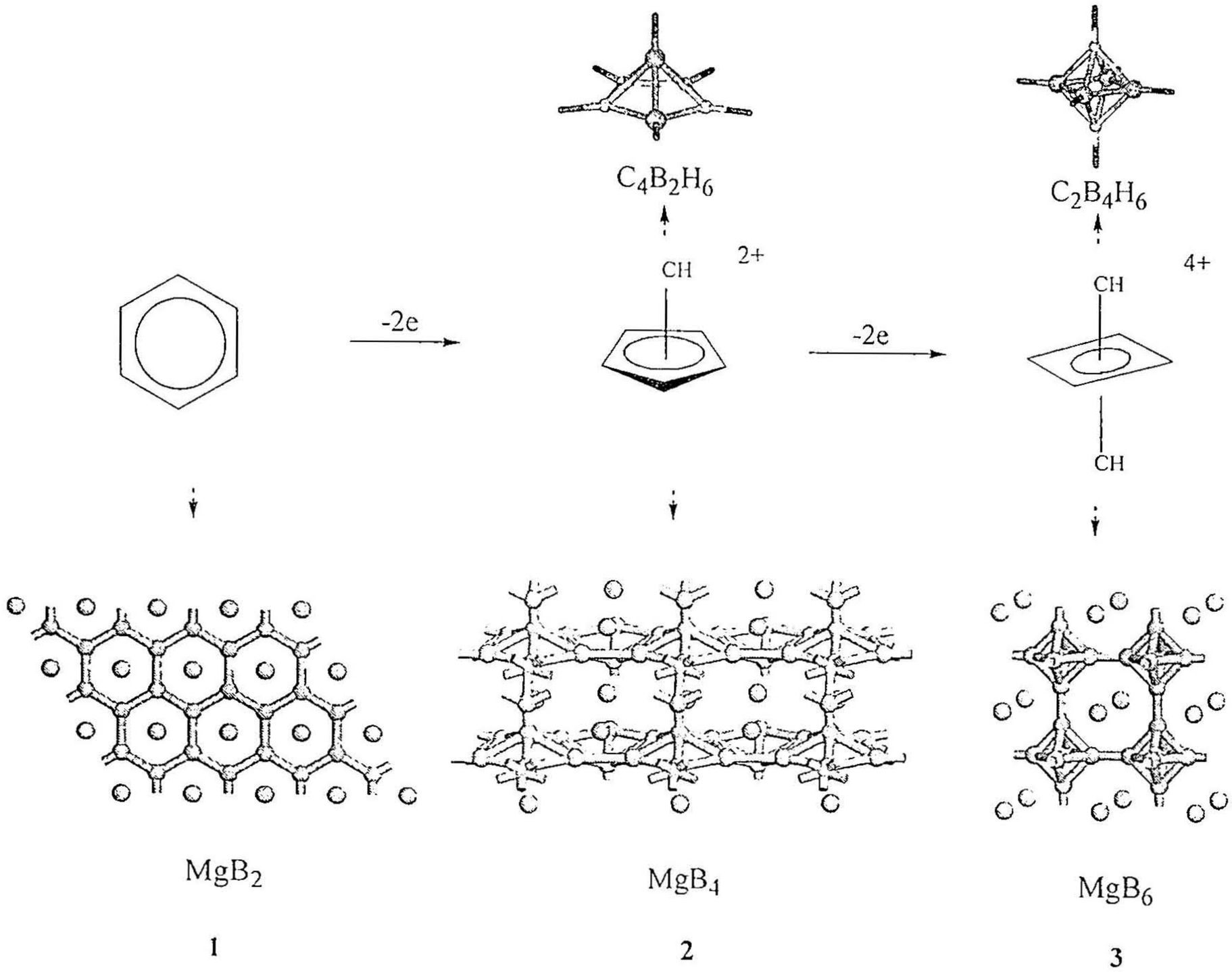

Figure 4.1. The structural similarities between hydrocarbons and the magnesium borides. (**1**) benzene and MgB_2. The diagram indicates the projection of a graphite-like boron sheet and a magnesium sheet into one plane. There is one magnesium on each B_6 hexagon; (**2**) pentagonal pyramidal $C_6H_6^{+2}$, $C_4B_2H_6$ and MgB_4 obtained by edge-sharing of pentagonal pyramidal B_6 units; (**3**) octahedral $C_6H_6^{+4}$, $C_2B_4H_6$, and MgB_6.

The large family of three-dimensional polyhedral structures represented by $B_nH_n^{-2}$ and $C_2B_{n-2}H_n$ is well known.[1,8] Schematically we can remove electrons from benzene and get $C_6H_6^{+2}$ (Figure 4.1). While there are several structures that may be envisaged for the

dication, the one that relates to boron most easily is the pyramidal cation; a permethyl derivative with a similar structure is known in solution.[9] This also satisfies Wade's Rule for *nido* structures (polyhedron with one missing vertex).[10] Replacement of one or more carbons by B^- results in $C_5BH_6^+$,[11] $C_4B_2H_6$[12] and B_6H_{10} ($B_6H_6^{-4}$ with 4 bridging hydrogens to neutralize the charge),[13] all known experimentally with pentagonal pyramidal structure. When another pair of electrons is taken away we have $C_6H_6^{+4}$, unrealistic in view of the high charge. Replacing four carbons by four B^- and the neutral $C_2B_4H_6$ gives an octahedral structure;[14] an all-boron octahedron has two negative charges ($B_6H_6^{-2}$), compensated by an accompanying cation.[15] A similar procedure of removing electrons and arriving at the three-dimensional structures can be applied to the cyclopentadienyl anion as well. Removal of two electrons from $C_5H_5^-$ leads to square pyramidal $C_5H_5^+$;[16] isoelectronic and isostructural B_5H_9 [17] is familiar with 4 bridging hydrogens. Removal of another electron pair leads to $C_5H_5^{+3}$; the *closo*-$B_5H_5^{-2}$ and the $C_2B_3H_5$ are well-known.[18]

4.1.3. Connection between organic structures and magnesium borides

The isoelectronic and isostructural relationship of pentagonal pyramidal $C_6H_6^{+2}$ and square bipyramidal $C_6H_6^{+4}$ to polyhedral molecules, $B_6H_6^{-4}$ and $B_6H_6^{-2}$ is explained earlier. The relationship between benzene and the periodic two-dimensional sheet structure of MgB_2 is also obvious (Figure 4.1). A three-dimensional structure is easily seen for the B_6^{-2} octahedra where each B atom bonds to another B atom of the adjacent B_6 unit by a two center-two electron (2c-2e) bond. Divalent metal ions in the interstitial space of this $(B_6^{-2})_n$ solid make a neutral MB_6 network. Molecular structures with an empirical formula of MB_6 are well known with divalent metals such as Ca, Sr and Ba; the crystal structure

consists of an octahedral B_6 unit surrounded by 8 metal atoms at each corners of the cubic unit cell.[19] It is only a question of time until MgB_6 is also studied structurally.

While $B_6H_6^{-2}$ could condense to give periodic structures through 2c-2e bonds, the electronic requirement for condensation of pentagonal pyramidal $B_6H_6^{-4}$ or $C_4B_2H_6$ is less obvious. By the *mno* rule, an edge-shared *bisnido* polyhedral borane $B_{10}H_8$ should have a charge of –6 (m=2, n=10, o=0, p (no. of missing vertices) =2.) (Figure 4.2).

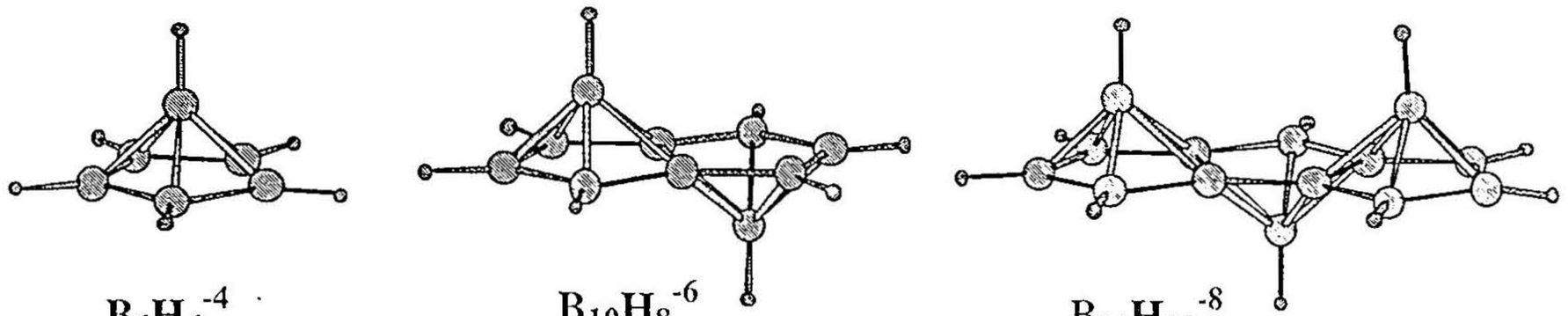

Figure 4.2. The edge shared products of pentagonal pyramid $B_6H_6^{-4}$. The difference of B_4^{-2} between the two consecutive fused products is obvious. The electron counting according to the *mno* rule is also indicated.

A second condensation leads to $B_{14}H_{10}^{-8}$. Thus condensation of each pentagonal pyramid results in the addition of a B_4 unit and an increase of -2 charges. An analysis of this process also suggests the structure of MgB_4.[20] The chains of pentagonal pyramidal units are connected to each other by removing the hydrogen atoms of the remaining BH bonds and forming 2c-2e B-B bonds to complete the three-dimensional structure of MgB_4! Thus we find the relationship between the three organic-based structures and metal borides in terms of MgB_2, MgB_4 and MgB_6-based structures (Figure 4.1).

The structure of another possible magnesium boride can be explained by relating to the elemental boron. The structure of the most stable polymorph, β-rhombohedral boron, starts out in the most natural way by building 12 icosahedra around an icosahedron, but

there are many problems with this perfect packing as it would not lead to three-dimensional periodicity.[21] Incidentally 12 B_{12} around a B_{12} is indeed a part of boron chemistry, but to sustain this arrangement requires electron donors in the form of metals as in YB_{66}.[22] The 12 outer icosahedra are not completed in β-boron; only the pentagonal pyramidal half is retained (Figure 4.3), so that a B_{84} unit is generated ($B_{12}@B_{12}@B_{60}$, Figure 4.4).[2]

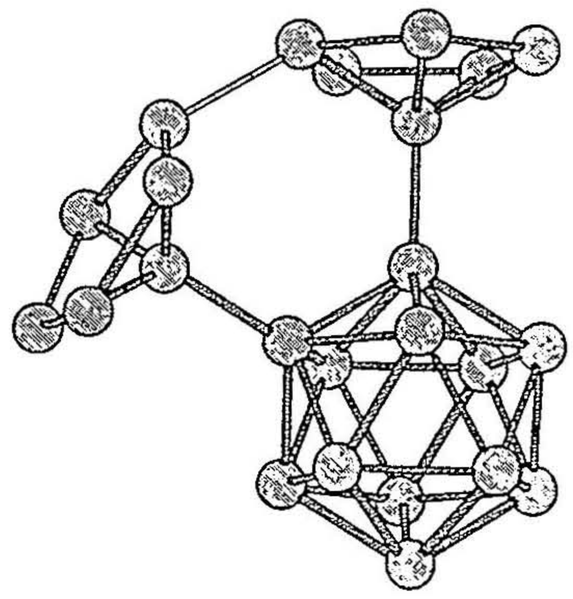

Figure 4.3. A fragment of B_{84} which shows the building up of B_{84}. Each vertex of B_{12} is connected to one pentagonal pyramidal B_6 unit thus leading to the formation of B_{84} unit.

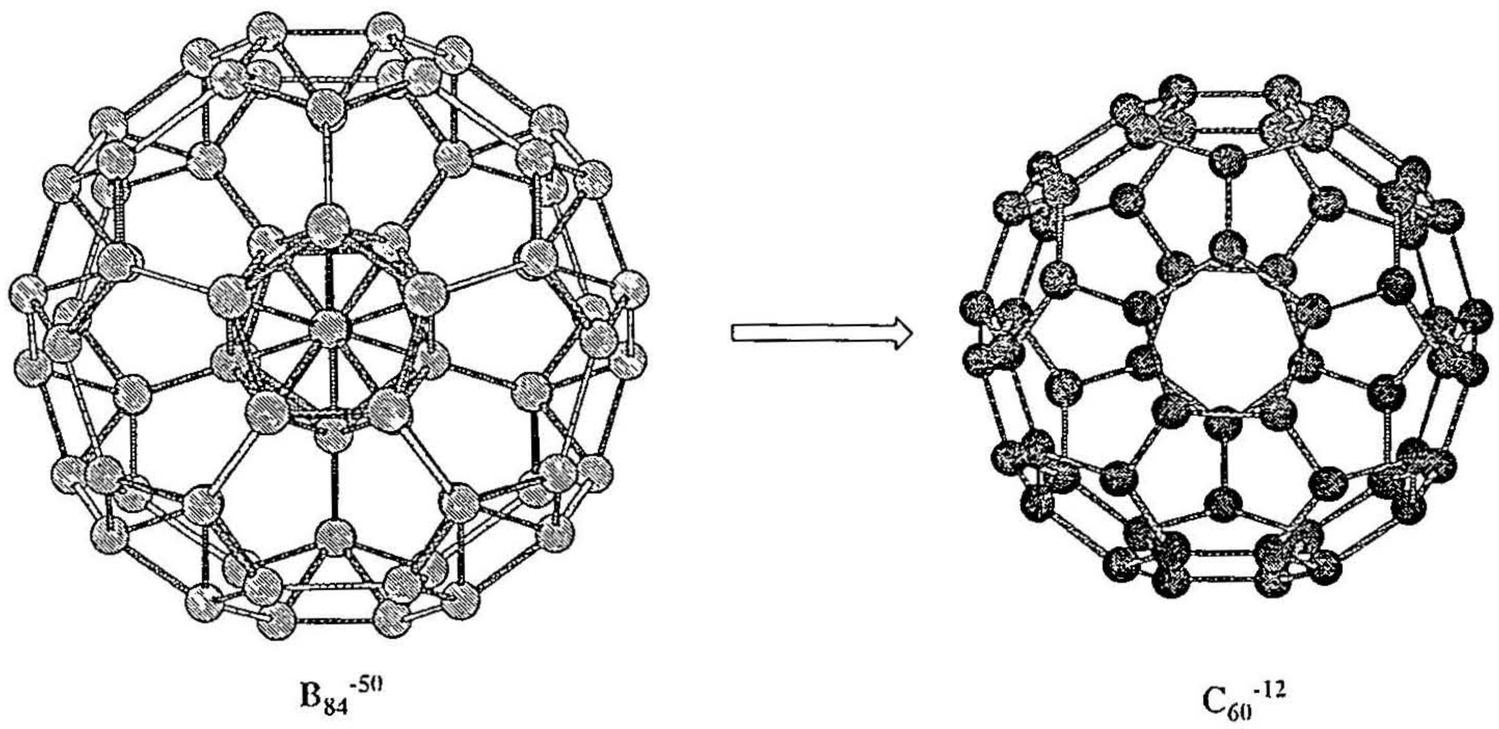

Figure 4.4. The B_{84} fragment of β-rhombohedral boron and fullerene are related structurally and electronically. The replacement of 12 pentagonal pyramidal B_6^{-4} by 12 C_5^- and the removal of the inner B_{12} unit of the B_{84} leads to the fulleride anion, C_{60}^{-12}.

ıen two of these B_{84} units come together, two half icosahedra form a new icosahedron ıgure 4.5).

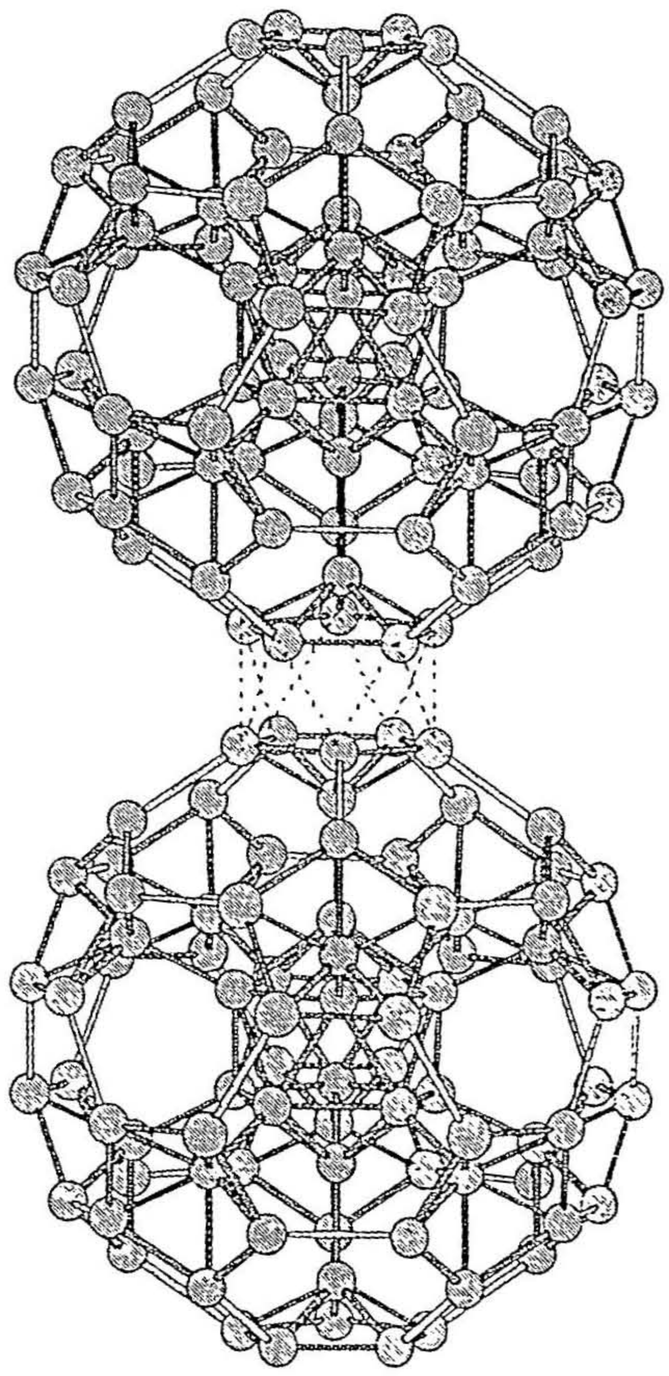

Figure 4.5. The arrangement of 2 B_{84} units in the β-rhombohedral boron. The six pentagonal pyramidal B_6 units on the surface of B_{84} complete the icosahedral framework with similar B_6 units on other B_{84} units as shown.

The size of B_{84} restricts the total number of units that can come around any one B_{84} in this fashion to six. Nature finds a way to generate icosahedra out of the remaining six half-icosahedra of B_{84} by adding a B_{10} unit, which, by its unusual symmetry, provides three half-icosahedra (Figure 4.6). Three B_{84} units can be brought around this B_{10} unit. Two of these giant $(B_{84})_3B_{10}$ units are connected to each other by a single boron atom.

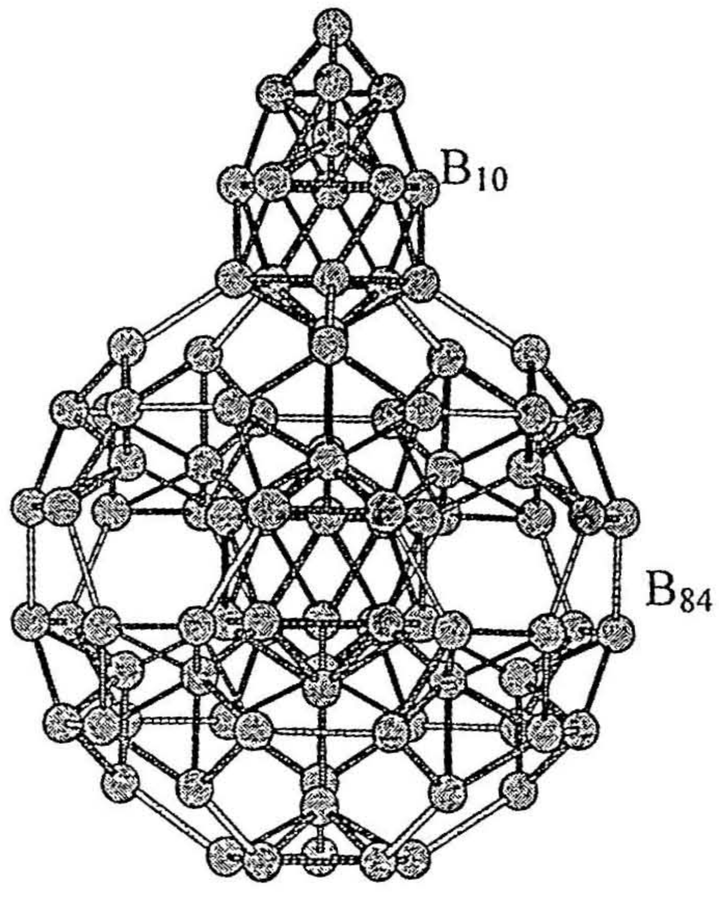

Figure 4.6. The 6 B_6 units on the B_{84} surface form an icosahedron with B_6 units of the B_{10} fragments.

Removing the symmetry-related atoms, one gets the unit cell 84+10+10+1 = 105. This also generates a new structural type that can be separated by breaking 2c-2e bonds, the B_{57} unit B_{28}-B-B_{28} (Figure 4.7).

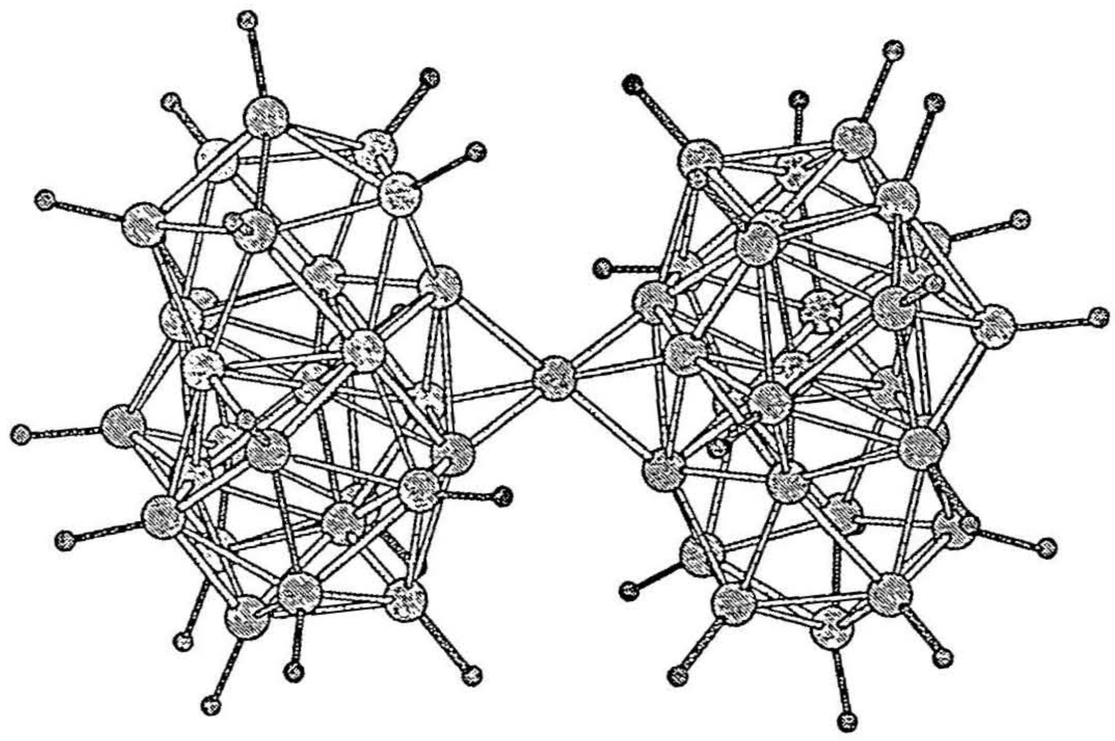

Figure 4.7. B_{57} unit in the β-rhombohedral boron. It consists of 2 B_{28} units which are connected through one boron atom. Each B_{28} unit has three icosahedral B_{12}s with each B_{12} sharing a face with the other two B_{12}s.

The electron requirement for this large structure is worked out using the *mno* rule by adding hydrogens to the dangling valencies.[2d] According to this the B_{57} unit has three

extra electrons and should have a +3 charge, (The *mno* count of $B_{57}H_{36}$ molecule is 8+57+1=66; 36 electron pairs are obtained from BH vertices and 31.5 electron pairs are provided by the remaining boron vertices making the molecule in excess of 3 electrons) which is confirmed computationally as well.[2d] The remaining B_{48} unit (out of the B105) has 4 icosahedral B_{12} units and must have –8 charges. Thus the unit cell, B_{105}, will be deficient by 5 (=8-3) electrons. An early band structure calculation by Bullet confirmed this deficiency in the B_{105} structure.[23] However, properties of elemental boron do not support this. More recent X-ray studies indicate that the unit cell is $B_{106\,66}$ and there are 20 symmetry equivalent atomic positions in the unit cell, of which 6 are partially occupied.[24] Among these, one has six fold symmetry and a partial occupancy of about 5/6 and belongs to the B_{57} part. This missing boron atom with its 3 valence electrons takes care of the +3 charge. The unit cell still requires eight electrons; these are provided by the extra occupancy of 2.66 (106.66-104) boron atoms in the many holes inside B_{84} ($2.66\times3\approx8$). Counter ions can also impart neutrality to the structure. Lithium boride, LiB_{13}, with β-rhombohedral structure, is known experimentally.[25] Here the deficiency of electrons is taken care of by lithium atoms (Li_8B_{104}). This points to the possibility of MgB_{26} with a β-rhombohedral structure, thus adding one more candidate to the list of magnesium borides.

4.1.4. Fullerene (C_{60}) and β-rhombohedral boron

With the discovery of fullerenes, chemists have been fascinated by the endohedral chemistry possible by encapsulating large atoms inside the vacant cavity (stuffing). Were the B_{84} ($B_{12}@B_{72}$) (Figure 4.4) unit electron sufficient, it would be a remarkably stable stuffed boron fullerene similar to the endohedral fullerenes with 24 boron atoms inside borafullerene, B_{60}. The electron deficiency of B_{84} can be easily calculated. The 12

pentagonal pyramidal B_6 units in B_{84} require 4 electrons each (a la $C_4B_2H_6$), totaling 48 electrons. An additional two electrons are required for the central B_{12}. Thus a B_{84}^{-50} should be appropriate! Therefore, we could anticipate a stable isoelectronic $Si_{50}B_{34}$ with 50 Si atoms and 10B atoms on the fullerene-like surface.[26] The molecular species $B_6H_6^{-4}$ (C_{5v}) could compensate the charge by replacing $4B^-$ by 4C;[12] an additional way that nature has found is to protonate four times as in B_6H_{10} (Figure 4.8).[13]

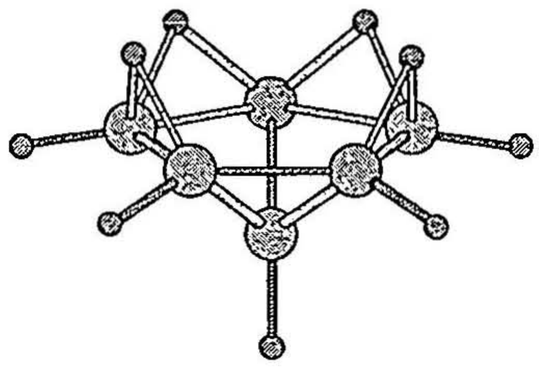

Figure 4.8. The structure of well-known B_6H_{10}. The charge of $B_6H_6^{-4}$ is compensated by 4 bridging hydrogens.

An analogous $B_{84}H_{48}^{-2}$ species where each of the 12 five-membered B_5 ring is quadruply protonated must be electron sufficient.[27] We have carried out PM3 calculations on $B_{84}H_{50}$ structures obtained by adding two bridging hydrogen atoms to the $B_{84}H_{48}^{-2}$ isomer with a D_{3d} symmetry. (There are 1256602779 isomers possible for $B_{84}H_{50}$ including geometrical and optical isomers, the number obtained from the enumeration of isomers reported for $C_{60}H_{50}$.)[28] The calculations showed this isomer of neutral $B_{84}H_{50}$ to be a minimum on the potential energy surface (Figure 4.9).

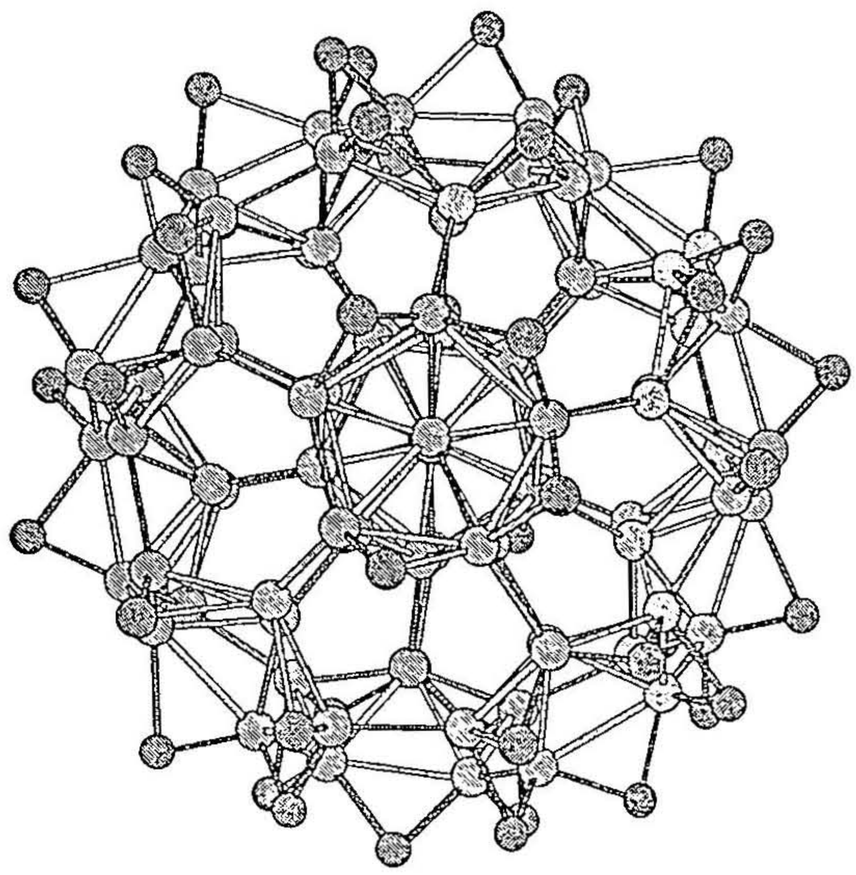

Figure 4.9. The structure of $B_{84}H_{50}$. The electron deficiency of B_{84} is compensated by adding 50 bridging hydrogens.

A more direct connection between fullerenes and β-boron is available through the *arachno* formulation of polyhedral boranes. Removal of the axial BH group from the *nido* pentagonal pyramidal $B_6H_6^{-4}$ leads to the *arachno* planar $B_5H_5^{-6}$ (Figure 4.10).

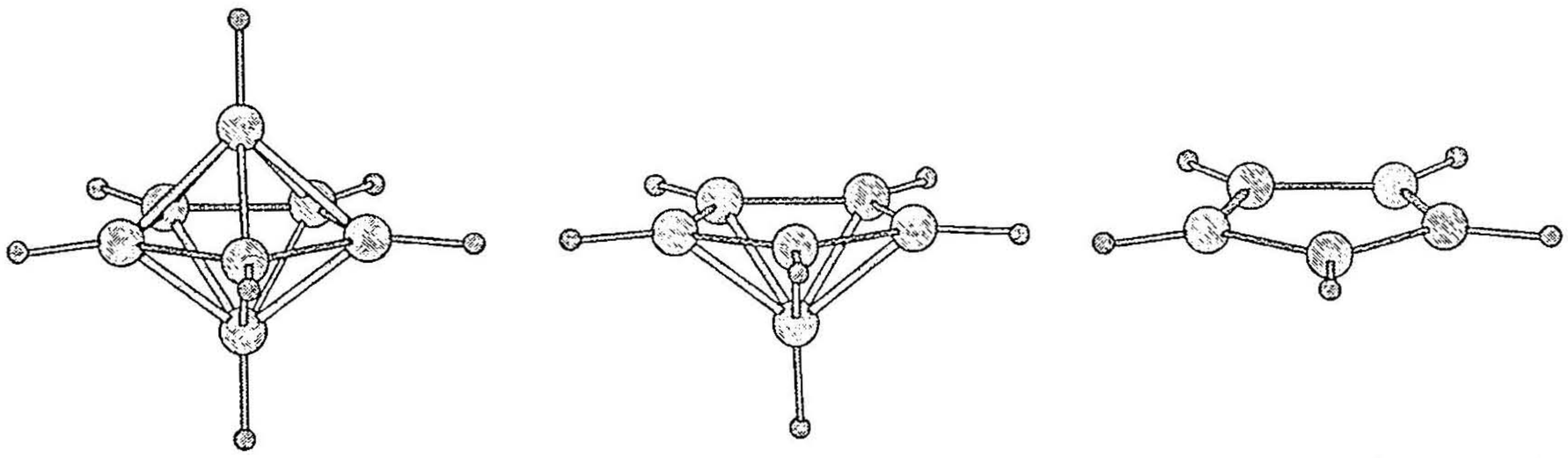

closo-$B_7H_7^{-2}$ *nido*-$B_6H_6^{-4}$ *arachno*-$B_5H_5^{-6} \approx C_5H_5^{-1}$

Figure 4.10. The isoelectronic equivalence of *arachno*-$B_5H_5^{-6}$, evolved from the *closo*-$B_7H_7^{-2}$ by removing 2 vertices, with $C_5H_5^{-1}$ is shown.

This is isoelectronic with the aromatic cyclopentadienyl anion $C_5H_5^-$. If the central B_{12} of the B_{84} is removed and the 12 pentagonal pyramidal B_6 units are replaced by 12 C_5^- units, what remains is C_{60}^{-12} (Figure 4.4). This has already been generated from C_{60} as $C_{60}Li_{12}$

and $C_{60}K_{12}$.[29] There is also experimental evidence now of the stable neutral structure $C_{48}N_{12}$.[30]

4.1.5. Conclusions

The structural connections between the compounds of boron and carbon are extended using the *mno* rule beyond the borane-carbocation continuum, the lithium boride-polycarbyne analogy and the magnesium boride (MgB_2)-graphite equivalence to β-rhombohedral boron and fullerenes. The structural similarity of the pentagonal pyramidal $C_6H_6^{+2}$ and MgB_4 is established. An interesting electronic structural relationship between the B_{84} fragment of the β-rhombohedral boron and the fulleride anion, C_{60}^{-12}, is derived by replacing the 12 pentagonal pyramidal B_6^{-4} units by isoelectronic C_5^- units and removing the central B_{12} from the electron deficient B_{84} unit. This relation is well supported by the experimental realization of $C_{60}M_{12}$ (M=Li, K) and $C_{48}N_{12}$.

4.2. The stability of 3-dimensional *closo*-polycondensed polyhedral boranes:- A comparative study with benzenoids.

4.2.1. Introduction

Benzene and $B_{12}H_{12}^{-2}$ are the prototypes of two- and three-dimensional aromatic compounds. Icosahedral $B_{12}H_{12}^{-2}$ is the most stable of all mono cage boranes owing to the coincidence that the orientation of the exohedral BH bonds in relation to the B_5H_5 rings dictated by icosahedral symmetry is close to the orientation required for ideal overlap in a pentagonal pyramidal B_6H_6. Thus it occupies a unique place in borane chemistry as its counterpart benzene. The relationship between boranes and benzenoids is well exploited by six interstitial electron rule using ring cap fragmentation of boranes.[31] While aromatic delocalization of $B_{12}H_{12}^{-2}$ and benzene share much in common, they differ in many ways.

Benzene can be represented by many resonance forms and can be compared with the hypothetical cyclohexatriene for resonance energy estimates. The delocalization of benzene can be forced to break down by forming exo-double bonds as in quinonoids, whereas placing an exo-double bond on any *closo* borane is proved difficult, as the cage will break apart.[32] The other structural patterns of polyhedral boranes, *nido* and *arachno* boranes try to attain the aromatic stability by forcing bridging hydrogens on the open face, a phenomenon that is seldom observed in the chemistry of benzenoids.[33] Carbon atoms tend to avoid bridging hydrogens even when they are implanted in the borane cage. These discrepancies in the properties show that the sigma skeleton of benzene does not depend on the stability due to aromaticity whereas for $B_{12}H_{12}^{-2}$ and other polyhedral boranes structure and aromatic stability are sides of the same coin.

While there are many studies on the energetic consequence of condensation of benzenoid aromatics, such analysis on polyhedral boranes are unknown. Macropolyhedral boranes, which comprise of more than one polyhedral borane unit sharing some common vertices is an intriguing area of research. Despite the intense activity in the experimental chemistry of macropolyhedral boranes, it is crippled by the lack of understanding of their structures and energetics. An analysis on these macropolyhedral boranes by carrying out theoretical calculations based on DFT is presented here. The ability of condensed macropolyhedral boranes to sustain the three-dimensional aromaticity of the individual cages after fusion is analyzed by taking polycyclic aromatic hydrocarbons (PAH) as a reference. The charge of all the structures studied here has been evaluated using the *mno* rule.[34]

4.2.2. Energetics of various fusion modes

The energetic consequences of polycondensation are examined by equations similar to (1–2).

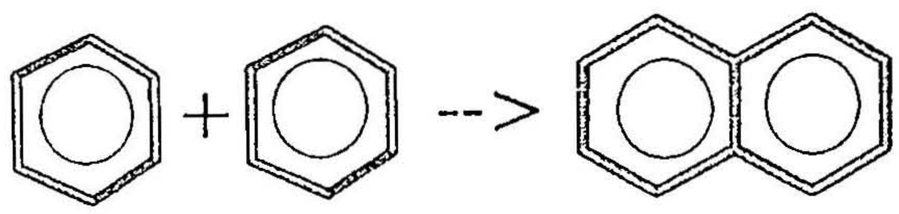

$$+ \quad 2CH_2 \qquad (4.1)$$

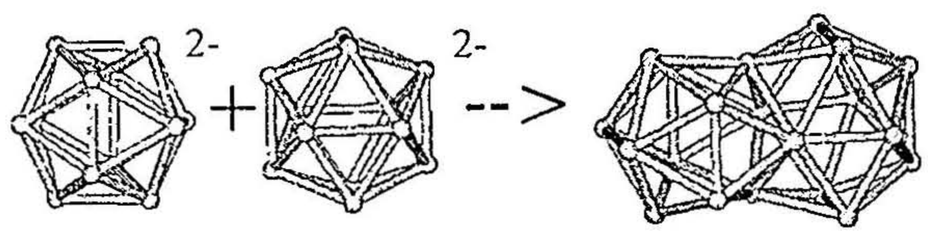

$$+ \quad 4BH_2^- \qquad (4.2)$$

All the condensed systems can be compared with the fused hydrocarbons employing the above equations that can be thought of as an effective approximation since BH_2^- and CH_2 are isoelectronic and minima in their singlet state. For example, condensation of two benzenes sharing an edge to give naphthalene **(1)** by the elimination of two carbenes (calculated as singlet for uniformity) is endothermic by 218.4 kcal/mol (Table 4.1). Similarly, in the case of boranes condensation requires elimination of BH_2^-. To compare across these structurally diverse systems ΔE is divided by the number of the isoelectronic CH_2 or BH_2^- groups that are generated (ΔE_{av} , Table 4.1). Even these ΔE_{av} values cannot be compared directly between the benzenoid aromatics and polyhedral boranes, as the differential contribution of CH_2 or BH_2^- to energetics cannot be easily estimated. However the relative trends of these values can be contrasted and the stability of the corresponding compounds can be predicted. Lower endothermicity from these equations predicts favorable condensation.

i. Benzenoids

The decrease in aromatic stability of benzenoid rings when condensed together to share an edge is well documented. Condensation forces some vertices to be shared which are simultaneously involved in the delocalisation of multiple aromatic units and though all their four orbitals are used up in the process, they are still two orbitals short when compared to isolated monomers. The resonance energy of naphthalene is decreased by 12 kcal/mol when compared with the sum of the resonance energies of individual benzene rings. It is generally agreed that there is a minimum decrease of 5 kcal/mol per each fusion. The ΔE_{av} for the formation of naphthalene is 109.2 kcal/mol by using the earlier equation. The ΔE_{av} does not change considerably in going to anthracene **(2)**, phenanthrene **(3)** or naphthacene **(4)**. This is illustrated graphically in Figure 4.11. There appears to be minimal energetic changes with each added benzenoid ring.

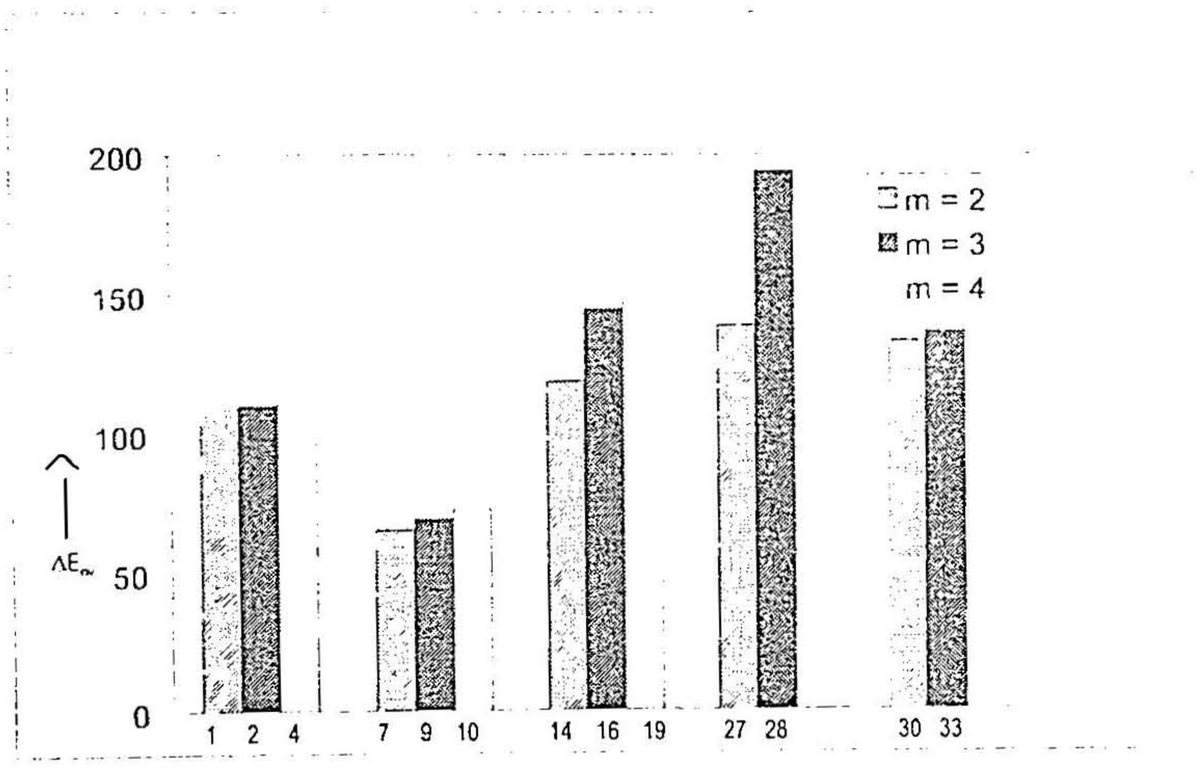

Figure 4.11. The variation of ΔE_{av} as a function of number of individual polyhedral units. The increase in ΔE_{av} per added polyhedra is nearly a constant for edge-sharing condensation (**1**, **2**, **4**; **7**, **9**, **10**; **30**, **33**). With three (**14**, **16**, **19**) and four atom (**27**, **28**) sharing condensation, ΔE_{av} increases with increase in the number of individual polyhedral units. The condensation between same cages are considered for plotting.

ii. Edge-sharing condensation

Edge sharing condensation of two *closo*-$B_{12}H_{12}^{-2}$, unlike benzenoids, is not practical due to geometrical constraints on the $B_{22}H_{20}^{-2}$ generated. The strain is so high that the skeleton breaks down on optimization of geometry shown in Figure 4.12. One B_{12} cage retains the skeleton while the other loses its *closo* deltahedral geometry. The hydrogen on the boron cap (as is defined in Figure 4.16) of the unperturbed B_{12} skeleton is bonded to the boron cap of the broken cage in a bridged manner. The bond between the capped boron of the broken cage and the shared boron is broken (BH-B=2.591 Å). The B-B bonds near the condensation site of the broken *closo* cage are elongated and the B-B bonds away from the fused site are reasonable and essentially bonding. However the distances between the nonbonded cap atoms are still short (BHcap-BHcap =1.952 Å; Hbridge-Hcap =1.694 Å). This is clearly reflected in the very high and endothermic ΔE_{av} value (169.0kcal/mol). However such condensation is ideally possible with $B_7H_7^{-2}$ and $B_6H_6^{-2}$ (Figure 4.13). Edge sharing between two octahedral B_6, $B_{10}H_8^{-2}$ **(5)** is found to be -

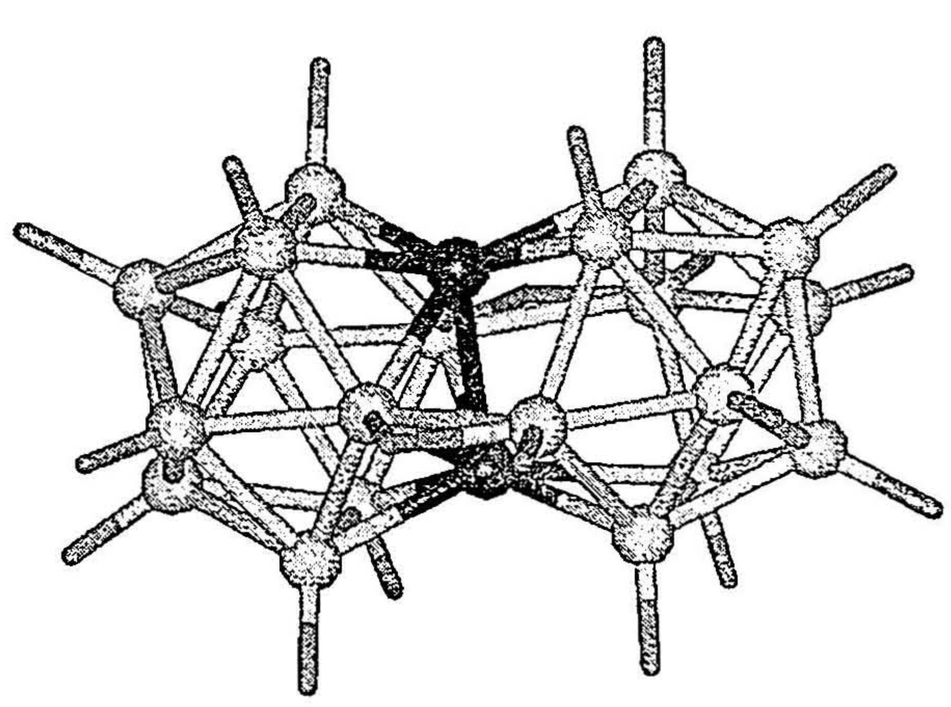

Figure 4.12. The optimized geometry of the $B_{22}H_{20}^{-2}$, an edge sharing polyhedron between two B_{12} units.

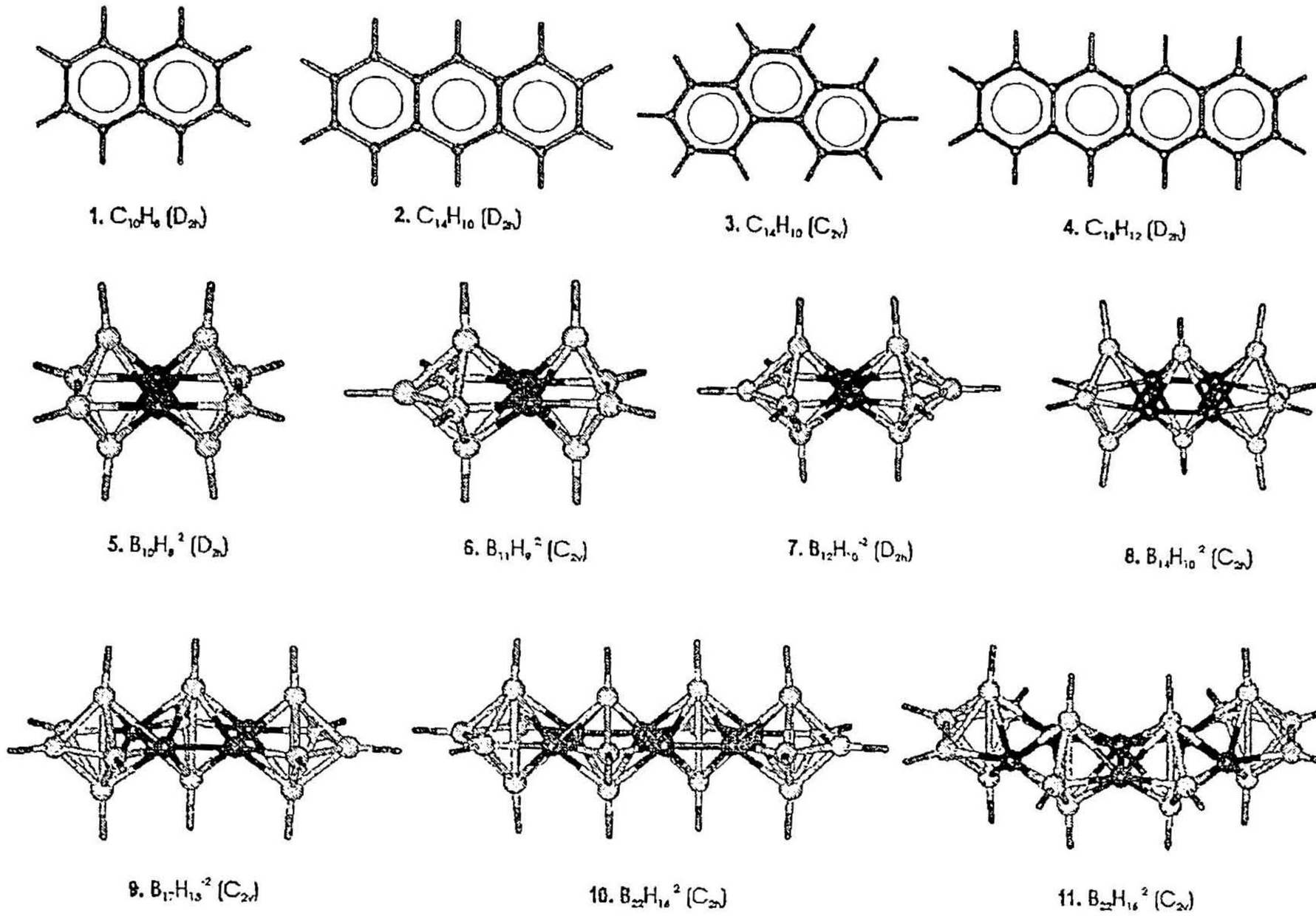

Figure 4.13. Optimized edge sharing condensed structures **(1-18)** at B3LYP/6-31G*

favorable in spite of the short Bcap-Bcap distance (2.113 Å, Hcap-Hcap=2.353 Å) with a ΔE_{av} value of 69.6 kcal/mol (equation 4.3).

$$2B_6H_6^{-2} \rightarrow B_{10}H_8^{-2} + 2BH_2^{-} \; ; \; \Delta E_{av} = 69.6 \text{ kcal/mol} \qquad (4.3)$$

Similarly the edge sharing condensation between octahedral B_6 and pentagonal bipyramidal B_7 results in $B_{11}H_9^{-2}$ **(6)** which is the most preferred structure with a ΔE_{av} value 65.5 kcal/mol and large cap-cap distance (2.332 Å, 2.379 Å). $B_{12}H_{10}^{-2}$ **(7),** a condensed product between two $B_7H_7^{-2}$ units, is a minimum with the ΔE_{av} value of 65.3kcal/mol, which is almost identical to that of $B_{11}H_9^{-2}$. A neutral carbaborane analogue $C_2B_{10}H_{10}$ of **(7)** must be a practical target.[35] $C_2B_{10}H_{10}$ isomer where the two carbons are in the opposite ends of the two 5-membered rings in **(7)** is calculated to be lower in energy

than the icosahedral monocage $C_2B_{10}H_{10}$ (orthocarboryne)[35b] reported experimentally[35c] by 6.5 kcal/mol. This substantiates the credibility of ΔE_{av} values used in discussing the results throughout this paper and the possibility of experimental realisation of the favorable compounds.

Extending $B_{10}H_8^{-2}$ **(5)** to one more octahedral B_6 cage leads to a structure, $B_{14}H_{10}^{-2}$ **(8)** with D_{2h} symmetry, which is not a minimum on the PES due to the unfavorable interaction between the capping hydrogen atoms (Bcap-Bcap=2.072 Å, Hcap-Hcap=2.203 Å). On following the lower frequency, the C_{2h} structure is favorable with a ΔE_{av} value of 80.2 kcal/mol. The capped atoms are slightly distorted away from the plane with a H-B(cap1)-B(cap2)-H dihedral angle of 34.538° thus reducing the capped H-H interactions (Bcap-Bcap=2.022 Å, Hcap-Hcap=2.395 Å). Extending $B_{12}H_{10}^{-2}$ **(7)** to $B_{17}H_{13}^{-2}$ **(9)** by condensing an additional B_7 unit does not alter the ΔE_{av} significantly as in the case of anthracene (Table 4.1). Energetics did not change much even when the fourth $B_7H_7^{-2}$ is condensed to give $B_{22}H_{16}^{-2}$ **(10,11)**. Between the two isomers possible for the $B_{22}H_{16}^{-2}$, the linear C_{2h} isomer **(10)** is the more stable one than the angular C_{2v} form **(11)** by 2.0 kcal/mol. The preference for the C_{2h} isomer over the C_{2v} is validated by the ΔE_{av} values and the cap-cap distances, which is given in Table 4.1. This theoretical result is against the stability of edge sharing PAHs where the angular isomer is more stable than the linear one. Almost constant value of ΔE_{av} (Figure 4.11) and the constancy in the charge requirements render the edge sharing polyhedra ideal for condensation based polymeric forms. Structural patterns based on edge sharing pentagonal pyramids are already observed in some boron rich solids such as MgB_4.[20]

iii. Face-sharing condensation

With aromatic hydrocarbons, condensation by sharing more than two atoms is not possible. However, polyhedral boranes present a bonanza. Face sharing condensation between two octahedral B_6 results in $B_9H_6^-$ **(12)** and is akin to $B_{10}H_8^{-2}$ **(5)** and $B_{17}H_{13}^{-2}$ **(9)** in its ΔE_{av} value (69.0 kcal/mol) (Figure 4.14). From the energetics this is the most stable condensed polyhedra among the face sharing systems. A face sharing polyhedra $B_{15}H_{12}^-$ **(13)** between an icosahedral B_{12} and octahedral B_6 falls near to $B_9H_6^-$ **(12)** in the stability but the higher value of ΔE_{av} in the former (82.4 kcal/mol) can be attributed to the short cap-cap distance (2.593 Å) than in the latter (2.883 Å). Two molecules of $B_{12}H_{12}^{-2}$ can condense by sharing a triangular face to give $B_{21}H_{18}^-$**(14)** with ΔE_{av} of 118.9kcal/mol.

$$2B_{12}H_{12}^{-2} \rightarrow B_{21}H_{18}^- + 3BH_2^- \quad ; \Delta E_{av} = 118.9 \text{ kcal/mol} \qquad (4.4)$$

The ubiquitous presence of 3-atom sharing icosahedral arrangement in many boron rich solids[21,24] and in *nido* boranes[36] shows that $B_{21}H_{18}^-$ is a reachable experimental target. This also leads to a variety of possible neutral $CB_{20}H_{18}$ isomers.

When $B_9H_6^-$ **(12)** is extended to one more cage by condensing one more octahedron, $B_{12}H_6$ **(15)** results with a ΔE_{av} value of 103.8 kcal/mol. This shows further condensation to be less favorable than the preceding condensed product. The extension of $B_{21}H_{18}^-$ **(14)** to one more cage results in three different fusion isomers for $B_{30}H_{24}$ **(16-18)**. Among these, D_{3d} structure **(16)** is more stable followed by C_{2v} **(17)** and C_2 **(18)**. This and the result of edge sharing polyhedral borane, $B_{22}H_{16}^{-2}$ **(10,11)** show that the angular fusion, which was favored in benzenoid hydrocarbons is not a pronounced choice with polyhedral

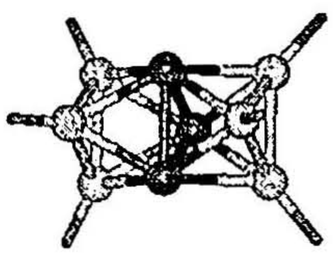

12. B_6H_6 (D_{6h})

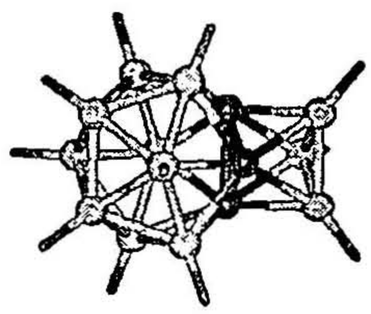

13. $B_{12}H_{12}^{-}$ (C_{5v})

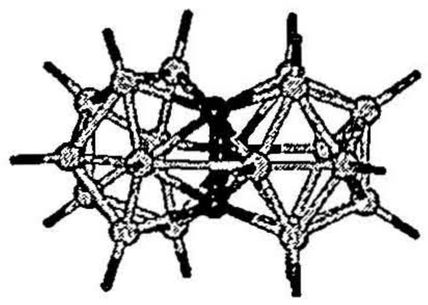

14. $B_{21}H_{18}^{-}$ (D_{3h})

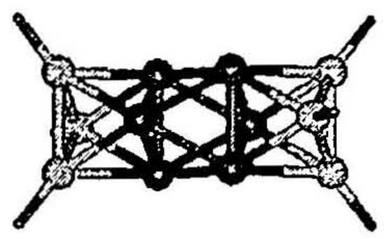

15. $B_{12}H_6$ (D_{3d})

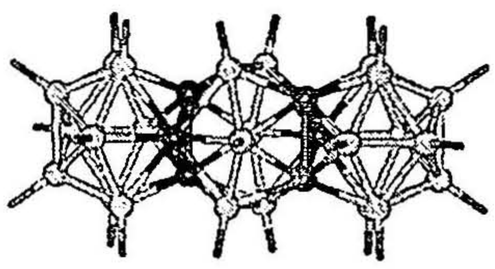

16. $B_{30}H_{24}$ (D_{3d})

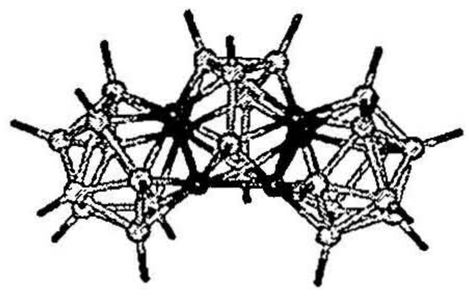

17. $B_{36}H_{24}$ (C_{2v})

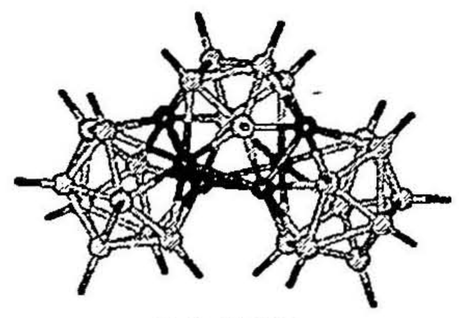

18. $B_{30}H_{24}$ (C_2)

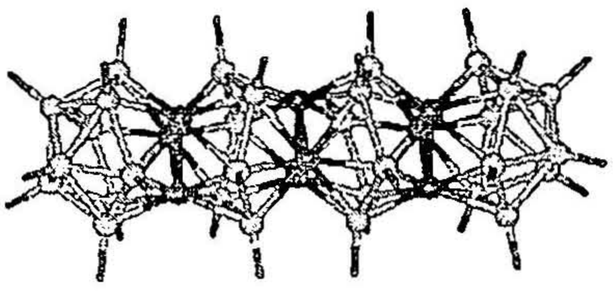

19. $B_{39}H_{30}^{+}$ (D_{6h})

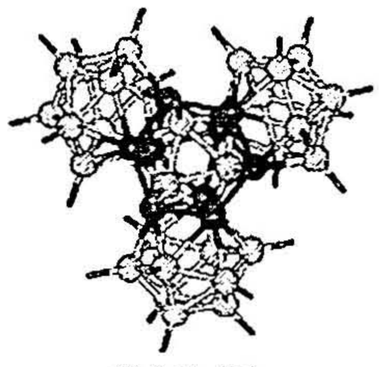

20. $B_{39}H_{30}$ (C_3)

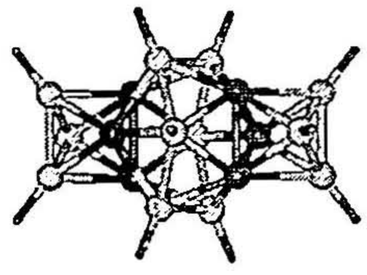

21. $B_{18}H_{12}$ (D_{3d})

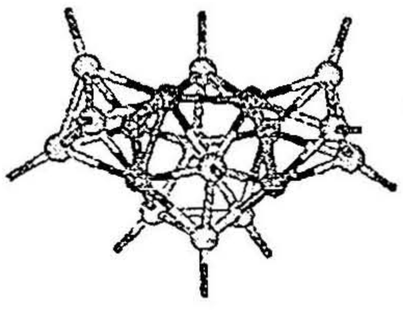

22. $B_{18}H_{12}$ (C_{2v})

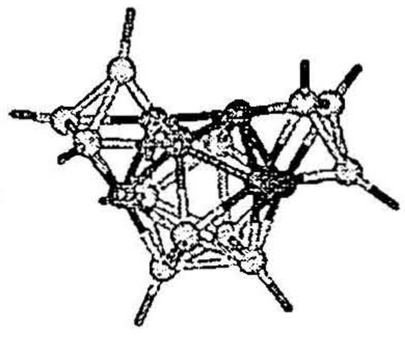

23. $B_{18}H_{12}$ (C_2)

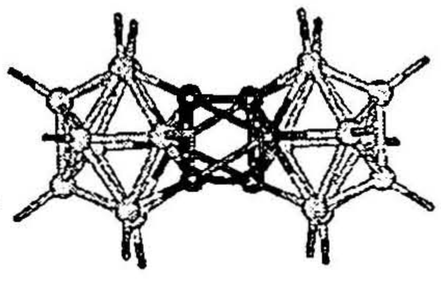

24. $B_{24}H_{18}$ (D_{3d})

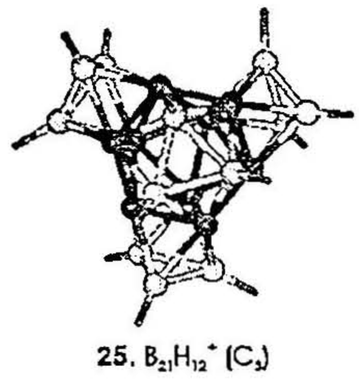

25. $B_{21}H_{12}^{+}$ (C_s)

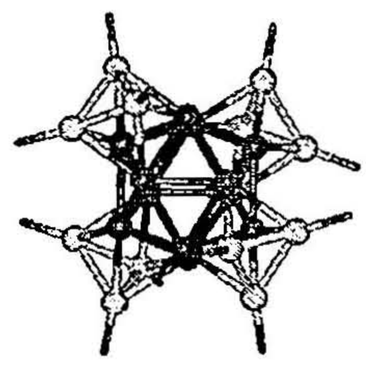

26. $B_{24}H_{12}^{+2}$ (T)

Figure 4.14. Optimized geometries of face sharing condensed products

boranes. Two isomers of the next analogue, $B_{39}H_{30}^{+}$ **(19,20)** are calculated next. The increased ΔE_{av} makes them less attractive. Further face sharing condensation is likely to

be less favorable with the increased positive charge. Adding one more B_6 cage to $B_{15}H_{12}^-$ on the icosahedral side leads to neutral $B_{18}H_{12}$, **(21-23)** which as well has three isomers. In this the angular isomer is the more preferred one both by relative energy measurements and by the ΔE_{av} values as in the case of polycondensed aromatic hydrocarbons. Thus the C_{2v} isomer **(22)** is more stable than D_{3d} form **(21)** only by 0.2 kcal/mol and the C_2 isomer **(23)** is the least stable one among them by 6.9 kcal/mol. These two results illustrate that the steric factors that is more pronounced in the angular isomer of the $B_{30}H_{24}$ causes it to be more energetic than the linear isomer and in $B_{18}H_{12}$ this steric strain is less due to the condensation of still small B_6 cage on to icosahedral B_{12}.

On the other hand neutral $B_{24}H_{18}$ **(24)** obtained as a result of the face sharing condensation of icosahedral B_{12} with $B_{15}H_{12}^-$ **(13)** on the octahedral part yields only one structural pattern and is found to be still more destabilized than the neutral $b_{18}H_{12}$ with a ΔE_{av} difference of 20.5 kcal/mol. This confirms that extended condensation of any condensed product with an icosahedron will be less favorable than with a smaller cage due to steric factors.

iv. Four-atom sharing condensation

Four atom sharing condensation of $B_{12}H_{12}^{-2}$ leads to the experimentally known $B_{20}H_{16}$ **(27,** Figure 4.15) .[37] The ΔE_{av} (138.5kcal/mol) for this system (equation. 4.5) can be used as an experimental upper limit.

$$2\ B_{12}H_{12}^{-2} \rightarrow B_{20}H_{16} + 4BH_2^-;\ \Delta E_{av} = 138.5\ \text{kcal/mol} \qquad (4.5)$$

This implies that with ΔE_{av} values below 138.5 kcal/mol, many edge sharing and face sharing systems described earlier should be within the realm of the possible. Another four atom sharing B_{12} unit on $B_{20}H_{16}$ **(27)** leads to $B_{28}H_{20}^{+2}$ **(28)** with the ΔE_{av} value of 194.1

kcal/mol, indicating that further condensation is still less favorable. We did not consider a fourth polyhedron in the 4-atom sharing condensation as the application of the *mno* rule leads to the tetracation $B_{36}H_{20}^{+4}$. Obviously the infinite extension of four-vertex sharing condensation[38] proposed earlier is improbable without substitutions that compensate the positive charge apart from the jumping up of ΔE_{av} values.

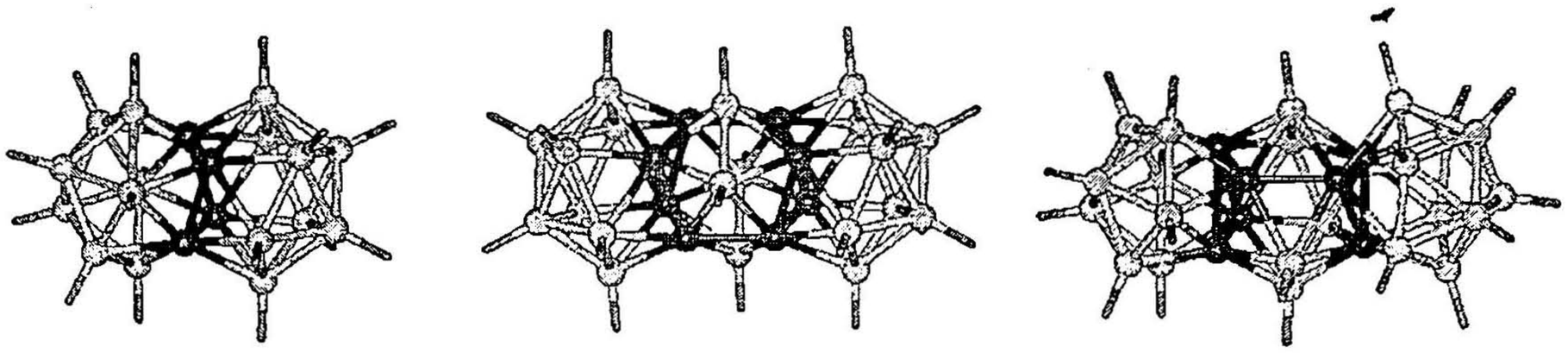

27. $B_{20}H_{16}$ (D_{2d}) 28. $B_{28}H_{20}^{+2}$ (D_{2h}) 29. $B_{29}H_{22}^{+}$ (C_s)

Figure 4.15. Optimized geometries of four vertex sharing condensed products

4.2.3. Aromaticity and NICS values

The above results can be further validated by adding the computed NICS values. For this purpose the isotropic chemical shift at the central position of the each cage of the condensed system is given in Table 4.1. It can be observed that for edge sharing systems the NICS values does not change much as more and more cages are getting condensed. For example, the NICS of $B_{10}H_8^{-2}$ is -21.91 and that of the end cage of $B_{14}H_{10}^{-2}$ is -22.13. This is what is obtained from the equation discussed earlier. This behavior is identical to that observed in benzenes (Table 4.1). The NICS value of the central cage in the case of $B_{14}H_{10}^{-2}$ (-14.55) and $B_{17}H_{13}^{-2}$ (-8.84) is reduced considerably compared to their parent B_6 (-27.05) and B_7 (-21.33) cages. This is in contrast to what is observed in anthracene where it is increased (-12.56) from the parent benzene (-9.66). But phenanthrene shows a similar trend as that of the polyhedral cages (Table 4.1). NICS value goes down with increase in the number of cages for face sharing and 4-vertex sharing systems and the magnitude of

the reduction is high for the 4-vertex sharing systems. For $B_{21}H_{18}^-$, the NICS value is -20.72 and for $B_{30}H_{24}$ it is -18.62 whereas for the four-vertex shared systems $B_{20}H_{16}$ it is -23.63 and for $B_{28}H_{20}^{+2}$ it is -16.49. However a comparison across the various fusion modes shows the 4-vertex sharing $B_{20}H_{16}$ to be more delocalized. As the number of shared atoms increases the system tends to remain as a single cage and hence delocalization becomes more with 4-vertex sharing systems. In general, it is observed that the NICS value of the condensed cages is reduced compared to the parent polyhedral cages.

4.2.4. Geometrical features of the condensed systems

The trends observed in the above energetic analysis are reflected in the geometric data as well. The magnitude of the distance between the cap atoms B1 and B4 incident to a shared edge B2-B3 and the dihedral angle DH (B1B2B3B4) reflects the stability of the condensed systems (Figure 4.16).

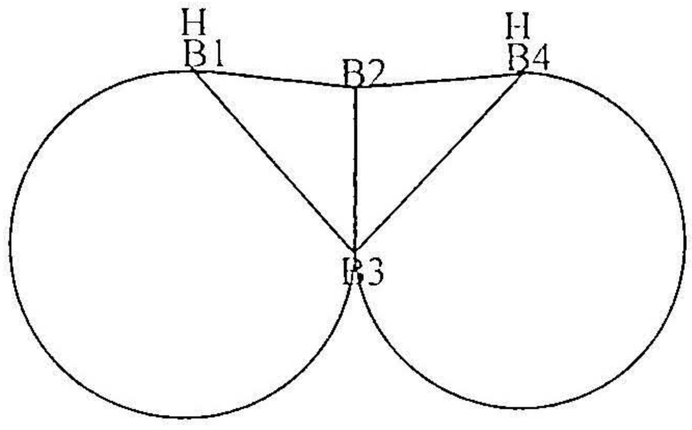

Figure 4.16. The dihedral angle B1B2B3B4 (DH) around a shared bond B2-B3.
B1 and B4 are the capping atoms.

Ideal tetrahedral arrangement of these four atoms will have the dihedral angle of 70.529° ($2\sin^{-1}(1/\sqrt{3})$) where all six B-B distances will be equal. The distance between the capping groups B1 and B4 should ideally fall in the nonbonding range. Comfortable nonbonding distances are achieved by stretching the B1-B2 and B1-B3 bonds and/or by increasing the

DH. Table 4.1 lists the minimum DH observed in the equilibrium geometry, the longest distance between the shared atom to the cap and the shortest cap-cap distance.

The condensed products obtained by edge sharing are the systems where the geometry itself induces shorter cap-cap distances. But the energetics favors them to be more favorable than any other possible mode. This can be attributed to the number of orbitals involved in the delocalization of the resulting condensed system. When two cages are condensed the atoms at the condensed sites donate all their orbitals for bonding. However the number of orbitals used up in delocalisation in the condensed product is still less than the sum of orbitals for the isolated monomers. Lesser the number of orbitals exhausted in delocalization less will be the stability of the associated compounds. This argument favors the preference for edge sharing condensation over three and four atom sharing fusion. Moreover the reduction in the s character of the orbitals of the atoms at the condensed sites involved in condensation also reduces the stability as one goes from the edge sharing, face sharing to four atom sharing systems. The edge sharing system $B_{12}H_{10}^{2-}$ (7) is more comfortable with a DH of 95.303°. A good correlation exists between the ΔE_{av}, DH and the given bond distances (Table 4.1) as is obvious from the table. In each category where the value of 'm' is constant, the most favorable compound will be the one with longest NH (nonbonding distance between capped hydrogen atoms) distance and a DH, which is reasonable with the angle specified above.

For three atom sharing, depending upon the geometry of the individual cages involved the DH will change. $B_9H_6^-$ **(12)** and $B_{15}H_{12}^-$ **(13)** are characterized with optimum Max values and large NB and DH values that will completely forbid any unwanted interactions between the nearest atoms among the different cages and thus these are turn

out to be the most favorable ones among the face sharing systems. The 3-vertex sharing systems between icosahedral B_{12} cages try to reduce the nonbonding interactions by adjusting the DH and the Max. Structure **(14)** has DH value less than 90°. Hence, to avoid shorter NB and NH values, the bond between the cap and the shared atom is elongated (1.9017, Table 4.1) and, thus maximizes the cap-cap distance (2.330). Similar is the case with structures **(16-18)** and **(19,20)** as is shown in Table 4.1. In general, the longest bond is found between the cap and the shared boron (B1-B2). The interatomic distances and the energetics show the extended systems of $B_{30}H_{24}$ **(16-18)** to be favorable, contradicting the earlier predictions.[36b]

For four-atom sharing between the icosahedra **(27** and **28)**, the DH values are in the range 110°-115° and hence B1-B2 bond elongation is not observed.

The immediately perceivable difference in all these condensed systems is the higher co-ordination number (6-8) of the shared boron atoms. This is a major obstacle only in the non-shared site due to ring-cap mismatch and several open and stable macropolyhedral boranes are isolated experimentally. The higher coordination at the shared site in itself is not a destabilizing factor as several known condensed open systems and B_{12} based solids exhibit even 9 and 10 coordination.[39] Theoretically, it is reported to accommodate 12 neighbours.[39c]

The geometries and the energies predict greater favorability for condensed systems in the order edge shared systems> face shared systems> 4-vertex shared systems. But the nuclear independent chemical shift values show that the delocalization is more for the 4-vertex shared $B_{20}H_{16}$ rather than $B_{21}H_{18}^-$. This, in turn points out that the delocalization cannot be attributed directly to the stability.

Table 4.1. Total Energies in a.u. at the B3LYP/6-31G* level for structures 1-19; $\Delta E_{av,}$ average energy (kcal/mol) deduced from Equation 1;[‡] m, number of cages; n, number of vertices; c, number of condensed atoms; DH, dihedral angles (degrees) between a shared edge and the adjacent caps(B1, B2, B3, B_4); Max, longest bond length between the shared atom (B2 or B3) and cap (B1 or B4); NB, Non-bonding distance between two capping borons(B3, B4); NH, the non-bonding distance between two Hs connected to the capping borons. The definition of B1, B2, B3, B4 is illustrated in Figure 4.16. NICS values computed for the condensed cages are also given.

No	Molecule	B3LYP/ 6-31G* (a.u)	ΔE_{av} Kcal/ mol	m	n	c	DH	Max (Å)	NB (Å)	NH (Å)	NICS
1	$C_{10}H_8$ (D_{2h})	-385.89273	109.2	2	10	2	---	---	---	---	-9.96
2	$C_{14}H_{10}$ (D_{2h})	-539.53052	110.2	3	14	4	---	---	---	---	-8.82, -12.56
3	$C_{14}H_{10}$ (C_{2v})	-539.53866	108.9	3	14	4	---	---	---	---	-10.04, -6.80
4	$C_{18}H_{12}$ (D_{2h})	-693.16581	110.8	4	18	6	---	---	---	---	-7.83,-12.57
Edge sharing condensed polyhedra											
5	$B_{10}H_8^{-2}$ (D_{2h})	-253.28709	69.6	2	10	2	80.700	1.872	2.113	2.353	-21.91
6	$B_{11}H_9^{-2}$ (C_{2v})	-278.79148	65.5	2	11	2	87.884	1.964	2.332	2.379	-18.98,-17.68
7	$B_{12}H_{10}^{-2}$ (D_{2h})	-304.28365	65.3	2	12	2	95.303	1.924	2.537	2.419	-14.76
8	$B_{14}H_{10}^{-2}$ (C_{2h})	-353.85472	80.2	3	14	4	77.510	2.142	2.023	2.395	-22.13,-14.55
9	$B_{17}H_{13}^{-2}$ (C_{2v})	-430.39702	69.6	3	17	4	94.567	1.960	2.498	2.384	-15.13,-8.84
10	$B_{22}H_{16}^{-2}$ (C_{2h})	-556.49335	72.8	4	22	6	94.291 94.125	1.979	2.495 2.483	2.384 2.380	-14.57,-9.35
11	$B_{22}H_{16}^{-2}$ (C_{2v})	-556.49014	73.1	4	22	6	93.752 94.625	1.951	2.470 2.475	2.375 2.371	-14.49,-9.23
3-vertex sharing condensed plyhedra											
12	$B_9H_6^-$ (D_{3h})	-227.28188	69.0	2	9	3	141.731	1.751	2.883	4.147	-14.97
13	$B_{15}H_{12}^-$ (C_{3v})	-380.25676	82.4	2	15	3	111.511	1.793	2.593	2.959	-18.54,-21.97
14	$B_{21}H_{18}^-$ (D_{3h})	-533.12037	118.9	2	21	3	88.271	1.902	2.330	2.106	-20.72
15	$B_{12}H_6$ (D_{3d})	-301.57912	103.8	3	12	6	143.193	1.802	2.984	---	-8.70, 15.67
16	$B_{30}H_{24}$ (D_{3d})	-760.30385	144.7	3	30	6	87.867	1.937	2.359	2.096	-18.62,-21.88
17	$B_{30}H_{24}$ (C_{2v})	-760.30300	144.8	3	30	6	87.150	1.954	2.310	2.019	-18.57,-19.61
18	$B_{30}H_{24}$ (C_2)	-760.30041	145.0	3	30	6	88.427	1.984	2.374	2.097	-15.36,-18.98
19	$B_{39}H_{30}^+$(D_{3h})	-987.34351	163.3	4	39	9	87.368	1.966	2.386	---	-15.10, -20.62
20	$B_{39}H_{30}^+$ (C_3)	-987.29795	166.5	4	39	9	87.995 87.368	1.966	2.386 2.369	2.099 2.086	-17.67,-21.54
21	$B_{18}H_{12}$ (D_{3d})	-454.63439	102.0	3	18	6	110 277	1.813	2.611	2.934	-14.63,-21.22
22	$B_{18}H_{12}$ (C_{2v})	-454.63472	102.0	3	18	6	110 809	1.824	2.591	2 964	-16.41,-21.48
23	$B_{18}H_{12}$ (C_2)	-454.62372	103.2	3	18	6	112.806	1.825	2.621	2.986	-15.62,-21.07
24	$B_{24}H_{18}$ (D_{3d})	-607.46582	123.7	3	24	6	110.322	1.852	2.667	---	-21.36,-19.91
25	$B_{21}H_{12}^+$ (C_3)	-528.82183	121.9	4	21	9	113.893	1.844	2.645	---	-13.56,-25.84
26	$B_{24}H_{12}^{+2}$ (T)	-602.87115	139.0	5	24	12	114.971	1.852	2.668	---	-12.76,
4-vertex sharing condensed polyhedra											
27	$B_{20}H_{16}$ (D_{2d})	-506.90851	138.5	2	20	4	113.660	1.870	2.683	2.720	-23.63
28	$B_{28}H_{20}^{+2}$(D_{2h})	-707.41872	194.1	3	28	8	110.091	1.908	2.673	2.656	-16.49,-16.91
Mixed condensation product											
29	$B_{29}H_{22}^+$ (C_s)	-733.93621	166.2	3	29	7	87.6783 111.948	1.915	2.329 2.675	2.097 2.640	-16.20,-23.71

[a] The total energies required in addition are C_6H_6 (D_{6h}) : -232.24866; $B_{12}H_{12}^{-2}$ (I_h): - 305.69021; $B_7H_7^{-2}$ (D_{5h}) : -178.14319; $B_6H_6^{-2}$(O_h): -152.65161; CH_2 (C_{2v}) : -39.12825 ; BH_2^- (C_{2v}) : -25.89723, $C_2B_{10}H_{10}$(condensed)= -330.780560; $C_2B_{10}H_{10}$(monocage)=-330.770183, all at the same level. NICS values in addition are C_6H_6=-9.66; $B_6H_6^{-2}$ = -27.05; $B_7H_7^{-2}$ = -21.33; $B_{12}H_{12}^{-2}$ = -25.92

4.2.5. Conclusions

Obviously several unknown condensed systems are energetically more favorable than the known $B_{20}H_{16}$. Due to the reduction in the number of delocalized orbitals, aromaticity is reduced during condensation. The reduction in stabilization is directly proportional to the number of shared atoms as seen in going from (7) to (14) and (24) (Table 4.1). Stability reduces further with the extended condensation except in the case of edge sharing systems. This clearly delineates the candidates for possible synthesis of condensation-based polyhedral borane polymers. These examples are only illustrative. In view of the large number of polyhedral boranes, the possibilities for polycondensation are endless. The current results help to select the energetically more favorable candidates.

4.3. Benzocarboranes: A comparative analysis on their stability and aromaticity

4.3.1. Introduction

Many compounds are known either with a basic unit of benzene or with a basic unit of mono polyhedral cage present in their structural framework. The structures where both these units are present invite a special scenario where many interesting characteristics are yet to unravel. The only possible mode of mixed condensation between benzenoid aromatics and polycondensed boranes is by two-atom sharing. The benzocarborane was first synthesized by Matteson and Hota in 1968, where the question of aromaticity and the stability factors were raised.[40] This synthesis is followed by the study of many related systems and all studies came to the same conclusion that the benzene ring does not possess substantial π-delocalization.[41,42] The structure of naphthocarborane and anthracarborane were subsequently characterised.[43,44] These interesting structures and many related

hypothetical systems are studied theoretically to uncover their peculiar geometrical features and the extent of delocalization. The previous section pointed out that the edge-sharing fusion is suitable to be considered for the extended condensation based on their ΔE_{av} values. A similar comparative study is made here as well on these edge-fused 2d- 3d systems.

The ability to sustain the delocalization in polyhedral boranes is well known whereas compounds with delocalization broken for benzenoids as in quininoid systems by external perturbation exist. This undoubtedly points out the necessity of delocalization in polyhedral boranes more than in a benzenoid system. We have taken fused systems of benzene with the most stable monopolyhedral cages such as 6-vertex, 7-vertex, 10-vertex and 12-vertex boranes. The charge of the molecules is decided by the *mno* rule. We have calculated the structures where the fused atoms are both borons, one boron and one carbon, and both carbons so that a cross comparison can be made. All the structures discussed here are calculated using B3LYP/6-31G* method implemented in Gaussian 94 programme package.

There are three structural varieties in each case depending on the type of atoms which is being shared; the structures with the sharing sites are occupied by two boron atoms (**a**), one boron and one carbon (**b**), and two carbon atoms (**c**), are separately discussed below. The structures with two carbon atoms at the shared site are neutral, the latter ones have -2 and -1 charge respectively by *mno* rule. The energetic consequences of these edge sharing structures are examined by equation (4.6).

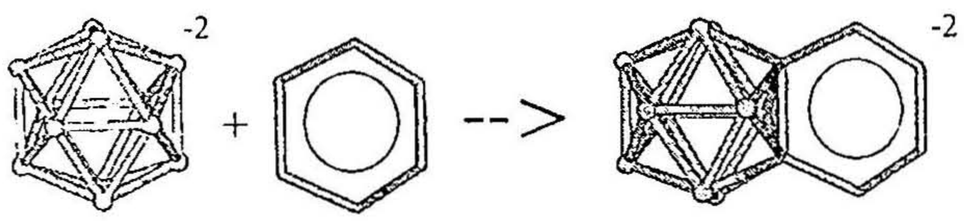

$$+ 2BH_2^- \qquad (4.6)$$

Depending on the condensed products the fragments that are to be eliminated varies, such as 2 CH_2 for structures **a**; 1 CH_2 and 1 BH_2^- for structures **b** and 2 BH_2^- for structures **c**. The values are approximated on the assumption that the differential contribution of isoelectronic fragments BH_2^- and CH_2 to energetics are comparable.

4.3.2. Condensed product of planar 6-membered ring and 12-vertex icosahedral borane

The condensed products of benzene and $B_{12}H_{12}^{-2}$, $C_4B_{12}H_{14}^{-2}$ (**1a**) and $C_5B_{11}H_{14}^{-1}$ (**1b**), though not known experimentally are found to be minimum on their respective potential energy surfaces. The structure **1a** can be considered as a product of $B_{12}H_{12}^{-2}$ and *cis*-butadiene from their geometries. The B-B bond lengths (1.780Å, 1,790Å) are correlating with that in icosahedral $B_{12}H_{12}^{-2}$ (1.787Å) calculated at the same level. The C-C bond lengths 1.350 Å and 1.460 Å in **1a** can be equated with that of *cis*-butadiene. Similarly, in the case of **1b** the geometrical parameters are in agreement with the parent cage $CB_{11}H_{12}^{-1}$ and the *cis*-butadiene. The ΔE_{av} value for **1a** and **1b** are estimated using the equations given below.

$B_{12}H_{12}^{-2} + C_6H_6 \rightarrow C_4B_{12}H_{14}^{-2} + 2CH_2$; $\Delta E_{av} = 116.2$ kcal/mol

$B_{12}H_{12}^{-2} + C_6H_6 \rightarrow C_5B_{11}H_{14}^{-1} + BH_2^- + CH_2$; $\Delta E_{av} = 97.8$ kcal/mol

1b is found to be energetically more favourable than **1a**.

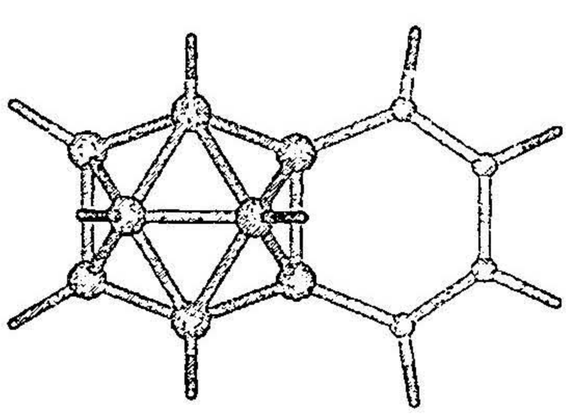

$C_4B_{12}H_{14}^{-2}$ **(1a)**

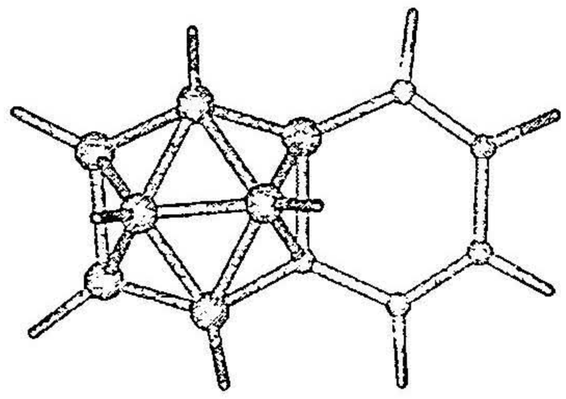

$C_5B_{11}H_{14}^{-1}$ **(1b)**

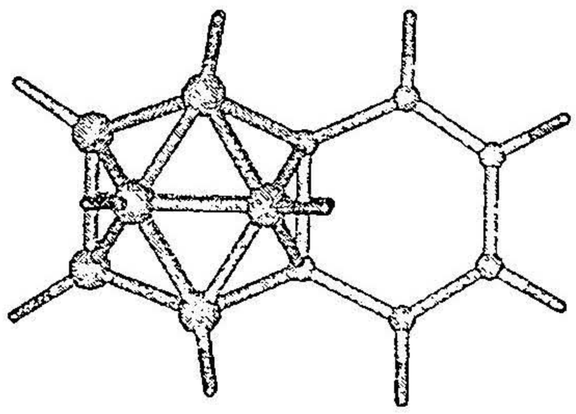

$C_6B_{10}H_{14}$ **(1c)**

Indeed the product of condensation of $B_{12}H_{12}^{-2}$ and C_6H_6 (1**c**) is already known though the starting materials are different.[40,41] This is the fused product of two different delocalized bonding systems where the benzenoid ring is sharing an edge with the icosahedral polyhedral borane cage. The ΔE_{av} value for the equation,

$$B_{12}H_{12}^{-2} + C_6H_6 \rightarrow C_6B_{10}H_{14} + 2BH_2^- \; ; \; \Delta E_{av}=137.9 \text{ kcal/mol} \qquad (4.7)$$

is 137.9 kcal/mol for $C_6B_{10}H_{14}$ **(1c)**. We have calculated all the possible isomers of this compound, which retain the *ortho* carbaborane skeleton (Table 4.2). These isomers can be categorized into three: one where both the carbon atoms are at the shared position (one isomer), where only one carbon atom at the shared site (two isomers) and both the carbon atoms are located away from the fused site (six isomers). The isomer where both the carbon atoms **($1c_c$)** are at the condensed site is the least stable isomer. This is synthesized from 1,2-dilithiocarborane and cis-1,4-dichloro-2-butene and then the dehydrogenation of the resulting 1,4-dihydrobenzocarborane by NBS.[40] The spectral studies indicated a partial aromatic character in the 6-membered ring. Theoretically the relative energies of all the isomers lay within a range of 5 kcal/mol to each other except the least stable one whose relative energy is 9.64 kcal/mol. The more favorable isomer among the structures of $C_6B_{10}H_{14}$ where the condensation involves only the *ortho*-carbaborane unit has two boron atoms at the shared position **($1c_a$),** showing the preference for boron at the condensation site. The high bond alternation and the minimal downfield shift observed in the ^{1}H-NMR of C-H protons indicate practically no aromaticity in the six membered ring.[41] In this respect the carbocycles are different from the boranes.[40] The latter requires aromaticity for its very existence. Localization of benzenoid structures on the other hand is possible with different chemistry, eg. the quinones. In all the isomers of this category the C-C bond

lengths and the planarity shows the C_4 part of 6-membered ring to be like a 1,3-butadiene moiety. The alternate bond lengths are within the range, C_1-C_2, and C_3-C_4=1.354 Å-1.359 Å and C_2-C_3=1.463 Å -1.466 Å. The next favorable category where one carbon is at the fused site also shows the same trend in these bond lengths. One among these isomers (Isomer no. 7, Table 4.2) is known experimentally.[41] The bond length variation obviously points to the localized nature of bonds in the 6-membered ring even though a slight ring current is being observed by experiments in the known forms. However the bond length variation of B-B bonds in the *closo*-borane part is at the second decimal position. All bond distances fall within the range 1.750 Å -1.800 Å indicating that the 3-dimensional delocalization is retained in the cage even after the condensation. Condensing one more icosahedral cage to the benzene unit of **(1c)** gives $C_6B_{20}H_{22}$ **(1d)**. Among the possible isomers, the linear D_{2h} isomer is not a minimum as it forbids double bond localization in the hexagonal ring. But the angular C_{2v} isomer **(1d)**, which resembles phenanthrene has ΔE_{av} values almost constant and is the ideal fusion mode for extended condensation.

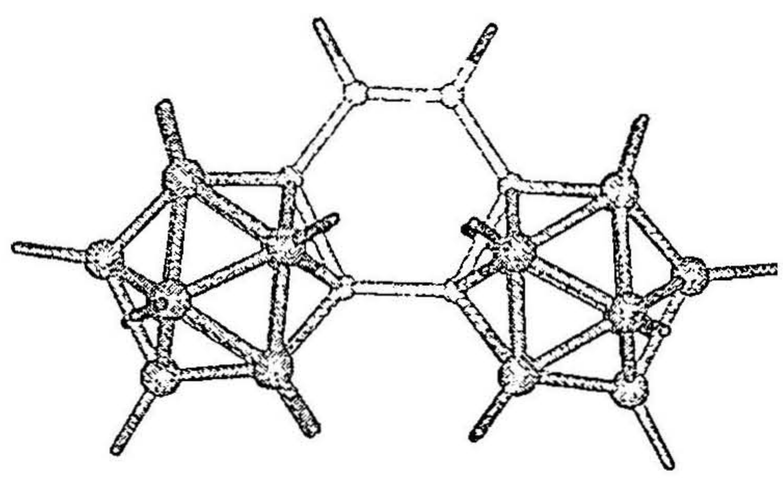

(1d)

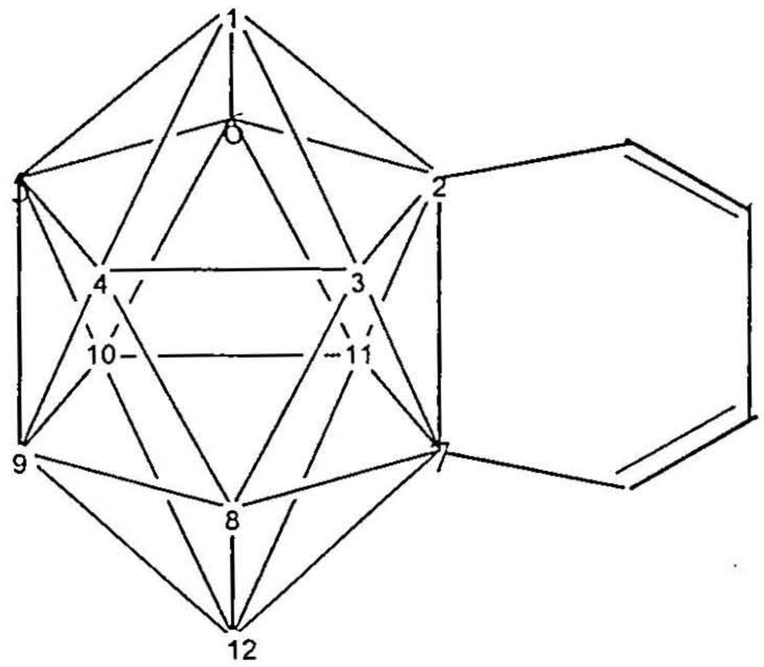

Table 4.2. The total energies (a.u); and the relative energies, RE (kcal/mol) of all the possible isomers of the mixed condensed polyhedron of benzocarborane $C_6B_{10}H_{14}$ which retains an *ortho*-position for the carbon atoms. The position of carbon atoms on the polyhedral cage is specified in the table.

No	Isomer	B3LYP/ 6-31G* (a.u)	RE,(kcal/ mol)
1.	3,8-	-485.720139	0.0
2.	3,4-	-485.719459	0.4
3.	5,9-	-485.717928	1.4
4.	1,6-	-485.717439	1.7
5.	4,9-	-485.716979	2.0
6.	1,5-	-485.716956	2.0
7.	2,3-	-485.714788	3.4
8.	1,2-	-485.713838	4.0
9.	2,7-	-485.704781	9.6

4.3.3. Condensed product of planar 6-membered ring and 10-vertex polyhedral borane

The geometrical parameters of $C_4B_{10}H_{12}^{-2}$ (**2a**) which consists of a B10 unit and a *cis*-butadiene unit are in well agreement with these parent molecules. Similarly the geometrical parameters of $C_5B_9H_{12}^{-1}$ (**2b**) and $C_6B_8H_{12}$ (**2c**) are almost identical to their parent molecules $CB_9H_{10}^{-1}$ and *cis*-butadiene, and $C_2B_8H_{10}$ and *cis*-butadiene respectively. Thus, the planar six-membered ring loses its identity on fusion with any polyhedral borane or carbaboranes. The ΔE_{av} values shows the same trend as observed in icosahedral condensed products. The isomer **2b** is found to be energetically more favorable with a

ΔE_{av} value of 91.4 kcal/mol; **2a** comes next with a ΔE_{av} value of 114.9 kcal/mol and **2c** has a ΔE_{av} value of 127.1 kcal/mol.

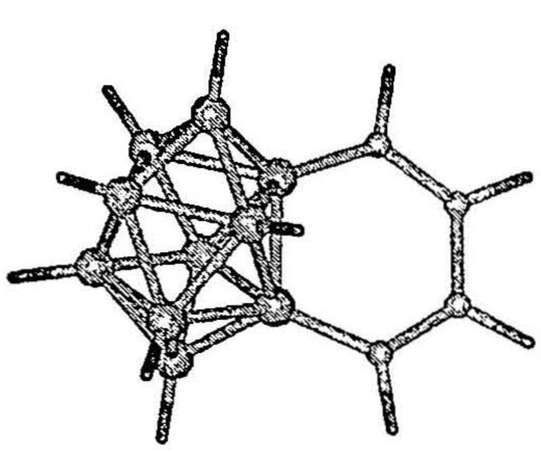

$C_4B_{10}H_{12}^{-2}$ **(2a)**

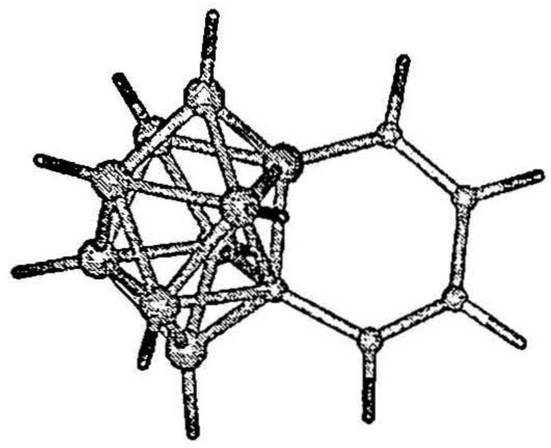

$C_5B_9H_{12}^{-1}$ **(2b)**

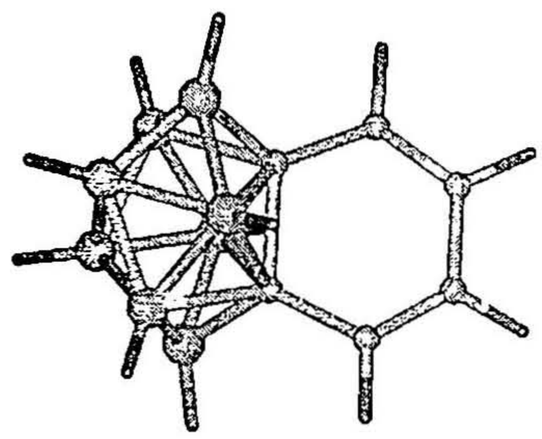

$C_6B_8H_{12}$ **(2c)**

4.3.4. Condensed product of planar 6-membered ring and 7-vertex polyhedral borane

Here each structure can be looked upon as the product of the respective parent polyhedral cage and *cis*-butadiene. $C_4B_7H_9^{-2}$ **(3a)** is a combination product of $B_7H_7^{-2}$ and *cis*-butadiene. Similarly, $C_5B_6H_9^{-1}$ **(3b)** and $C_6B_5H_9$ **(3c)** are the combination products of corresponding monocarbaborane and *cis*-butadiene, and dicarbaborane and *cis*-butadiene. **3a** has a ΔE_{av} value of 110.7 kcal/mol, **3b** has a ΔE_{av} value of 65.5 kcal/mol and **3c**, a ΔE_{av} value of 85.3 kcal/mol.

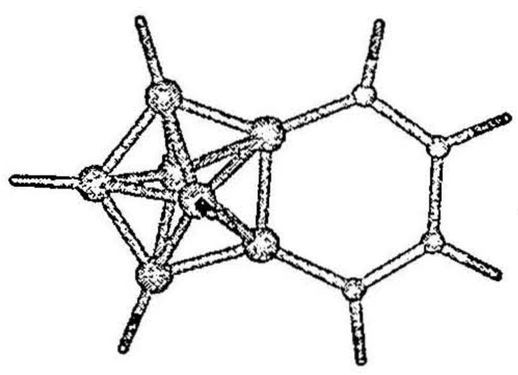

$C_4B_7H_9^{-2}$ **(3a)**

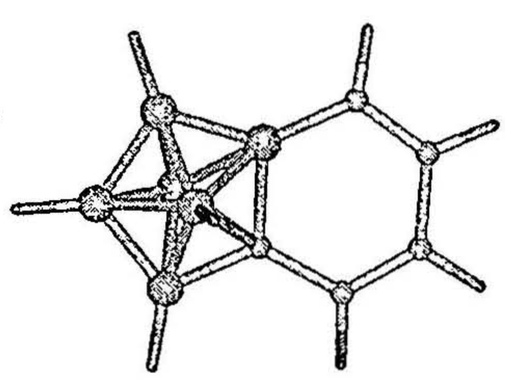

$C_5B_6H_9^{-1}$ **(3b)**

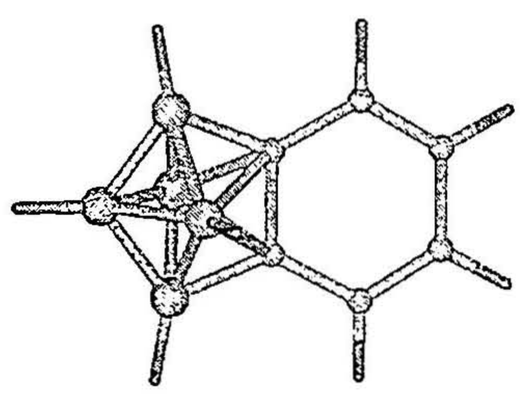

$C_6B_5H_9$ **(3c)**

4.3.5. Condensed product of planar 6-membered ring and 6-vertex polyhedral borane

The geometrical parameters of all the structures **4a**, **4b**. and **4c** are in accordance with the earlier observation that they can be considered as the product of corresponding

polyhedral borane cage and *cis*-butadiene. The ΔE_{av} values calculated are 112.1, 64.8 and 83.9 kcal/mol respectively.

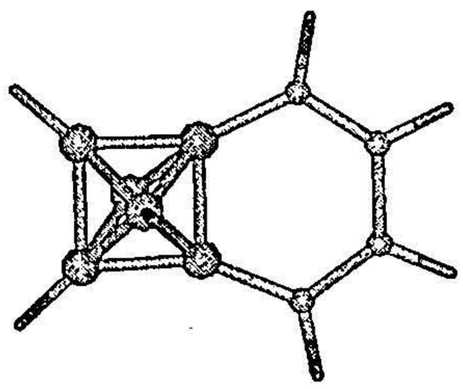

$C_4B_6H_8^{-2}$ **(4a)**

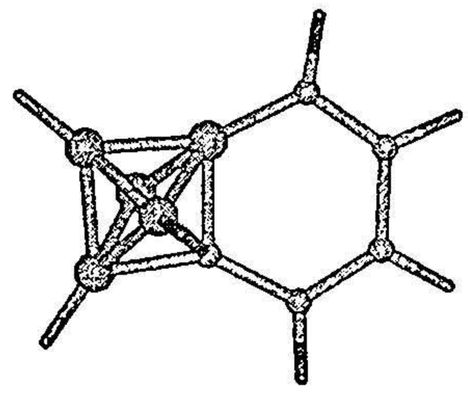

$C_5B_5H_8^{-1}$ **(4b)**

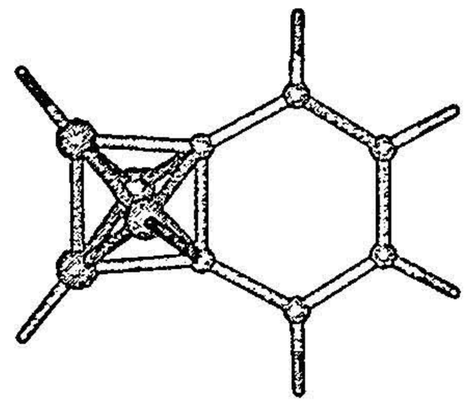

$C_6B_4H_8$ **(4c)**

4.3.6. Aromaticity and NICS values

It has been found that the planar ring loses its aromatic π-delocalization by the condensation with polyhedral cages. The degree of delocalization in both 3-dimensional polyhedral cage and 2-dimensional planar ring after the condensation can be evaluated by calculating the NICS values. It is tabulated in Table 4.3. The values show that the NICS values of the polyhedral cages in the condensed product (Table 4.3; I) are approximately equal or slightly greater than the NICS values calculated for the parent polyhedral cages (Table 4.3; I'). Thus, there is no destruction of the delocalized stability for the cage by the fusion. But on the other hand, the ring current of the six-membered ring has reduced substantially compared to that of benzene. The NICS of benzene is -9.65, but after the condensation the NICS value of the ring in all the compounds has reduced. These values fall within the range 1-3. This substantiates the earlier geometrical observation that all the condensed products can be considered as the product of *cis*-butadiene and the related polyhedral cage.

Table 4.3. The total energies (au); the NICS values for the polyhedral cage of the condensed product (I), of the parent polyhedral cage (I'), and of the 6-membered ring; the lowest vibration frequency; and the ΔE_{av} values (kcal/mol) calculated using the eqn (5.1).

No	Molecule	B3LYP/ 6-31G* (a.u)	NICS I	NICS I'	NICS II	Low Freq	ΔE_{av} (kcal/mol)
1.	$C_4B_{12}H_{14}^{-2}$ (1a)	-459.311914	-26.09	-25.92	-1.72	146.3	116.2
2.	$C_5B_{11}H_{14}^{-1}$ (1b)	-472.601720	-26.26	-26.33	-1.73	155.1	97.8
3.	$C_6B_{10}H_{14}$ (1c)	-485.704781	-26.03	-26.19	-1.68	167.6	137.9
4.	$C_4B_{10}H_{12}^{-2}$ (2a)	-408.269931	-26.47	-25.86	-2.17	143.8	114.9
5.	$C_5B_9H_{12}^{-1}$ (2b)	-421.575610	-27.39	-27.25	-2.32	147.9	91.4
6.	$C_6B_8H_{12}$ (2c)	-434.693096	-27.86	-29.10	-2.55	163.1	127.1
7.	$C_4B_7H_9^{-2}$ (3a)	-331.782582	-22.63	-21.33	-1.91	138.3	110.7
8.	$C_5B_6H_9^{-1}$ (3b)	-345.157520	-18.39	-21.97	2.76	147.4	65.5
9.	$C_6B_5H_9$ (3c)	-358.325427	-23.29	-22.16	-1.32	155.3	85.3
10.	$C_4B_6H_8^{-2}$ (4a)	-306.286470	-27.22	-27.05	-5.81	168.0	112.1
11.	$C_5B_5H_8^{-1}$ (4b)	-319.668158	-29.27	-28.58	-3.73	168.7	64.8
12.	$C_6B_4H_8$ (4c)	-332.838404	-30.05	-29.06	-2.85	184.3	83.9

4.3.7. Conclusions

All the edge-shared condensed products of planar 6-membered ring and the polyhedral borane cages are found to be stable on the potential energy surface. The benzenoid ring loses its aromatic π-delocalisation after the condensation substantially which is reflected in the bond lengths and the NICS values. The ΔE_{av} values, which reflects the stability of the condensed product, shows that the structure with one boron and one carbon at the shared site is energetically more favorable than the other two isomers.

References

1. (a) Lipscomb, W. N. *Boron Hydrides*, Benjamin, New York, **1963**. (b) Lipscomb, W. N. *J. Less- Common Met.* **1981**, *82*, 1.
2. (a) Buschbeck, K. C. *Boron compounds: Elemental boron and boron carbides*; Gmelin Handbook of Inorganic Chemistry, XIII, Supplement 2; Springer, Berlin, **1981**. (b) Wells, A. F. *Structural Inorganic Chemistry*; Oxford University press, Oxford, **1975**. (c) King, R. B. *Chem. Rev.* **2001**, *101*, 1119. (d) Jemmis, E. D.; Balakrishnarajan, M. M. *J. Am. Chem. Soc.* **2001**, *123*, 4324.
3. (a) Pople, J. A.; Lathan, W. A.; Hehre, W. J. *J. Am. Chem. Soc.* **1971**, *93*, 808. (b) Raghavachari, K.; Whiteside, R. A.; Pople, J. A.; Schleyer, P. v. R. *J. Am. Chem. Soc.* **1981**, *103*, 5649. (c) Kaldor, A.; Porter, R. F. *J. Am. Chem. Soc.* **1971**, *93*, 2140.
4. (a) Olah, G. A.; Westerman, P. W.; Mo, Y. K.; Klopman, G. *J. Am. Chem. Soc.* **1972**, *94*, 7859. (b) Rasul, G. A.; Olah, G. A. *Inorg. Chem.* **1997**, *36*, 1278. (c) DePuy, C. H.; Gareyev, R.; Hankin, J.; Davico, G. E.; Damrauer, R. *J. Am. Chem. Soc.* **1997**, *119*, 427. (d) Olah, G. A.; Rasul, G. *J. Am. Chem. Soc.* **1996**, *118*, 8503.
5. Worle, M.; Nesper, R. *Angew. Chem. Int. Edition.* **2000**, *39*, 2349.
6. Jones, M. E.; Marsh, R. E. *J. Am. Chem. Soc.* **1954**, *76*, 1434.
7. Nagamatsu, J.; Nakagawa, N.; Muranaka, T.; Zenitani, Y.; Akimitsu, J. *Nature.* **2001**, *410*, 63.
8. (a) Aihara, J.-I. *J. Am. Chem. Soc.* **1978**, *100*, 3339. (b) King, R. B.; Rouvray, D. H. *J. Am. Chem. Soc.* **1977**, *99*, 7834. (c) Shapiro, I.; Good, C. D.; Williams, R. E. *J. Am. Chem. Soc.* **1962**, *84*, 3837.

9. (a) Hogeveen, H.; Kwant, P. W. *J. Am. Chem. Soc.*, **1974**, *96*, 2208. (b) Hogeveen, H.; Kwant, P. W. *Acc. Chem. Res.* **1975**, *8*, 413.

10. (a) Wade, K. *Chem. Commun.* **1971**, 792. (b) Wade, K. *Adv. Inorg. Chem. Radiochem.* **1976**, *18*, 1.

11. (a) Jutzi, P.; Seufert, A. *Angew. Chem. Int. Ed.* **1977**, *16*, 41. (b) Brown, H. C.; Ravindran, N. *J. Org. Met. Chem.* **1978**, *61*, C5-C7. (c) Jutzi, P.; Seufert, A.; Buchner, W. *Chem. Ber.* **1979**, *112*, 2488. (d) Jutzi, P.; Dohmeier, C.; Koppe, R.; Robl, C.; Schnockel, H. *J. Org. Met. Chem.* **1995**, *487*, 127.

12. (a) Binger, P. *Tetrahedron Lett.* **1966**, *7*, 2675. (b) Onak, T. P.; Wong, G. F. *J. Am. Chem. Soc.* **1970**, *92*, 5226. (c) Miller, V. R.; Grimes, R. N. *Inorg. Chem.* **1972**, *11*, 862. (d) Pasinski, J. P.; Beudet, R. *J. Chem. Phys.* **1974**, *61*, 683. (e) Herberhold, M.; Bertholdt, U.; Milius, W.; Glockle, A.; Wrackmeyer, B. *Chem. Commun.* **1996**, 1219.

13. (a) Hirschfeld, F. L.; Eriks, K.; Dickerson, R. E.; Lippert, E. L, Jr.; Lipscomb, W. N. *J. Chem. Phys.* **1958**, *28*, 56. (b) Stock, A., *Hydrides of Boron and Silicon*, Cornell University Press, Ithaca, New York, **1957**, 74.

14. Shapiro, I.; Keilin, B.; Williams, R. E.; Good, C. D. *J. Am. Chem. Soc.* **1963**, *85*, 3167.

15. Schaeffer, R.; Johnson, Q.; Smith, G. S. *Inorg. Chem.* **1965**, *4*, 917.

16. (a) William, R. E. *Inorg. Chem.* **1971**, *10*, 210. (b) Masamune, S.; Sakai, M.; Ona, H. *J. Am. Chem. Soc.* **1972**, *94*, 8955.

17. (a) Dulmage, W. J.; Lipscomb, W. N. *J. Am. Chem. Soc.* **1951**, *73*, 3539. (b) Hedberg, K.; Jones, M. E.; Schomaker, V. *J. Am. Chem. Soc.* **1951**, *73*, 3538.

18. *The Borane, Carborane, Carbocation Continuum*, Casanova, J. Ed., John Wiley, New York, **1998**.

19. Blum, P.; Bertaut, F. *Acta Crystallogr.*; **1954**, *7*, 81.

20. Naslain, R.; Guette, R.; Barret, M. *J. Solid State. Chem.* **1973,** *8*, 68.

21. (a) Hoard, J. L.; Sullenger, D. B.; Kennard, C. H. L.; Hughes, R. E. *J. Solid State Chem.* **1970**, *1*, 268.

22. Richards, S. M.; Kaspar, J. S. *Act. Crystallogr.* **1969**, *B25*, 237.

23. Bullet, D. W. *J. Phys. C.* **1982**, *15*, 415.

24. (a) Slack, G. A.; Hejna, C. I.; Garbauskar, M. F.; Kasper, J. S. *J. Solid State Chem.* **1988**, *76*, 52. (b) Slack, G. A.; Hejna, C. I.; Garbauskar, M. F.; Kasper, J. S. *J. Solid State Chem.* **1988**, *76*, 64.

25. Kobayashi, M.; Higashi, I.; Matsuda, H.; Kimura, K. *J. alloys. Compd.* **1995**, *221*, 120.

26. (a) Jemmis, E. D.; Kiran, B. *Current Science*. **1994**, *66*, 766. (b) Jemmis, E. D.; Kiran, B. Comput. Chem: Reviews of Current Trends, Vol.1; Leszczynski, J., Ed; World Scientific, Singapore. **1996**, 175.

27. Yao. H-J.; Hu, C-H.; Sun, J.; Jin, R-S.; Zheng, P-J.; Bould, J.; Greatrex, R.; Kennedy, J. D.; Ormsby, D. L.; Thornton-Pett, M. *Collect. Czech. Chem. Commun.* **1999**, *64*, 927.

28. Balasubramanian, K. *Chem. Phys. Lett*. **1991**, *182*, 257.

29. (a) Martin, T. P.; Malinowski, N.; Zimmermann, U.; Näher, U.; Schaber, H. *J. chem. Phys.* **1993**, *99*, 4210. (b) Cristofolini, L.; Ricco, M.; De Renzi, R. *Recent*

Advances in the Chemistry and Physics of Fullerenes and Related Materials, Kadish, K. M. and Ruoff, R. S., Ed.; **1998**, *6*, 667.

30. (a) Hultman, L.; Stafström, S.; Czigány, Z.; Neidhardt, J.; Hellgren, N.; Brunell, I. F.; Suenaga, K.; Colliex, C. *Phys. Rev. lett.* **2001**, *87*, 225503. (b) Manaa, M. R.; Sprehn, D. W.; Ichord, H. A. *J. Am. Chem. Soc.* **2002**, *124*, 13990.

31. Jemmis, E. D.; Schleyer, P. v. R. *J. Am. Chem. Soc.* **1982**, *104*, 4781.

32. Brown, D. A.; Clegg, W.; Colquhoun, H. M.; Daniels, J. A.; Stephenson, I. R.; Wade, K. *J. chem. Soc. Chem. Commun.* **1987**, 889.

33. Muetterites, E. L. Ed. *Boron Hydride Chemistry*; Academic Press: New York, **1975.**

34. Jemmis, E. D.; Balakrishnarajan, M. M.; Pancharatna, P. D. *J. Am. Chem. Soc.* **2001**, *123*, 4313.

35. (a) $C_2B_{10}H_{10}$ isomer where the two carbons are in the opposite ends of the two 5-membered rings in **(5)** is calculated to be lower in energy than the icosahedral $C_2B_{10}H_{10}$ (orthocarboryne)[18b] reported experimentally[18c] by 6.5 kcal/mol: (b) Jemmis, E. D.; Kiran, B. *J. Am. Chem. Soc.* **1997**, *119*, 4076. (c) Gingrich, H. L.; Ghosh, T.; Huang, Q.; Jones Jr, M. *J. Am. Chem. Soc.* **1990**, *112*, 4082.

36. (a) Hosmane,N. S.; Franken, A.; Zhang, G.; Srivastava, R. R.; Smith, R. Y.; Spielvogel, B. F. *Main Group Met. Chem.* **1998**, *21*, 319. (b) Enemark, J. H.; Friedman, H.; Lipscomb, W. N. *Inorg. Chem.* **1966**, *5*, 2165. (c) Lipscomb, W. N. *Inorg. Chem.* **1980**, *19*, 1415. (d) Shea, S. L.; McGrath, T. D.; Jelinek, T.; Stibr, B.; Thornton-Pett, M.; Kennedy, J. D. *Inorg. Chem. Commun.* **1998**, *1*, 97. (e) Shea, S.

L.; Jelinek, T.; Stibr, B.; Thornton-Pett, M.; Kennedy, J. D. *Inorg. Chem. Commun.* **2000**, *3*, 169.

37. (a) Miller, H. C.; Muetterties, E. L. *J. Am. Chem. Soc.* **1963**, *85*, 3506. (b) Dobrott, D. R.; Friedman, L. B.; Lipscomb, W. N. *J. Chem. Phys.* **1964**, *40*, 866. (c) Miller, N. E.; Forstener, J. A.; Muetterties, E. L. *Inorg. Chem.* **1964**, *3*, 1690.
38. J. D. Kennedy in *Advances in Boron Chemistry*, (Ed. *W. Siebert*) Royal society of Chemistry, Heidelberg, **1997**.
39. (a) Hughes, R. E.; Kennard, C. H. L.; Sullinger, K. G.; Weakleim, H. A.; Sands, D. E.; Hoard, J. L. *J. Am. Chem. Soc.* **1963**, *85*, 361. (b) Slack, G. A.; Hejna, C. I.; Garbauskar, M. F.; Kasper, J. S. *J. Solid State Chem.* **1988**, *76*, 64. (c) Jemmis, E. D.; Balakrishnarajan, M. M. *J. Am. Chem. Soc.* **2001**, *123*, 4324.
40. Hota, N. K.; Matteson, D. S. *J. Am. Chem. Soc.* **1968**, *90*, 3571.
41. Hota, N. K.; Matteson, D. S. *J. Am. Chem. Soc.* **1971**, *93*, 2893.
42. Wu, S.; Jones Jr., M. *Inorg. Chem.* **1988**, *27*, 2005.
43. Bradley, A. Z.; Link, A. J.; Biswas, K.; Kahne, D.; Schwartz, J.; Jones Jr., M.; Zhu, Z.; Platz, M. S. *Tetrahedron Lett.* **2000**, *41*, 8691.
44. Bradley, A. Z.; Cohen, A. D.; Jones, A. C.; Ho, D. M.; Jones Jr., M. *Tetrahedron Lett.* **2000**, *41*, 8695.

CHAPTER 5

CO Vertices in Polyhedral Boranes: A New Class of *Hypercloso*-systems

5.0. Abstract

A theoretical analysis on the benzoquinone analogues of polyhedral boranes showed that the polyhedral cage retains the aromatic delocalization in contrast to its 2-dimensional organic counterparts. Jahn-Teller distortion is observed in the p-isomers due to the presence of partially filled degenerate frontier orbitals. The corresponding quinolate anlogues, dianionic isomers have more electron delocalization and are found to be favorable.

5.1. CO vertices in polyhedral boranes: a new class of *hypercloso*-systems

5.1.1. Introduction

The results of the previous chapter showed that the polyhedral borane cage retains three dimensional delocalization even after condensation. How does it change when a carbonyl group is introduced in to the polyhedral borane cage? The carbonyl is an important functional group in organic chemistry. Carbon monoxide is a well-known σ-donor and π-acceptor ligand in transition metal complexes. When CO groups are incorporated into the benzenoids the cyclic delocalization disappears as seen in quinones. Compounds involving quinone structures are abundant in nature. The presence of a low lying LUMO in quinones leads to interesting properties. They are used as organic conductors based on charge transfer complexes[1] and some of them show antitumor activity.[2] Though, there are many such studies on quinones in the literature, there is only one report of a polyhedral borane structure with CO vertex.[3] The characterized structure is with a CO vertex capping a *nido*-$CB_{11}H_{11}$ cage, 1,2-$C_2B_{10}H_{11}O$. The polyhedral boranes with CO vertices demand a deeper understanding of their structure and bonding,

which may provide another link in connecting the electron deficient polyhedral boranes and well-known organic compounds.

By the electron counting rules benzene requires 9 electron pairs (arachno structure, n+3; n=6) which is provided by the 6 carbon vertices. The benzoquinone structure is deficient of one electron pair demanded by the electron counting rules which also explains the presence of a low lying empty orbital whereas the quinolate ion, $C_6H_4O_2^{-2}$ is electron sufficient (Figure 5.1). The corresponding polyhedral carbaborane analogs, the dianionic $C_2B_{n-2}H_{n-2}O_2^{-2}$, are quinolate analogs which are electron sufficient. The neutral ones are benzoquinone analogs. Thus, the benzoquinone equivalent polyhedral carbaboranes, *closo*-$C_2B_{n-2}H_{n-2}O_2$ are n vertex- n electron systems and come under the category '*hypercloso*'.[4] *Hypercloso* structures are *closo* systems with the number of skeletal electrons short of what is needed by the electron counting rules. The idea of exohedral multiple bonding on polyhedral boranes have been discussed in the literature.[5]

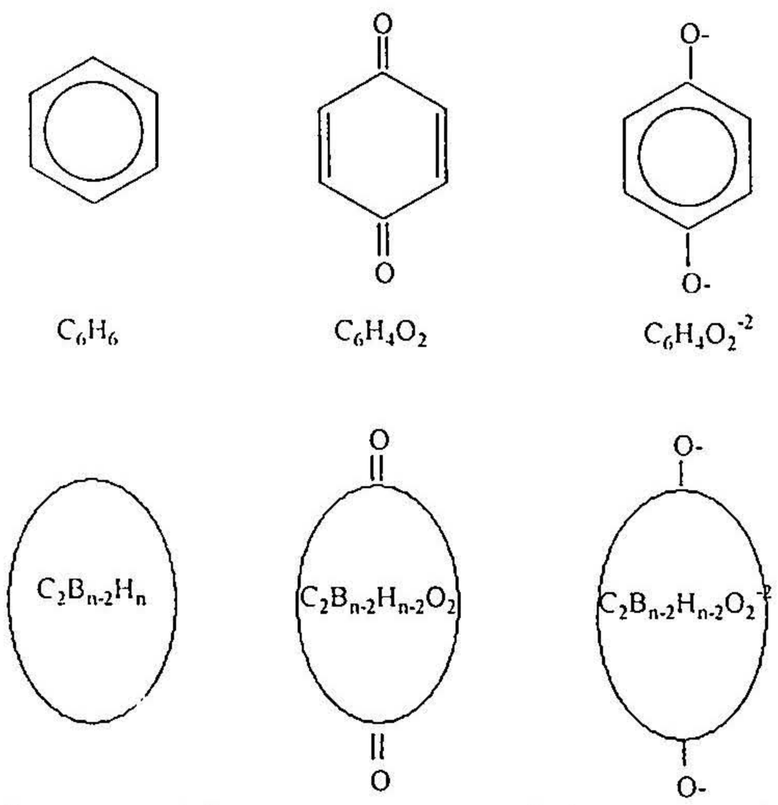

Figure 5.1. All the three benzenoid structures need (m+n+p=1+6+2) 9 electron pairs by electron counting rule. The six carbon atoms in benzene provide 6 electron pairs each and is neutral. The CO vertex can give only two electrons for skeletal bonding, thus benzoquinone $C_6H_4O_2$ is short of an electron pair. The quinolate ion $C_6H_4O_2^{-2}$ is electron sufficient. Their analogous polyhedral carbaborane cages are also shown.

A quantitative treatment is needed to understand the nature of CO bond and the geometrical changes of the polyhedra in these neutral and dianionic clusters. With this aim, a theoretical investigation on the structure and stability of dianionic and neutral $C_2B_{n-2}H_{n-2}O_2$ isomers (n=6,7,10,12) are carried out. The polyhedral carbaboranes with one CO vertex $CB_{n-1}H_{n-1}O^{-2}$ (n=6,7,10,12) are also calculated. These structures are discussed first. In both the cases the structures with 5-membered rings are discussed first and are numbered accordingly followed by the structures with 4-membered rings. Structure with one CO vertex and one 5-membered ring is structure (**1**) and structures with one CO vertex and two 5-membered rings is structure (**2**). Octahedral and bicapped square antiprismatic structures with one CO vertex are numbered **3** and **4**. Then the dianionic isomers with two CO vertices are numbered, first the pentagonal bipyramidal structures (**5-8**) and icosahedral structures (**9-11**) followed by octahedral (**12.13**) and bicapped square antiprism structures (**14-20**). The neutral isomers are numbered by adding "a" to the number of the corresponding dianionic isomers. A comparative analysis of quinone equivalent polyhedral carbaboranes with benzoquinones is also included in the current study.

5.3.2. Polyhedral boranes with one CO vertex

The dianionic mono CO substituted polyhedral boranes, $CB_{n-1}H_{n-1}O^{-2}$ retain the *closo*-skeleton (Figure 5.2) and are equivalents of $CB_{11}H_{12}^-$ where C-H is replaced by C-O^-. The significant change observed is the elongation of B-C bonds when compared to the parent monocarboranes. The frontier π-bonding molecular orbitals (BMO) of the open cage interacts with the CO π* orbitals which are higher lying than the CH p-orbitals. Thus, there is a destabilization of the resulting π-BMOs of the CO substituted cage

compared to the parent carbaboranes. Since these BMOs are essentially ring-cap bonding the destabilization should lengthen the ring-cap distance. In the CO substituted polyhedral boranes the shift of electrons is more towards the oxygen reducing the charge on carbon as well as on the boron atoms to which this carbon is connected. The calculated reduced overlap population values support this argument (Table 5.1):[6] the overlap population of B-C bonds are reduced in the CO substituted boranes compared to the parent carbaborane. The CO bond lengths in these structures approximately fall in the CO bond length range observed for phenolate ions (1.260 Å, calculated at B3LYP/6-31G*). The CO bond lengths observed in the carbonyl substituted polyhedral boranes ($B_{12}H_{10}(CO)_2$) comes around 1.21 Å which is close to the normal carbonyl length.[7]

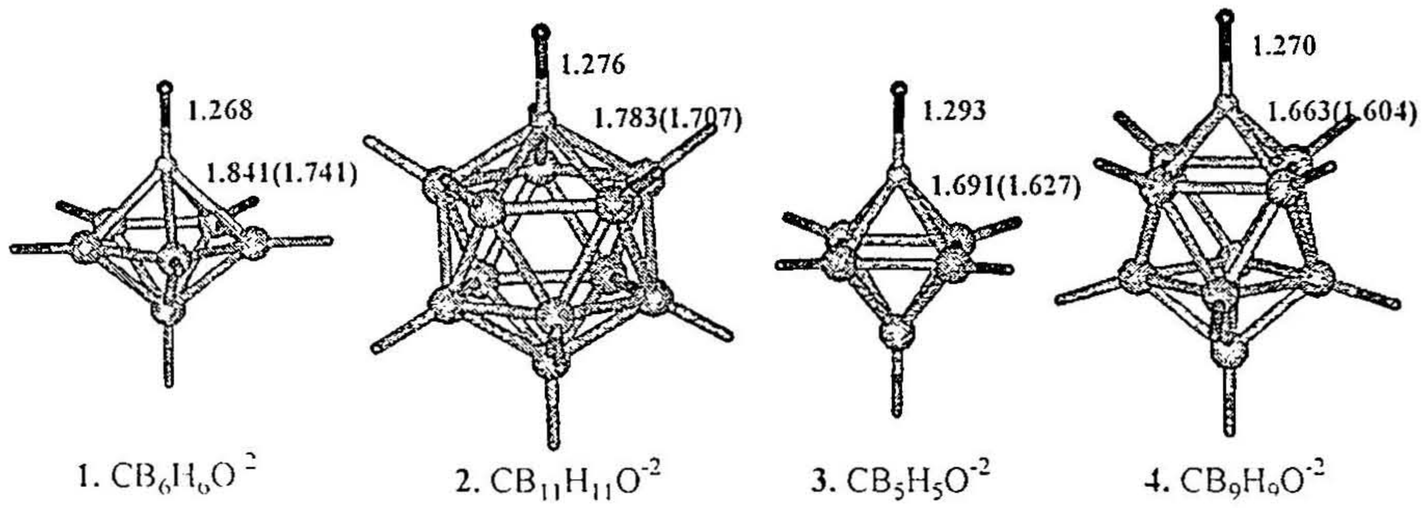

Figure 5.2. The optimized geometries of dianionic mono (CO) substituted polyhedral boranes. The numbers in the parenthesis shows that of parent carbaboranes.

Table 5.1. The overlap population of B-C bonds in the dianionic mono (CO) substituted polyhedral boranes and the parent polyhedral carbaborane cages and the total energy of the $CB_{n-1}H_{n-1}O^{-2}$ isomers.

No.	n	Overlap Population		Total energy,au
		$CB_{n-1}H_n^-$	$CB_{n-1}H_{n-1}O^{-2}$	
		B-C	B-C	
1	7	0.42	0.31	-265.966434
2	12	0.47	0.36	-393.500441
3	6	0.55	0.45	-240.506900
4	10	0.58	0.48	-342.489345

5.3.3. Polyhedral boranes with two CO vertices

i. Clusters involving 5-membered rings:- Icosahedral and pentagonal bipyramidal structures, $C_2B_{n-2}H_{n-2}O_2$ (n=7,12) are included in this part of the discussion. The isomers with adjacent carbon atoms are included under the *ortho* isomers; the isomers with carbon atoms as caps and are opposite to each other are categorized under the *para* isomers and the remaining ones are included in the *meta* category.

In the dianionic o-isomer 2.3-$C_2B_5H_5O_2^{-2}$ (**5**) where the carbon atoms are on the ring, the BH caps move away from the ring centre, thus, getting opened up with a B-C bond length of 2.130 Å. This structure is in contrast to the structure of its parent dicarbaborane where the BH caps are bonded to all the ring atoms.[8] Here the destabilizing π-BMOs due to the interaction of the higher lying CO π* orbitals have large coefficients on the carbon atoms than on the boron atom leading to the slipping of the caps away from carbon atoms. A similar distortion with the capping atoms deviating from ring centre is observed in the other o-isomer, 1,2-$C_2B_5H_5O_2^{-2}$ (**6**) which has one carbon on the ring and one carbon atom as the cap and in the icosahedral o-isomer, 1,2-$C_2B_{10}H_{10}O_2^{-2}$ (**9**). In isomer (**6**) the capping CO carbon is bonded to the ring boron atoms with B-C bond lengths 1.598 Å. The remaining B-C bond distance is 2.331 Å and the C-C bond length is 2.719 Å. The other BH cap moves away from ring carbon, thus, the B-C bond is elongated to 2.245 Å. In the case of icosahedral isomer (**9**) C-C bond is lengthened to 2.120 Å compared to 1.625 Å in the parent *ortho* dicarbaborane. An interaction diagram showing the interaction of the frontier molecular orbitals of the *nido* cage and the CO orbitals in the dianionic icosahedral o-isomer is given in Figure 5.4.

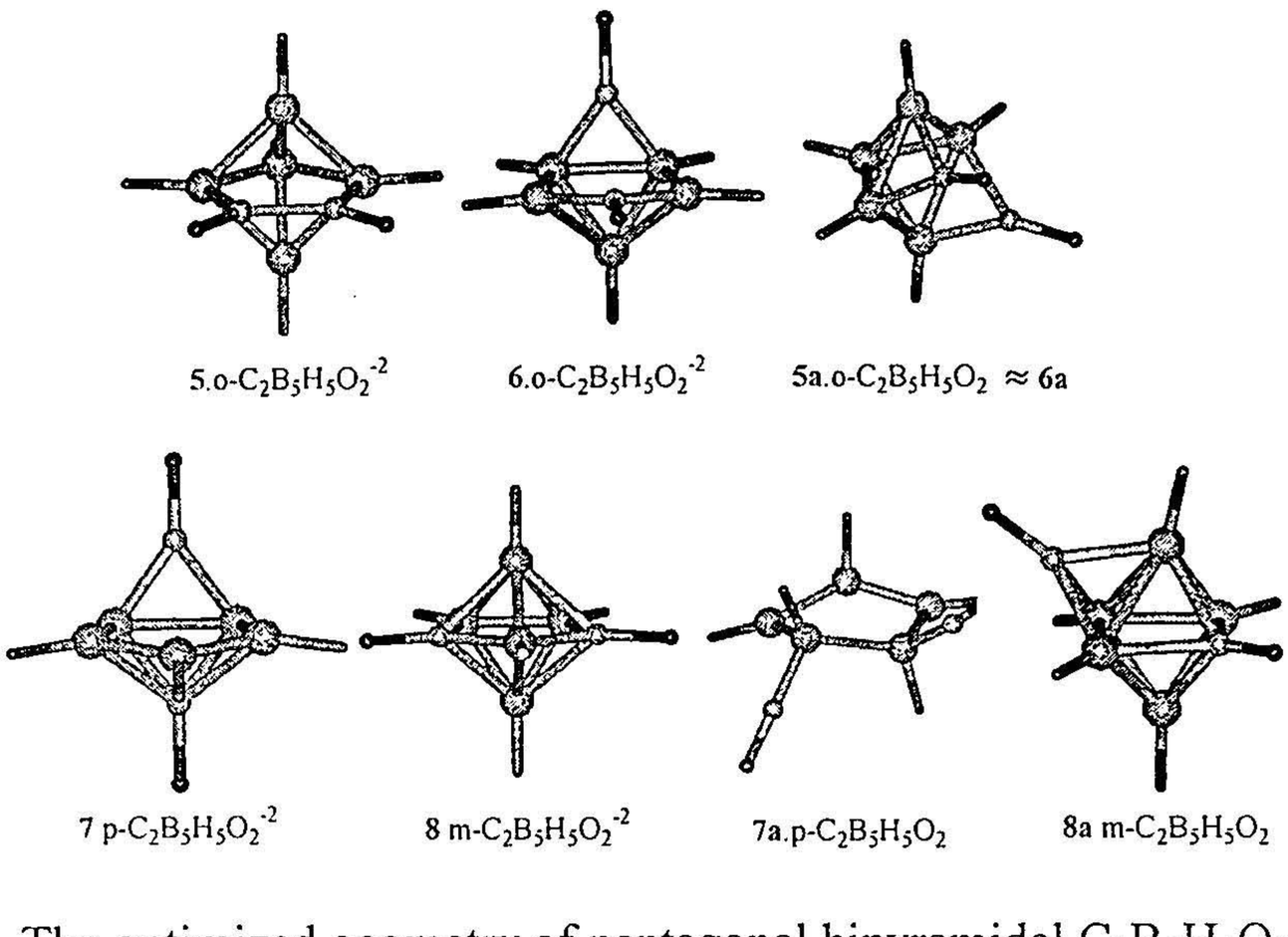

Figure 5.3. The optimized geometry of pentagonal bipyramidal $C_2B_5H_5O_2^{-2/0}$ isomers

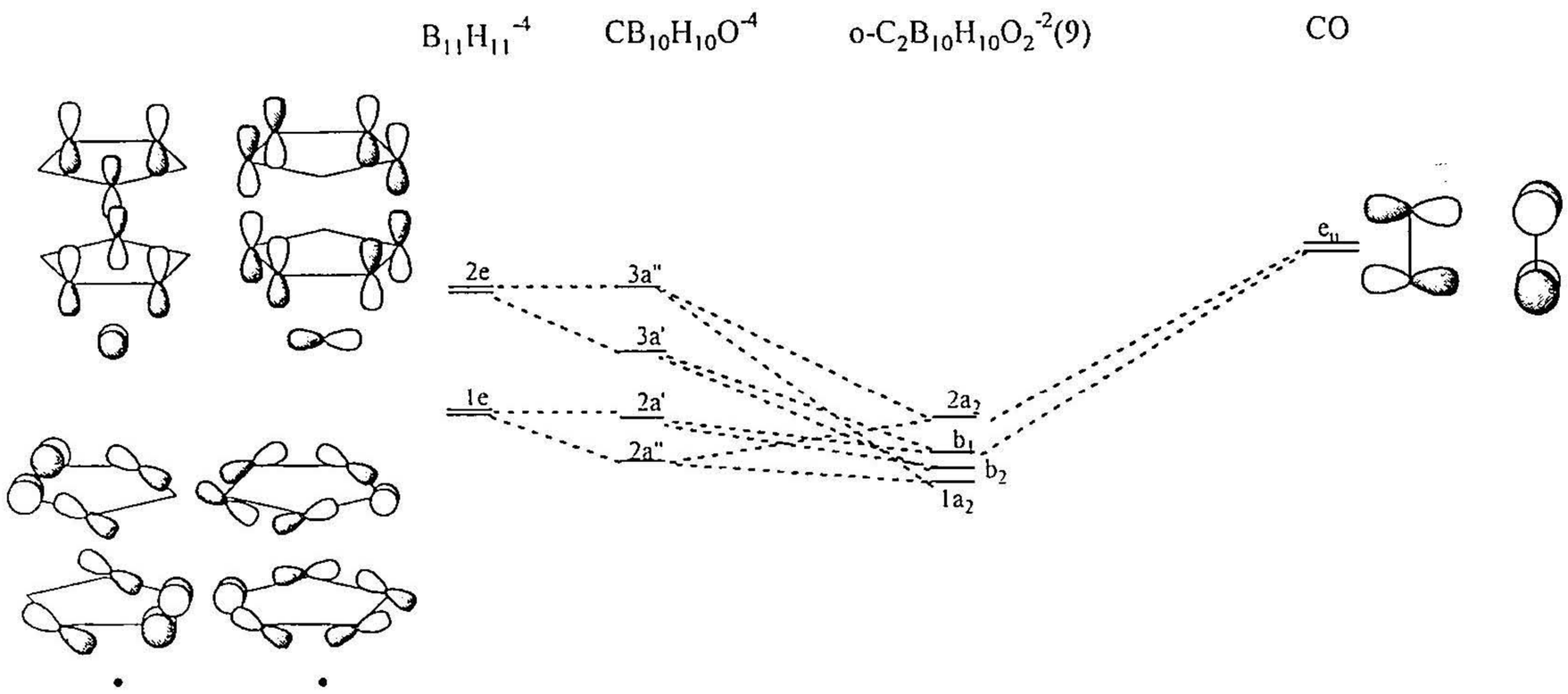

Figure 5.4. A diagram showing the interaction of the CO antibonding orbitals with the parent *nido* system $CB_{10}H_{10}O^{-4}$. The CO vertex in $CB_{10}H_{10}O^{-4}$ is on the open face. The shifting of the degeneracy by replacing a BH vertex in $B_{11}H_{11}^{-4}$ by CO and the secondary interactions taking place in the o-isomer $C_2B_{10}H_{10}O_2^{-2}$ is shown.

When a BH vertex is replaced by a CO on the open face in $B_{11}H_{11}^{-4}$ the frontier orbitals, 1e and 2e shift their degeneracy. When the carbon atom is on the open face the splitting of the degenerate orbitals are higher than in any other positions. When one more CO is placed as cap to the open face, the CO antibonding orbitals interact with the frontier orbitals of the cage, which are the primary interactions. The π-type HOMO 3a" interacts

much strongly with the CO orbitals since their energies are closer. The resulting bonding molecular orbital ($2a_2$, BMO) of the o-$C_2B_{10}H_{10}O_2^{-2}$ is being pushed up by secondary interaction with the in-plane BMO, 2a″. The interaction between the remaining π-MO, 3a′ and the in-plane orbital, 2a′ is also significant. The overall result of this secondary interaction is that it leads to the frontier orbitals with major contribution from the in-plane orbitals in o-$C_2B_{10}H_{10}O_2^{-2}$. The MO, which has major contribution from the π-MO is stabilized and becomes HOMO-3. HOMO-1 with major contribution from the in-plane orbital is found to be stabilized to a greater extent when compared to the orbitals of corresponding dianionic icosahedral m- (**10**) and p-isomers (**11**). This stabilization along with strong $O^-...O^-$ repulsion causes the distortion of the cage and deviation of the cap orbitals from the ring centre in (**6**) and (**9**). Moreover carbon cap on a 5-membered ring has ring-cap compatibility problems as well.[9] All these factors lead to the observed structural deviation.

Marked geometry changes are seen on optimization in the corresponding neutral isomers. There are two o-isomers for the pentagonal bipyramidal species. They are one with two COs on the ring (**5**) and another isomer with one CO on the ring and one CO as cap (**6**). The corresponding neutral isomers converge to identical structure while optimizing (**5a, 6a**). One of the vertex moves to cap a trigonal face apart from the structural deviation observed due to the incorporation of CO vertices as is seen in dianionic isomers. The *hypercloso* structures of B_nH_n are found to have a face capped BH after optimization.[4] The neutral form of the icosahedral o-isomer $C_2B_{10}H_{10}O_2$ (**9a**) also forms a geometry with one of the CO vertex moving to a face capping position. The CO bond lengths and their vibrational frequencies show significant variations in both

dianionic and neutral isomers (Table 5.2). The CO bond length in the dianionic isomers are found to be 1.263 Å (WBI=1.452) in **5**, 1.230 Å (cap(CO);WBI=1.605) and 1.279 Å (WBI=1.461) in **6**; and 1.259 Å (WBI=1.393) in **9**. Similarly the CO bond length in their neutral isomers are 1.170 Å (WBI=1.987) in **5a** and **6a** and 1.189 Å (WBI=1.892) in **9a**.

In the dianionic p-isomer 1,7-$C_2B_5H_5O_2^{-2}$ (**7**) of the pentagonal bipyramidal geometry, both CO caps depart from the ring centre. One of the CO caps is slightly deviated with one longer B-C bond (1.950 Å). The second CO cap deviates more and bridges an edge with three longer B-C bonds (3.110 Å and 2.580 Å). This unsymmetrical distortion can be explained on the basis of ring-cap orbital overlap.[9] The ring hydrogens are bent towards one of the carbon vertex in order to attain the better ring cap-overlap. However, this reduces the overlap of the other carbon cap and the ring. The former carbon vertex thus shifted slightly and the latter, more. This type of distortion is not found in the dianionic icosahedral p-isomer, 1,7-$C_2B_{10}H_{10}O_2^{-2}$ (**10**). It retains its D_{5d} symmetry though the B-C bond length is larger (1.786 Å) than the parent dicarbaborane (1.708 Å). The elongation of B-C bond lengths can be explained on the basis of the charge transfer due to the electron withdrawing nature of the CO vertex. The CO bond lengths in 7 are 1.273 Å (WBI=1.351) and 1.229 Å (WBI=1.664) and that in **10** is 1.276 Å (WBI=1.316).

The neutral p-isomer of the pentagonal bipyramid (1,7-$C_2B_{10}H_{10}O_2$, **7a**) has a doubly degenerate HOMO with only two electrons. This leads to a structural distortion so that the degeneracy can be iifted (Jahn-Teller distortion). Thus on optimization, a distorted structure (**7a**) is obtained with one of the frontier π-MO being destabilized to a greater extent. One of the bonds (B-B bond, each of this boron is bonded to one CO and

one hydrogen, **7a**) is elongated to 1.812 Å and the vertex, which is opposite to this bond comes closer thus causing an out of plane distortion of the 5-membered ring. Each of the CO is bonded to one of the vertex with B-C bond length 1.490 Å (WBI=1.193). The CO bond length is 1.150 Å (WBI=2.167).

The neutral icosahedral p-isomer, $C_2B_{10}H_{10}O_2$ is optimized (**10a**) in C_{2v} symmetry and is a minimum on the potential energy surface with low vibrational frequency value 89.52. Though it loses its symmetry from D_{5d} to C_{2v}, it still retains the *closo* form with reasonable bond lengths. The CO bond length is found to be 1.254 Å (WBI=1.415). The attempt of the 12-vertex polyhedral species to retain its icosahedral framework at any expense is obvious here.

The m-isomer, 2,4-$C_2B_5H_5O_2^{-2}$ (**8**) of the pentagonal bipyramid retains its *closo* skeleton with CO bond length 1.291 Å (WBI=1.314). Its neutral isomer (**8a**) is optimized to an octahedral geometry with a CO vertex capping one of the trigonal faces. This is in agreement with the *hypercloso*-geometry obtained for the B_nH_n species. The CO bond lengths obtained are 1.193 Å (cap CO; WBI=1.764) and 1.217 Å (WBI=1.560). The dianionic icosahedral m-isomer 2,4-$C_2B_{10}H_{10}O_2^{-2}$ (**11**) also retains the *closo*-structure. The distortion observed among the o-isomer (**6**) is not found as the secondary interactions mentioned above are not prominent here. The CO bond length is 1.275 Å (WBI=1.310). The icosahedral framework is retained in the neutral form (**11a**) with CO bond length 1.254 Å (WBI=1.403).

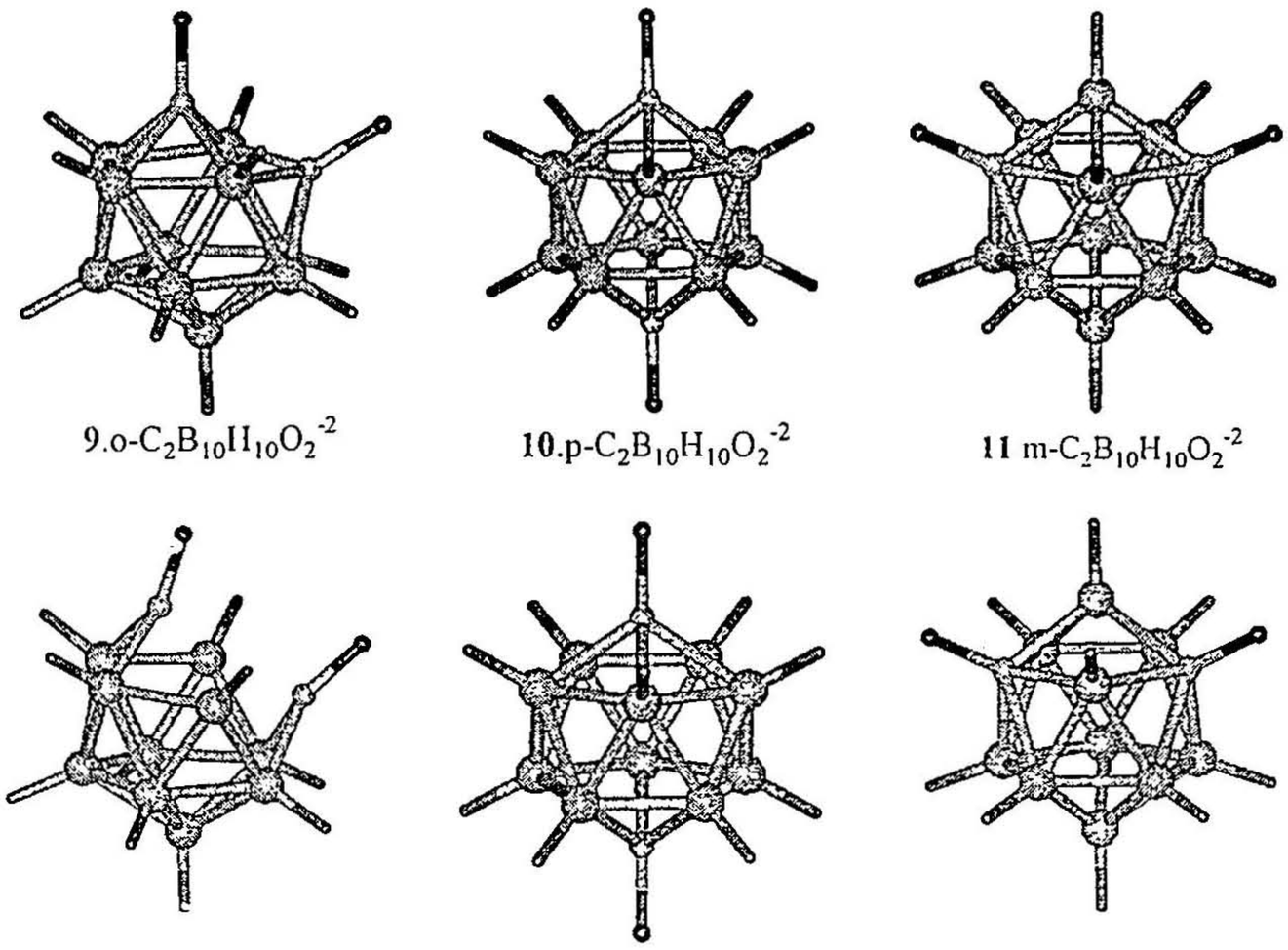

9.o-$C_2B_{10}H_{10}O_2^{-2}$ **10**.p-$C_2B_{10}H_{10}O_2^{-2}$ **11** m-$C_2B_{10}H_{10}O_2^{-2}$

9a.o-$C_2B_{10}H_{10}O_2$ **10a**.p-$C_2B_{10}H_{10}O_2$ **11a** m-$C_2B_{10}H_{10}O_2$

Figure 5.5. The optimized geometries of icosahedral $C_2B_8H_8O_2^{-2/0}$ isomers

ii. Clusters involving 4-membered rings:- In the case of o-isomers, when we compare the parent dicarbaboranes and the dianionic 1,2-$C_2B_4H_4O_2$ (**12**) the obvious distinction is in the C-C bond length which is elongated to 1.870 Å from 1.540 Å.

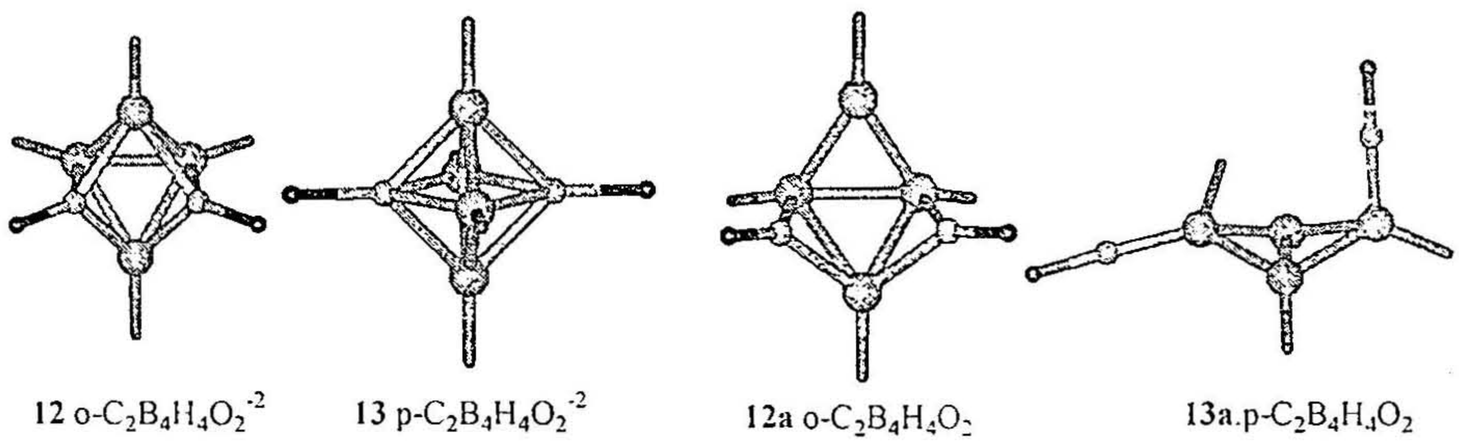

12 o-$C_2B_4H_4O_2^{-2}$ **13** p-$C_2B_4H_4O_2^{-2}$ **12a** o-$C_2B_4H_4O_2$ **13a**.p-$C_2B_4H_4O_2$

Figure 5.6. The optimized geometries of octahedral $C_2B_4H_4O_2^{-2/0}$ isomers

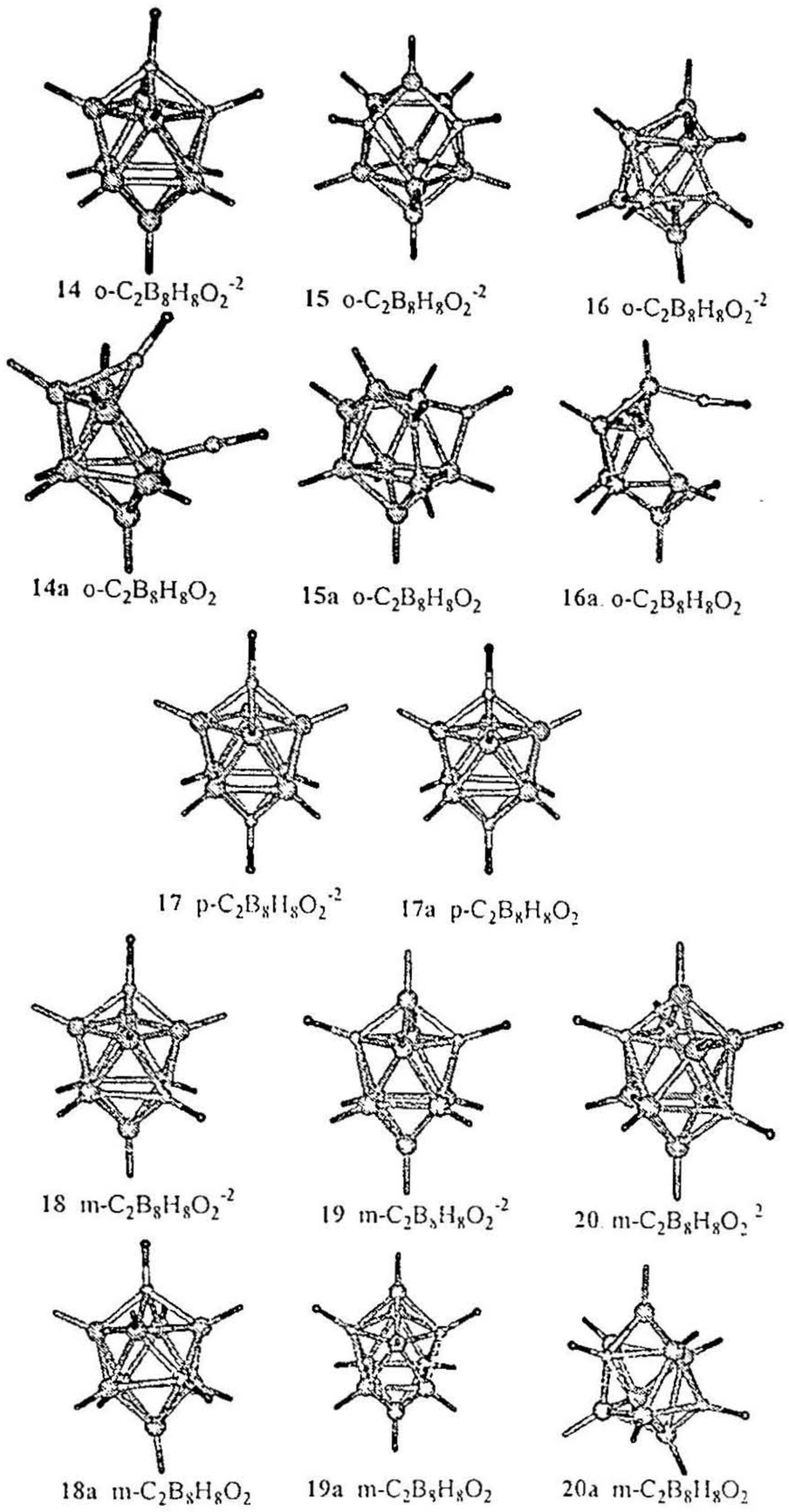

Figure 5.7. The optimized geometries of 10-vertex $C_2B_8H_8O_2^{-2/0}$ isomers

This can be attributed to the destabilization of the in-plane bonding molecular orbital with large coefficients on the carbon atoms due to the interaction with higer lying CO antibonding orbitals.

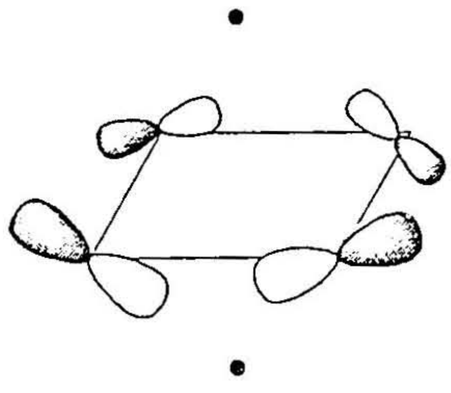

Similarly in the neutral quinone analog (**12a**) an electron pair is removed from this destabilized MO (shown above) and the 2 π-MOs shown below are stabilized.

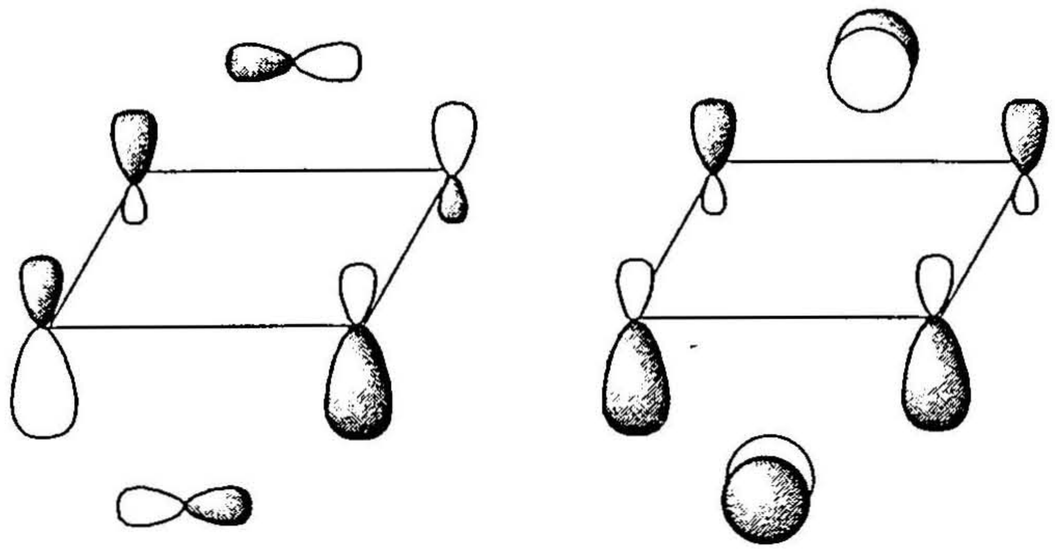

The *closo*-geometry is broken and one of the BH cap goes away from the symmetry axis and bridges an edge. The unsymmetric distortion is caused by the bending of ring hydrogens and the large coefficients on the carbon atom and thus favors maximum ring-cap orbital overlap. The CO bond length in the dianionic form (**12**) is 1.275 Å (WBI=1.364) and that in the neutral form (**12a**) it is 1.181 Å (WBI=1.940).

There are three o-isomers for 10-vertex polyhedron (**14,15,16**). Among the dianionic o-isomers, the C-C and B-C bond elongation can be explained based on the charge transfer and the destabilization of the π-BMOs. Apart from this bond length elongation one of the CO is shifted to a face capping position in their neutral counterparts (**14a,15a,16a**).

In contrast to the o-isomers 1,2-$C_2B_4H_4O_2^{-2}$ (**12**) where the in-plane bonding MO is destabilized, the in-plane BMO is stabilized and the degenerate π-bonding MOs are destabilized in the dianionic p-isomer 1,6-$C_2B_4H_4O_2^{-2}$ (**13**) in comparison to the parent p-dicarbaborane, thus leading to the shortening of the B-B bonds and lengthening of the B-C bonds. But (**13**) has a D_{4d} structure with a CO bond length of 1.298 Å (WBI=1.268). The neutral D_{4d} structure has its frontier electrons in a doubly degenerate level, a case

similar to the neutral p-isomer of the pentagonal bipyramid (**4a**). Thus, on optimization, Jahn-Teller distorted structure is obtained. The diagonal atoms in the 4-membered ring come closer. Each of the caps which had bonding interaction with these diagonal atoms going towards the remaining diagonal atoms with the B-C bond length of 1.470 Å (WBI=1.244). The CO bond length is calculated to be approximately 1.156 Å with a WBI of 2.109. The dianionic p-isomer (**17**) of the 10-vertex family shows similar trends in their geometry. The neutral isomer (**17a**) undergoes Jahn-Teller distortion reducing the symmetry to C_{2v}. The opposite ring B-B bonds are elongated and the remaining ring bonds are shortened. The dianionic m-isomers (**18,19,20**) show B-C bond elongation and their neutral counterparts (**18a,19a,20a**) has one CO moving to a face capping position. The CO bond lengths in the dianionic isomers are longer than that in the neutral isomers as observed earlier (Table 5.2).

5.3.4. Comparison of the stability with benzoquinones

The aromatic destabilization due to the loss of cyclic delocalization in benzoquinone and their polyhedral analogues is calculated by employing similar equations given below. The LHS of the equation involves the delocalized benzene or the dicarbaborane and the RHS involves the quinones or its analogues of polyhedral carbaboranes. All the other systems involved in the equation do not possess any cyclic delocalization and thus the ΔH evolving from the equation is an indicator of the loss of aromatic stabilization in the quinone ring or the cage.

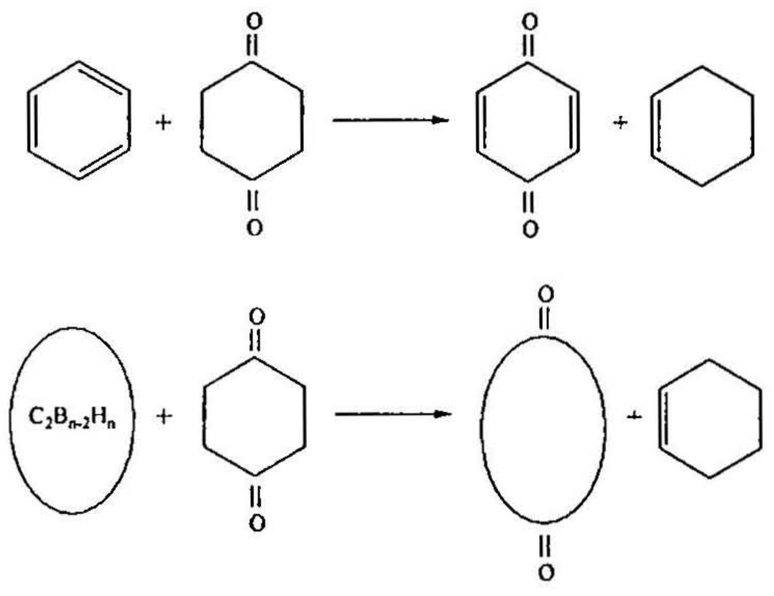

The p-benzoquinone is computed to be deprived of aromatic stability by 29.5 kcal/mol compared to benzene. The ΔH of the equation involving the o-isomer is 36.6 kcal/mol and that of the m-quinone is 82.5 kcal/mol. The high ΔH value of the m-quinone is supported by its unavailability. In the case of carbaborane analogues, the ΔH values show that there are potential candidates, which can be accessible experimentally. The p-isomers of the quinone analogs of polyhedral boranes are open structures due to Jahn-Teller distortion except 12-vertex species. The ΔH values of the octahedral quinone equivalents are computed to be 52.5 kcal/mol and 59.7 kcal/mol for p- and o-isomer respectively. The pentagonal bipyramidal isomers may be even more accessible. The isomers with CO caps are calculated to have less ΔH values compared to benzoquinones. The distorted p-isomer with 2 CO caps (**7a**) has a ΔH value of 21.3 kcal/mol and the o-isomer with one CO cap (**6a**) has a ΔH value of 26.0 kcal/mol. The loss of aromatic delocalization in the icosahedral isomers is found to be very high. The p-isomer (**10a**) is less stable with a ΔH value of 127.0 kcal/mol, m-isomer (**11a**) with 128.0 kcal/mol and the o-isomer (**9a**) with 91.2 kcal/mol than their corresponding parent dicarbaborane cages. This makes them less favorable though their dianionic structures should be accessible.

Table 5.2:- The total energy (au), the delocalization energy (ΔH in kcal/mol), the CO bond lengths (r in Å), the asymmetric and symmetric CO stretching frequency (υ in cm^{-1}), the Wiberg Bond Indices of the CO bond (WBI), and the NICS values. The NICS values in the parentheses are that of the corresponding parent dicarbaborane.

Isomer	Total Energy,au	ΔH(kcal /mol)	r(C-O) (Å)	υ(C-O) cm^{-1}	WBI	NICS
o-$B_5H_5(CO)_2^{-2}$ **(5)**	-353.849391		1.263	1533,1605	1.452	-22.17
o-$B_5H_5(CO)_2$ **(5a)**	-353.874142	50.38	1.170	1948,2018	1.987	-15.93 (-22.73)
o-$B_5H_5(CO)_2^{-2}$ **(6)**	-353.849429		1.230©,1.270	1519,1723	1.605,1.461	-17.83
o-$B_5H_5(CO)_2$ **(6a)**	-353.874259	26.01	1.170©,1.150	1938,2136	1.987	-11.95 (-21.56)
p-$B_5H_5(CO)_2^{-2}$ **(7)**	-353.785984		1.273,1.220	1452,1735	1.351,1.664	-10.28
p-$B_5H_5(CO)_2$ **(7a)**	-353.841502	21.29	1.151,1.140	2141,2161	2.167	-17.08 (-21.68)
m-$B_5H_5(CO)_2^{-2}$ **(8)**	-353.847591		1.291	1433,1449	1.314	-23.17
m-$B_5H_5(CO)_2$ **(8a)**	-353.846924	84.44	1.210©,1.190	1721,1850	1.560,1.764	-10.74 (-22.98)
o-$B_{10}H_{10}(CO)_2^{-2}$**(9)**	-481.315903		1.259	1491,1553	1.393	-27.12
o-$B_{10}H_{10}(CO)_2$**(9a)**	-481.209435	91.17	1.189	1828,1867	1.892	-9.51 (-26.22)
p-$B_{10}H_{10}(CO)_2^{-2}$**(10)**	-481.305326		1.276	1423,1436	1.316	-23.54
p-$B_{10}H_{10}(CO)_2$**(10a)**	-481.182573	127.05	1.254	1463,1465	1.415	-139.95 (-27.63)
m-$B_{10}H_{10}(CO)_2^{-2}$**(11)**	-481.306108		1.275	1423,1436	1.310	-25.99
m-$B_{10}H_{10}(CO)_2$**(11a)**	-481.176708	128.00	1.253	1451,1467	1.403	148.21(-27.00)
o-$B_4H_4(CO)_2^{-2}$**(12)**	-328.358235		1.275	1528,1532	1.364	-36.11
o-$B_4H_4(CO)_2$**(12a)**	-328.386153	59.73	1.181	1899,1976	1.940	-8.17 (-29.34)
p-$B_4H_4(CO)_2^{-2}$**(13)**	-328.345223		1.298	1409,1495	1.268	-29.74
p-$B_4H_4(CO)_2$**(13a)**	-328.411281	52.52	1.156	2136,2190	2.109	-9.45 (-29.81)
o-$B_8H_8(CO)_2^{-2}$**(14)**	-430.300525		1.274©,1.250	1490,1536	1.325,1.397	-22.96
o-$B_8H_8(CO)_2$**(14a)**	-430.257765	68.34	1.180©,1.150	1944,2140	1.953,2.152	-10.26 (-24.28)
o-$B_8H_8(CO)_2^{-2}$**(15)**	-430.293003		1.267	1482,1519	1.416	-18.48
o-$B_8H_8(CO)_2$**(15a)**	-430.220904	74.11	1.173,1.190	1826,1955	1.948,1.883	-3.92 (-27.71)
o-$B_8H_8(CO)_2^{-2}$**(16)**	-430.306691		1.245	1630,1653	1.605	-7.65
o-$B_8H_8(CO)_2$**(16a)**	-430.257532	51.41	1.159	2078,2109	2.097	-10.95 (-28.90)
p-$B_8H_8(CO)_2^{-2}$**(17)**	-430.328978		1.287	1423,1469	1.280	-20.85
p-$B_8H_8(CO)_2$**(17a)**	-430.258234	108.09	1.232	1588,1608	1.541	140.59(-23.30)
m-$B_8H_8(CO)_2^{-2}$**(18)**	-430.301137		1.286©,1.270	1445,1469	1.277,1.364	-22.01
m-$B_8H_8(CO)_2$**(18a)**	-430.232699	102.49	1.235©,1.231	1576,1595	1.505,1.490	14.01 (-25.50)
m-$B_8H_8(CO)_2^{-2}$**(19)**	-430.270923		1.278	1422,1465	1.329	-22.99
m-$B_8H_8(CO)_2$**(19a)**	-430.209531	91.54	1.232	1584,1609	1.495	3.95 (-29.08)
m-$B_8H_8(CO)_2^{-2}$**(20)**	-430.274726		1.272	1458,1464	1.362	-22.65
m-$B_8H_8(CO)_2$**(20a)**	-430.208737	96.45	1.211,1.220	1627,1728	1.622,1.508	4.21 (-29.15)

©CO bond lengths of cap CO vertices

5.3.5. Aromaticity and NICS values

The variation in aromaticity is studied by the nuclear independent chemical shift (NICS) values.[10] All the quinone analogs are found to have small NICS values compared to the corresponding dianionic isomers. The benzoquinones are found to be antiaromatic by NICS values, the magnitude of which is high for the known p- (8.42) and o- isomers (10.12) of the benzoquinones and less for the m-quinone (0.26). The quinone analogs of polyhedral boranes are found to have reasonable aromatic NICS values. The NICS values of the dianionic isomers and the corresponding parent dicarbaboranes are comparable where as that of quinone analogs the magnitude is comparatively smaller (Table 5.2). The aromatic destabilization energies and the NICS values indicate potential candidates for experimental scrutiny.

5.3.6. Conclusions

Benzoquinone analogues of polyhedral carbaboranes are found to be favorable on the potential energy surface. They can be grouped under the *hypercloso*-category as they are n vertex-n electron systems. The p-isomers show Jahn-Teller distortion due to the presence of partially occupied frontier degenerate orbitals. The corresponding dianionic isomers are found to be more favorable by NICS values.

References

1. (a) Eriksson, L. A.; Himo, F.; Siegbahn, P E. M.; Babcock, G. T. *J. Phys. Chem. A.*, **1997**, *101*, 9496. (b) Khodorkovsky, V.; Becker, J. Y. In Organic Conductors; Farges, J.-P., Ed.; Marcel Dekker: New York, 1994. (c) Ohtsuka, Y.; Ohkawa, K.; Nakatsuji, H. *J. Comput. Chem.* **2001**, *22*, 521.
2. Lown, J. W. *Chem. Soc. Rev.* **1993**, *22*, 165.
3. Brown, D. A.; Clegg, W.; Colquhoun, H. M.; Daniels, J. A.; Stephenson, I. R.; Wade, K. *J. Chem. Soc., Chem. Commun.* **1987**, 889.
4. (a) Baker, R. T. *Inorg. Chem.* **1986**, *25*, 109. (b) Kennedy, J. D. *Inorg. Chem.* **1986**, *25*, 111. (c) Johnston, R. L.; Mingos, D. M. P. *Inorg. Chem.* **1986**, *25*, 3321. (d) Mckee, M. L. *Inorg. Chem.* **1999**, *38*, 321. (e) Mckee, M. L.; Wang, Z-X.; Schleyer, P. v. R. *J. Am. Chem. Soc.* **2000**, *122*, 4781.
5. (a) Balakrishnarajan, M. M.; Hoffmann, R. *Angew. Chem Int. Edition.* **2003**, *115*, 3907. (b) Balakrishnarajan, M. M.; Hoffmann, R. *Inorg. Chem.* **2004**, *43*, 27.
6. Mulliken, R. S. J. Chem. Phys. **1955**, *23*, 1833, 1841. 2338. 2343.
7. Rudolph, R. W.; Pelug, J. L.; Bock, C. M.; Hodgson. M. *Inorg Chem.* **1970**, *9*, 2274.
8. The Borane, Carborane, Carbocation Continuum: Casanova. J. Ed; John Wiley & Sons., 1998.
9. Jemmis, E. D. *J. Am. Chem. Soc.* **1982,** *104*, 7017.
10. Schleyer, P. v. R.; Maerker, C.; Dransfeld, A.; Jiao, H.; Hommes, N. J. v. E. *J. Am. Chem. Soc.* **1996**, *118*, 6317.

List of Publications

- "Cationic *Closo* Carboranes- Promising Weakly Coordinating Ions" Jemmis, E. D.; Ramalingam, M.; **Jayasree, E. G.**; *J. Comput. Chem.*; **2001**, *22*, 1542-1551.
- "The Relation between Polyhedral Borane Sandwiches and Endohedral Complexes; the Electronic Structure and Stability of $X@Y_mB_nH_{n+m}^q$ (X=He,Ne,Li,Be; Y=B,C,Si; m=0-3; n=12-9; q=-2 to+2); $(C_2B_4H_6)_2X^q$ (X=Li,Al,Si; q=-3,-1,0) and $X_2@B_{17}H_{17}^q$ (X=He,Li; q=-2,0)" Jemmis, E. D.; **Jayasree, E. G.**; *Collect. Czech. Chem. Commun.*; **2002**, *67*, 965-990.
- "Ab initio Molecular Orbital Studies on the Structural Isomers of $C_3Si_2H_4$" Jemmis, E. D.; Saradha, R.; Saieswari, A.; **Jayasree, E. G.** *J. Ind. Chem. A.;* **2003**, 2382-2391.
- "Analogies between Boron and Carbon" Jemmis, E. D.; **Jayasree, E. G.** *Acc. Chem. Res.* **2003**, *36*, 816-824.
- "The Rearrangement of Dicarboranyl Methyl Cation: A Possible Synthetic Strategy towards Cationic *closo*-Tricarbaboranes" Jemmis, E. D.; **Jayasree, E. G.** *Inorg.Chem.*; **2003**, *42*, 7725-7727.
- "Does a sterically bulky group occupy the equatorial site in trigonal bipyramidal phosphorous?" Kommana, P.; Kumar, S, N.; Vittal, J. J.; **Jayasree, E. G.**; Jemmis, E. D.; Kumara Swamy, K. C. *Org. Lett.*; **2004**, 6, 145-148.
- "A Comparative Analysis of Polycondensed Aromatics: Benzenoids and Polyhedral Boranes" Jemmis, E. D.; **Jayasree, E. G.**; Balakrishnarajan, M. M. Manuscript under preparation.
- "Stable $B_{12}H_{10}$, $B_{12}H_{11}$ and Related Species" Anoop, A.; **Jayasree, E. G.**; Balakrishnarajan, M. M.; Sharma, P. K.; Jemmis, E. D. Manuscript under preparation.
- "CO vertices in Polyhedral Boranes: A new class of *hypercloso* systems" Jemmis, E. D.; **Jayasree, E. G.** Manuscript under preparation.
- "Structures with Hypercarbon" Jemmis, E. D.; **Jayasree, E. G.** manuscript under preparation.